

Lawrence Berkeley National Laboratory

Recent Work

Title

ELECTROCHEMICAL BEHAVIOR OF THE ALKALI METALS IN PROPYLENE CARBONATE

Permalink

<https://escholarship.org/uc/item/7g05n7gp>

Author

Jorne, Jacob.

Publication Date

1972-09-01

RECEIVED
LAWRENCE
RADIATION LABORATORY

LBL-1111

NOV 20 1972

LIBRARY AND
DOCUMENTS SECTION

ELECTROCHEMICAL BEHAVIOR OF THE
ALKALI METALS IN PROPYLENE CARBONATE

Jacob Jorné
(Ph. D. thesis)

September 1972

AEC Contract No. W-7405-eng-48

For Reference

Not to be taken from this room



LBL-1111

DISCLAIMER

This document was prepared as an account of work sponsored by the United States Government. While this document is believed to contain correct information, neither the United States Government nor any agency thereof, nor the Regents of the University of California, nor any of their employees, makes any warranty, express or implied, or assumes any legal responsibility for the accuracy, completeness, or usefulness of any information, apparatus, product, or process disclosed, or represents that its use would not infringe privately owned rights. Reference herein to any specific commercial product, process, or service by its trade name, trademark, manufacturer, or otherwise, does not necessarily constitute or imply its endorsement, recommendation, or favoring by the United States Government or any agency thereof, or the Regents of the University of California. The views and opinions of authors expressed herein do not necessarily state or reflect those of the United States Government or any agency thereof or the Regents of the University of California.

UNIVERSITY OF CALIFORNIA
Lawrence Berkeley Laboratory
Berkeley, California

January 9, 1973

ERRATA

To: All recipients of LBL-1111.
From: Inorganic Materials Research Division and Technical Information
Division
Subject: LBL-1111, "Electrochemical Behavior of the Alkali Metals in
Propylene Carbonate", by Jacob Jorné, dated September 1972.

Please make the following corrections on subject report.

On page 55 please change the following reference numbers:

- Line 14: Reference 3 should be reference 8.
- Line 17: Reference 6 should be reference 91, reference 7 should
be 38 and reference 8 should be 92.
- Line 20: Reference 11 should be 95, reference 12 should be 96
and reference 13 should be 97.
- Line 25: Reference 3 should be reference 91.
- Line 27: Reference 9 should be reference 8.

"Much important chemistry has been obscured
by our slavish devotion to water."(1)

ELECTROCHEMICAL BEHAVIOR OF THE ALKALI METALS IN PROPYLENE CARBONATE

Contents

Nomenclature	ix
Abstract	1
I. Introduction and General Background	3
1.1. Introduction	3
1.2. Electrodeposition of the Alkali Metals From Nonaqueous Solvents	6
1.3. Solubilities and Conductance Studies in PC	9
1.4. Conductance in Dilute Regions	11
1.5. Conductance Measurements of $AlCl_3$ in PC	15
1.6. Diffusion Coefficients	21
1.7. Reference Electrodes in PC	22
1.8. Electrode Kinetics of the Alkali Metals in PC	26
1.9. Thermodynamics of the Alkali Metals in PC and Related Aprotic Solvents	29
1.10. Double-Layer Capacity Measurements in PC	38
II. Experimental	40
2.1. General	40
2.1-1. Solvent Purification	40
2.1-2. Glove Box Operation	43
2.2. Solubilities and Deposition Measurements	45
2.2-1. Solubilities	45
2.2-2. Electrodeposition of the alkali metals	46
2.2-3. Cyclic Voltammetry Measurements	46
2.2-4. Electrodeposition of the Alkali Metals in a Rotating Disk System	48

2.3. Potential Measurements	54
2.3-1. Electrolytic Solutions	54
2.3-2. Reference Electrode	55
2.3-3. Preparation of Tl(Hg)/TlCl Reference Electrode	56
2.3-4. Preparation of the Alkali Metal Electrodes . .	58
2.3-5. Preparation of the Alkali Metal Amalgam Electrode	58
2.3-6. Cell for Potential Measurements	59
2.3-7. Assembly of Cell	62
2.3-8. Cell Potential Measurements	63
2.4. Electrode Kinetics Measurements	64
2.4-1. Electrode Kinetics of the Alkali Metals	64
2.4-2. Electrode Kinetics of the Alkali Metal Amalgams	67
2.5. Conductance Measurements	69
2.5-1. Preparation of Solutions	69
2.5-2. Conductance Measurements	70
2.6. Density Measurements	72
III. Results	73
3.1. The Electrodeposition of the Alkali Metals From Various Solutions in PC	73
3.1-1. Lithium	73
3.1-2. Sodium	80
3.1-3. Potassium	89
3.1-4. Rubidium	96
3.1-5. Cesium	98

3.2. Cell Potentials of the Alkali Metal Chlorides in AlCl ₃ (1 m)-PC Solutions	106
3.3. Activity Coefficients of the Alkali Metal Chlorides in AlCl ₃ (1 m)-PC Solution	118
3.4. Conductance of the Alkali Metal Chlorides in AlCl ₃ (1 m)-PC Solution	121
3.5. Density Measurements	125
3.6. Micropolarization Measurements of the Alkali Metals in Their Chloride Solutions in AlCl ₃ (1 m)-PC	129
3.7. Enthalpy of Activation at Zero Polarization of Lithium in LiCl Solution in AlCl ₃ (1 m)-PC	129
3.8. Micropolarization Experiments of the Alkali Metal Amalgams in Their Chloride Solutions in AlCl ₃ (1 m)-PC	136
3.9. Tafel Polarization of Potassium Amalgam in KAlCl ₄ (1 m)-PC Solution	142
3.10. Electrodeposition of Lithium in the Tafel Region	145
IV. Discussion	149
4.1. The Electrodeposition of the Alkali Metals	149
4.2. Cell Potentials of the Alkali Metal Chlorides in AlCl ₃ (1 m)-PC Solutions	154
4.3. Estimation of the Standard Potentials of the Alkali Metals in Pure PC	165
4.4. Conductance Measurements	167
4.5. Density Measurements and Excess Volumes	173
4.6. Micropolarization of the Alkali Metals in Their Chloride Solutions in AlCl ₃ (1 m)-PC	177

4.7. Nonuniform Current Distribution and Ohmic Drop Effects in Micropolarization Measurements	182
4.8. Micropolarization of the Alkali Metal Amalgams in Their Chloride Solutions in AlCl_3 (1 m)-PC	188
V. The Thermodynamics of Ion Solvation in Propylene Carbonate .	199
5.1. Introduction	199
5.2. Medium Effect or Solvent Activity Coefficient	199
5.3. Free Energies of Solvation of Individual Ions	201
5.4. Empirical Methods of Estimation of the Free Energies of Solvation of Individual Ions	204
5.5. Free Energies of Solvation of Single Ions in AlCl_3 (1 m)-PC Solution	205
5.6. Free Energy of Transfer	210
5.7. Standard Entropies of Transfer of the Alkali Metal Chlorides in AlCl_3 (1 m)-PC Solution	211
VI. Electrode Kinetics and Medium Effects	214
6.1. Introduction	214
6.2. Kinetics of Simple Electrode Process	217
6.3. Exchange Currents in Different Solvents	221
6.4. Rate Constants of the Alkali Metal Amalgams in AlCl_3 (1 m)-PC	222
6.5. Double Layer Correction of the Rate Constant	225
6.6. Individual Ion Solvation and Its Effect on Electrode Kinetics in AlCl_3 (1 m)-PC Solution	225
6.7. Conclusions	230

VII. Electrorefining and Separation of the Alkali Metals at	
Ambient Temperature	231
7.1. Conclusions of the Present Work	231
7.2. Electrorefining and Separation of the Alkali Metals	
at Ambient Temperature	232
7.3. Notes on the preliminary Design of a PC Electrorefining	
Cell	234
Appendix I. Properties of Propylene Carbonate	237
I.1. Preparation of PC	237
I.2. Purification of PC	237
I.3. Physical Properties of Propylene Carbonate	239
Appendix II. General Properties of the Alkali Metals	241
Appendix III. Chemicals	242
Appendix IV. The Deposition of Magnesium From PC and Related	
Solvents	244
IV.1. Experimental	245
IV.2. Results and Discussion	246
IV.2-1. Deposition From PC Solution	246
IV.2-2. $Mg(BF_4)_2$, $Mg(PF_6)_2$ and $Mg(PCl_6)_2$	253
IV.2-3. The Borohydride Solutions	255
IV.2-4. Ethyl Pyridinium Bromide Solution	256
IV.2-5. $MgX_2 + Mg$ Mixtures in PC	257
IV.3. The Mechanism of Mg^{2+} Reduction in PC	258
IV.4. Electrodeposition of Mg From related Solvents	260
IV.5. Electrodeposition of Calcium	262

Appendix V. The Electrodeposition of Titanium From PC and Related	
Solvents	263
V.1. Experimental	263
V.2. Results and Discussion	264
Appendix VI. The Electrodeposition of Molybdenum From PC and	
Pyridine Solution	268
VI.1. Experimental	268
VI.2. Results and Discussion	268
Acknowledgements	270
References	271

NOMENCLATURE

A	electrode area (cm^2)
A	electron affinity
A	Debye-Huckel constant (mole/Kg) ^{-1/2}
A_η	Jones-Dole coefficient
a_i	activity coefficient of solute i
B_η	Jones-Dole coefficient
C	concentration (mole/l)
c_i^s	bulk concentration (mole/l)
D	diffusion coefficient (cm^2/sec)
d	interplanar spacing, X-ray analysis, (\AA)
E	potential (volt)
E_1	cell potential (volt)
E_1°	standard oxidation potential of the alkali metal in pure PC with respect to Tl/TlCl, (volt)
E_2	$E_1 + 2RT/F \ln m_{\text{MCl}}$ (volt)
E_2°	standard oxidation potential of the alkali metal in $\text{AlCl}_3(\text{lm})$ -PC solution, with respect to Tl/TlCl, (volt)
E_m°	molar standard potential (volt)
E_c°	molar standard potential (volt)
E_N°	mole fraction standard potential (volt)
$E_{\text{M-M(Hg)}}$	potential difference between the pure alkali metal and its amalgam (volt)
E'	potential difference between the alkali metal amalgam and Tl(Hg)/TlCl reference electrode (volt)

E_z	potential of the point of zero charge (volt).
e	electron charge (coul.)
F	Faraday constant, 96500 coul./eq.
ΔG°	standard free energy (cal/mole).
ΔG_2°	standard free energy of the cell reaction (cal/mole).
ΔG_{emf}°	standard free energy of the cell reaction (cal/mole).
ΔG_{solv}°	standard free energy of solvation (cal/mole).
ΔG_t°	standard free energy of transfer (cal/mole).
ΔG_{conv}°	conventional free energy (cal/mole).
ΔG_{lat}°	lattice free energy (cal/mole).
ΔG_f°	standard free energy of formation (cal/mole).
$\overrightarrow{\Delta G}_\#^\circ$	the difference in the chemical standard free energy of the transition state and the solvated ion (cal/mole).
$\overleftarrow{\Delta G}_\#^\circ$	the difference in the chemical standard free energy of the transition state and the metal or the amalgam state (cal/mole).
ΔH°	standard enthalpy (cal/mole).
ΔH_2°	standard enthalpy of the cell reaction (cal/mole).
ΔH_{solv}°	standard enthalpy of solvation (cal/mole).
ΔH_t°	standard enthalpy of transfer (cal/mole).
ΔH_o^*	enthalpy of activation at zero polarization (cal/mole).
I	current (Ampere).
i	current density (mA/cm ²).
i_a°	apparent exchange current density (mA/cm ²).
I	ionization potential (e.v.).
i_t°	standard true exchange current density (mA/cm ²).

$(i_t^0)_r$	relative standard true exchange current density (mA/cm ²).
J	$= (\alpha_c + \alpha_a) Fr_o i^0 / RTk_\infty$
K	association constant of Cl ⁻ and Al ³⁺ in PC.
k_t^0	standard true rate constant (cm/sec).
k_a^0	standard apparent rate constant (cm/sec).
k_{s_2}	equilibrium constant of AgCl ₂ ⁻ .
k	Boltzmann constant.
m	molality (mole/Kg solvent).
M. W.	molecular weight.
M	alkali metal.
M(Hg)	alkali metal amalgam.
M [#]	activated complex or transition state.
p	pressure (atm).
q	charge density (coul/cm ²).
R	gas constant.
r_i	crystal radii (Å).
r	distance from the center of the rotating disk (cm).
r_o	radius of the disk (cm).
ΔS^0	standard entropy (cal/mole °K).
ΔS_2^0	standard entropy of the cell reaction (cal/mole °K).
ΔS_{solv}^0	standard entropy of solvation (cal/mole °K).
T	temperature (°K)
V	potential (volt).
v	specific volume (cm ³ /g).

v_{excess}	excess specific volume (cm^3/g).
v^m	molar volume (cm^3/mole).
X_M	mole fraction of the alkali metal M in its amalgam.
z	ionic valency.
α_c	cathodic transfer coefficient.
α_a	anodic transfer coefficient.
β	Guggenheim constant.
γ	activity coefficient.
γ_i^s	salt effect activity coefficient.
γ_i^m	medium effect.
$\Delta\alpha_t^o$	real standard free energy of transfer (cal/mole).
δ	Latimer, Pitzer and Slansky's solvent parameter (\AA).
δ	boundary layer thickness (cm).
ϵ	dielectric constant.
η	viscosity (c.p.).
η_o	solvent viscosity (c.p.).
η	overpotential (volt).
θ	time (sec).
κ	specific conductance ($\text{ohm}^{-1}\text{cm}^{-1}$).
Λ	equivalent conductance ($\text{ohm}^{-1}\text{cm}^2\text{eq}^{-1}$).
Λ_o	equivalent conductance at infinite dilution ($\text{ohm}^{-1}\text{cm}^2\text{eq}^{-1}$).
λ^o	ionic equivalent conductance at infinite dilution ($\text{ohm}^{-1}\text{cm}^2\text{eq}^{-1}$).
ρ	density (g/cm^3).
τ	transition time (sec).

ϕ_M^e	equilibrium potential (volt).
ϕ_M^o	standard equilibrium potential (volt).
ϕ_2	potential of the outer Helmholtz layer (volt).
χ	surface potential (volt).
ω	rotation speed (rpm).

ELECTROCHEMICAL BEHAVIOR OF THE ALKALI METALS IN PROPYLENE CARBONATE

Jacob Jorné

Inorganic Materials Research Division, Lawrence Berkeley Laboratory and
Department of Chemical Engineering, University of California
Berkeley, California

ABSTRACT

The electroreduction of active metals from aqueous solution is restricted primarily by thermodynamic limitations, because of preferential decomposition of the solvent. The most reactive of these, the alkali metals, cannot be deposited at all from aqueous solutions. Propylene carbonate (PC), a highly polar aprotic compound, was used as solvent medium for the deposition of the alkali metals at ambient temperature. Li, Na, K, Rb, and Cs were deposited successfully from their chlorides in AlCl_3 solution in PC. AlCl_3 served as a complexing agent. The experimental program included:

1. Equilibrium potential measurements which yielded activity coefficient data, and served to establish a relative standard potential scale in AlCl_3 -PC.
2. Conductance, density measurements.
3. Micropolarization measurements, for obtaining kinetic information (exchange current densities, transfer coefficients) on the alkali metals and their amalgams in AlCl_3 -PC.
4. Electrodeposition studies in the Tafel region.

A new process is proposed for the production and separation of the alkali metals at ambient temperature. Alkali amalgam from commercial mercury-chlorine cells is transferred into an AlCl_3 -PC electro-refining cell, where the alkali metal is dissolved anodically from the amalgam,

and deposited in a pure metallic form at the cathode. The lean amalgam is returned to the chlorine cell where it is again enriched with respect to the alkali metal.

I. INTRODUCTION AND GENERAL BACKGROUND

1.1. Introduction

The electrodeposition of metals from aqueous solution is restricted primarily by thermodynamic limitations. Metals which have significantly higher electrode potentials than hydrogen cannot be deposited from aqueous solution; the solvent is decomposed instead. In certain cases (e.g., Zn, Cd, Fe) nature was generous enough to extend the deposition of metals up to approximately 1 volt, because of high overpotential for hydrogen evolution; however, most metals are above this limit and cannot be reduced from aqueous solution. The alkali metals are the most reactive and cannot be deposited at all from aqueous solution, as they react violently with water. In addition, the alkaline earth metals and most of the transition metals cannot be electrodeposited from their aqueous solutions. The alternative use of nonaqueous solvents has been recognized for many years,^{1,2} and the search for the "magic" solvent that would permit a wider range of potentials for oxidation or reduction, turned during the years into a wide and very promising field--the chemistry of nonaqueous solvents.

The search for an alternative to water as a solvent was started in the beginning of the century by Walden.³ An early review on the deposition of metals from various nonaqueous solvents was written by Audrieth and Nelson,⁴ and later by Audrieth and Kleinberg.¹ Brenner⁵ reviewed the deposition of metals from organic solvents up to 1964. Most of the work in this field was unsystematic and covered only the most familiar organic solvents, in particular, pyridine, formamide, acetamide, acetonitrile, and alcohols.

Of all the classes of solvents, the aprotic solvents proved to be the most promising. Aprotic solvents do not contain proton available for reduction. These solvents have high dielectric constants (greater than 30), have weak acidic and basic character, and are difficult to oxidize or reduce. The most commonly used aprotic solvents are acetonitrile, dimethyl sulfoxide (DMSO), dimethyl formamide (DMF), N-methylformamide (NMF), propylene carbonate (PC) and 4-butyrolactone. These solvents dissolve moderate concentrations of ionic salts and permit a wide range of potentials, which enable, in some cases, the reduction of the most active metals, without decomposition of the solvent.

The present work concentrates on the possible electroreduction of the alkali metals, at ambient temperature, from their solutions in propylene carbonate. The goal was to develop a new process for the electrorefining and separation of the alkali metals at ambient temperature, as an alternative to the high temperature molten salt processes, by which these metals are currently produced. In addition, the electrodeposition of magnesium, calcium, titanium and molybdenum was investigated, and the results, mostly qualitative, are presented separately in Appendix IV, V, VI.

Propylene carbonate (PC), originally proposed for electrochemical applications by Harris and Tobias,⁶ is a member of a group of cyclic esters. PC is a dipolar aprotic solvent with high dielectric constant, low melting and high boiling point, dissolves many inorganic salts giving solutions of moderate conductance. The decomposition potential of PC is above 4 volts. Some selected properties of PC are presented in Table 1-1. A more complete review on the properties, preparation and purification of PC is given in Appendix I.

Table 1-1. Selected properties of propylene carbonate.

Formula	$ \begin{array}{c} \text{CH}_3 - \text{CH} - \text{CH}_2 \\ \quad \quad \\ \text{O} \quad \quad \text{O} \\ \quad \quad \diagdown \quad / \\ \quad \quad \text{C} \\ \quad \quad \\ \quad \quad \text{O} \end{array} $
Molecular weight	102
Dielectric constant	65 at 25°C
Melting point	-49°C
Boiling point	241°C
Density	1.2 at 25°C
Viscosity	2.5 cp at 25°C
Colorless, odorless.	

The initial electrochemical study of PC⁶ was quickly followed by a large number of exploratory government sponsored projects on the development of high energy batteries in which lithium served as an anode. The most popular electrolytic solutions used in these projects were LiClO₄ and LiAlCl₄ solutions in PC. Recently, PC has been used as a nearly ideal structureless solvent for better understanding of solution chemistry.

The electrochemistry and application of PC was reviewed recently by Jasinski,⁷ and therefore only relevant information concerning the immediate subject of the present work is being reviewed in this chapter. On the subject of high energy density batteries the reader is referred to Jasinski.²⁹ Over 200 papers and reports have been published on the electrochemistry of PC since Harris' thesis. A comprehensive review by Butler⁸ on reference electrodes in aprotic solvents contains useful information and an excellent list of references. The general subject

of electrochemistry of nonaqueous solvents was recently covered by Mann,^{9,10} Givens¹¹ and Adams.¹² Strehlow¹³ reviewed the electrode potentials in nonaqueous solvents; still other reviews covered the field of polarography in nonaqueous solvents.^{14,15,16} Payne¹⁷ reviewed the subject of the electrical double layer in nonaqueous solvents. The chemistry of nonaqueous solvents is reviewed in recently published books edited by Waddington¹⁸ and Lagowski.¹⁹ The rest of this chapter is restricted to a review of the behavior of the alkali metal in PC.

1.2. Electrodeposition of the Alkali Metals from Nonaqueous Solvents

Although the alkali metals are the most active metals and have the most negative electrode potentials in aqueous solution, their electrodeposition from various nonaqueous solvents seemed feasible. The general properties of the alkali metals are presented in Appendix II. Previous investigations of the electrodeposition of the alkali metals were qualitative in nature, incomplete and in many cases unreliable. Of the alkali metals only lithium, sodium and potassium were electrodeposited, mostly in impure forms, while rubidium and cesium were not obtained at all, probably because of their high reactivity.

Lithium is in general more readily deposited from various organic solvents. Lithium was deposited for the first time in 1895 from LiCl solution in acetone²⁰ and in pyridine.^{21,22,23} In a more detailed work^{24,25} lithium was obtained from LiCl solution in acetone, pyridine and various aliphatic alcohols. An extensive work was done by Müller

and his co-workers²⁶ on the electrodeposition of various metals, including lithium, from pyridine and other solvents. Lithium was obtained from solutions of lithium iodide in ether or nitromethane.²⁷ G. N. Lewis and F. G. Keyes²⁸ measured the standard electrode potential of lithium in propylamine, and the stability of the metal toward the solvent was very high. Harris and Tobias⁶ obtained metallic lithium from various solutions in several cyclic esters, in particular from propylene carbonate solutions. The stability and reversibility of lithium in propylene carbonate (PC) and other aprotic solvents were adopted in a series of projects, sponsored mainly by NASA, in order to develop secondary high energy batteries for space application. Since this topic is beyond the scope of the present work, and since the subject had been reviewed by Jasinski,^{29,7} only results which are related directly to the deposition of lithium are mentioned here. The aprotic solvents are the most suitable medium for the reduction of the alkali metals. Most of the work in this field was concerned with the following aprotic solvents: Acetonitrile (AN), dimethyl sulfoxide (DMSO), dimethyl formamide (DMF), and PC. Lithium was deposited from LiClO_4 solution in PC,³⁰⁻³⁶ and from the following salt solutions in PC: LiAlCl_4 ,^{47,7,77,159} LiBr ,⁶ LiPF_6 ,³⁶ LiBF_4 ,³⁶ LiAsF_6 .³⁶ Lithium behaves reversibly and can be deposited from the following systems: 4-butyrolactone, DMF and DMSO,³⁶ dimethylsulfite,³⁷ LiCl in DMSO,^{38,39} LiI in propylamine,²⁸ and from LiClO_4 solution in ethylene carbonate.^{40,41} Fried and Barak⁴² studied the reduction of the alkali metals on platinum substrates in PC by voltammetric technique. Alloying of electrodeposited lithium with Pt, Sn, Pb, Al, Au, Zn, Cd, Hg, and Mg is reported by Dey.⁴³ A Li/LiBr-PC system was used to

investigate the thermodynamics of lithium isotope exchange reaction.^{44,45} The kinetics of the electrodeposition of lithium from LiClO_4 , LiAlCl_4 , LiPF_6 and LiBF_4 is reported by Meibuhr.^{46,47} The kinetics of the Li electrode in LiClO_4 solution in PC is also reported by Scarr,⁴⁸ and the influence of water on the exchange current density is discussed by Butler, et al.⁴⁹ The kinetics of Li(Hg) in LiCl solution in DMSO was investigated.⁵⁰

The electrodeposition of sodium and potassium from nonaqueous solvents was reviewed by Brenner.⁵ Doubtful deposits of sodium⁵¹ and potassium^{20,21,23,52} were obtained from their pyridine and acetone solutions. Sodium and potassium have been obtained at somewhat elevated temperatures ($100^\circ\text{--}150^\circ\text{C}$) from their iodides in ethylene diamine.^{53,54} Potassium was obtained from KCl in AlBr_3 -nitromethane solution.⁵⁵ Russian workers intensively studied the electrodeposition of the alkali metals from various combinations of the alkali metal halides and aluminum halides in nitrobenzene;^{56,57} however, they concluded that nitro compounds are not suitable for commercial electrodeposition of the alkali metals. Sodium was electrodeposited from a solution of sodium trimethoxyborohydride in glycol dimethyl ether,⁵ and from sodium fluoroborate in diethylene glycol dimethyl ether⁵ at current densities above 500 mA/cm^2 . The Ziegler process⁵⁹ for the electrodeposition of sodium from molten $\text{NaAl(C}_2\text{H}_5)_4$ or $\text{NaB(C}_2\text{H}_5)_4$ should be mentioned here, although it is more of a molten salt electrolysis bath, and operates at a somewhat elevated temperature (150°C).

Harris and Tobias⁶ obtained light deposits of sodium and potassium from NaI and KI solutions in PC, ethylene carbonate and some lactones.

Meibuhr investigated the kinetics of sodium deposition from NaClO_4 solution in PC,⁶⁰ and obtained moderately high exchange current densities. Potassium was reported by several workers⁷ to be unstable and reactive in PC. The deposition of Na and K on Pt electrode from their chlorides in DMSO was reported by Avria and his co-workers.⁶¹ Sodium was found to be stable in ethylamine^{64,65} and in diethylamine.⁶⁵ Potassium was stable in ethylamine.⁶² Ethylamine and diethylamine were used in these works to determine, for the first time, the standard potentials of sodium and potassium in aqueous solution.^{62,64,65}

Rubidium and cesium have not been deposited from nonaqueous solution, probably due to their high reactivity and experimental difficulties. However, rubidium was found to be relatively stable in ethylamine, and its standard potential was measured in this solvent by G. N. Lewis and W. L. Argo.⁶⁶ The standard potential of cesium was measured in dimethylamine by Bent and his co-workers.⁶⁷

1.3. Solubilities and Conductance Studies in PC

Solubilities and conductivities are of importance in selecting electrolytes for batteries and electrolysis cells, and in designing cell configurations. Since the early research on PC was oriented toward the development of high energy batteries, most of the conductance data was obtained at high concentrations. More recently, measurements were performed in the dilute range in order to gain better understanding about solvent-solute interactions.^{68,72,81,82,79}

Most of the data on solubilities and conductivities is summarized in Jasinski's review,⁷ and the reader is referred to Table XIII and XIX in that review. Solubilities in PC are lower than in water. The

maximum solubilities are in the range of 2-3 M. A more valid comparison can be made on a mole fraction scale, since the molecular weight of PC is more than 5 times greater than that of water. Therefore solubilities of the order of 2 M in PC are equivalent to approximately 10 M in aqueous solutions, since both have the same mole fraction ratio. Solubilities of highly soluble salts in PC taken from the literature are presented in Table 1-2.

Table 1-2. Selected solubilities in PC.

Salt	Concentration	Reference
LiBr	2.43 m	68
LiI	1.365 m	68
LiPF ₆	0.763 M	69
LiPF ₆	0.55 M	70
LiClO ₄	2.1 M	71
LiBF ₄	0.42 M	70
NaClO ₄	>2 M	72
NaI	1.10 M	72.6
NaPF ₆	0.86 M	70
KI	0.23 M	72
KI	0.223 M	6
KPF ₆	1.2 M	31a

Salts with large anions are generally more soluble in PC. The solubilities of lithium salts are higher than the rest of the alkali metals; the solubility drops with increasing cation size. Small cations are strongly solvated by the localized negative pole of the PC molecule.

Specific conductivities in PC are in general one order of magnitude lower than in water, and range between 10^{-3} to 10^{-2} ohm⁻¹ cm⁻¹. The relatively low conductance is attributed to the higher viscosity of PC and to ion association at high concentration. Of special interest are the solutions of AlCl₃, BF₃ and PF₅ in PC. These solutes are strong Lewis acids and coordinate strongly with the negative pole of the solvent molecule. Since the present work deals mainly with solutions of AlCl₃ in PC, a separate section is dedicated to the solubility and conductance of AlCl₃ in PC. Selected conductance data is presented in Table 1-3.

Transference numbers of different salts in PC were measured using concentration cell with transference⁷⁹ and Hittorf cells.^{71,69,80} In the case of LiClO₄, the transference number of Li⁺ was below 0.5, similar to aqueous solution.

1.4. Conductance in Dilute Regions

Conductance measurements in dilute solutions can reveal important information about the solvent-solute interactions. Most of the work was performed in order to get the equivalent conductance at infinite dilution, where ions behave independently. The equivalent conductances at infinite dilution, Λ_0 , were obtained in most cases by extrapolation of a plot of Λ vs. $c^{1/2}$ to infinite dilution.

Table 1-3. Specific conductivities of soluble salts in PC.

Salt	Concentration	Conductivity $\text{ohm}^{-1}\text{cm}^{-1}$	Reference
LiAlCl_4	1 N	$6.57 \cdot 10^{-3}$	73
	0.75 M	$5.1 \cdot 10^{-3}$	74
AlCl_3	1.01 N	$7.0 \cdot 10^{-3}$	73,75
LiClO_4	1 N	$5.6 \cdot 10^{-3}$	73
	1.1 N	$4.97 \cdot 10^{-3}$	73
	0.9 M	$5.2 \cdot 10^{-3}$	76
LiPF_6	0.76 N (sat)	$5.83 \cdot 10^{-3}$	69
	0.55 M (sat)	$4.49 \cdot 10^{-3}$	70
LiBr	2.4 m	$5.0 \cdot 10^{-3}$	6
	1.15 m	$1.8 \cdot 10^{-3}$	77
LiBF_4	0.42 M (sat)	$2.5 \cdot 10^{-3}$	70
NaPF_6	1 N	$1.67 \cdot 10^{-3}$	69
	0.86 M (sat)	$6.8 \cdot 10^{-3}$	70
NaI	1.1 m	$5.8 \cdot 10^{-3}$	6
NaClO_4	1.22 N	$6.75 \cdot 10^{-3}$	76
KPF_6	0.5 N	$6.8 \cdot 10^{-3}$	69
	sat.	$3.12 \cdot 10^{-3}$	70
KCNS	1.55 M	$8.95 \cdot 10^{-3}$	31
PF_5	0.5 M	$1.3 \cdot 10^{-3}$	78
CaBr_2	0.75 m	$3.3 \cdot 10^{-4}$	6
$\text{Mg}(\text{ClO}_4)_2$	0.4 M	$4.7 \cdot 10^{-3}$	77

Harris⁶ obtained Kohlrausch plots for NaI and KI in PC, and the equivalent conductances were 28.3 and 31.0 $\text{ohm}^{-1} \text{cm}^2$, eq^{-1} , respectively. The slopes of the straight lines were in good agreement with the Onsager limiting law equation. Fuoss, et al.⁶⁸ studied the conductance of tetra-n-butylammonium tetrphenylboride in PC and concluded that ion association was negligible. Wu and Friedman⁷² investigated the conductances and heats of solution of several alkali metal iodides, perchlorates, trifluoroacetates and tetrphenylborates in PC. The perchlorates were found to be strong electrolytes, whereas the trifluoroacetates showed considerable ion association. Keller, et al.⁸¹ measured the equivalent conductance of LiClO_4 , LiCl , LiBr , TBABR, TMAPF₆ in PC, and obtained the equivalent conductance at infinite dilution. Mukherjee and Boden⁸² made conductance and viscosity measurements of LiCl , LiBr , LiClO_4 , Et_4NCl , Et_4NClO_4 , $n\text{-Bu}_4\text{NBr}$ and $n\text{-Bu}_4\text{NClO}_4$ in PC. The method of Fuoss and Accascina⁸³ was used to obtain Λ_0 and the individual ion conductances Λ_+^0 and Λ_-^0 . LiCl and LiBr were found to be associated, whereas no association could be detected for the other salts.

Table 1-4 presents the equivalent conductances and ionic conductances at infinite dilution for several electrolytes in PC. The ionic conductance of Li^+ is the lowest, which means that the ion has a large effective size. The ionic conductance of ClO_4^- , I^- , Br^- and Cl^- are approximately the same. Anions are poorly solvated in PC, and their ionic conductance is higher than the conductance of the cations.

A somewhat related series of papers by Yao and Bennion^{84,85,86} needs mention. Conductances and viscosities of several salts in DMSO

Table 1-4. Equivalent conductance and ionic conductance in PC.

Salt	Λ	λ_+	λ_-	Reference
LiCl	25.6			81
	26.2			81
	27.5	7.30	20.20	82
LiBr	26.2			81
	27.35	7.30	20.05	82
LiClO ₄	25.6			81
	26.2			69,72
	26.08	7.30	18.78	81
	26.3			87
NaI	28.2			6
NaClO ₄	28.3			72
KI	30.75	11.97	18.78	79
	31.0			6
KClO ₄	30.75	11.97	18.78	79
Et ₄ NC10 ₄	32.06	13.28	18.78	79
n-Bu ₄ NC10 ₄	28.17	9.39	18.78	79
n-Bu ₄ NBr	28.65	9.39	19.26	79
(i-Am) ₄ N(i-Am) ₄ B	16.37	8.185	8.185	79
(i-Am) ₄ NI	26.95	8.185	18.675	79

were measured over a wide range of concentrations and temperatures and the transport properties were calculated and interpreted. Melendres^{86a} determined the solubilities of chlorides, nitrates, perchlorates and bromides of the alkali, alkaline earth and several transition metals.

1.5. Conductance Measurements of AlCl_3 in PC

AlCl_3 , a strong Lewis acid which is very soluble in PC (3.2 M), increases the solubility of salts that are insoluble in pure PC by forming complex ions with the anions of these salts. AlCl_3 in combination with LiCl was investigated as an electrolyte for high energy batteries (Refs. 87,88,81,159,108,161,109). Conductance measurements and NMR studies were performed in order to understand the transport properties and the species present in AlCl_3 solutions in PC. Boden⁸⁷ measured the specific conductance of AlCl_3 in PC over a wide concentration range (Fig. 1-1). The maximum specific conductance of approximately $10^{-2} \text{ ohm}^{-1} \text{ cm}^{-1}$ occurs at an AlCl_3 concentration of 1.2 M. The specific conductance falls off at higher concentrations because of the increasing viscosity of the solution and due to ion association at high concentrations. Breivogel and Eisenberg⁸⁸ measured the equivalent conductance of dilute solutions of AlCl_3 and LiCl-AlCl_3 in PC, using a dc conductivity method. The results were interpreted through the Onsager equation, after being corrected for viscosity effect using the Walden rule. A plot of the equivalent conductances vs. $C^{1/2}$ for LiAlCl_4 and AlCl_3 in PC are shown in Fig. 1-2 and Fig. 1-3, respectively. The experimental slope in the case of LiAlCl_4 did not agree with the calculated Onsager slope. Breivogel and Eisenberg⁸⁸ attempted to explain the anomalous minimum in the equivalent conductance of AlCl_3 (Fig. 1-3) by the presence of different ionic species in different concentration regions. The rapid increase in was explained as being caused by an increase in the number of ions per mole of solute as the concentration increases. The following equilibrium

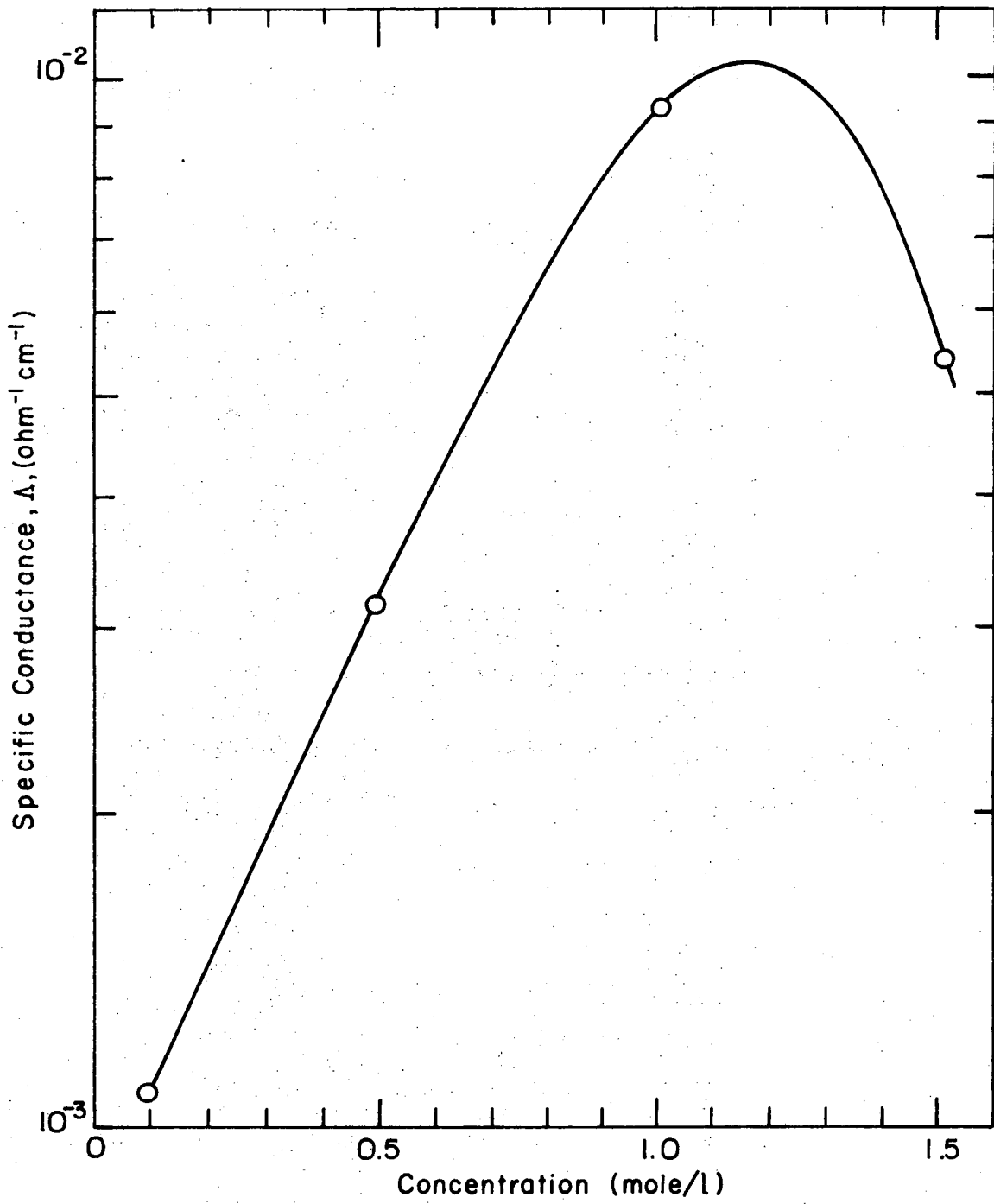


Fig. 1-1 Specific Conductance of AlCl₃ Solution in PC.

After Boden.⁸⁷

XBL72I-6004

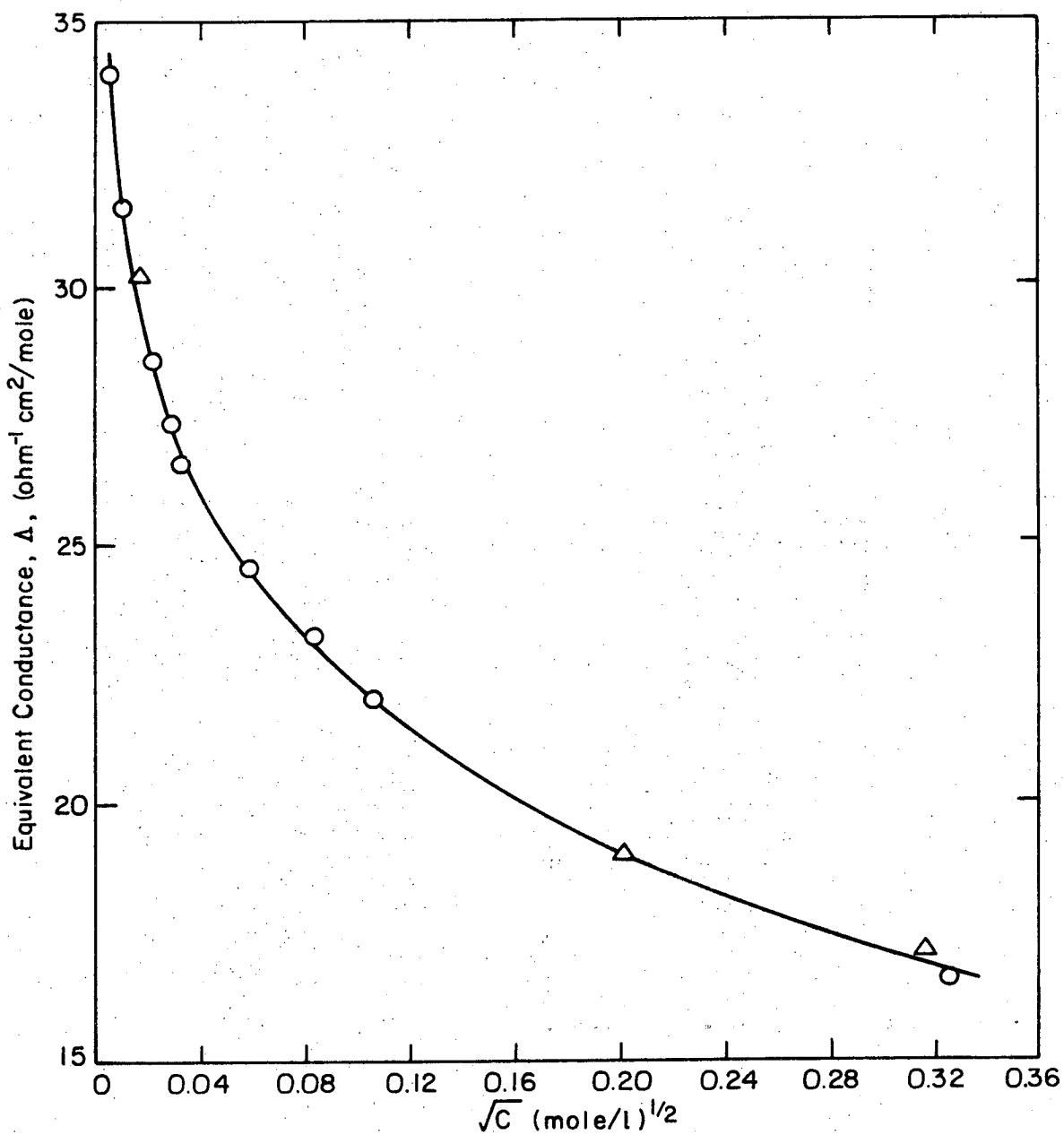
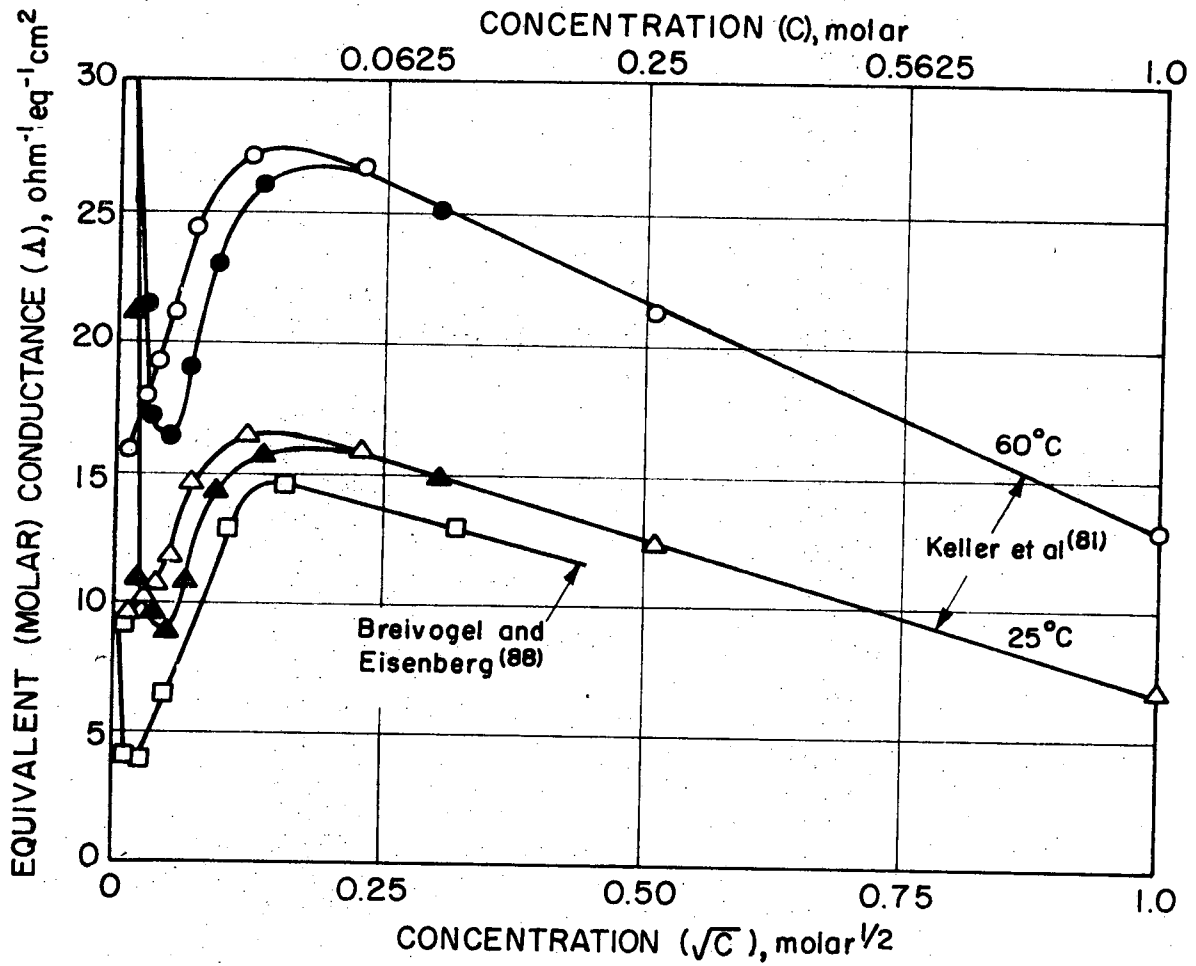


Fig.1-2 Equivalent Conductance vs. $C^{1/2}$ for LiAlCl₄ in PC.⁸⁸

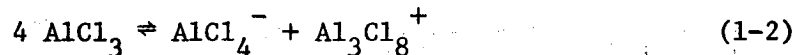
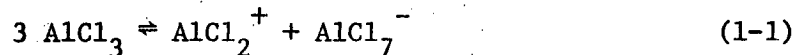
XBL72I-6003



XBL 728-6729

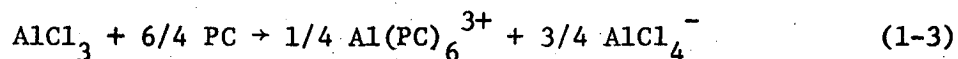
Fig. 1-3. Equivalent molar conductance of AlCl₃ in PC at 25 and 60°C.

reactions were proposed as being able to explain such an increase in the specific conductance:



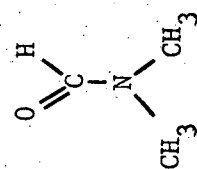
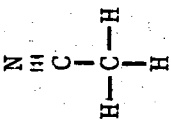
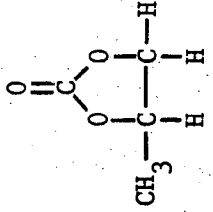

Although either of the equations can explain qualitatively the anomalous behavior, further work is required to confirm this hypothesis. A different approach was proposed by Keller, et al.,⁸¹ who found the same anomalous behavior of AlCl_3 at low concentrations. The minimum in the plot of Λ_0 vs. $C^{1/2}$ was explained by the hydrolysis of AlCl_3 with traces of water to give aluminum hydroxide and HCl . The limiting equivalent conductance of LiAlCl_4 was estimated to be $34.5 \text{ ohm}^{-1} \text{ eq}^{-1} \text{ cm}^2$, (see Fig. 1-2) although the extrapolation was somewhat uncertain.

Keller, et al.⁸¹ also studied directly the ionic equilibria of AlCl_3 in PC, using NMR techniques. From the Al^{27} spectra, Keller concluded that the main species are $\text{Al}(\text{PC})_n^{3+}$ and AlCl_4^- , similar to the species present in an AlCl_3 solution in acetonitrile. High resolution H^1 spectra of 1 M AlCl_3 -PC indicates peaks due to coordinated PC as well as bulk PC. From the H^1 and the Al^{27} spectra, Keller showed that the Al coordination number (n) is six. Therefore, the dissolution of AlCl_3 in PC proceeds according to

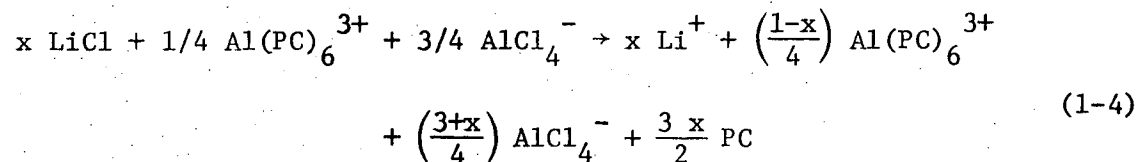


Furthermore, it was observed that the addition of LiCl to an AlCl_3 -PC solution reduces the concentration of the coordinated Al species, and at the saturation point, where the $\text{LiCl}:\text{AlCl}_3$ ratio is 1:1, the coordinated Al species disappears. Such observations can be explained by the reaction

Table 1-5. Summary of complexing property of solvents. 81

	DMF	AN	PC	Water
Solvent Structure				
Dielectric Constant	~35	~35	~65	~80
Dipole Moment	3.9	2.7	~4 (?)	1.8
Basicity	High	Low	Low (?)	---
Species in AlCl ₃	Al[DMF] ₆ ⁺³ + Cl ⁻	Al[AN] ₆ ⁺³ + AlCl ₄ ⁻ + Cl ⁻ (?)	Al[PC] ₆ ⁺³ + AlCl ₄ ⁻ + Cl ⁻ (?)	Al[H ₂ O] ₆ ⁺³ or [Al(OH) ₄] ⁻ + Cl ⁻
Change in Species on Addition of LiCl	As Above + Li ⁺ + Cl ⁻	Al[AN] ₆ ⁺³ + AlCl ₄ ⁻ + Li ⁺	Al[PC] ₆ ⁺³ + AlCl ₄ ⁻ + Li ⁺	
Change in Species on Addition of HClO ₄	As above + Li + ClO ₄ ⁻	Al[AN] ₆ ⁺³ + [A](AN) _x (ClO ₄) _y ^{+3-y} (?) + Li ⁺ + ClO ₄ ⁻		

between LiCl and $\text{Al}(\text{PC})_6^{3+}$ to give AlCl_4^- , according to the following reaction:



At the saturation point, where $x = 1$, all the coordinated $\text{Al}(\text{PC})_6^{3+}$ converted to AlCl_4^- , and the species present are Li^+ and AlCl_4^- .

Table 1-5 summarizes the results of Keller, et al.,⁸¹ for solutions of AlCl_3 in DMF, AN, PC and water. The complexing strength of Al^{3+} toward Cl^- is stronger than toward PC, AN and water, but weaker than toward DMF. This ionic equilibria analysis of AlCl_3 in PC, according to Keller, et al. is in contrast to the analysis of Brievogel and Eisenberg.⁸⁸ Neither of these workers succeeded in explaining quantitatively the minimum in the equivalent conductance plot of AlCl_3 in PC.

1.6. Diffusion Coefficients

Diffusion coefficients of lithium salts in several aprotic solvents were measured by Sullivan, Hanson and Keller,¹⁷⁴ using a porous disk method. According to this method, a porous disk, filled with the solution to be studied, was suspended in a large volume of pure solvent, and the integral diffusion coefficient was calculated from the weight change. Table 1-6 presents the results of their measurements.

A direct correlation can be seen between the diffusion coefficient and the solvent viscosity. Since for the above solvents the product $D \cdot \eta_{(\text{solvent})}$ is constant within $\pm 16\%$, this correlation can be used to estimate diffusion coefficients for various solute-solvent combinations.

Table 1-6. Diffusion coefficients of lithium salts in several aprotic solvents.

Electrolyte	D, cm ² sec ⁻¹
LiClO ₄ (1 M) in PC	2.58 10 ⁻⁶
LiCl (0.7 M) + AlCl ₃ (1 M) in PC	3.04 10 ⁻⁶
LiCl (1 M) in DMF	7.29 10 ⁻⁶
LiClO ₄ (1 M) in AN	1.71 10 ⁻⁵
LiClO ₄ (1 M) in MF	1.68 10 ⁻⁵
LiAsF ₆ (1.1 M) in MF	1.54 10 ⁻⁵

The diffusion coefficients of the other alkali metals are expected to be somewhat higher than for the heavily solvated Li⁺ ion with its low mobility.

1.7. Reference Electrodes in PC

A reference electrode is an important tool in most electrochemical studies. Reference electrodes are widely used in thermodynamic and kinetic studies of electrode reactions, and are very important tools in many electroanalytical methods. An excellent review on reference electrodes in aprotic solvents was written by Butler⁸ and includes a large list of references.

The essential criteria for satisfactory reference electrode are: 1) stable potential with time, 2) reversibility under polarization in both cathodic and anodic directions, 3) Nernstian behavior with respect to some species in the electrolyte, 4) for reference electrode of the second kind, the solid phase must not be appreciably soluble in the electrolyte solution. Reference electrodes must have a well defined reaction

which determines its potential at equilibrium, although in many cases, undefined reference electrodes, such as platinum and silver wires or mercury pools were used. Although many electrodes show stable potentials, very few behave reversibly according to the Nernst equation. This requirement is essential when the reference electrode is used to measure thermodynamic data. Reference electrodes of the second kind are suitable for emf and activity coefficient measurements; however, a search for a satisfactory reference electrode of the second kind involves the quest for a salt whose metal ion forms a reversible electrode couple, and at the same time is relatively insoluble in solutions containing a large excess of the common anion. Because of the dramatic changes in solubilities and complex stabilities from one solvent to the other, the search for a satisfactory reference electrode is not an easy task, and projections from the aqueous system to nonaqueous systems are mostly incorrect.

The most widely used nonaqueous reference electrode is based on the Ag/Ag^+ couple. Unfortunately, the reference electrode of the second kind Ag/Ag^+ cannot be used in PC because of the much higher stability of the complexes of silver with chlorides and other anions.⁸ As Butler pointed out,⁸ the establishment of a satisfactory $\text{Ag}/\text{AgCl}(\text{s})$ reference electrode depends primarily on the equilibrium constant K_{s_2} for the reaction



The forward reaction is accelerated in the presence of an excess of chloride ions. If the concentration of AgCl_2^- is relatively high, a liquid junction potential will result because the mobilities of

AgCl_2^- and Cl^- are not the same. Butler⁸ presents a comprehensive table of the solubilities and complex formations of silver salts in many aprotic solvents. The equilibrium constant for reaction¹⁻⁵ in PC is quite high, $K_{s_2} = 1.0$, and means that most of the anionic species are AgCl_2^- rather than Cl^- .^{89,90} The high value of K_{s_2} in most aprotic solvents can be explained by the fact that AgCl_2^- is more strongly solvated than Cl^- , which is in agreement with the observation that salts with large anions are more soluble in PC (e.g., ClO_4^- , BF_4^- , PF_6^- , AlCl_4^-).

The most promising reference electrodes of the second kind are those based on Thallium (I) salts.⁸ Thallous chloride is only slightly soluble in PC and does not dissolve in an excess of chloride. Earlier investigations in this laboratory revealed the excellent nature of thallium amalgam (or thallium metal)-thallous halide electrodes in PC and DMSO.^{91,38,92} This reference electrode was applied to the cell Li/LiX in $\text{DMSO/TlX(s)/Tl(Hg)}$ to determine activity coefficients and standard potentials.^{92,93,94} Salomon^{95,96,97} used the thallium amalgam-thallous halide reference electrodes in PC to determine activity coefficients and standard potentials. The Tl(Hg)/TlCl electrode was found to be reversible and stable in DMF.^{98,99} Baucke and Tobias⁹¹ studied the performance of Tl(Hg)/TlX and Tl/TlCl in PC, where X was either Cl^- , Br^- or I^- . The solubilities of TlCl , TlBr and TlI in PC are in the order of 5×10^{-6} , 1×10^{-6} and 2×10^{-6} M, respectively. The solubility products of TlCl and TlBr in PC are $10^{-12.4}$ and $10^{-12.66}$, respectively, being much lower than in DMSO, for example. This is the reason for their excellent performance in PC. A solid thallium-thallous chloride electrode showed somewhat less reproducible behavior than the corresponding amalgam

electrode. Rock, et al.^{44,45} used Tl(Hg)/TlBr reference electrode in PC to determine the thermodynamics of lithium exchange reactions. However, the cell potential was somewhat erratic and irreproducible.⁴⁴ Synnot and Butler¹⁰⁰ reported the use of Tl(Hg)/TlCl in PC.

Other reference electrodes of interest were reported by several investigators and are reviewed briefly here. Fried and Barak¹⁰¹ studied the "calomel" reference electrode in PC. The following systems were tested: Hg/Hg₂Cl₂(s)/(C₂H₅)₄NCl(satd.), Hg/Hg₂Cl₂(s)/(C₄H₉)₄NCl(1F) and Hg/Hg₂I₂(s)/(C₂H₉)₄NI(1F). The exchange current densities of these electrodes were 4.8×10⁻⁶, 3.7×10⁻⁵ and 4.3×10⁻⁵ A/cm², respectively. Piljac and Iwamoto¹⁰² investigated the mercury/mercury (I) systems: Hg/Hg₂Cl₂, NaCl(satd.) (C₂H₅)₄-NClO₄; Hg/Hg₂I₂, KI; Hg/Hg₂SO₄; and in particular Hg/Hg₂Cl₂, KCl, (C₂H₅)₄NClO₄ for which the exchange current density is 4.5×10⁻⁶ A/cm². Kirowa-Eisner and Gileadi¹⁰³ developed the Ag/Ag⁺ reference electrode in PC. The Ag/AgClO₄ reference electrode was found to be very suitable, easy to prepare and showed a high exchange current density, in the order of 2×10⁻⁵ A/cm². The use of this type of reference electrode is reported by Biegler and Parsons,¹⁰⁴ who used the electrode Ag/Ag⁺ (0.05 M), NaClO₄ (0.5 M) in their electrical double layer measurements on mercury in PC. Caiola, et al.¹⁰⁵ studied the behavior of the electrodes Li/LiCH₃CO₂, Hg/Hg₂(CH₃COO)₂ and Cu/Cu(CH₃COO)₂ in PC and DMSO. The Li/LiCH₃CO₂ behaved reversibly in PC, while cupric acetate dissolved due to complex formation.

The reversible behavior of Li(s)/Li⁺ reference electrode in PC received much attention, especially due to the extensive research on lithium high energy batteries. Burrows and Jasinski³³ investigated the

reversible behavior of Li/LiClO_4 reference electrode in PC. Meihbur^{46,47} and Scarr⁴⁸ investigated the kinetics of Li/Li^+ electrodes, and showed that the exchange currents are in the order of $1 \text{ mA}/\text{cm}^2$. However, Butler, et al.⁴⁹ found that the exchange current of lithium electrodes depends strongly on the water content of the solution, and decreases rapidly during the first hour, from a value of $10.2 \text{ mA}/\text{cm}^2$ at the first second, to $1.6 \text{ mA}/\text{cm}^2$ after one hour, despite the fact that the water level was quite low ($<0.001 \text{ m}$). The $\text{Li}(\text{Hg})/\text{Li}^+$ reference electrode in PC was investigated by Butler.¹⁰⁷ The kinetics of a sodium electrode in NaClO_4 -PC solution was investigated by Neibuhr,⁶⁰ and the exchange current density of Na/NaClO_4 (1 M) in PC was $0.21 \text{ mA}/\text{cm}^2$ at 19°C . Anodization of the electrode was necessary to obtain reproducible results.

1.8. Electrode Kinetics of the Alkali Metals in PC

The great interest in nonaqueous high energy batteries produced an increasing number of investigations concerning the electrochemical behavior of nonaqueous solvents. Lithium metal is the leading anodic material for high energy batteries due to its high energy density. Despite the increasing interest in dissolution-deposition processes, few investigations dealt directly with the kinetics of the electrode process. Moreover, most of the literature dealt exclusively with lithium systems. Although the work of Harris and Tobias⁶ included deposition tests of metals from cyclic esters, these were mostly qualitative in nature, and did not reach the stage of systematic kinetic measurements.

The electron transfer kinetics of Li/Li^+ reaction in PC was studied by several laboratories. Burrows and Jasinski³³ measured the exchange

current density of Li(s) in 1 M LiClO₄-PC at 28°C, using micropolarization measurements. However, the reported exchange current density appears too low (0.0275 mA/cm²), probably due to the inclusion of an ohmic drop in the potential measurements. Meibuhr⁴⁶ measured the exchange currents of lithium in different LiClO₄ concentrations in PC, at temperatures up to 70°C. At 28°C, for 1 M LiClO₄-PC solution, the exchange current, $i_0 = 0.95 \text{ mA/cm}^2$, and the transfer coefficient, $\alpha = 0.67$, were calculated from the linear polarization curves and from the concentration dependence of the exchange current. The solution was stirred by bubbling argon, and the ohmic drop was excluded using pulse technique. The Nernstian behavior of the Lithium electrode was confirmed by concentration cells. The enthalpy of solvation at zero polarization was estimated as 8.5 Kcal/mol, and the reaction order was one, which reaffirmed the assumption that the charge transfer was the rate-determining step. In a second article, Meibuhr⁴⁷ studied the anion effect on the electrode kinetics of Li/Li⁺ in PC. The exchange currents for unit molarity solutions of LiAlCl₄, LiPF₆ and LiBF₄ are 0.40, 0.29 and 0.5 mA/cm², respectively. The transfer coefficient for LiAlCl₄ was $\alpha = 0.8$. The water content of the solutions had a major influence on the electrode performance. Scarr⁴⁸ measured the kinetics of lithium electrode in different concentrations of LiClO₄ in PC. Film formation, and two levels of activity were observed, depending on the pretreatment of the electrode. The film was broken at high currents. The exchange current density of a film free electrode in 1 M LiClO₄ PC solution is $1.78 \pm 0.33 \text{ mA/cm}^2$. Generally, good agreement was found between Meibuhr's and Scarr's results, which are complementary, since Scarr worked at moderately high currents, while Meibuhr's work is

restricted to the zone of linear current-potential dependence. Butler, Cogley and Synnot⁴⁹ studied the aging effect on the kinetics of lithium in LiClO_4 solution in PC. Even when the solvent was quite "dry" ($<0.001 \text{ m H}_2\text{O}$), the exchange current dropped from 10.2 mA/cm^2 at 1 second after the exposure of the freshly cut lithium surface, to 1.6 mA/cm^2 after 1 hour. The effect of water was also dramatic; the presence of $0.02 \text{ m H}_2\text{O}$ reduced the exchange current to 0.026 mA/cm^2 after one hour. It seems that most measurements were taken on aged surfaces; the exchange currents of fresh surfaces may have no practical meaning. The effect of water content on the behavior of lithium electrodes in LiClO_4 ^{35,107} showed that LiOH was formed on the electrode during the deposition of lithium from LiClO_4 solution in PC.

The anodic polarization of lithium in 1.0 m AlCl_3 PC solution was investigated by Jackson and Blomgren,¹⁰⁸ using an interrupter and a constant load pulse technique. Severe polarization of the concentration type was observed, which would be caused by the formation of LiCl layer during the anodic discharge. Sufficient stirring removed the product, which dissolved in AlCl_3 solution and eliminated the severe concentration polarization.

In a study of the anodic behavior of sodium in NaClO_4 PC solution, Meibuhr⁶⁰ reports that the exchange current depends strongly on the Na^+ concentration. At 1 M NaClO_4 and at 19°C , the exchange current was 0.21 mA/cm^2 .

The behavior of lithium in related solvents is reported in several papers. The electrochemical behavior of Li in solutions of LiClO_4 , KPF_6 , KCNS in ethylene carbonate was reported by Pistoia, et al.^{40,41}

Ethylene carbonate was proposed as a superior solvent for high energy batteries due to its higher conductance and lower viscosity, and due to the better anodic polarization characteristics found for Li in $\text{LiClO}_4\text{-EC}$ solution.

The kinetics of Li(Hg) in LiCl solution in DMSO was reported by Cogley and Butler.^{109,50} The Tafel equation with cathodic transfer coefficient $\alpha = 0.75$ was obeyed over the current density range of 10^{-5} to $3 \times 10^{-3} \text{ A/cm}^2$. The exchange currents were in the order of $0.1 - 1.0 \text{ mA/cm}^2$.

1.9. Thermodynamics of the Alkali Metals in PC and Related Aprotic Solvents

Aqueous solutions are believed to be very complicated because of their specific interactions and structure. It is often said that in order to gain a better understanding of electrolytic solutions, further work should be done in nonaqueous solvents, which have less complicated structure. As a result, there is a strong interest in thermodynamic measurements in polar aprotic solvents, since some of them are considered to be structureless, and do not show specific interactions with the solutes. The evaluation of single ion solvation energies in nonaqueous solvents are of great importance since it can reveal information about medium effects and establish a universal scale of standard potentials. In addition, there is a growing interest in organic and inorganic ionic reactions in aprotic solvents. Recent interest in the possible use of aprotic solvents as a medium for high energy batteries also prompted a number of potentiometric studies of lithium salts in several promising aprotic solvents.

Thermodynamic measurements in aprotic solvents can be divided into two main categories: 1) *Emf* measurements for obtaining standard potentials and activity coefficients, and 2) direct calorimetric measurements of enthalpies of solution. Standard potentials can be used to estimate free energies of solvation of individual ions. The entropies of solvation of individual ions can be estimated from either the temperature dependence of the standard potentials or from the combined free energy and enthalpy measurements. Individual ionic solvation entropies can be interpreted in terms of the structural effects on the solvent.

The following brief review covers thermodynamic measurements in PC and related aprotic solvents; the direct work in PC is presented at the end of this section in greater detail. Potentiometric studies using cells without transference lead to the determination of standard potentials and of activity coefficients. Comparison between different solvents yields information on medium effects. Most of the studies were performed in the common aprotic solvents: acetonitrile (AN), formamide (FA), N-methylformamide (NMF), dimethyl sulfoxide (DMSO) and propylene carbonate (PC).

Luksha and Criss¹¹⁰ measured electrode potentials for cells of the type $M(\text{Hg})/\text{MX}$, $\text{NMF}/\text{AgX}/\text{Ag}$ in NMF, where M is Li, Na, K, or Cs and X is either Cl^- or Br^- . These potentials were used to evaluate standard potentials for cells of the type M/MX , $\text{NMF}/\text{AgX}/\text{Ag}$ for which standard free energies of formation and activity coefficients of LiCl , NaCl , KCl , CsCl and NaBr in NMF were obtained. The free energies were used in conjunction with previous heat of solution data¹¹¹ to obtain the standard

partial molal entropies of the corresponding electrolytes. Thermodynamic properties of some alkali metal halides in N, N-dimethylformamide (DMF) were measured and calculated by Held and Criss,¹¹² and by Criss and Luksha.¹¹³ The entropies of solvation and the partial molal entropies of alkali metal and halide ions were estimated in DMF. A compilation of partial molal entropies of 1:1 electrolytes in seven nonaqueous solvents is presented by Criss, et al.¹¹⁴ The ionic entropies were estimated and their relationship to the structure of the electrolytic solutions was discussed. Butler and Synnott⁹⁸ measured potentials of the cell $\text{Li(Hg)/LiCl, DMF/TlCl(s)/Tl(Hg)}$ in DMF. LiCl concentration varied from 0.001 to 2.0 m. The standard potential, free energy, enthalpy and entropy for the reaction $\text{Li}^+ + \text{Cl}^- + \text{Tl(s)} \rightarrow \text{Li(s)} + \text{TlCl(s)}$ and for the reaction $\text{Li}^+ + \text{Tl(s)} \rightarrow \text{Li(s)} + \text{Tl}^+$, as well as activity coefficients for LiCl in DMF, were obtained. Ion pairing between Li^+ and Cl^- was found to be weak, and the Guggenheim equation gave the most accurate empirical description of the activity coefficients. Measurements by the emf method for the activity coefficients of LiCl in DMSO were reported by Smyrl and Tobias⁹² and by Butler, et al.^{109,115} The agreement between the two works is quite good, although two other measurements of the activity coefficients of LiCl in DMSO by the freezing point method,^{116,117} show wide disagreement. It seems that the emf results are more reliable.⁸ Salomon measured the thermodynamic properties of LiBr and LiI in DMSO^{93,94} using the emf method with thallium amalgam/thallic halide reference electrode.

Agarwall and Nayak^{118,119} measured the emf of the cell $\text{Pt, H}_2/\text{HCl}/\text{AgCl/Ag}$ in formamide. The standard potential, the activity coefficients

and the standard thermodynamic values ΔG° , ΔH° and ΔS° for the cell reaction were determined. The potentials were determined by extrapolation to zero time, since the measured potentials dropped slowly with time. This was believed to be the result of a decomposition of the solvent, and the extrapolation to zero time corresponds to zero decomposition of the solvent. The standard potential of Ag/AgCl electrode in formamide was evaluated by the emf method, with respect to the normal hydrogen electrode.¹²⁰ Similar measurements as well as the solubility product and equilibrium constant for AgCl in formamide were reported elsewhere.¹²¹ Again, the emf values were extrapolated to zero time because of the decomposition of the solvent. The activity coefficients of LiCl in acetonitrile were measured by the emf method by Spiegel and Ulich.¹²² Solute-solvent interactions in acetonitrile and the evaluation of relative activities of cations and anions in acetonitrile are reported by Coetzee and Campion.^{123,121}

Enthalpies of solution are of interest in calculating individual ionic entropies, as well as for obtaining temperature coefficients of cell potentials. Enthalpies of solvation were obtained mostly by direct calorimetric measurements in formamide,^{125,126} N-methylformamide, (Refs. 125,111,112,127,128) dimethylformamide,^{111,112,129} DMSO^{130,125} and propylene carbonate.^{125,72,13}

In a series of papers, H. L. Friedman and his co-workers estimated the enthalpies of transfer of ions from water to PC.^{72,131} The individual ionic enthalpies of transfer were estimated using the method of Latimer, Pitzer and Slansky.¹³² Ion associations in PC were checked by conductance measurements.⁷² Regularities and specific effects in enthalpies of

transfer of ions from water to PC, DMSO, FA and N-MF were discussed by Friedman.¹³³ The trend of the halide ions is the same in each case, while a varying trend of the alkali metal ions reflects differences in solvent basicity. The basicity of the solvent is suggested to be in the order $PC < FA < DMSO < N-MF$. The assumption that PC is a nearly ideal solvent for ions is discussed in light of the disagreement with the Born equation, although the agreement is better for PC than for water. A summary of the solvation enthalpies of various ions in water, PC and DMSO is presented by Krishnan and Friedman.¹³⁴ Again the large enthalpies of transfer from DMSO to PC are related to the difference in basicity of the two solvents. Solvation enthalpies of nonelectrolytes, mostly alcohols and hydrocarbons, were measured in water, PC and DMSO.¹³⁵ Enthalpies of transfer of various 1:1 electrolytes from PC to methanol and DMF are presented elsewhere.¹³⁶ Solvation enthalpies of hydrocarbons and normal alcohols in several highly polar solvents, including PC, are reported by Krishnan and Friedman.¹³⁷

The extensive work of M. Salomon on the thermodynamics of ion solvation in PC is presented here in more detail because of its direct relevance to the present work. The thermodynamics of LiCl and LiBr,⁹⁵ NaI,⁹⁶ LiI and KI⁹⁷ were measured by the emf method. The potentials of the cell-type: M/MX in $PC/TlX(s)/Tl(Hg)$ were measured, where M represents Li, Na and K, and X represents Cl^- , Br^- and I^- . In the case of the potassium system, potassium amalgam replaced the metallic potassium, and the data was corrected for the free energy of formation of the amalgam. The measured emf was converted to the emf of the cell M/MX in $PC/TlX(s)/Tl(s)$ using the data of Richards and Daniels¹³⁸ for the emf's

of the thallium amalgam cell $Tl/Tl^+/Tl(Hg)$. The standard potentials were obtained by extrapolation to infinite dilution following Guggenheim equation¹⁵⁰

$$-\ln \gamma_{\pm} = \frac{A m^{1/2}}{1+m^{1/2}} + 2 \beta m \quad (1-6)$$

The thermodynamic quantities ΔG° , ΔH° , and ΔS° for the cell reactions were calculated from the standard potentials and their temperature dependence. The results are summarized in Table 1-7. The molal activity coefficients for the alkali metal halides in PC were calculated using the extrapolated standard potentials. It should be mentioned here that Salomon made a mistake in the thallium amalgam corrections in his work with LiCl and LiBr in PC.⁹⁵ The corrections at 25°C for thallium amalgam compositions of 3.147 and 7.76%wt are 112.5 and 78.6 mV respectively, as is evident from the work of Daniels and Richards, and not 135.34 and 94.6 mV as reported by Salomon.⁹⁵ The results obtained on the other systems studied by Salomon cannot be checked, as detailed data is not available. Table 7-1 gives the corrected results. However, the uncorrected results are given (in parentheses), since there is a possibility that the amalgam compositions were in error rather than the corresponding emf corrections. The calculated free energies and enthalpies of solvation for various salts in PC are given by Salomon.¹³⁹

The main observations and conclusions from Salomon's emf work are the following:

1. The order in the series of standard potentials of the alkali metals in PC does not follow the order in aqueous solution. Potassium has a higher standard potential in PC than lithium, while sodium has

Table 1-7. Thermodynamic quantities for the general cell M/MX-PC/TlX, Tl at 25°C.

Cell	E° (volt)	-ΔG°	-ΔH°	-ΔS°
Li/LiCl-PC/TlCl, Tl	1.85080 (1.83480)	42.690 (42.312)	50.730 (50.354)	26.98 (26.98)
Li/LiBr-PC/TlBr, Tl	1.84223 (1.81939)	42.490 (41.962)	49.746 (49.156)	24.35 (24.35)
Li/LiI-PC/TlI, Tl	1.8452	42.55	50.01	25.03
Na/NaI-PC/TlI, Tl	1.6188	37.33	43.02	19.09
K/KI-PC/TlI, Tl	1.934	44.61	49.31	15.77

Taken from Salomon.^{95,96,97}

Units are based on molal scale. ΔG°, ΔH° are in Kcal/mole; ΔS° is in cal/mole °K.

Values in parentheses reported by Salomon⁹⁵ in error. (See text)

the lowest standard potential among the alkali metals.

2. Potassium was found to be reactive toward PC.

3. The potentials of the LiCl and LiBr cells tailed off the Guggenheim plots at low molalities. This phenomenon was observed by others in DMSO^{38,92} and in NMF.¹¹⁰ Symrl and Tobias³⁸ explained the deviations from the Guggenheim equation by the solubility of TlX in DMSO, which can cause concentration gradients across the cell, resulting in a lowering of the observed emf. Salomon⁹⁵ attempted to explain the observed deviations in PC as possible reactions between the solvent and the lithium electrode. The solubility products of TlCl and TlBr in PC are extremely low, $10^{-12.4}$ and $10^{-12.66}$, respectively, and cannot be responsible for large liquid junction potentials.

4. Anions are poorly solvated in PC; the solvation of anions increases from Cl^- to I^- . This behavior is opposite to that found in water.

5. LiCl and LiBr are associated in PC solutions. LiCl shows strong ion-pairing effects, as can be seen from the large negative constant in the Guggenheim equation. However, LiI, NaI and KI do not show any signs of ion association.

The thermodynamics of single ion solvation in PC and water is summarized by Salomon.¹³⁹ The free energies and enthalpies of solvation of individual ions were evaluated from the corresponding values of the salts, and by extrapolation (to infinite ionic radius) of the plot of the differences of cation and anion conventional energies vs. $1/r$. This method of splitting the solvation energies into individual ionic contributions is advantageous, according to Salomon, over the traditional method of Latimer, Pitzer and Slansky,¹³² which introduces a single adjusting parameter to the Born equation. The individual free energies and enthalpies of solvation are of fundamental importance, since they represent the ion-solvent interactions. Table 1-8 presents selected free energies and enthalpies of solvation of individual ions in PC and water, as well as the free energies and enthalpies of transfer from water to PC.

Cogley, Butler and Grunwald¹⁴⁰ studied the selective solvation of ions by water in PC. The equilibrium constants for the association of water with individual ions were obtained under a relatively mild set of extrathermodynamic assumptions, from protic magnetic resonance (chemical shift) measurements. The affinity of water at low concentrations in

Table 1-8. Energetics of single-ion solvation in water and PC at 25°C.

Ion	PC		H ₂ O		ΔG_t°	ΔH_t°
	$-\Delta G_{\text{solv.}}^\circ$	$-\Delta H_{\text{solv.}}^\circ$	$-\Delta G_{\text{solv.}}^\circ$	$-\Delta H_{\text{solv.}}^\circ$		
Li ⁺	95.0	106.2	97.8	107.6	+2.8	+1.4
Na ⁺	71.9	80.5	72.4	80.2	+0.5	-0.3
K ⁺	56.6	64.4	54.9	60.2	-1.7	-4.2
Rb ⁺	54.5	58.1	50.7	53.1	-3.8	-5.0
Cs ⁺	52.7	51.8	46.7	46.1	-6.0	-5.7
Ag ⁺	85.4	96.3	87.9	96.0	+2.5	-0.3
Tl ⁺	56.7	----	56.9	62.0	+0.2	----
Cl ⁻	88.2	101.4	100.3	106.0	+12.1	+4.6
Br ⁻	84.0	96.4	94.2	101.6	+10.2	+5.2
I ⁻	78.0	91.2	85.7	88.8	+7.7	-2.4
ClO ₄ ⁻	----	59.8	----	56.2	---	-3.6

Taken from Salomon.¹³⁹ Units are in Kcal/mole.

PC for alkali metal cations correlated well with the free energy of transfer of these ions from PC to bulk water.

Parker¹⁴¹ gives an extensive review on the protic-dipolar aprotic solvent effects on rates of organic bimolecular reactions. The observations that dipolar aprotic solvents are excellent media for many organic reactions are explained by positive free energies of transfer of anions. The review contains extensive and very useful information on the solvation of ions in aprotic solvents and on the solvent activity coefficients (medium effects).

On the general subject of solvation of individual ions in nonaqueous solvents, the reader is referred to the view of Popovych.¹⁴² The commonly used extrathermodynamic assumptions were critically reviewed, and the

establishment of universal solvent-independent scales for ion activities and electrode potentials was discussed. The review by Butler⁸ on reference electrodes in aprotic solvents contains very useful data concerning standard potentials, activity coefficients and other thermodynamic data. This review contains an excellent list of references.

1.10. Double-Layer Capacity Measurements in PC

Preliminary measurements by Payne¹⁴³ on the capacity of the electrical double-layer of a mercury electrode in 0.1 M KPF_6 in PC and related solvents, revealed the presence of a hump in the capacity-potential curve. These results show clearly that the capacity hump is not a unique property of aqueous solutions, as was widely thought for many years. Furthermore, the hump can occur also in solvents of only moderately high dielectric constants, and is not restricted only to high dielectric constant solvents. The hump might be due to a minimum in the orientation polarization of the adsorbed solvent dipoles occurring at the potential where their preferred orientation is reversed by the external field. Since the hump in PC and other aprotic solvents occurs on the anodic side of the electrocapillary maximum (ecm), the preferred orientation of the solvent dipole should be positive and toward the metal. However, there is a possibility that the hump is related to the adsorption of anions, since it occurs on the positive side of the point of zero charge (ecm). To illuminate this point, Biegler and Parsons¹⁰⁴ made further measurements on the capacitance of mercury electrode in NaClO_4 -PC solutions. The diffusion layer minimum is visible at concentrations as high as 0.1 M, and this observation suggests that anion adsorption is very weak. The agreement between the experimental and the calculated results under the assumption of the absence of specific

adsorption, proved that the specific adsorption of anions at the lower positive charges is low. The hump is again suggested to be the result of solvent reorientation rather than anion adsorption. On the negative side of the point of zero charge the capacity becomes almost independent of NaClO_4 concentration. The zero charge potential for 0.1 M KPF_6 in PC is -0.33 volts vs. nce. The electrical double layer in nonaqueous solutions was reviewed recently by Payne.¹⁴⁴

II. EXPERIMENTAL

The experimental studies of the electrochemical behavior of the alkali metals in propylene carbonate are divided into five categories:

1. Solubility and deposition measurements of the alkali metals from their salt solutions in PC.
2. Measurement of the potentials of the alkali metals using a cell without transference.
3. The electrode kinetics of the alkali metals and their amalgams in alkali metal chlorides in AlCl_3 (1 m)-PC solutions.
4. Conductance measurements of the alkali metal chlorides in AlCl_3 (1 m)-PC solutions.
5. Density measurements of the alkali metal chlorides in AlCl_3 (1 m)-PC solutions.

2.1. General

2.1-1. Solvent Purification

Propylene carbonate (Jefferson Chemical Company, Houston, Texas) was distilled at 0.5 mm Hg by means of a commercially available distillation column (Semi-CAL series 3650, Podbielniak, Franklin Park, Illinois) packed with stainless steel helices. The reflux ratio was 60 to 100 and the head temperature 65°C. The first 10% and the last 25% of the solvent were discarded. The receiver system of the column was rebuilt with glass drip tips and needle valve stopcocks (Delmar Scientific Laboratories, Inc., Maywood, Illinois) equipped with teflon "o" rings. Argon gas was bubbled through the solvent during distillation. The collection vessel was not detached from the column; the solvent was discharged directly into the dispensing vessel. The transfer was done under argon atmosphere. The

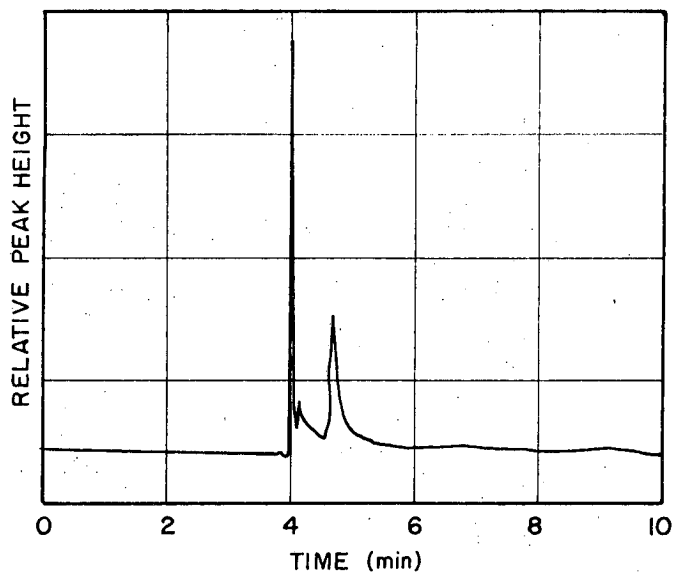
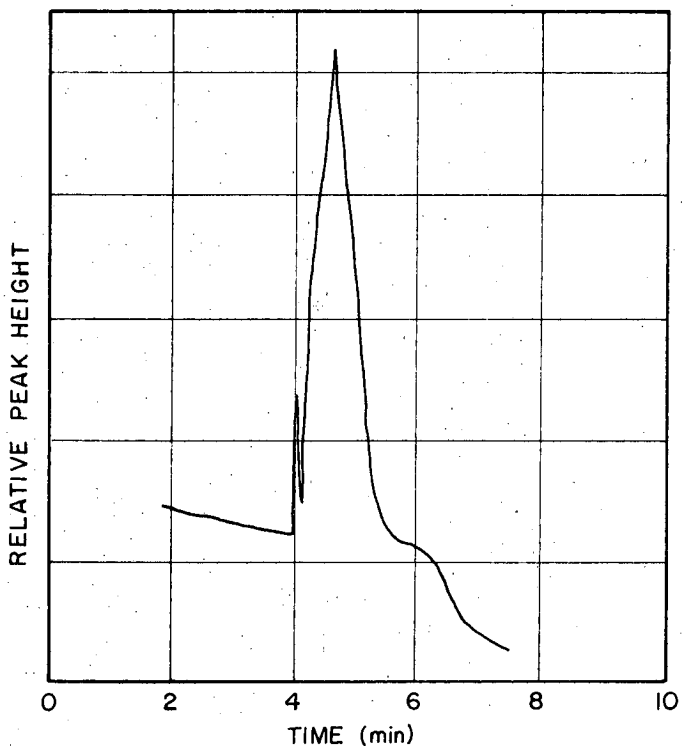


Fig. 2-1. Distilled PC after one month of storage in the glove box. The peak corresponds to about 10 ppm water. The propylene oxide peak disappeared.



XBL 728-1450

Fig. 2-2. Distilled PC after deliberate addition of 200 ppm H₂O.

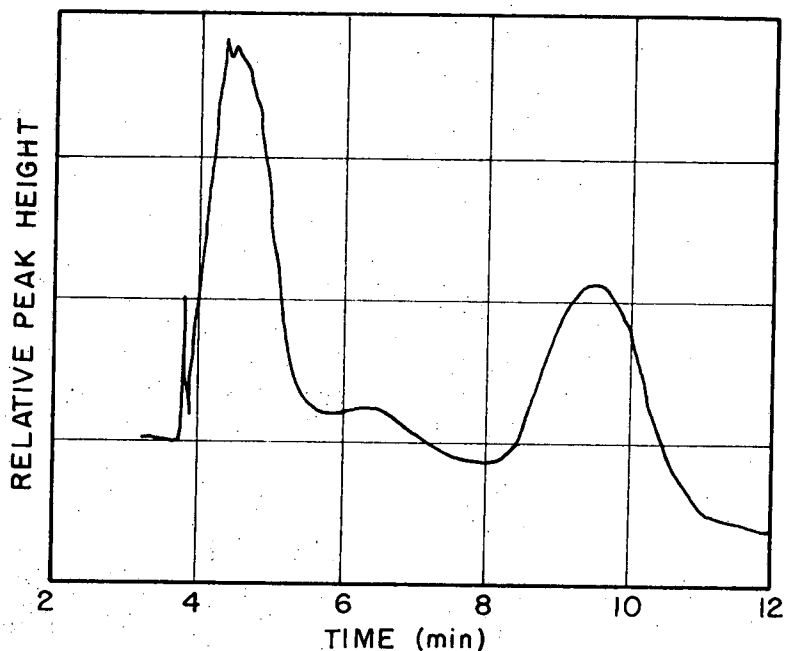
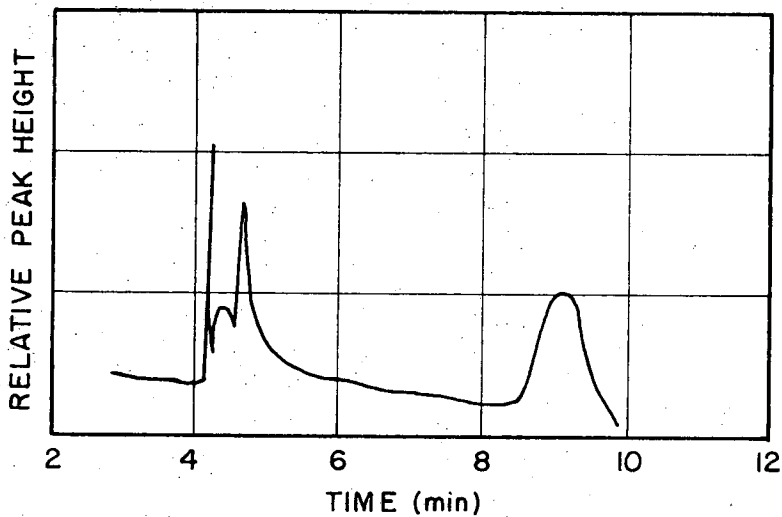


Fig. 2-3. "As received" PC after a treatment with Linde 5A molecular sieves. The peak on the left-H₂, on the right-PC.



XBL 728-1448

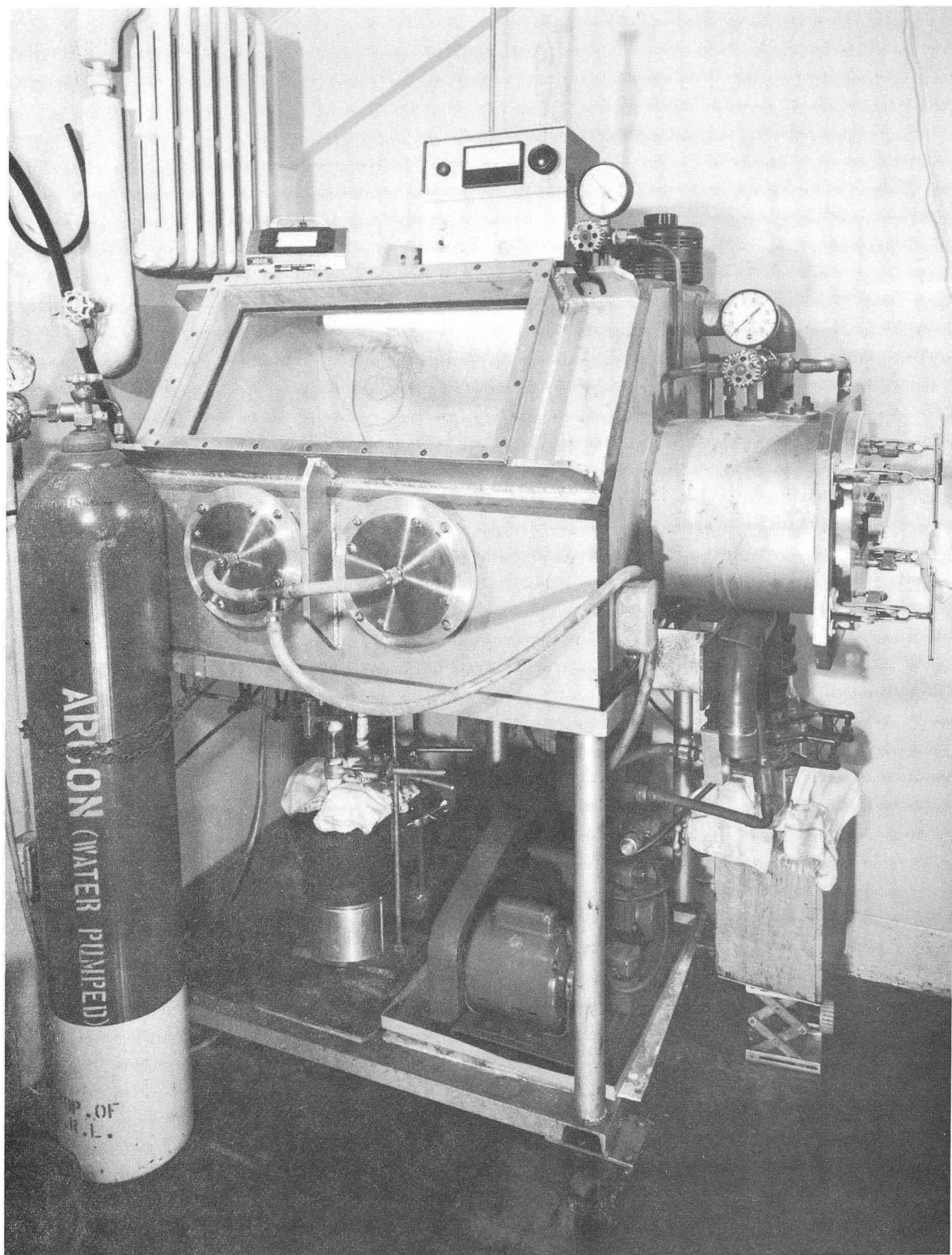
Fig. 2-4. Distilled PC after deliberate addition of 240 ppm propylene oxide.

dispensing vessel was evacuated on the vacuum line to approximately 50 μ Hg, closed tightly and transferred into the glove box.

The "as received" solvent contains a few tenths of a percent of the following impurities: water, propylene glycol, propion aldehyde, propylene oxide.¹⁴⁵ Gas chromatographic analysis of the product performed in this laboratory showed the water content to be always below 50 ppm. Typical gas chromatographic analysis is shown in Fig. 2-1. The presence of a second impurity at a very low concentration was identified as propylene oxide, and its concentration was estimated below 1 ppm. Figures 2-2 and 2-4 show gas chromatograms of samples which were deliberately contaminated with water and propylene oxide, respectively. Figure 2-3 shows that molecular sieves are ineffective in removing propylene oxide from PC.

2.1-2. Glove Box Operation

The vacuum glove box was a Lawrence Livermore Laboratory design. It was equipped (see Fig. 2-5) with an antechamber, glove ports for one operator and an oil vacuum pump capable of evacuating the box to a few microns pressure. It was maintained under dry and oxygen-free argon. The atmosphere of the box could be replaced by evacuating it and refilling it with argon. The argon was passed through two magnesium perchlorate columns in order to remove moisture, and then through two columns of BTS catalyst to remove oxygen. The $Mg(ClO_4)_2$ was replaced periodically, and the BTS catalyst was regenerated periodically by reducing the CuO by a stream of hydrogen accompanied by heating. The water content of the inlet argon stream was measured by Moisture Monitor (Consolidated Electrodynamics Corporation, Model 26-303 ME) and was found to be below 1 ppm. The box's argon atmosphere was replaced once a week. Alkali metals exposed inside



BBC 679-5192

Fig. 2-5. General view of the glove box.

the glove box kept shining surfaces for at least a day. Figure 2-5 shows a general view of the glove box. All chemicals, solvents and solutions were kept covered and closed inside the box. During the time the box was not used and at nights, the glove ports were tightened and evacuated from the outside to minimize diffusion of moisture and air through the gloves. The gloves were made of neoprene. A small balance was used inside the glove box to prepare solutions and amalgams.

2.2. Solubility and Deposition Studies

2.2-1. Solubilities

The investigation of the feasibility of the deposition of the alkali metals from PC started with a search for a common anion which would permit high solubilities for all the alkali metals in PC. Solubility measurements revealed that all the chlorides, except LiCl, are quite insoluble. Of the bromides, only LiBr and NaBr are soluble. The iodides of rubidium and cesium are insoluble. The perchlorate series revealed that only lithium and sodium perchlorate are highly soluble. Of the tetrafluoroborates only LiBF₄ and NaBF₄ are soluble. From the hexafluorophosphate series, LiPF₆, NaPF₆ and KPF₆ are soluble, while RbPF₆ and CsPF₆ are practically insoluble.

The only common anion which yielded high solubilities for the entire alkali metal series was the chloride-aluminum trichloride complex:



where M is any alkali metal. It was found that in the presence of AlCl₃, which itself is highly soluble in PC (above 3 mole/lit.), the solubilities of the alkali metal chlorides rise to 1:1 ratio, except for NaCl. The solubility of NaCl is approximately 0.5 m in the presence of AlCl₃ (1 m) in PC (1:2 ratio).

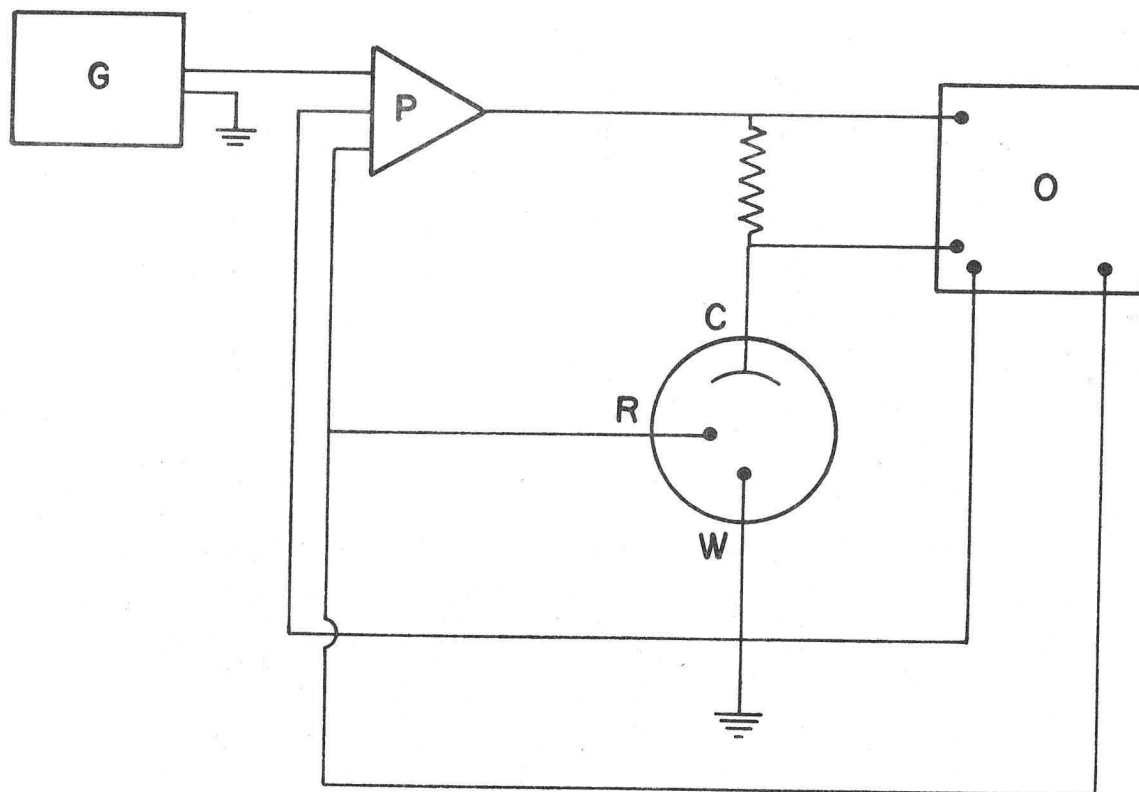
2.2-2. Electrodeposition of the Alkali Metals

Electrodeposition experiments were conducted in an H type cell, the two compartments being separated by a fritted glass. The anode and the cathode were made of platinum foils attached to platinum wires and were immersed in the solution. The area of the electrodes was approximately 1 cm^2 . Constant current of 1 mA was applied and the cathode was observed for the nature of the deposit. The solution was stirred during the experiment by a small magnetic stirrer.

The experiments were qualitative in nature and were conducted in order to screen the possible electrolytes. All the electrodeposition experiments were conducted inside the glove box under dry argon atmosphere. A constant current power supply (Model C 612 Electronic Measurements) was used and the applied potential was measured by an Electrometer (Keithly Model 60i).

2.2-3. Cyclic Voltammetry Measurements

The reversible behavior of the alkali metals and their amalgams in PC solutions was tested by the cyclic voltammetry technique, in which the potential between the working and the reference electrodes was scanned linearly around the equilibrium potential, both in the cathodic and anodic directions. The solutions were stirred during the experiments by a small magnetic stirrer. A slow sweep technique was used, for which the non-faradaic component of the current was very small. Because the sweep rate was in the slow range of the order of a few millivolts per second, and the solution was stirred, the technique is actually a polarization experiment in which the potential is scanned linearly and slowly instead of being increased manually, point by point. A block diagram of the



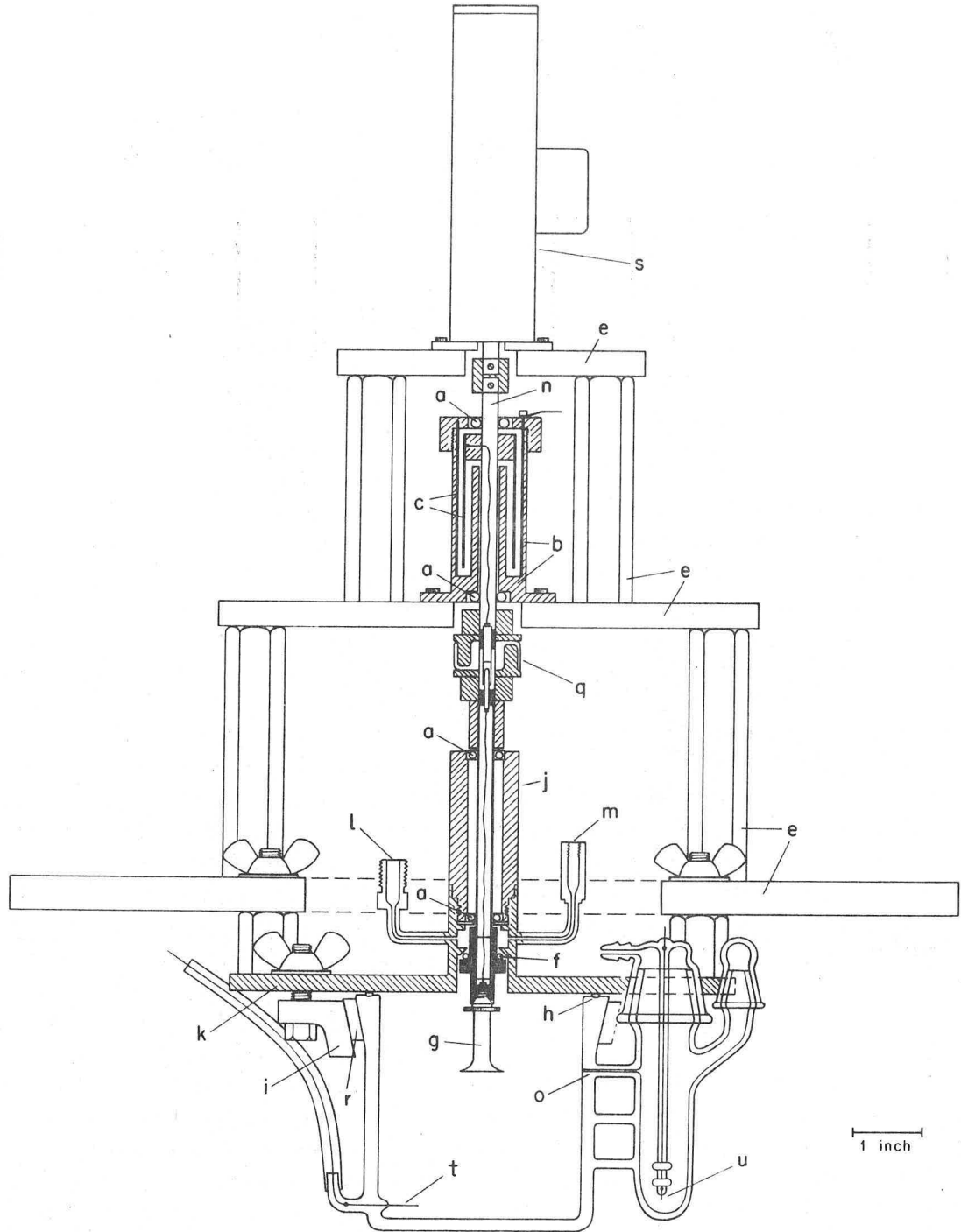
XBL 725- 6288

Fig. 2-6. Apparatus for cyclic linear voltammetry.
C -- counter electrode
G -- wave form generator
O -- oscilloscope, or x-y recorder
P -- potnetiostat
R -- reference electrode
W -- working electrode

experimental apparatus is shown in Fig. 2-6. Triangular potential waveform was generated by a Waveform Generator, Exact Model 100, connected to a Wenking Potentiostat. The current was recorded versus the scanned potential on an oscilloscope (Tektronix Oscilloscope) or on a fast X-Y recorder (Autocraft X-Y Recorder, Mosley). The working and the reference electrodes were identical in most cases, except when the working electrode was made of a clean platinum foil.

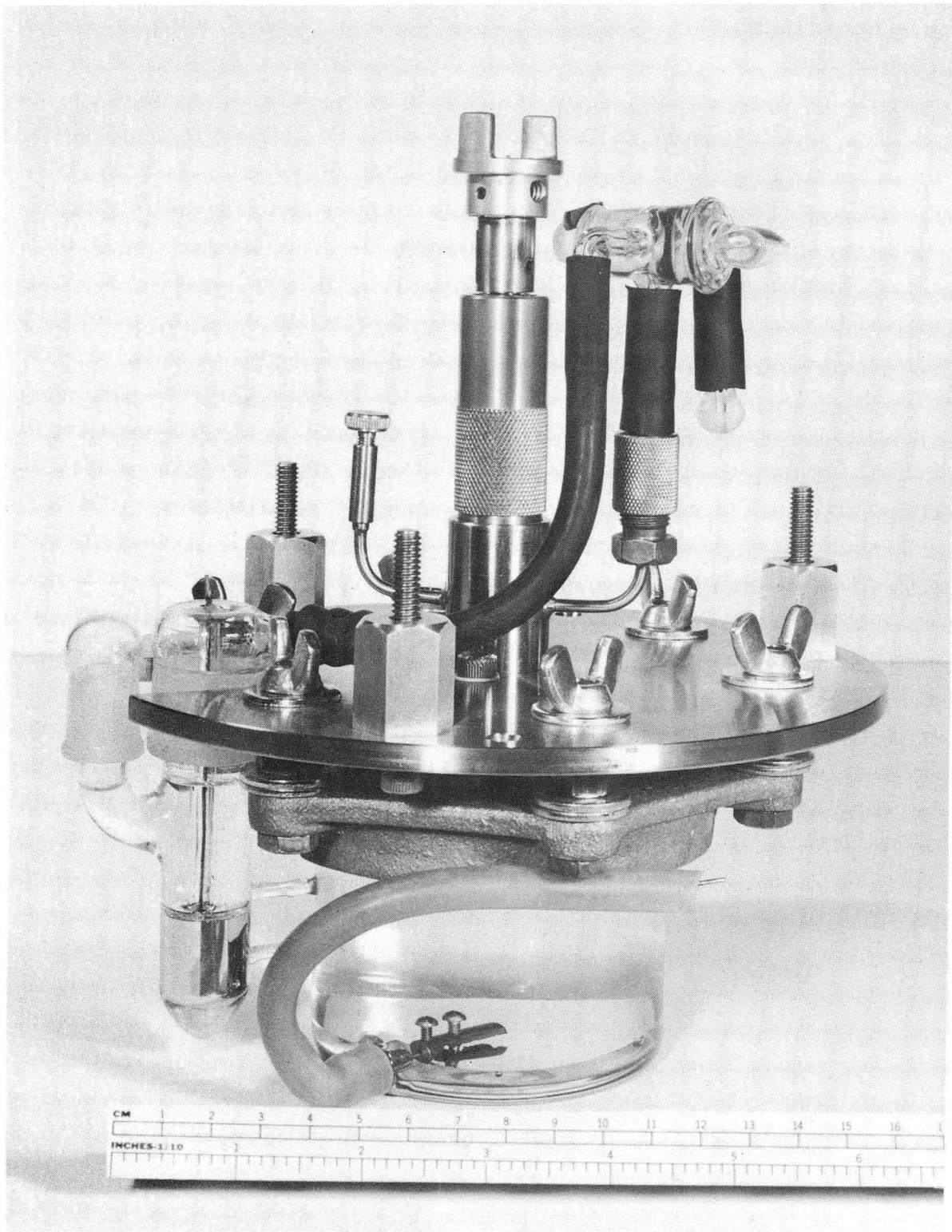
2.2-4. Electrodeposition of the Alkali metals in a Rotating Disk System

The electrodeposition of the alkali metals at relatively high current densities was investigated using a rotating disk system, especially designed for inert atmosphere conditions.¹⁴⁶ The rotating disk system is shown in Fig. 2-7 and the general view of the cell is shown in Fig. 2-8. The disk electrode is shown in Fig. 2-9. The disks were made of teflon, and the central electrodes were made of platinum, stainless steel or nickel. The area of the electrode was about 0.01 cm^2 , and the rotation speed varied from 0 to 3600 rpm. The electrodeposition experiments were conducted under a stream of dry argon, with the rotating disk serving as the cathode, and an amalgam of the particular alkali metal serving as the anode. A reference electrode was placed in a separate cell connected to the main cell by a small capillary. The tip of the capillary was in the plane of the disk, at 2.4 cm from the center. The reference electrode was made of the corresponding alkali metal, or an amalgam of identical composition to the counter electrode. The measurements were performed by a Wenking Potentiostat, where constant potentials were applied between the working and the reference electrode, and the resulting currents were read from the potentiostat dial. The currents were varied



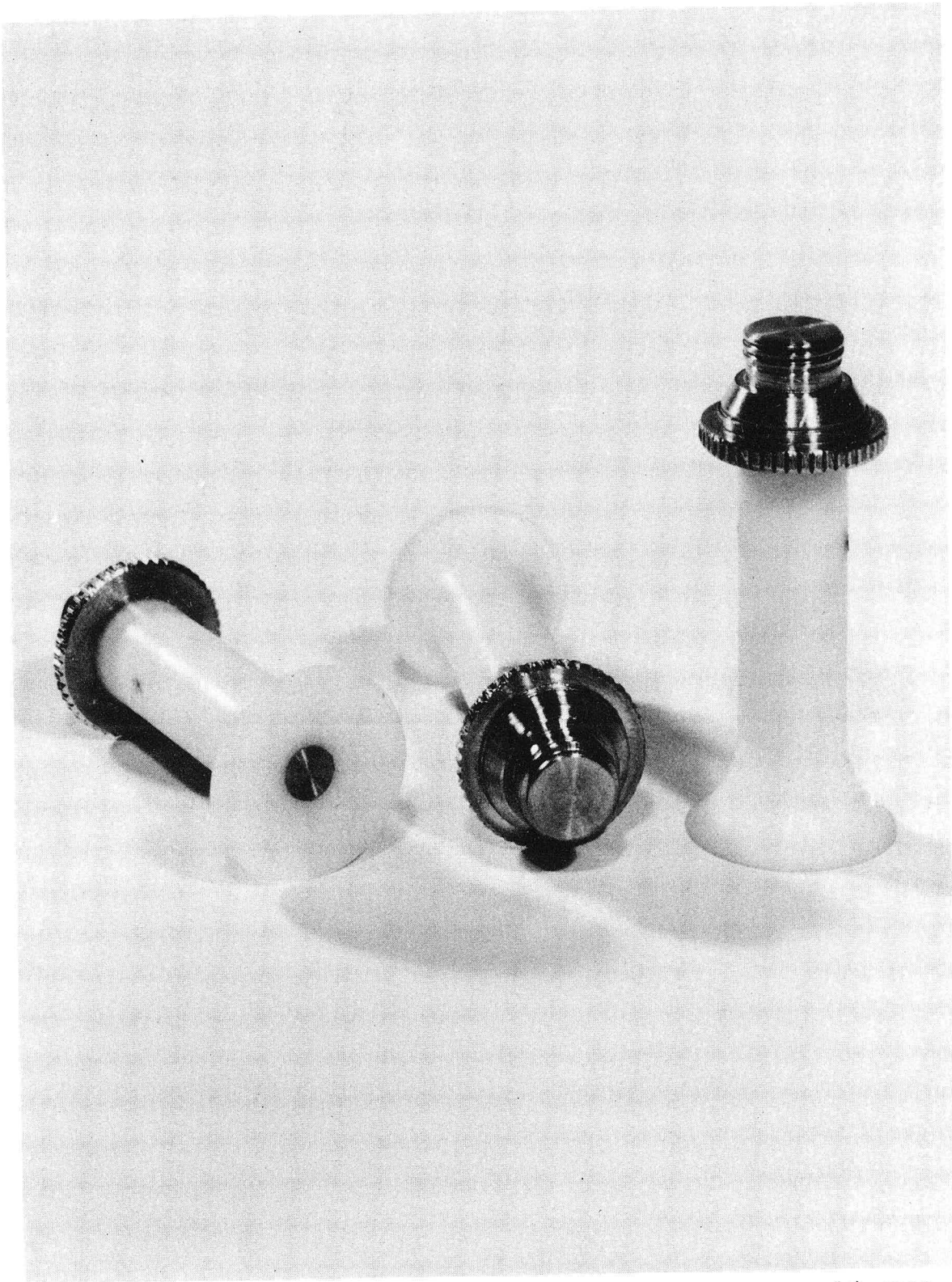
XBL6712-5883

Fig. 2-7. Rotating disk assembly.



BBC 679-5190

Fig. 2-8. The rotating disk cell.



XBB 674-5193

Fig. 2-9. Disk electrodes.

up to 5 mA, which corresponds to current density of 50 mA/cm^2 , a practical condition for a commercial electrolysis process. The ohmic drop was excluded from the total overpotential by a current interrupter technique, where the immediate drop in the potential was attributed to the ohmic resistance of the solution between the working electrode and the tip of the reference electrode's capillary. The pulse technique is described in detail in Section 2.4-1. The ohmic drop was calculated also according to the method of Newman and Hsueh^{147,148} using experimentally determined values of the specific conductivities of the solutions. When the Luggin capillary is located in the plane of the disk, the resistance of the solution between the working electrode and the Luggin capillary can be expressed as

$$R = \frac{\tan^{-1} \lambda_o}{2 r_o \kappa} \quad (2-2)$$

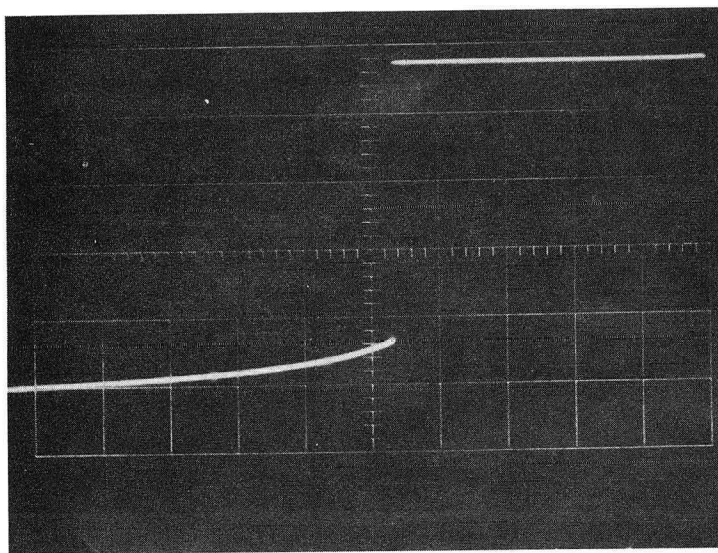
where

$$\lambda_o = (r/r_o - 1)^{1/2} \text{ at } z = 0, \text{ and} \quad (2-3)$$

r is the radial distance to the Luggin capillary, and r_o is the radius of the disk. In the present case, $r = 2.4 \text{ cm}$, $r_o = 0.33 \text{ cm}$ and the ohmic resistance as a function of the solution conductivity is given by:

$$R = 1.8034/\kappa \text{ ohm} \quad (2-4)$$

The ohmic resistances were calculated for each particular solution, and were found to be in good agreement with the IR drops obtained by pulse technique. The specific conductivities of the solutions of the alkali metal chlorides in $\text{AlCl}_3\text{-PC}$ are in the order of $6 \times 10^{-3} \text{ ohm}^{-1} \text{ cm}^{-1}$. Substituting this value in Eq. (2-4) gives resistance in the order of 300 ohm, which is the order of magnitude of the resistance obtained by the pulse



XBB 728-4115

Fig. 2-10. IR drop determination in the rotating disk cell using a current interrupter technique. Deposition of Li on a stainless steel disk electrode from LiAlCl_4 (1m)-PC solution at 25°C .

$I = 0.75 \text{ mA}$

Vertical scale: 50 mV/cm. Horizontal scale: 1 msec/cm.

Calculated ohmic resistance: $R = 280 \text{ ohm}$.

technique. The general agreement between calculated and experimentally obtained ohmic drop indicates that the resistance of the electrodeposited metals was quite low. Typical oscilloscope trace of the potential drop during a current interruption for the case of electroreduction of Li from 1.0 m LiAlCl_4 PC solution is shown in Fig. 2-10. The cathode in this case was fabricated of stainless steel.

2.3. Potential Measurements

2.3-1. Electrolytic Solutions

All solutions of the alkali metal chlorides in AlCl_3 (1 m)-PC were prepared by weighing the salts and the solvent inside the glove box. The 1.0 molal solutions of AlCl_3 in PC were made by adding the salt very slowly to the solvent, since the heat of solution is very high. The AlCl_3 in PC solutions were prepared inside the box under argon and were cooled with chloroform-carbon tetrachloride-dry ice bath mixture. Careless addition of AlCl_3 to PC resulted in a brown solution; this occurred particularly when the salt was not a fine powder, but rather in small granules, which upon addition to PC resulted in local heating and darkening of the solution.

The alkali metal chlorides were dried inside a vacuum oven (Hotpack, Philadelphia) at 200°C and approximately 50μ Hg for at least 24 hours. The amounts needed for the specific molalities were calculated each time from the weights of the solvent. Stirring for a few hours was required in order to achieve complete dissolution of the alkali metal chlorides. The final solutions were treated with molecular sieves (Linde 4A) in order to remove traces of water introduced by the salts. The molecular sieves were treated before use by heating (300°C), high vacuum and several

flashes with argon. This procedure was found effective in further removing traces of water and therefore increased the stability of the alkali metals during the potential measurements.

2.3-2. Reference Electrode

After the alkali metal chlorides in AlCl_3 (1 m)-PC solutions were selected as the most promising systems, a search began for a suitable reference electrode of the second kind which would be sensitive to chloride ion.

The most widely used nonaqueous reference electrode is based on the Ag/Ag^+ couple. Unfortunately, the reference electrode of the second kind Ag/AgCl cannot be used in PC because of the much higher stability of the complexes of silver with chloride and other anions.

The most promising reference electrodes of the second kind are those based on thallium (I) salts.³ Thallous chloride was found to be only slightly soluble in PC and does not dissolve in excess of chloride. Earlier investigations in this laboratory revealed the excellent nature of thallium amalgam-thallos halide electrodes in PC⁶ and DMSO.^{7,8} This reference electrode has been applied to the cell $\text{Li}/\text{LiX}(\text{DMSO})/\text{TlX}(\text{s})/\text{Tl}(\text{Hg})$ in order to determine the standard potential of the cell and the activity coefficients of LiX in DMSO. Salomon^{11,12,13} used this reference electrode to measure standard potentials and activity coefficients of alkali metal halides in PC. $\text{Tl}(\text{Hg})/\text{TlCl}$ electrode was found to be stable and reversible in DMF.⁹⁸

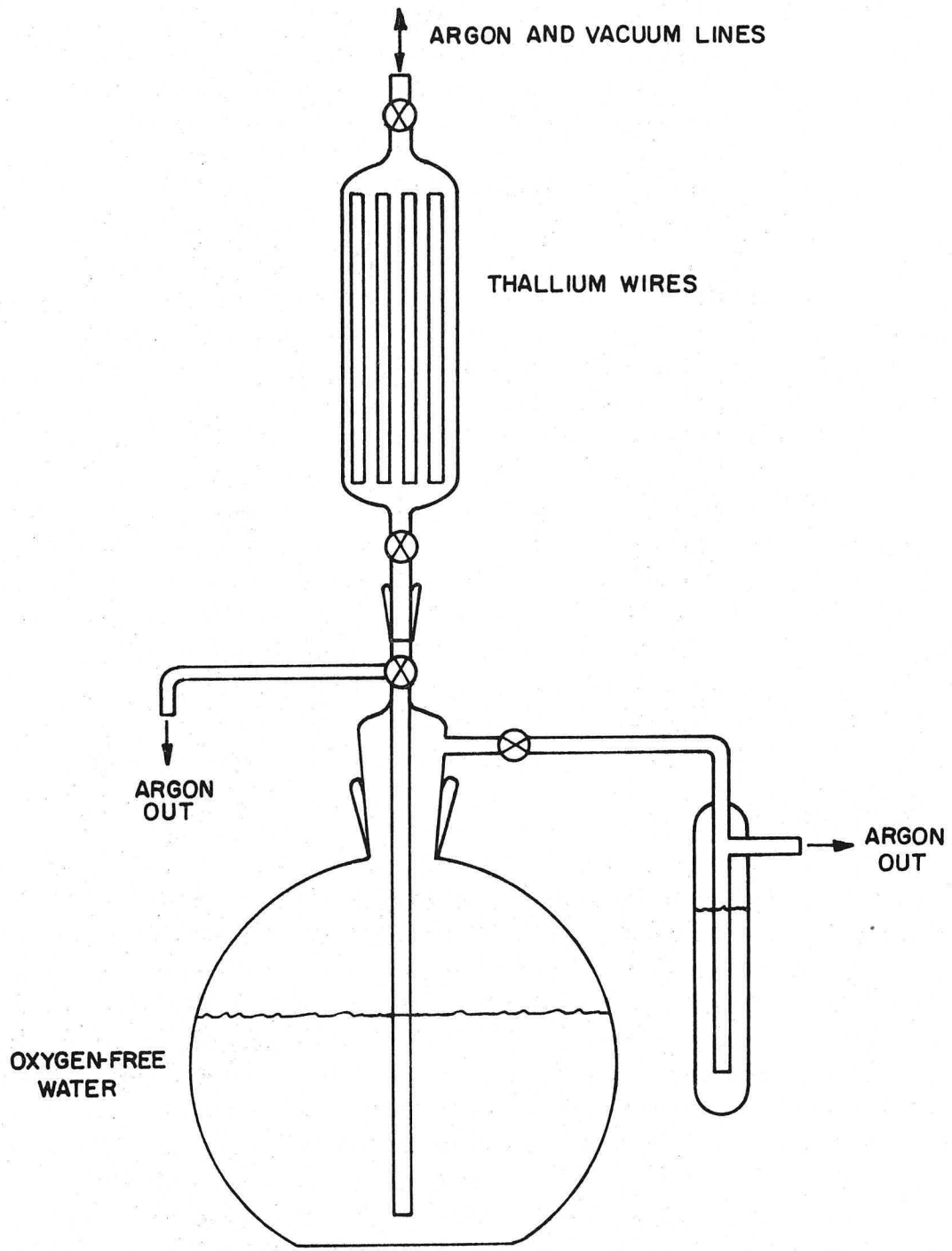
The performance of $\text{Tl}(\text{Hg})/\text{TlCl}$ electrode in PC was reversible with good stability. The solubility product of TlCl in PC is $K_{\text{sp}} = 10^{-12.43}$, extremely low even when compared with other aprotic solvents (e.g., for DMSO $K_{\text{sp}} = 10^{-6.26}$).⁹

Having established that the alkali metal halides AlCl_3 (1 m)-PC combination was stable toward the alkali metals, and that the reference electrode Tl(Hg)/TlCl showed reversible behavior and very small bias potentials (always below 1 mV), emf measurements began on the behavior of the alkali metals in their chloride solutions in AlCl_3 (1 m)-PC. The experiments consisted of measuring the potential between the alkali metal and the reference electrode in various alkali metal chloride concentrations in AlCl_3 (1 m)-PC solutions. Measurements were made at 25° and 35°C .

2.3-3. Preparation of Tl(Hg)/TlCl Reference Electrode

The thallium wire used for preparation of the amalgam was 99.999% pure (United Mineral and Chemical Corp., New York). The oxide coating on the metal was removed by successive washing with oxygen-free distilled water under argon atmosphere. The washing apparatus is shown in Fig. 2-11. The rinsing and drying of the thallium wires was performed by alternately raising and lowering the water level. The shining Tl was transferred directly into the glove box without exposure to air. The resulting silvery white metal dissolved readily in mercury. The amalgam concentration was prepared by weight. The thallium amalgam was then placed inside the electrode cups containing about 5 ml of the amalgam, exposing around 1 cm^2 of shiny surface (see Fig. 2-12). The amalgam surface was then covered with a thin adherent layer of fine TlCl . The electrode was gently shaken in order to get a complete and uniform coverage of the surface.

The electrical connection to the amalgam was through a platinum lead which was connected to a tungsten wire. All the connections and leads were overlaid with uranium glass for a vacuum tight seal. The platinum



XBL 725-6266

Fig. 2-11. Apparatus for washing thallium oxide off of thallium wires.

tip was immersed well beneath the surface of the amalgam to prevent creeping of the solvent between the amalgam and the glass. The mercury used was triple distilled.

2.3-4. Preparation of the Alkali Metal Electrodes

The preparation of rubidium and cesium electrodes was different from the rest of the alkali metals, since they are liquids at slightly above room temperature. Lithium, sodium and potassium electrodes were all prepared in a similar way. Wires of the metals were cut inside the glove box, the oxide layer was removed by a clean blade and the wires were rinsed with the solvent. The wires were connected to the alkali metal electrode holder (s-e Fig. 2-12) by a stainless steel connector. Electrodes which did not keep a bright surface were discarded. The connectors were always kept above the solution level.

The electrodes for Rb and Cs were prepared by heating the capsules of these metals to above their melting points 37° and 28.5° for Rb and Cs, respectively) and pouring the liquid metal into heated cup electrodes similar to the electrodes used as references. The cups were preheated to prevent solidifying of the metal on the edges of the cup. In this way the area exposed to the solution was calculated from the dimensions of the cup. The sources of the alkali metals are listed in Appendix III.

2.3-5. Preparation of the Alkali Metal Amalgam Electrodes

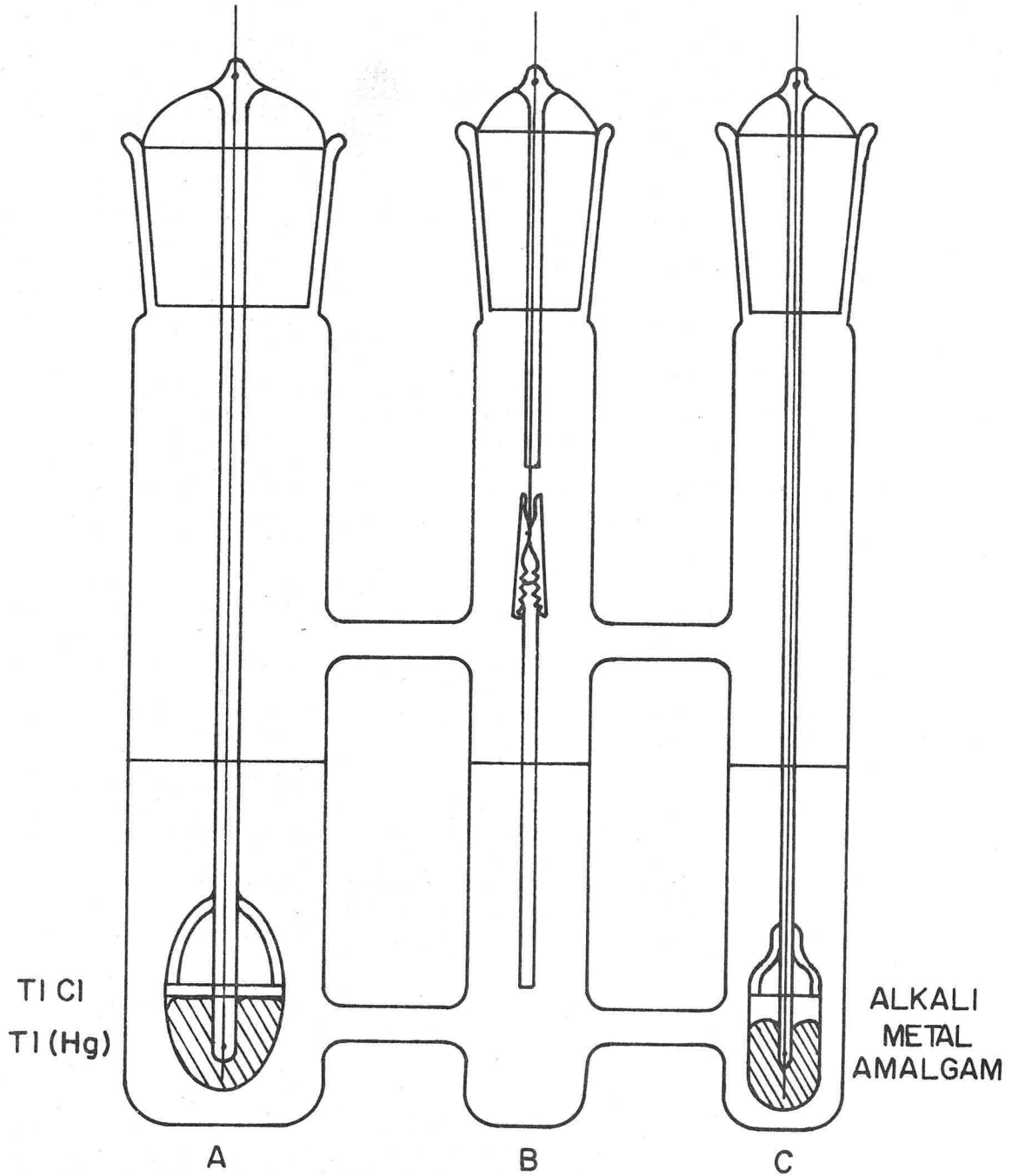
The alkali metal amalgams were prepared by combining weighed quantities of the appropriate alkali metal and mercury. The mercury was triple distilled, and the sources of the alkali metals are listed in Appendix III. The amalgams were washed with PC and filtered directly into the cup electrode through a capillary glass tube. In some cases, the amalgam

compositions had to be adjusted to specific values in order to match the only data available in the literature. This was done by diluting the amalgams to the specified concentrations. The platinum leads were kept well below the surface of the amalgam to prevent possible decomposition of the amalgam and consequent errors in the measured potentials.

2.3-6. Cell for Potential Measurements

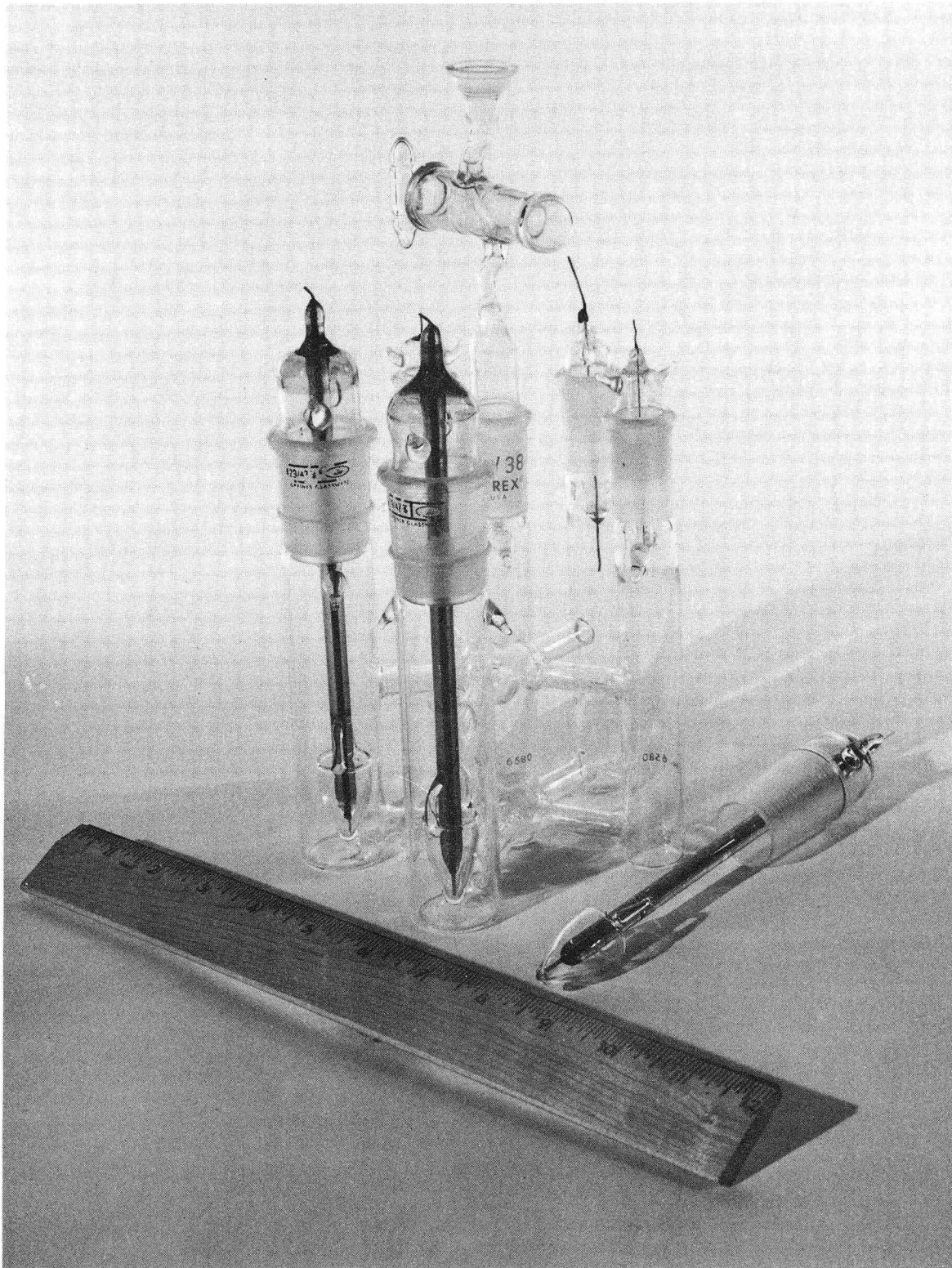
The cell used for potential measurements, shown in Fig. 2-13, was developed earlier by Smyrl.⁹² In this six compartment cell, each compartment is connected to the central one by a narrow pipe. The cup electrode for the thallium amalgam-thallos chloride reference electrode is shown in Fig. 2-12. A platinum lead projects into the cup and is connected to a tungsten wire which is in turn connected to a platinum lead on the exterior of the assembly. The tungsten and the connections to the platinum are overlaid with uranium glass for a vacuum tight seal. Only platinum is exposed to the amalgam in the cup and it is immersed well beneath the surface of the amalgam to prevent contact with creeping solution. The electrode holder for the solid alkali metals (Li, Na, K) is shown in Fig. 2-12. The alkali metal wire was attached to the platinum wire by a stainless steel connector. Alkali metal amalgam electrodes were prepared by pouring the amalgams into cup electrodes similar to those used for the reference electrodes.

Rubidium and cesium electrodes were prepared by heating the capsules in which these metals had been received, and the electrode's cups, and then pouring the liquid metals into the cups, well above the platinum leads. Lithium was obtained as 1/8 in. wire and was rinsed with the pure solvent. Sodium and potassium were obtained in the form of ribbons and



XBL725-6268

Fig. 2-12. Six-compartment cell for potential measurements.
(Only three compartments are shown.)
A - Reference electrode
B - Alkali metal electrode
C - Alkali metal amalgam electrode



IM-2453

Fig. 2-13. Six-compartment cell for potential measurements.

were extruded through a stainless steel extruder of 1.13 cm diameter, and then were washed with the pure solvent. All the alkali metal electrodes kept their shining surfaces during the measurements. Electrodes which turned grey or black after being immersed in the solution, consequently giving erratic potentials, were discarded.

The arrangement of the electrodes was the following: For every measurement there were two reference electrodes, two alkali metal electrodes and two alkali metal amalgam electrodes of identical composition. The cell, the electrode holders and the cup electrode, beside all volumetric flasks and glassware, were cleaned prior to each experiment by concentrated nitric acid and were rinsed several times with distilled water. Periodically the cells were cleaned with concentrated sodium hydroxide, dilute sulfuric acid and distilled water. Occasionally the cells and the cup electrodes were cleaned with an ultrasonic vibrator to remove solids from the glass. All glassware was dried in a vacuum oven at 50 microns and 200°C for at least 24 hours and then transferred quickly into the glove box.

2.3-7. Assembly of Cell

The six compartment cell was filled with approximately 100 cc solution of a specific concentration of the alkali metal chloride in AlCl_3 (1 m)-PC. Thallium amalgam was dispensed into the cup of each of the two reference electrodes, a small amount of TlCl was spread on the surface, the ground joints were lubricated, and the reference electrodes were inserted into the cell. The alkali metal amalgam was then dispensed into the cups of each of the two cup electrodes and was inserted into the cell. The alkali metal wire was cut, connected to the stainless steel holders and inserted

into the cell. The cell was then closed and removed from the glove box. The cell was next suspended in a constant temperature water bath for potentiometric and kinetic measurements. The measurements were done at 25°C and 35°C.

The water baths were thermostated at 25° and 35°C to $\pm 0.01^\circ\text{C}$. The baths were agitated by circulating pumps and mechanical stirrers. The bath temperature was measured with Beckmann differential thermometers which had been calibrated against National Bureau of Standards thermometers. The thermostats were Sargent Thermonitor, Model S, E. H. Sargent Co., Chicago, Illinois, and Resistotrol, Shell Development Design, Hallikainen Instruments, Berkeley, California.

2.3-8. Cell Potential Measurements

Measurements of the cell potentials were taken with a John Fluke Model 887--A differential voltmeter (accuracy ± 0.005 mV) which was calibrated against an Eppley Laboratory, low temperature coefficient standard cell.

The measurements began 15 minutes after the suspension of the cell in the bath. Measurements included:

(a) Cell potentials between the alkali metal electrodes and the reference electrodes.

(b) Cell potentials between the alkali metal amalgam electrodes and the reference electrodes.

(c) Potentials between the alkali metals and their amalgams.

(d) Bias potentials between the two alkali metal electrodes, the two alkali metal amalgam electrodes and the two Tl(Hg)/TlCl reference electrodes

The potential measurements were repeated each 30 minutes for the first

few hours and then were recorded several times each day for at least one week. The cell was then transferred to the 35°C bath and identical measurements were taken. The cell then was transferred back to the 25°C bath and the first series repeated.

Micropolarization measurements were conducted during the potential measurement period. The alkali metal electrodes were polarized in both cathodic and anodic directions and the reversibility of the electrodes was checked.

2.4. Electrode Kinetics Measurements

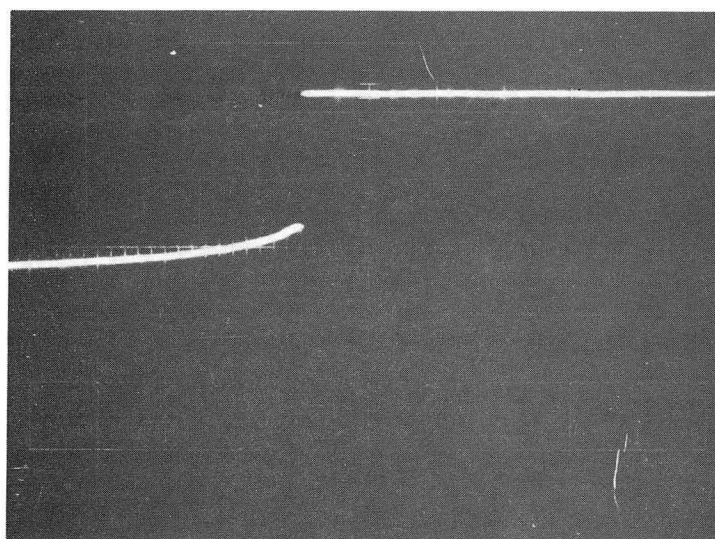
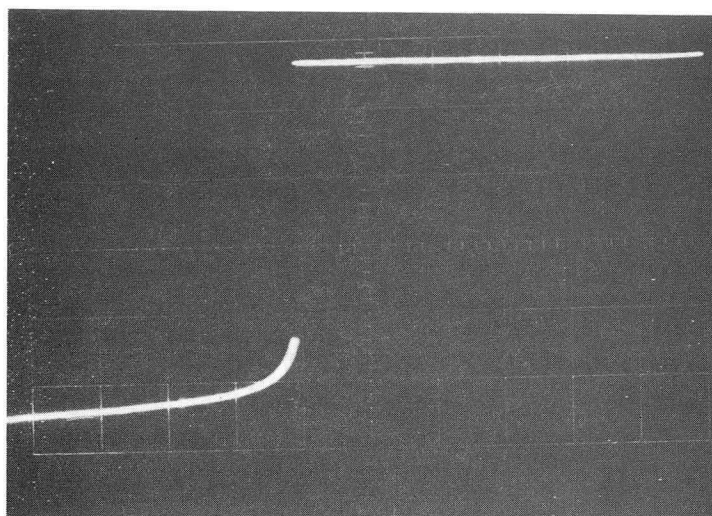
2.4-1. Electrodes Kinetics of the Alkali Metals

The micropolarization measurements of the alkali metals were performed in the same six-compartment cell where the cell potentials were measured. The galvanostatic experiments were conducted between two alkali metal electrodes where the central one served as the working electrode. The central working electrode was prepared in the glove box by sealing an approximately 5 cm long portion of a bright alkali metal wire, in epoxy resin. The end of the wire, not sealed in epoxy resin, was used for an electrical contact by attaching it to an alligator clip (see Fig. 2-12). The other end of the coated wire was cut at a right angle to the wire to expose the bright alkali metal surface, with an area equal to the cross sectional area of the wire. The other alkali metal electrodes were simply the original bright wires. In the cases of rubidium and cesium, the working electrodes, as well as the counter electrodes, were prepared by pouring the molten metals into cup electrodes, as has been described in the previous section. The solutions were stirred during the micropolarization experiments by a small magnetic stirrer at

the bottom of the central cell, just under the electrode's surface. The stirring was somewhat less efficient in the cases of Rb and Cs, because the stirrer was underneath the cup, while the active surface of the electrode was facing upward. The small currents employed insured that concentration overpotentials were negligible, even in the cases of Rb and Cs.

Pre-anodization was found necessary to obtain reproducible results. The standard procedure was to anodize the working electrode for 10 minutes at current density of 0.1 mA/cm^2 prior to each micropolarization cycle. The potential was measured between the central working electrode and one of the two Tl(Hg)/TlCl reference electrodes. The current was increased first in the anodic direction, then back toward the anodic direction, then back to the equilibrium state. The current was applied by a constant current power supply, Model C 612 Electronic Measurements, and was measured by a Keithley 601 Electrometer. The potential was measured by an AC/DC Differential Voltmeter, John Fluke Model 887-A. The cells were suspended in constant temperature baths at 25° and $35^\circ\text{C} \pm 0.01^\circ\text{C}$. The preparation of the electrodes and the assembly of the cells have been described already.

Because of the relatively low conductivity of the solutions ($10^{-3} - 10^{-2} \text{ ohm}^{-1} \text{ cm}^{-1}$), it was necessary to correct the overpotentials for ohmic drop between the working electrode and the tip of the reference electrode's connection. The ohmic drop was determined by a rapid current interrupter technique, in which the constant current was interrupted, and the potential was traced on a fast oscilloscope. The immediate drop in the potential was the IR drop, and the ohmic resistance was calculated by



XBB 728-4116

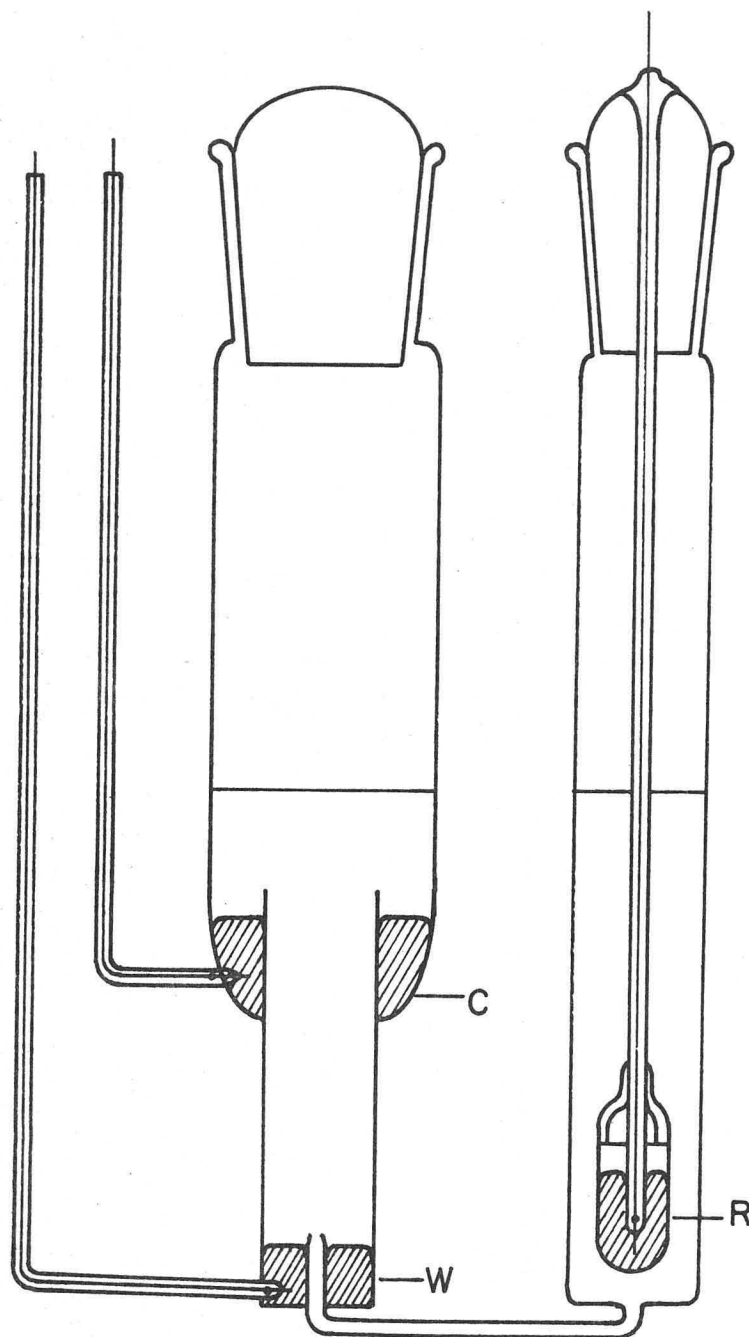
Fig. 2-14. IR drop determination in the six-compartment cell using a current interrupter technique.
Rb/RbCl(0.10 m) in AlCl_3 (1.0m)-PC 25°C.
Upper picture: Cathodic current, $I = 1.0$ mA.
Lower picture: Anodic current, $I = 0.5$ mA.
Vertical scale: 50 mV/cm. Horizontal scale: 1 msec/cm.

dividing it by the total current. The ohmic drop was then subtracted from the total overpotential. Rectangular wave form pulses were derived from an E. M. Test Pulser, Lawrence Berkeley Laboratory. The potentials were observed on a Tektronix Oscilloscope, and the potential trace was analyzed from the polaroid prints. The oscilloscope was operating at 0.01-1.0 m sec/cm and 50-200 mV/cm. The ohmic drop was determined at four different currents for each cell, both in anodic and cathodic directions. The currents employed during the pulse measurements were higher than the currents employed during the micropolarization experiments, and it has been assumed that the current distribution remained unchanged. Typical oscilloscope traces of the potential during current interruptions both in the cathodic and the anodic directions, are presented in Fig. 2-14. Currents were in the order of 0.1-1.0 mA, and the calculated ohmic resistances were in the order of 100-300 Ω . The calculated resistance from the four measurements agreed within 10%.

The polarization experiments were conducted at different alkali metal chloride molalities in AlCl_3 (1 m)-PC solution and at 25° and 35°C.

2.4-2. Electrode Kinetics of the Alkali Metal Amalgams

The micropolarization measurements of the alkali metal amalgams were conducted in a specially designed cell shown in Fig. 2-15. The working electrode, the counter electrode and the reference electrodes were all amalgams of identical composition. Because of the low conductance of the solutions, it was necessary to design the cell in such a way that the current distribution across the working electrode's surface would be fairly uniform. This was achieved by placing the working electrode at the bottom end of a cylindrical glass cell, approximately 5 diameters



XBL 725-6267

Fig. 2-15. Cell for kinetic measurements of the alkali metal amalgam.
W - working electrode
R - reference electrode
C - counter electrode

away from the annular counter electrode. The ohmic drop was minimized by designing the tip of the reference electrode's capillary just 1-2 mm above the surface of the amalgam. The platinum leads were kept well below the amalgam's surfaces.

After being filled with amalgams and solution, the cell was sealed, removed from the glove box and suspended in the constant temperature bath. The bias potential was measured between the three identical amalgams; it was always less than 1 mV. The galvanostatic polarization was conducted using a constant current power supply, Model C 612, Electronic Measurements. The current was measured by Keithly 601 Electrometer, and the potential between the working and the reference electrode by an AC/DC Differential Voltmeter, John Fluke Model 887-A. The ohmic drop was calculated from the potential traces resulting from constant current rectangular wave form pulses, which were driven from an E. M. Test Pulser, Lawrence Berkeley Laboratory. The potential traces were observed on a Tektronix oscilloscope operating at 10μ sec/cm and 50 mV/cm. For each solution the IR drop was determined at four different currents (2 anodic and 2 cathodic) and the calculated resistance was in the order of 10-30 ohm with up to 10% deviation.

2.5. Conductance Measurements

2.5-1. Preparation of Solutions

The solutions were prepared in the dry box by adding weighed amounts of the alkali metal chlorides to a 1 m AlCl_3 solution in PC. The volumetric concentrations in mol/lit were calculated from the densities of the solutions. The alkali metal chloride concentration varied from 0 up to 1 molal, all in the presence of AlCl_3 (1 m). The preparation of the solutions was very

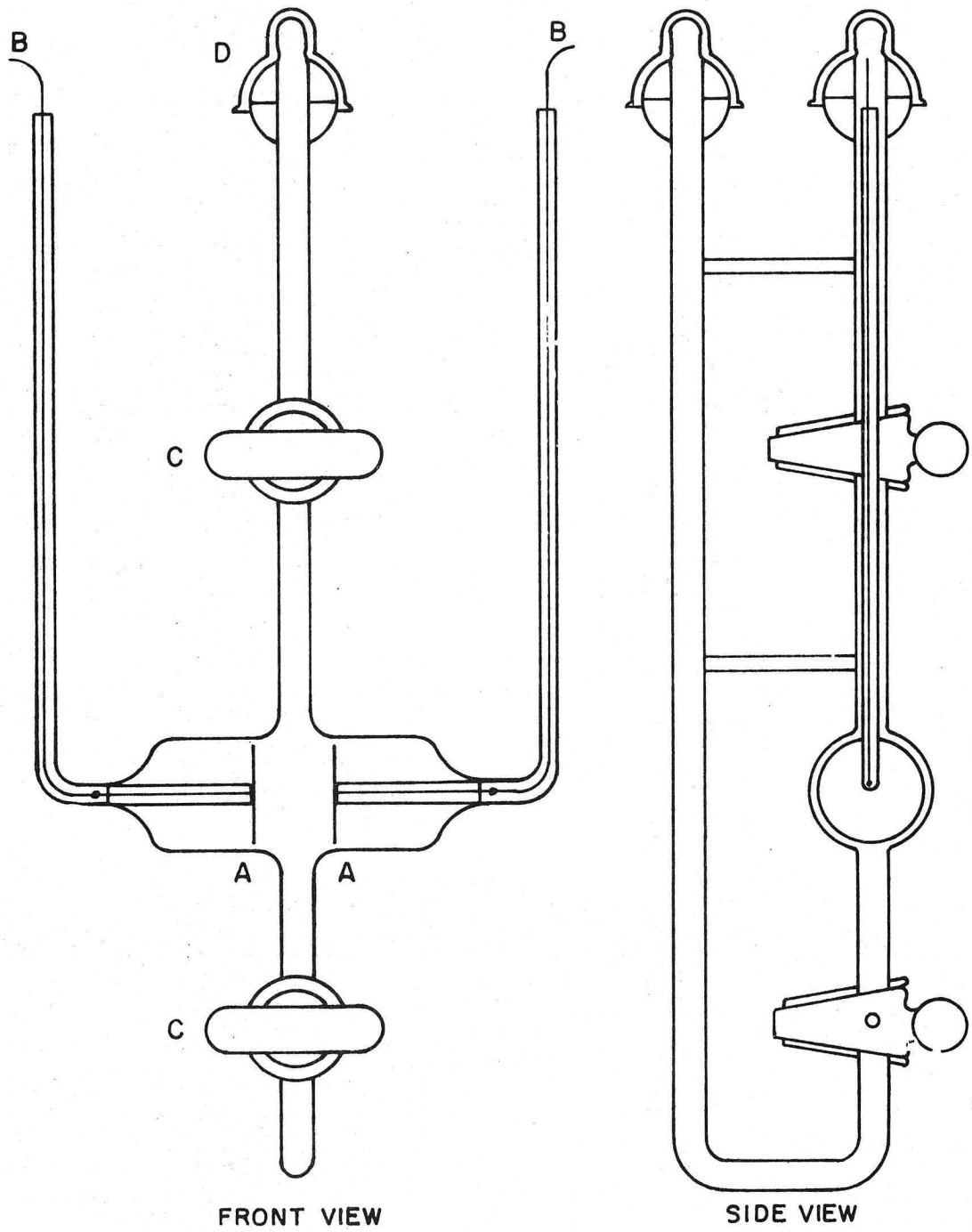
similar to the procedure described for the potential measurements. The AlCl_3 salt was added extremely slowly to PC to prevent heating and darkening of the solution. All glassware was cleaned in concentrated nitric acid, rinsed several times with distilled water and then was dried in a vacuum oven at 50 microns and 200°C for at least 24 hours.

2.5-2. Conductance Measurements

Conductivities of the alkali metal chloride in AlCl_3 -PC solutions were measured at 25° and 35°C , using an AC bridge. Sinusoidal signals at 20 kHz and amplitude of around 15 volts were generated by an AC Generator Detector, Model 861 A, Electro Scientific Industries, Portland, Oregon. The cell resistance and capacitance were balanced with an Impedance Bridge, Model 290 A, Electro Scientific Industries, Portland, Oregon, and with Variable Decade Capacitors, Model CDA-2 and CDA-3, Cornell-Dubilier Electronic Division, Federal Pacific Electric Division.

The conductance cell is shown in Fig. 2-16. It contained two parallel bright platinum disk electrodes. Because of the relatively low conductivities of the nonaqueous solutions, the cell was designed to give a relatively low cell constant. The cell constant, 0.439 cm^{-1} , was determined using 0.1 and 0.01 N aqueous KCl solutions.¹⁴⁹ All electrical wires were shielded. At the frequency of 20 kHz, the results were independent of the frequency.

The cell was filled with solution inside the glove box. The cell was sealed by closing the valves (Fig. 2-16), and then transferred into the constant temperature bath. Measurements were made first at 25° and then at 35°C . Temperatures were controlled to within 0.01°C by two thermostats



FRONT VIEW

SIDE VIEW

XBL 725-6269

Fig. 2-16. Conductivity cell.
 A - Platinum electrodes. C - stopcock.
 B - Lean-in. D - Ball joints.

2-6. Density Measurements

Density measurements of various molalities of the alkali metal chlorides in AlCl_3 (1 m)-PC solution were conducted at 25° and 35°C. The densities were measured with a picnometer. The volume of the picnometer was calibrated at 25° and 35°C by weighing distilled water.¹⁴⁹ The AlCl_3 -PC solutions were filled into the picnometer inside the glove box, and were transferred into a constant temperature water bath. Temperatures were maintained within $\pm 0.01^\circ\text{C}$ and a few hours were allowed to attain thermal equilibrium. The alkali metal chloride concentrations varied from 0 up to 1 m in AlCl_3 -PC solution.

III. RESULTS

3.1. The Electrodeposition of the Alkali Metals From Various Solutions in PC

The search for electrolytic solutions that will enable the deposition of the alkali metals started with a qualitative stage, in which the common alkali metal salts were tested for solubility, and the feasibility of deposition. High solubility is required in order to obtain a low ohmic drop and low concentration overpotential. It appears that a solubility in the order of 1 mole/l is necessary. This concentration corresponds to a specific conductance of approximately $10^{-2} \text{ ohm}^{-1} \text{ cm}^{-1}$, and permits a relatively wide range operation below the limiting current. The following anions were tested: chlorides, bromides, iodides, perchlorates, hexafluorophosphates, tetrafluoroborates and tetrachloroaluminates. The following results were observed:

3.1-1. Lithium

LiCl

The solubility of LiCl in PC is below 0.1 M; ($4.0 \cdot 10^{-2}$ M was reported by Butler, et al.⁴⁹) Li was deposited from the saturated solution; the applied potential was high because of the low conductance.

LiBr

LiBr is very soluble in PC, 2.43 M.⁶⁸ Lithium was deposited from 1 M solution of LiBr in PC at current density of 1 mA/cm^2 . The lithium deposit was grey and formed Li-Pt alloy with the platinum cathode. The alloy was similar to the one obtained during the electrodeposition from LiClO_4 solution in PC. X-ray analysis of the alloy is presented in Table 3-1. Figs. 3-1 and 3-2 show an electron microprobe analysis of

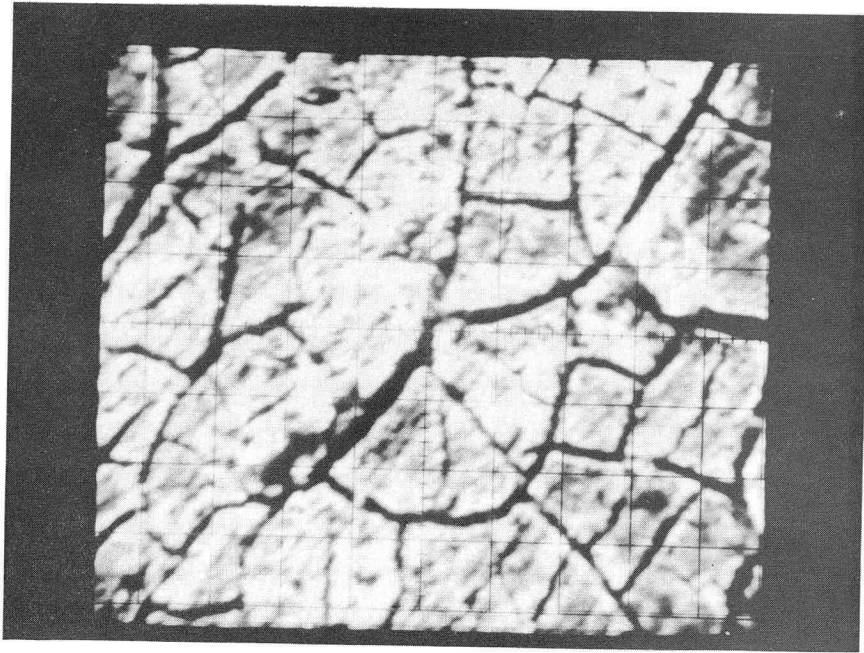
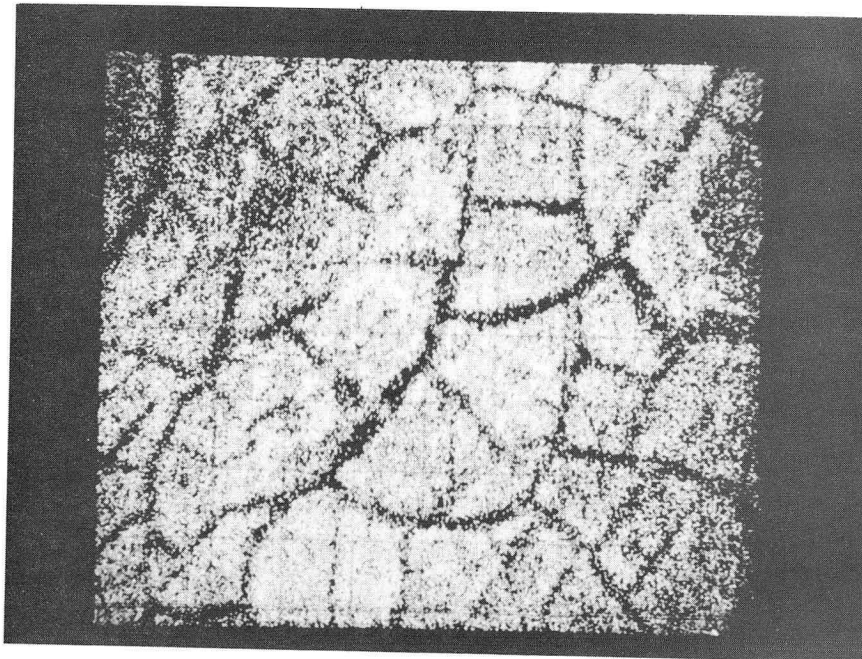


Fig. 3-1. Electron microprobe analysis of Li deposit on Pt electrode. Back scattered electron, primary: 15 kV. Magnification: x500



XBB 728-4114

Fig. 3-2. Electron microprobe analysis. X-rays for Pt. Magnification: x500. Light area: Pt. Dark lines: Lithium(?) or cracks.

Table 3-1. X-ray diffraction data for Li-Pt alloy.

Electrolyte: LiBr in PC	
d , (Å)	Relative Peak Height
2.794	medium
2.252	large
2.225	large
1.951	medium
1.381	medium
1.180	medium
1.129	small

the Li-Pt alloy, after the electrode was washed with water. The analysis was done using an Electron Microprobe, Material Analysis Corp., Model 400S. The dark lines appear to be Li-Pt alloy or deep cracks and are typical for all the lithium deposits which were obtained on a platinum substrate.

LiClO₄

LiClO₄ was found to be the best lithium electrolyte in PC. The solubility of LiClO₄ in PC is 2.1 M,⁷¹ and the conductivity is relatively high, $5.6 \cdot 10^{-3} \text{ ohm}^{-1} \text{ cm}^{-1}$, for 1 M solution at 25°C.⁸¹ Lithium was deposited from LiClO₄ (1 M)-PC solution at current densities of up to 10 mA/cm², without any sign of gas evolution or side reaction. The Li deposit was grey and formed an alloy with the Pt substrate. The Li-Pt alloy was stable toward air and water. Immersing the deposit in water resulted in violent reaction of the free lithium deposit, while the Li-Pt alloy remained stable. The platinum surface turned permanently grey and rough and there was no way to regain the bright appearance of platinum. The alloy was characterized by X-ray diffraction analysis (Cu α radiation

with nickel filter) and the diffraction data is given in Table 3-1 in terms of the interplanar spacings. Lithium metal was found to alloy with other metals, including noble metals.⁴³ The alloys were prepared by spontaneous electrochemical alloying in which a cell of the type Li/LiClO₄ (1 M), PC/Metal was shorted; Li formed an alloy with the metal at the cathode. The alloy between Li and Pt was analyzed to be Li₃Pt₂. The only intermetallic compound reported is LiPt₂ and the available data on this compound is limited. The fact that in the present work different diffraction data were obtained for each Li-Pt alloy might indicate different degrees of alloying. Alloying was not obtained when lithium was deposited on nickel or stainless steel cathodes.

Prolonged deposition of lithium led to the formation of the lithium trees shown in Fig. 3-3, which were obtained from a stagnant LiClO₄ (1 m) solution at 1 mA/cm².

LiPF₆

Lithium was deposited from 0.5 M LiPF₆ solution in PC. The current densities were in the range of 1-10 mA/cm² at relatively low applied potentials. The Li deposit was grey and very similar to the one obtained from LiClO₄ solution. The solubility of LiPF₆ is approximately 0.55 to 0.76 M.^{70,69}

LiBF₄

Lithium was deposited from a saturated solution of LiBF₄ in PC. The concentration was below 0.5 M. The solubility of LiBF₄ is 0.42 M.⁷⁰ Grey deposit was obtained at 1 mA/cm² and moderate applied potential.

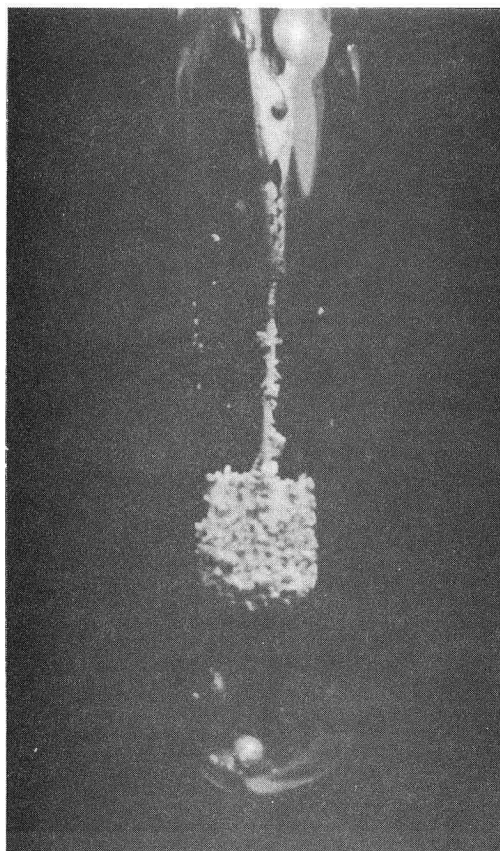
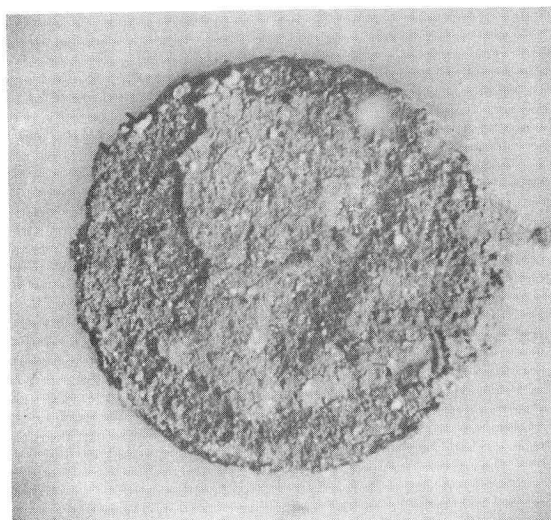


Fig. 3-3. Lithium deposit on Pt cathode from LiClO_4 (1M) solution in PC. Current density: 10 mA/cm^2 . Temperature: 25°C .



XBB 728-4117

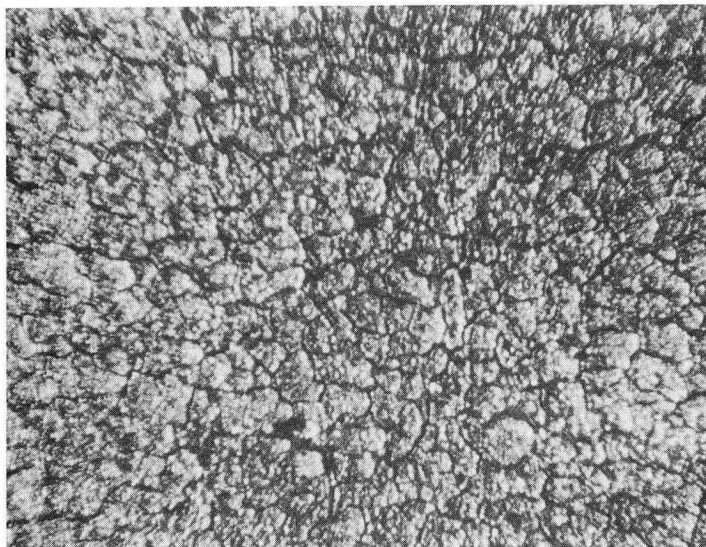
Fig. 3-4. Lithium deposit on a stainless steel disk cathode, from LiAlCl_4 (1M) solution in PC. Disk diameter: 0.33 cm. Current density: 10 mA/cm^2 . Temperature: 25°C .

LiAlCl₄

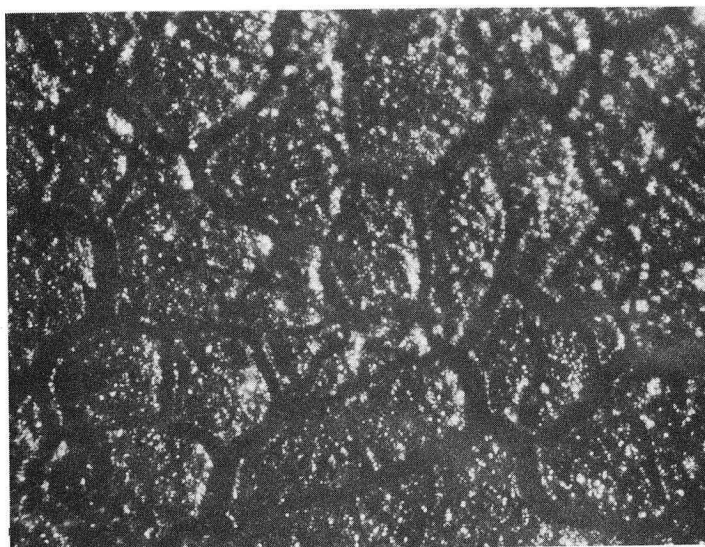
Lithium was deposited from 1:1 mixture of LiCl and AlCl₃ solution in PC. The solubility of LiCl in pure PC is low; however, in the presence of AlCl₃, which is highly soluble, the solubility of LiCl increases up to 1:1 ratio. Addition of AlCl₃ to PC results in violent reaction, accompanied by strong heating and darkening of the solution. This can be avoided by adding the LiCl first, then adding the AlCl₃ extremely slowly while cooling the solution with a cooling mixture of chloroform-carbon tetrachloride-dry CO₂. Solutions prepared in this way were almost colorless. Another successful method is to prepare the complex salt LiAlCl₄ by heating a stoichiometric mixture of LiCl and AlCl₃ at 200°C under dry argon atmosphere. Additions of LiAlCl₄, prepared in this way, to PC, resulted in no heating at all. Despite the superior solutions obtained by this method, in most experiments the solutions were prepared by careful addition of AlCl₃ to LiCl-PC mixture. The other method was inconvenient because of the strong sublimation of AlCl₃ at high temperature.

Lithium deposits formed alloys with Pt cathodes. Figure 3-4 shows a lithium deposit on a rotating disk stainless steel electrode. The current density was 50 mA/cm², and the rotation speed 1800 rpm. Figure 3-5 shows a typical Li-Pt alloy deposited from a LiAlCl₄ (1 m) solution in PC. The deposit was washed with water to remove the free lithium and to expose the alloy which is stable toward water and air. The dark "tunnels" probably correspond to Li-Pt alloy while the areas in between are mostly free of Pt (see Fig. 3-2 for electron microprobe analysis of the surface).

-79-



a. Side illumination, magnification: $\times 50$



XBB 728-4113

b. Side illumination, magnification: $\times 200$

Fig. 3-5. Lithium deposit on Pt electrode. Electrolyte: LiAlCl_4 (1m)-PC. Current density: 1 mA/cm^2 . The deposit was washed with water to expose the Li-Pt alloy.

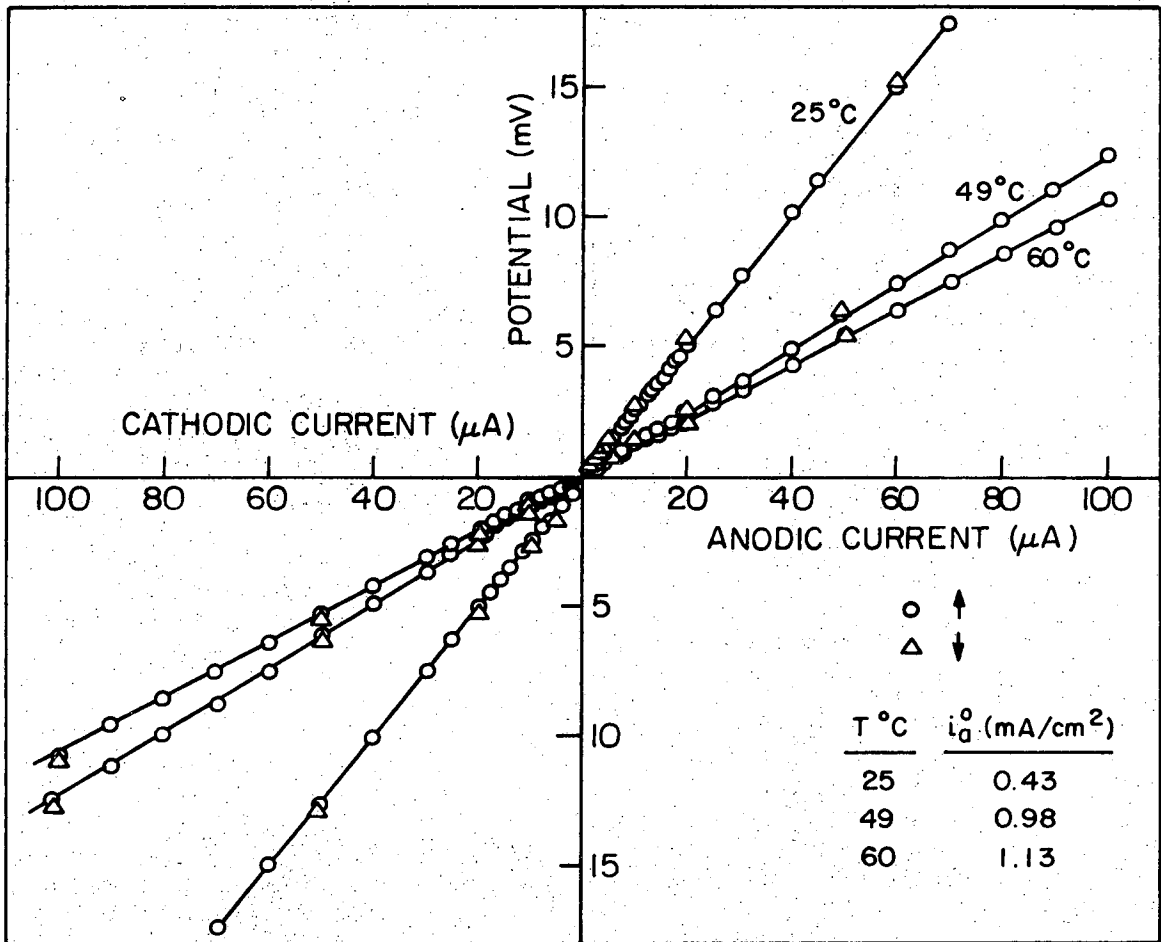
3.1-2. Sodium

NaCl and NaBr are practically insoluble in PC and therefore are not suitable for electrodeposition purposes. NaClO_4 , NaPF_6 , and NaAlCl_4 are quite soluble and therefore were tested. Furthermore, polarization and cyclic voltammetry experiments were performed for these electrolytes.

NaClO_4

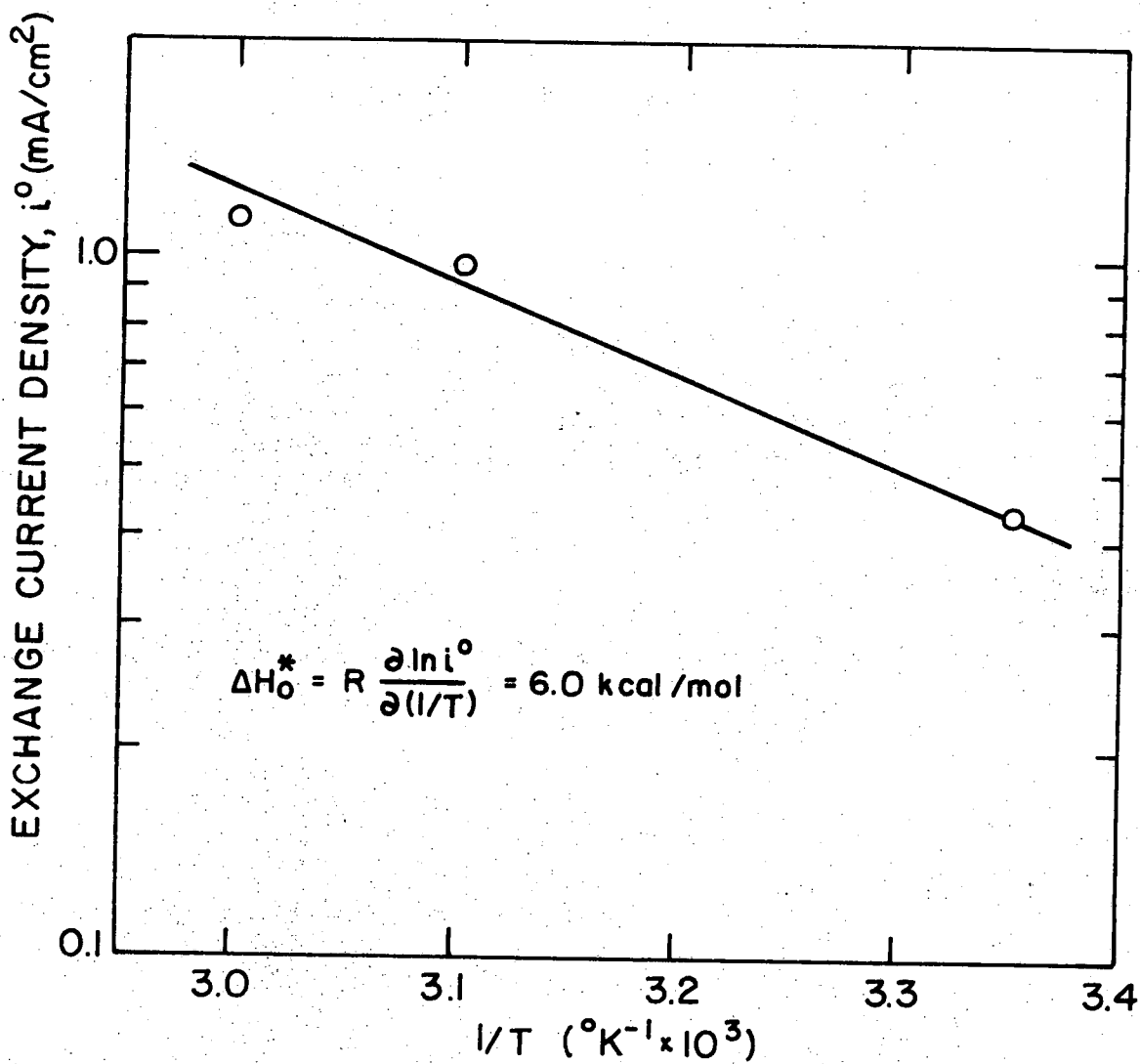
The solubility of NaClO_4 in PC is $>2 \text{ M}$.⁷² Sodium was deposited from 1 M NaClO_4 solution at current density of 10 mA/cm^2 without any visible sign of gas evolution or side reaction. The deposit was grey and did not form an alloy with the Pt cathode. In order to determine the exchange current density and the reversibility of the electrode reaction, several polarization experiments were carried out. The cell consisted of three compartments, in which three identical solid sodium electrodes were placed. The electrodes were prepared from sodium wires coated by epoxy resin, and fresh surfaces were prepared prior to each experiment by cutting the wires with a stainless steel blade, exposing bright sodium surfaces. The bias potentials between the Na electrodes were below 0.5 mV, even after a series of polarization experiments. The middle electrode served as the working electrode and the two side electrodes served as the counter and reference electrodes. The reference electrode compartment was connected to the working electrode compartment by a narrow capillary. The polarization experiments were described in detail in Chapter II.

Figure 3-6 show the polarizations of sodium in NaClO_4 (1 M) solution at 25° , 49° and 60°C after the overpotentials were corrected for ohmic drop, using a current interrupter technique. The exchange current densities



XBL 727-6637

Fig. 3-6. Polarization of Na(s)/NaClO₄ (1 M), PC.



XBL727-6627

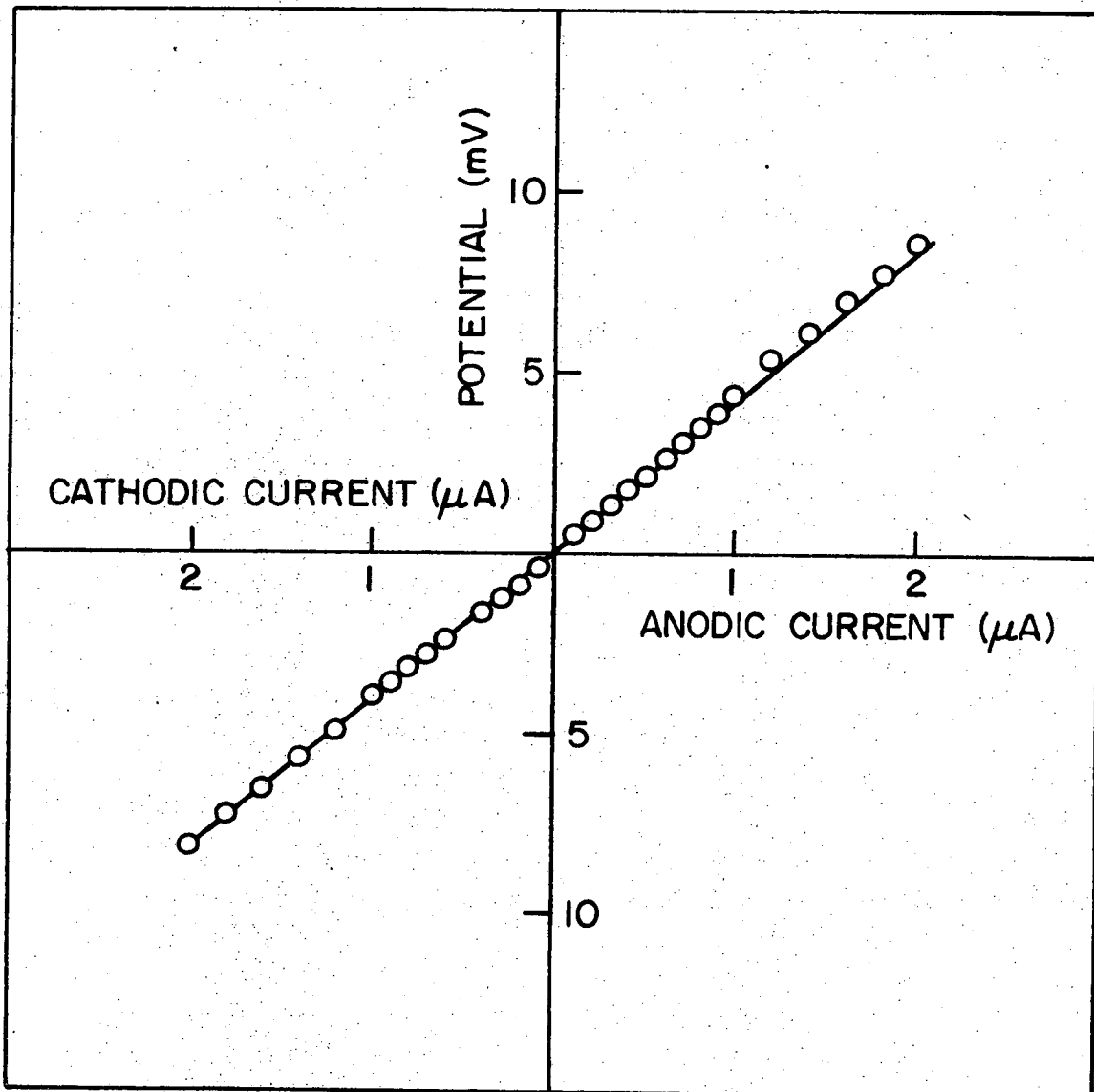
Fig. 3-7. Determination of the enthalpy of activation at zero polarization for Na(s)/NaClO₄ (1 M), PC.

were calculated from the slopes of the lines and from the area of the electrode. The exchange current densities are 0.43, 0.98 and 1.13 mA/cm² at 25°, 49° and 60°C, respectively. Figure 3-7 show the plot of the exchange current density vs. 1/T, and the enthalpy of activation at zero polarization, $\Delta H_0^* = 6.0$ kcal/mole, was calculated from the slope.

NaPF₆

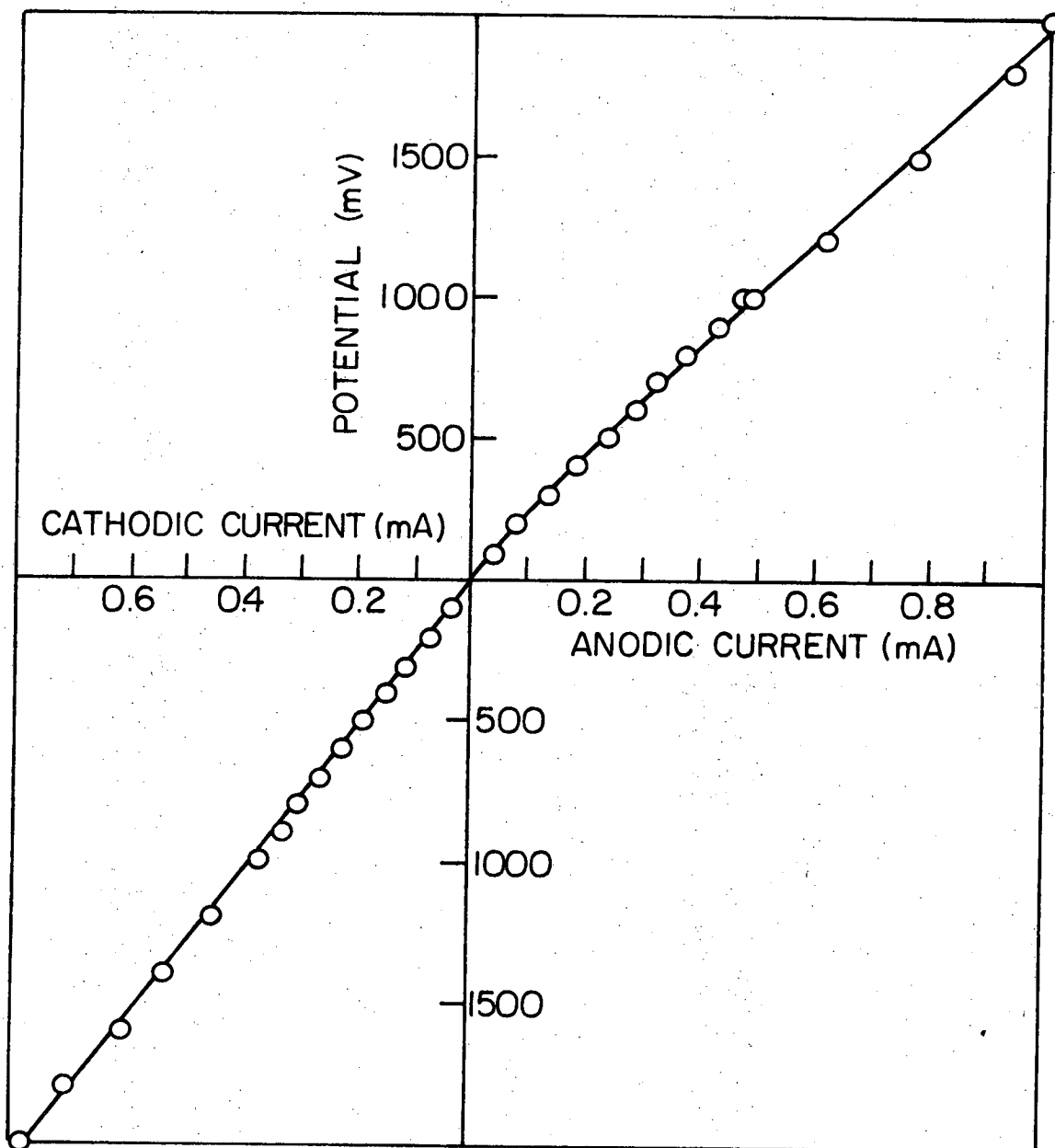
The solubility of NaPF₆ in PC is 0.86 M.⁷⁰ Sodium has been deposited from 0.5 M solution of NaPF₆ in PC at current densities of 1-10 mA/cm². The deposit was grey and there was no visible evidence of side reaction or gas evolution at the cathode. The potential between sodium electro-deposited on Pt electrode and a reference sodium electrode was below 1.15 mV, which is evidence for the pure quality of the deposit.

Polarization experiments were conducted to investigate the kinetic behavior of metallic sodium and sodium amalgam in NaPF₆ (0.5 M) solution in PC. The polarization experiments were done in a six-compartment cell in which two sodium, two sodium amalgam and two Pt electrodes were placed. The sodium electrodes were coated with epoxy resin and fresh surfaces were exposed by cutting the coated wires with a clean blade. The sodium amalgam concentrations were 0.286 and 0.351%wt, and the average potential difference between these electrodes and the sodium electrodes at 25°C were 831.88 and 734.70 mV, respectively. Constant current was applied in both cathodic and anodic directions between the sodium and the amalgam electrode while the two remaining electrodes served as reference electrodes. The measured overpotentials were corrected for ohmic drop by current interrupter pulse technique. The micropolarizations are presented in Figs. 3-8 and 3-9 for sodium and sodium amalgam electrodes, and the calculated



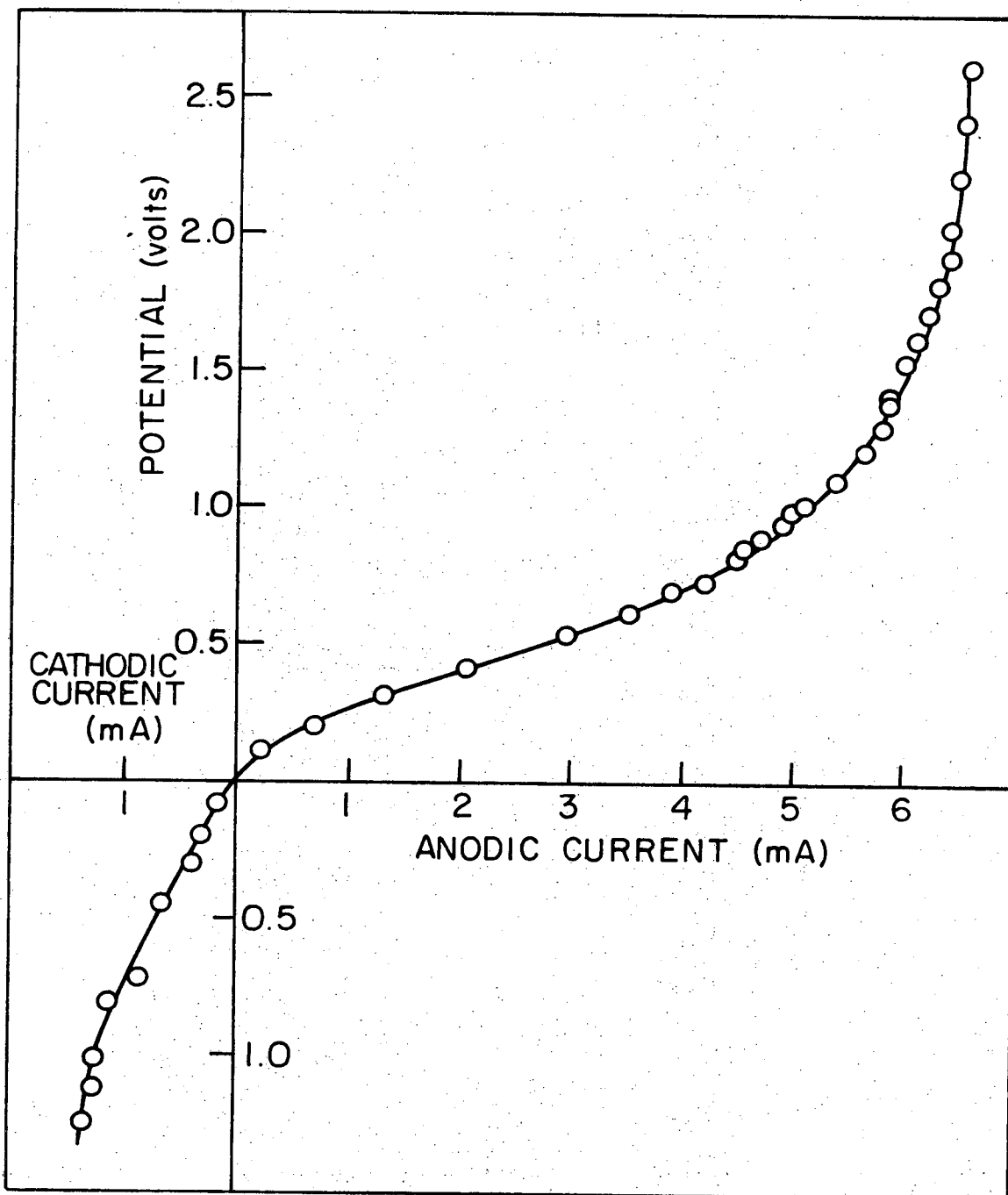
XBL727- 6632

Fig. 3-8. Micropolarization of Na(s)/NaPF₆ (0.5 M), PC. Reference electrode: Na(Hg). Area: 0.341 cm².
 $i^{\circ} = 18.1 \mu\text{A}/\text{cm}^2$.



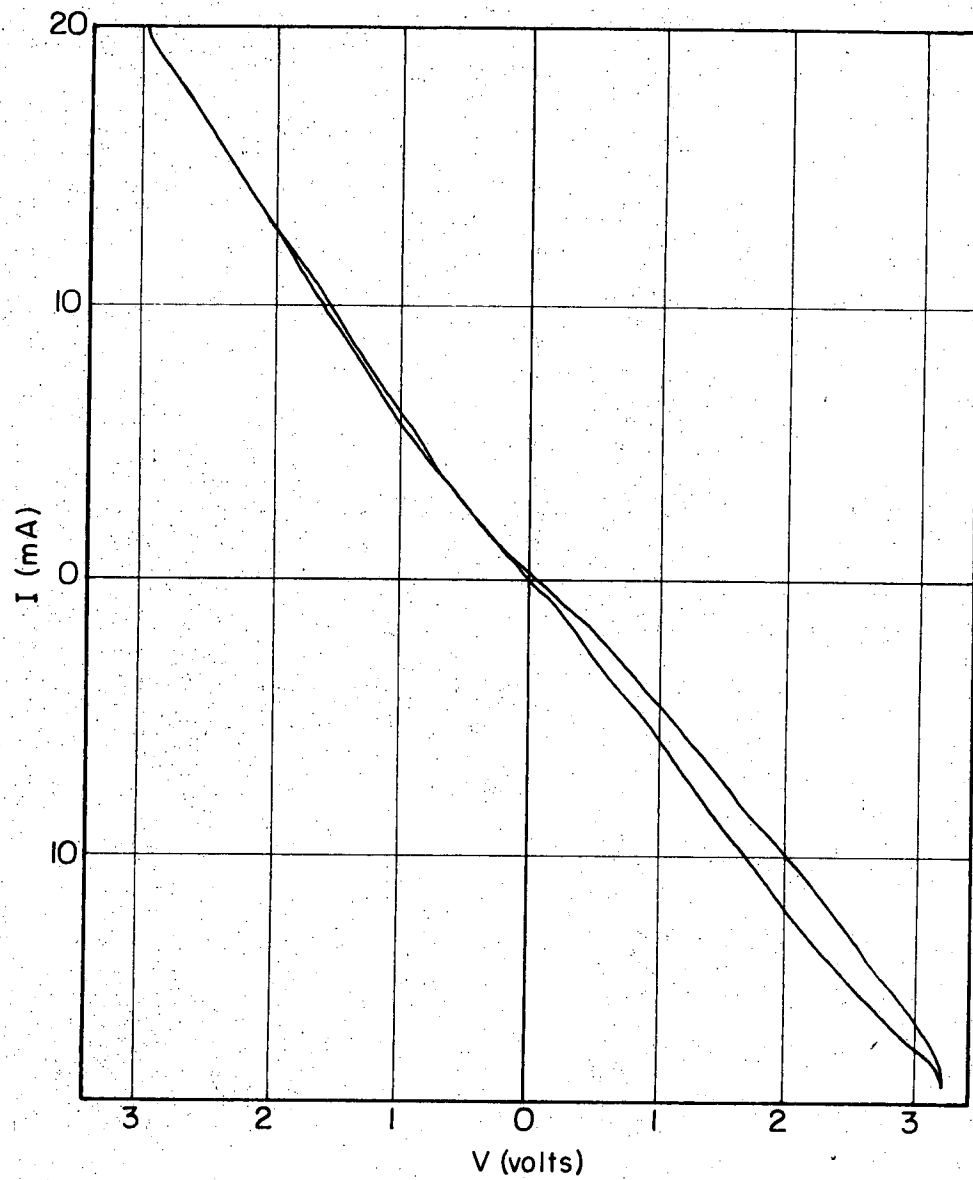
XBL727-6633

Fig. 3-9. Polarization of Na(Hg)/NaPF₆ (0.5 M), PC. Reference electrode: Na(Hg). Area: 0.965 cm².
 $i^{\circ} = 10.6 \mu\text{A}/\text{cm}^2$.



XBL 727 - 6635

Fig. 3-10: Polarization of Na(s)/NaPF₆ (0.5 M), PC. Reference electrode: Na(Hg), Electrode area: 0.341 cm².



XBL 727-6653

Fig. 3-11. Cyclic voltammogram for Na in NaPF_6 (0.5 M)-PC.

Reference electrode: Na
Sweep rate: 120 mV/sec

exchange current densities are 18.08 and 10.64 A/cm^2 , respectively. Figure 3-10 shows the polarization behavior of sodium in NaPF_6 (0.5 M) PC solution at higher currents. The solution was stirred during the experiments with a small magnetic stirrer at the bottom of the cell, just below the sodium electrode's surface. The stirring was necessary to minimize concentration overpotential which becomes appreciable at higher currents. Linear cyclic voltammogram for Na in NaPF_6 (0.5 M) is shown in Fig. 3-11. The sweep rate was quite high (120 mV/sec) and hysteresis is observed in the cathodic direction.

NaBF_4

Despite the low solubility of NaBF_4 in PC, 0.093 M,⁷⁰ sodium was deposited from a saturated solution at 1 mA/cm^2 and moderately high applied potential. The deposit was grey. The limiting current was undoubtedly exceeded, as evidenced by gas evolution observed along with sodium deposition.

NaAlCl_4

The solubility of NaCl in 1 m AlCl_3 solution in PC was found to be around 0.5 m, which is in contrast to the rest of the alkali metal chlorides. However, sodium was electrodeposited from NaCl (0.5 m)- AlCl_3 (1 m) in PC at current densities 1-10 mA/cm^2 without any sign of gas evolution or side reaction. The deposit was grey. Further thermodynamic, kinetic and conductance measurements are presented in the following sections.

3.1-3. Potassium

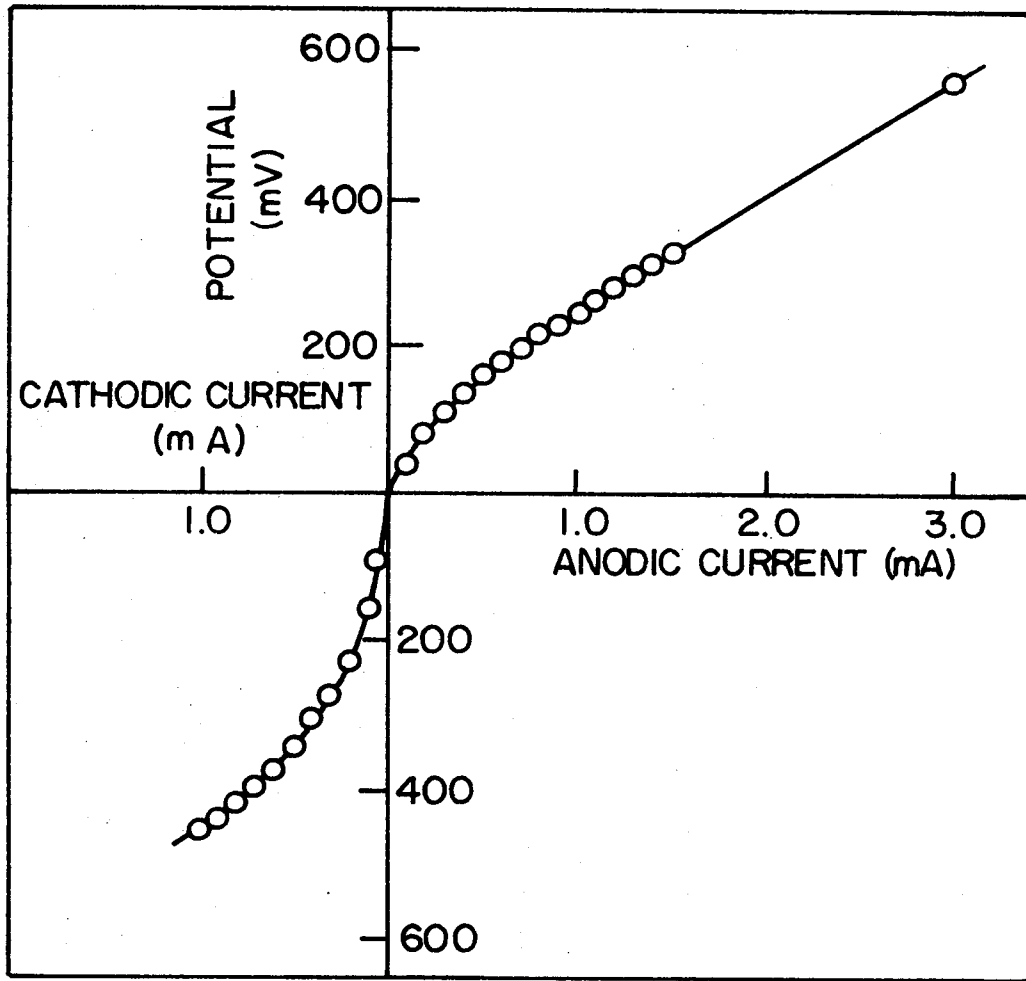
Potassium was found to be very reactive toward PC solutions. The surface of a bright potassium electrode turned purple within a few minutes in moderately dry PC (around 50 ppm H₂O). The stability of potassium increased significantly after the PC was treated with molecular sieves (Linde 4A). The molecular sieves, approximately 5% volume, were added to PC and the mixture stirred for several hours.

Due to the low solubility of KCl ($3.52 \cdot 10^{-4}$ M),⁷ KBr ($6 \cdot 10^{-3}$ M),⁶ KBF₄ (0.012 M)⁶ and KClO₄ in PC, the only practical possibilities were found to be KPF₆ and KAlCl₄. Nevertheless, potassium was electrodeposited from its perchlorate and tetrafluoro boride solutions in PC at very low current, 0.1 mA/cm², and high applied potentials.

KPF₆

Potassium was deposited from KPF₆ (0.5 M) solution in PC at currents up to 10 mA/cm². The solubility of KPF₆ in PC is 1.2 M.^{31a} Potassium wire served as the anode; normal anodic dissolution was observed, while the deposit on the platinum cathode was grey and loose. The bias potential between the deposited potassium and the potassium anode, after the deposition was completed, was less than 20 mV. The bias potential was probably caused by the different nature of the deposit on the Pt substrate.

Figure 3-12 shows polarization curves of potassium wire in KPF₆ (0.5 M) solution in PC. The reference electrode was an identical K wire and was connected to the working electrode compartment by a narrow capillary. Potentials were corrected for ohmic drop by current interruption technique. The solution was stirred by a small magnetic stirrer at the bottom of the working electrode compartment in order to minimize concentration polarization.



XBL 727 - 6636

Fig. 3-12. Polarization of K(s)/KPF₆ (0.5 M), PC.

KAlCl₄

Potassium was electrodeposited from 1:1 KCl-AlCl₃ (0.5 m) in PC. The electrodeposition was performed in a six-compartment cell, where potassium wire served as an anode, platinum foil served as a cathode, and the nature of the deposit was checked by measuring the bias potentials between the deposited potassium and reference potassium electrode, and another two potassium amalgam electrodes (0.231%wt). The potentials between the deposited potassium and the reference potassium electrode were always below 20 mV immediately after the deposition. However, within a few hours after the current was turned off the potential difference increased substantially, while it was observed that the potassium deposit became loose and the Pt substrate was exposed.

The potential differences between the potassium wire and the K(Hg) electrodes were measured and recorded over a period of 4 days at different temperatures. The electrodes underwent strong polarizations during this period, and despite this fact the potentials were constant within ±10 mV. Table 3-1a contains the results of the potential measurements between metallic potassium and potassium amalgam (0.231%wt) in 0.5 m KAlCl₄ solution in PC at different temperatures.

Table 3-1a: Potentials of K-K(Hg) 0.231%wt in 0.5 KAlCl₄ PC solution.

Temperature °C	Potential Volts
25	1.0067
29	1.013
30	1.016
43	1.057
50	1.064

The stability and the reversibility of potassium and its amalgam in KAlCl_4 solution in PC were tested by a linear cyclic voltammetry technique. The potential vs. K or K(Hg) reference electrode was scanned in a relatively slow sweep rate, and the resulting current was recorded. The solutions were stirred by a small magnetic stirrer. Figure 3-13 and Fig. 3-14 show two cyclic voltammograms for K in KAlCl_4 (0.5 M) PC solution, at 25° and 43°C, respectively. The sweep rate is 1.2 mV/sec, and no hysteresis was observed after a complete cycle. Figure 3-15 and Fig. 3-16 show cyclic voltammograms at 25°C and at the sweep rates of 4 and 40 mV/sec, respectively. The range of the scanned potential is wider, ± 1 volt, and the resulting currents are in the order of up to 7 mA. No hysteresis was observed at the low sweep rate; however, an hysteresis of about 120 mV was observed when the sweep rate was 40 mV/sec. The behavior of a clean platinum electrode in the same LiAlCl_4 (0.5 M) PC solution was investigated and is presented in Fig. 3-17. Three complete cyclic voltammograms were recorded, and the linear cathodic currents are in contrast to the small anodic currents. The peaks in the anodic direction followed the cathodic currents, and are the dissolution currents of the deposited potassium. The small anodic current on the clean Pt demonstrates the stability of the solvent at the far cathodic potential range.

Cyclic voltammogram for an amalgam of potassium in KAlCl_4 (0.5 M) PC solution is shown in Fig. 3-18. The behavior is quite reversible and no hysteresis was observed.

The behavior of potassium and potassium amalgam electrodes in KAlCl_4 (0.5 M) during several cycles is shown in Fig. 3-19 and Fig. 3-20. In both cases the current decreased with an increasing number of cycles.

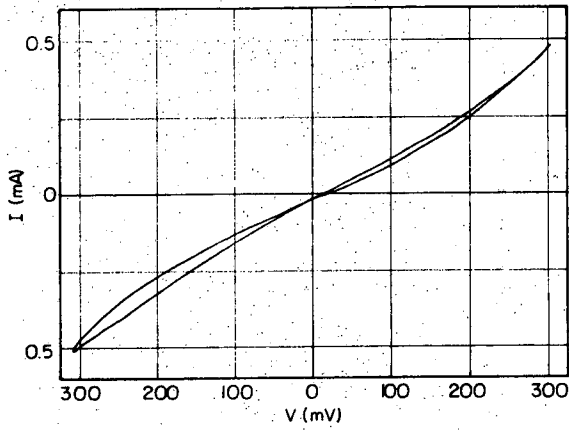


Fig. 3-13.

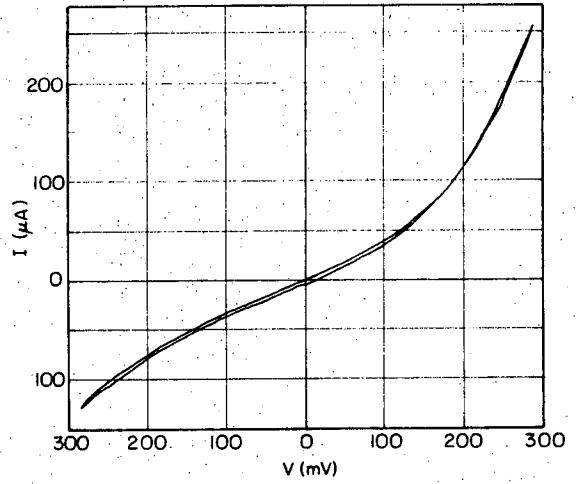


Fig. 3-14.

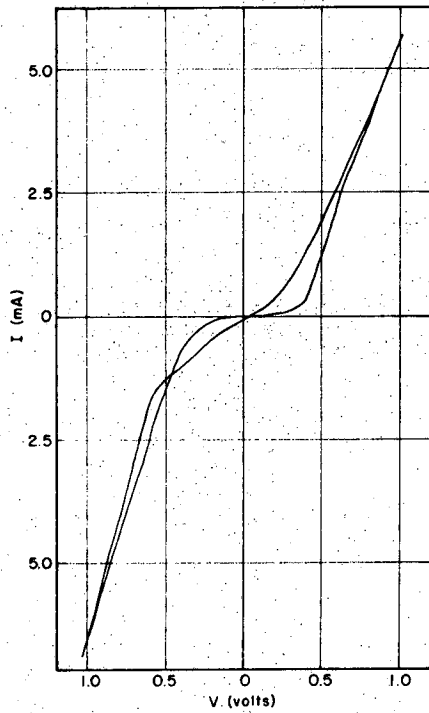


Fig. 3-15.

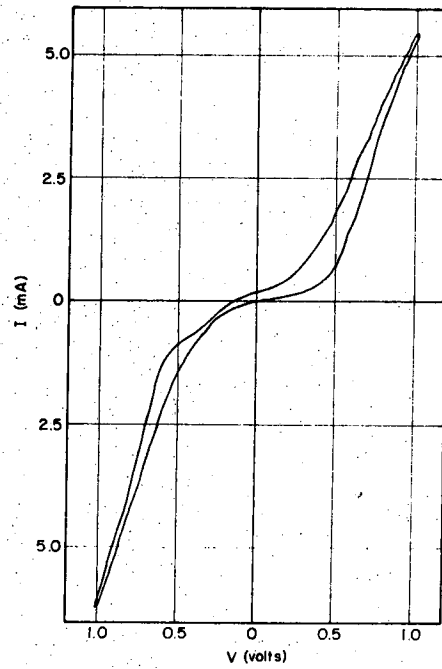


Fig. 3-16.

Fig. 3-13. Cyclic voltammogram for K in $\text{KAlCl}_4(0.5\text{M})\text{-PC}$.
Reference electrode: K
Sweep rate: 1.2 mV/sec.
Temperature: 25°C.

Fig. 3-14. Cyclic voltammogram for K in $\text{KAlCl}_4(0.5\text{M})\text{-PC}$.
Reference electrode: K
Sweep rate: 1.2 mV/sec.
Temperature: 43°C.

Fig. 3-15. Cyclic voltammogram for K in $\text{KAlCl}_4(0.5\text{M})\text{-PC}$.
Reference electrode: K
Sweep rate: 4 mV/sec.

Fig. 3-16. Cyclic voltammogram for K in $\text{KAlCl}_4(0.5\text{M})\text{-PC}$.
Reference electrode: K
Sweep rate: 40 mV/sec.

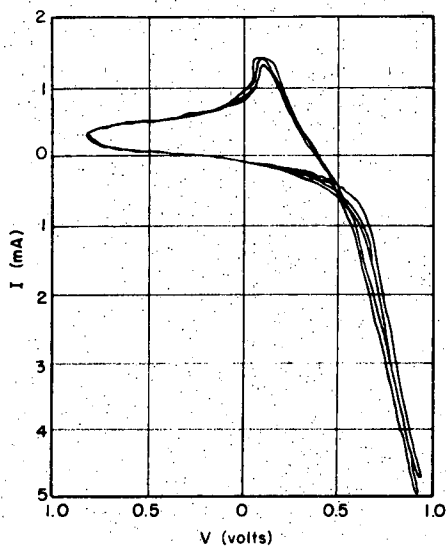


Fig. 3-17.

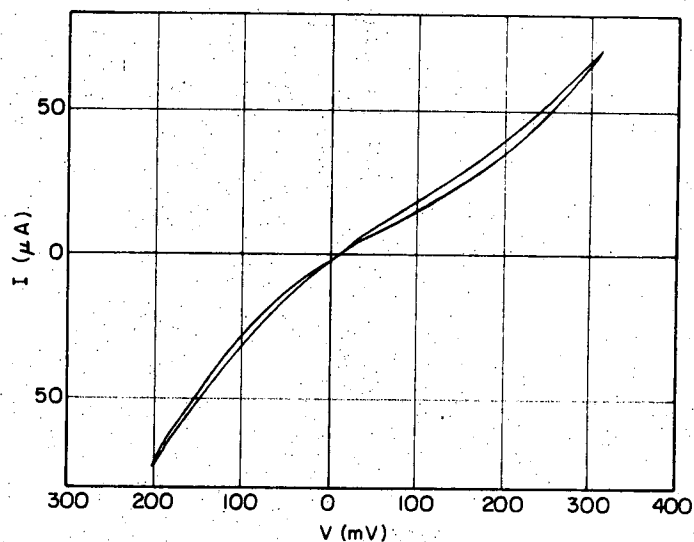


Fig. 3-18.

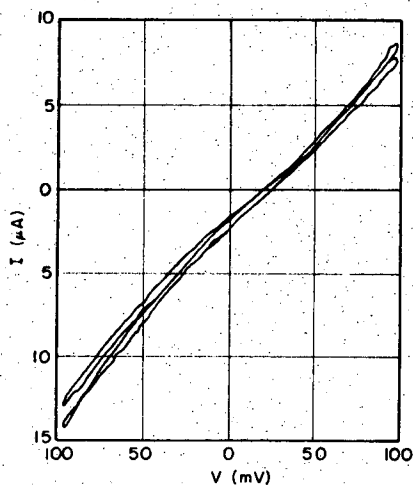


Fig. 3-19.

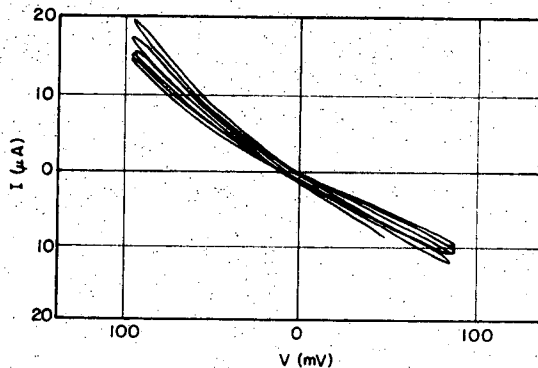


Fig. 3-20.

XBL 728-1440

Fig. 3-17. Cyclic voltammograms for Pt in $\text{KAlCl}_4(0.5\text{M})\text{-PC}$. Reference electrode: K(Hg) , Sweep rate: 0.4 mV/sec .

Fig. 3-18. Cyclic voltammogram for K(Hg) in $\text{KAlCl}_4(0.5\text{M})\text{-PC}$. Reference electrode: K(Hg) , Amalgam composition: $0.231\% \text{wt}$, Sweep rate: 1.2 mV/sec , Temperature: 30°C .

Fig. 3-19. Cyclic voltammogram for K in $\text{KAlCl}_4(0.5\text{M})\text{-PC}$. Reference electrode: K, Sweep rate: 0.4 mV/sec .

Fig. 3-20. Cyclic voltammogram for K(Hg) in $\text{KAlCl}_4(0.5\text{M})\text{-PC}$. Reference electrode: K(Hg) , Amalgam composition: $0.231\% \text{wt}$, Sweep rate: 4 mV/sec .

This is probably due to the increase in the ohmic resistance of the deposited metal, which is looser than the metallic potassium, or due to a buildup of an insulating layer on the electrode surface. It should be mentioned that the cyclic voltammograms were not corrected for the ohmic drop caused by the resistance of the solution and the electrode.

3.1-4. Rubidium

Due to the low solubility of most of the common Rb salts in PC, the only practical possibility found was the combination between RbCl and AlCl_3 .

Rubidium was deposited from a carefully dried 1:1 RbCl- AlCl_3 (1 M) solution in PC at currents up to 10 mA/cm^2 . The electrodeposition was done in a six-compartment cell, where metallic rubidium, rubidium amalgam (0.2306%wt) and a platinum electrode served as the anode, the reference electrode and the cathode, respectively. The potential between the metallic rubidium and the amalgam was recorded over a period of 4 days, and the average potential was 1.076 volts at 25°C , which is in good agreement with the value of 1.0745 volts measured by G. N. Lewis and W. L. Argo⁶⁶ in a series of measurements, in which they established the standard potentials of the alkali metals in aqueous solution. The composition of the amalgam matched exactly the amalgam composition used by Lewis, whose work provided the only available data.

The potential between the electrodeposited rubidium and the metallic rubidium was below 25 mV immediately after the electrodeposition, but dropped significantly after a few hours of standing when the deposit became loose and the platinum substrate was exposed.

Cyclic voltammograms of Rb and Rb(Hg) in RbAlCl_4 (0.5 M) are shown

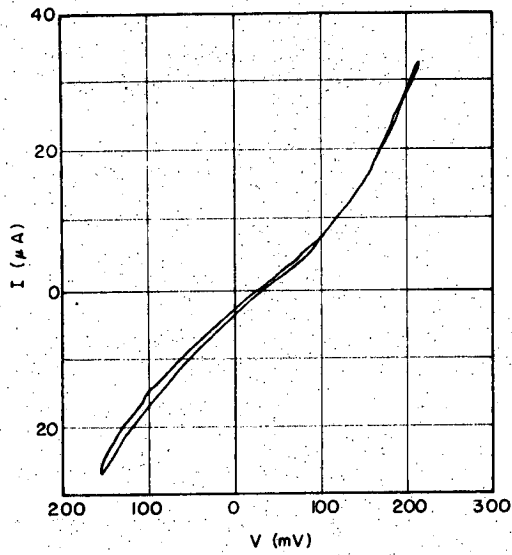
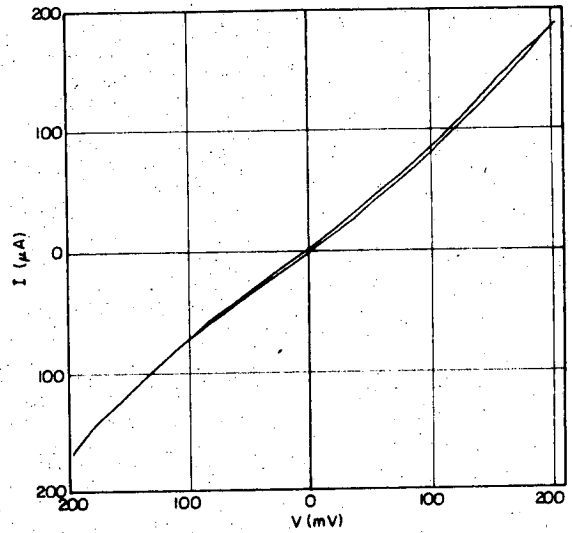


Fig. 3-21.
 Cyclic voltammogram for Rb in
 RbAlCl_4 (0.5 M)-PC.
 Reference electrode: Rb
 Sweep rate: 0.8 mV/sec
 Temperature: 30°C



XII. 728-1445

Fig. 3-22.
 Cyclic voltammogram for Rb(Hg) /
 RbAlCl_4 (0.5 M)-PC.
 Reference electrode: Rb(Hg)
 Amalgam composition: 0.2306%wt
 Sweep rate: 4 mV/sec.

in Figs. 3-21 and 3-22, respectively. Reversible behavior can be observed in both cases, and Tafel like behavior is evident at higher currents.

3.1-5. Cesium

Of the common cesium salts tried, only CsAlCl_4 ($\text{CsCl} + \text{AlCl}_3$) gave good solubility and a good deposit in PC. Cesium was deposited from CsClO_4 solution in PC, but because of the low solubility the current was very low and was accompanied by high applied potential. Gas evolution was observed during this experiment.

CsCl was found soluble in AlCl_3 solution in PC, while CsBr was found insoluble in the same AlCl_3 solution. Cesium was deposited from carefully dried CsAlCl_4 (0.25 m) solution in PC. Cesium deposit on a platinum electrode is shown in Fig. 3-23. A needle shaped cesium deposit is shown in Fig. 3-24. The experiment was conducted in a six-compartment cell, where two cesium electrodes, two cesium amalgam (0.302%wt) cup electrodes and two platinum electrodes served alternately as anode, reference electrode and cathode. The potential between the deposited cesium and the metallic cesium was below 20 mV and dropped significantly after a few hours of standing, due to the re-exposure of the platinum substrate. The composition of the Cs amalgam did not match the composition of the amalgam used by Bent, Forbes and Forziati,⁶⁷ who measured for the first time the standard electrode potential of cesium using a CsI solution in dimethylamine. The potential difference obtained in the present work was 1.017 ± 0.010 volts (0.302%wt), as compared to 1.119 volts (0.1875%wt) obtained by Bent, et al. at 25°C.

Micropolarizations of cesium in CsAlCl_4 (0.25 M) at four different temperatures are shown in Fig. 3-25. The exchange current densities i^0

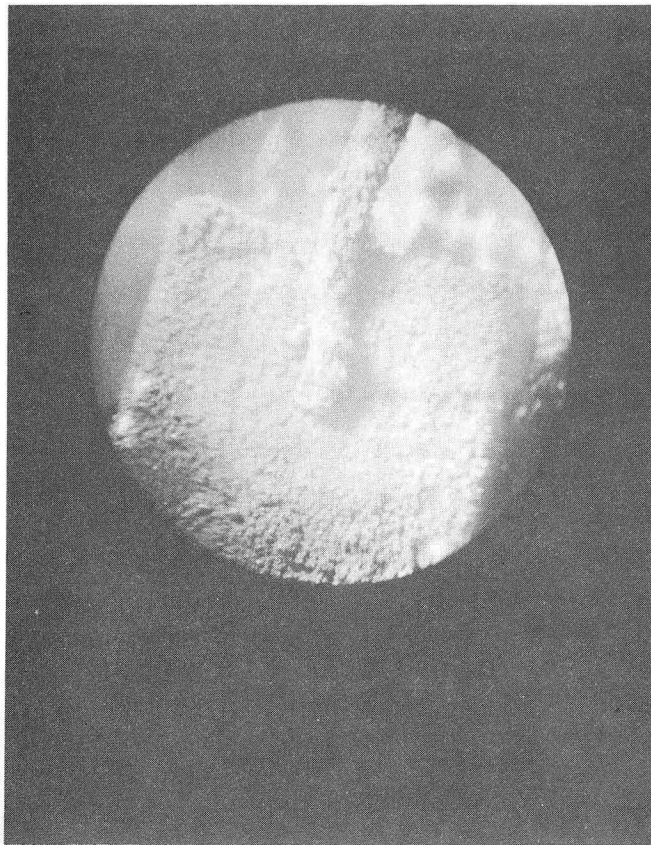
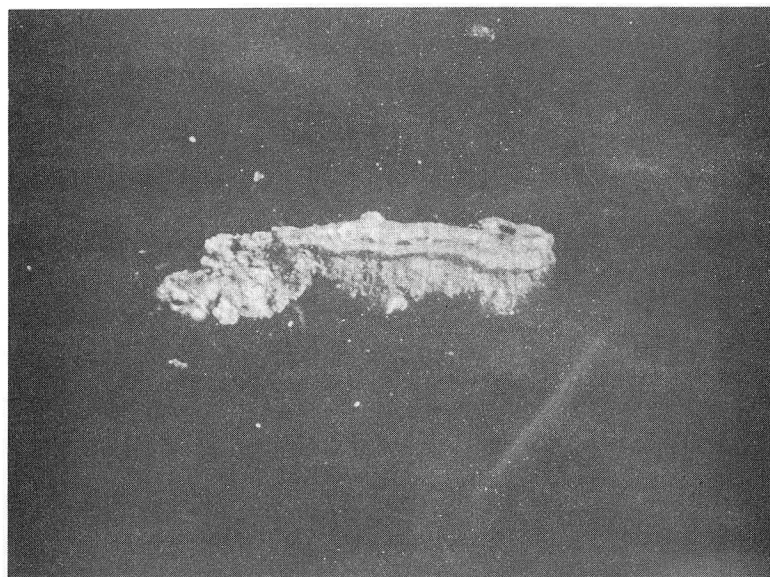
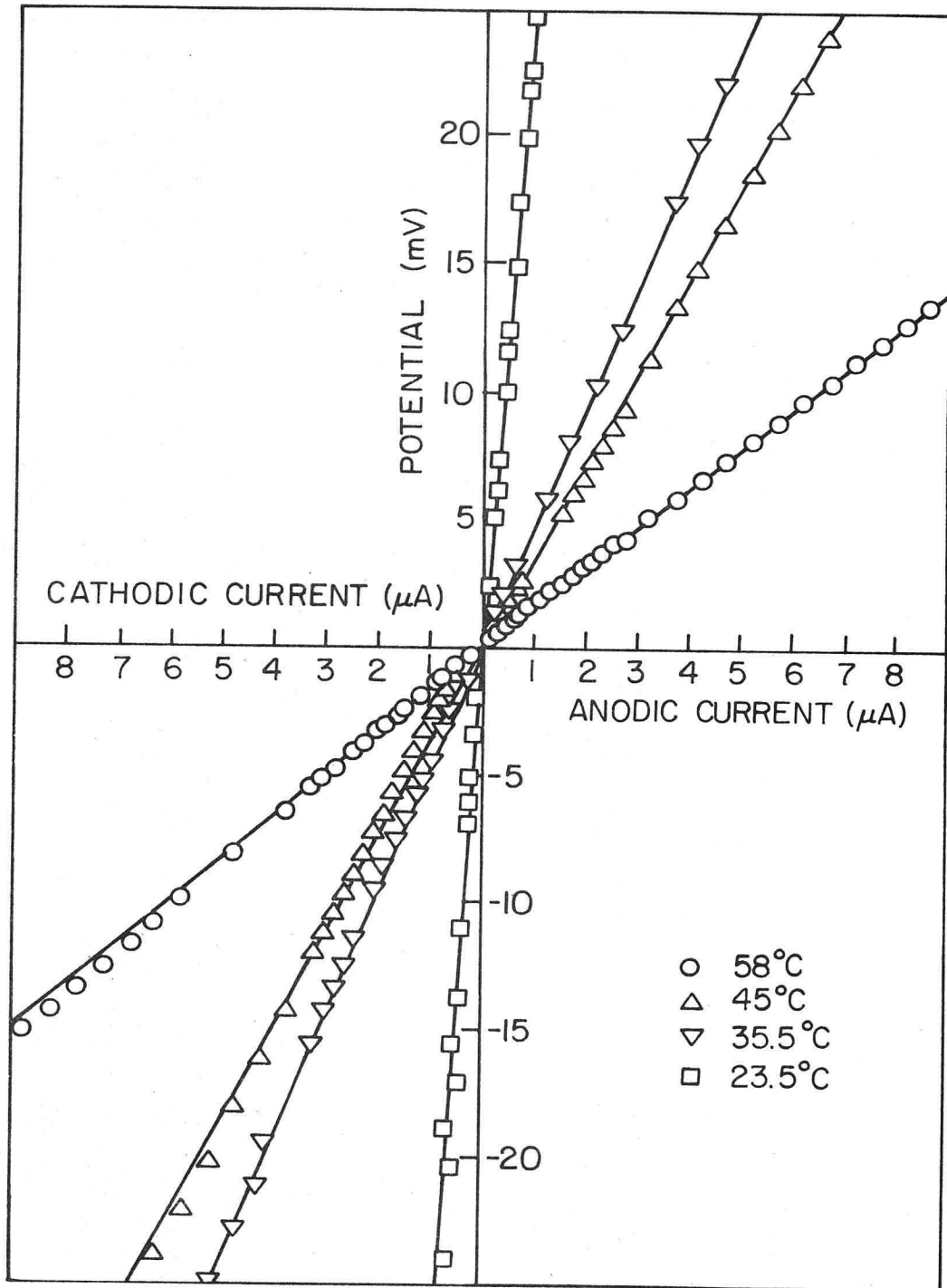


Fig. 3-23. Cesium deposit on a Pt foil cathod, from CsAlCl_4 (0.25m) solution in PC. Current density: 1 mA/cm^2 . Temperature: 25°C . Remark: Globules of molten Cs can be observed on the surface.



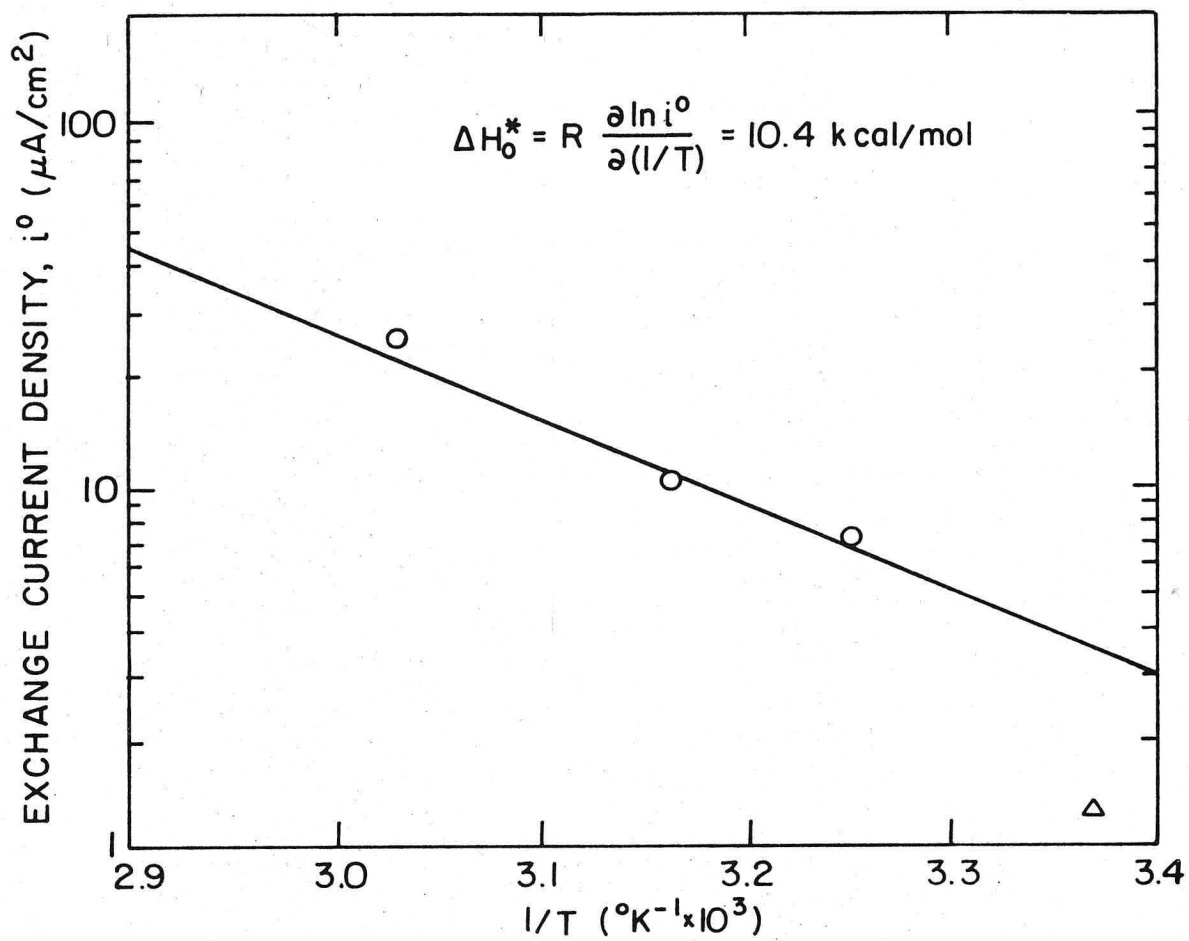
XBB 728-4118

Fig. 3-24. Needle-shape cesium deposit from CsAlCl_4 (1m) solution in PC. Current density: 2.0 mA/cm^2 . Temperature: 25°C . Length of the needle: 5 mm.



XBL 727-6643

Fig. 3-25. Micropolarization of Cs(s)/CsAlCl₄(0.25 M) in PC.



XBL 727-6628

Fig. 3-26. Determination of the enthalpy of activation at zero polarization of Cs(s)/CsAlCl₄(0.25 M), PC.

○ Solid Cs. △ Liquid Cs.

were calculated from the slopes and are plotted vs. $1/T$ in Fig. 3-26. The enthalpy of activation at zero polarization was calculated from the slope to be $\Delta H_o^* = 10.4$ kcal/mole. The exchange current at 23.5°C was lower than expected, probably because at 23.5°C Cs is a solid, while the other three temperatures were above the melting point of cesium, 28.4°C .

In addition to the galvanostatic deposition experiments, the deposition-dissolution of cesium on platinum electrode was investigated by a linear cyclic voltammetry technique. The potential between the working electrode and a reference cesium electrode was scanned in the cathodic and the anodic directions, and the current was recorded on an oscilloscope from the ohmic drop across a standard resistance. The solution was stirred during the experiment. The oscillograms in Figs. 3-27- 3-30 show the behavior of platinum, deposited cesium, metallic cesium and cesium amalgam in CsAlCl_4 (0.25 M) in PC at 25°C . The scanning rate was 0.25 V/sec.

Figure 3-27 shows the behavior of a clean platinum electrode. The anodic current is negligible due to the absence of active metal on the electrode. The cathodic current increases linearly with the scanning potential. The anodic branch following a single cathodic cycle shows a small current due to the redissolution of the deposited cesium. Scanning started from the far anodic side. Figure 3-28 shows the behavior of electrodeposited cesium on platinum substrate after four hours of cathodic deposition at 1 mA/cm^2 . The behavior is quite reversible and very similar to the behavior of pure metallic cesium in the same solution which is shown in Fig. 3-29. Figure 3-30 shows the behavior of cesium amalgam (0.2306%wt) in the same CsAlCl_4 (0.25 M) PC solution. The

-103-

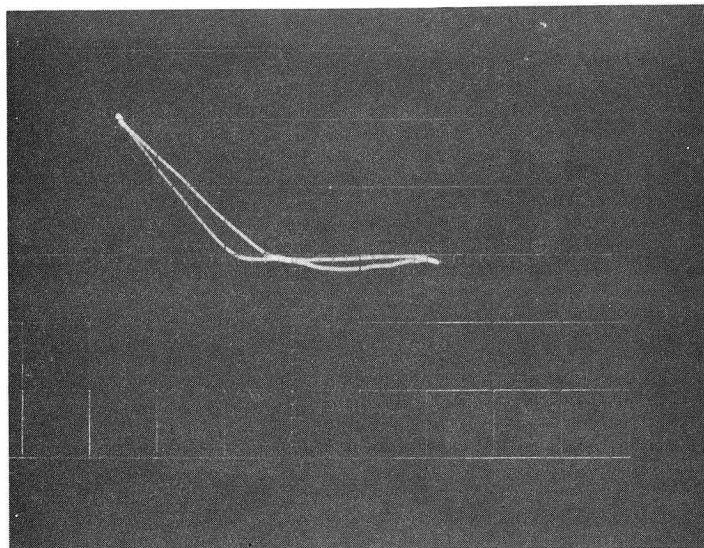
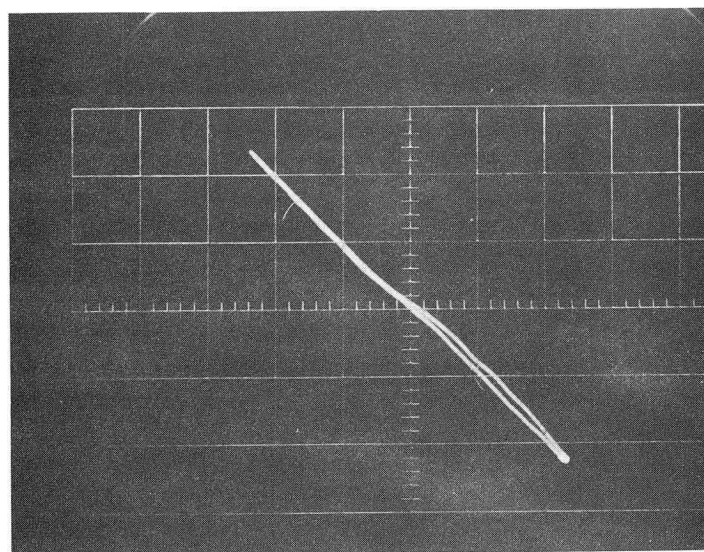


Fig. 3-27. Cyclic voltammogram of clean anodized Pt in CsAlCl_4 (0.25M). Scanning rate: 0.25 V/sec. Reference electrode: Cs. 0.8 V/cm, 0.25 mA/cm.



XBB 728-4112

Fig. 3-28. Cyclic voltammogram of Cs deposit on Pt electrode, in CsAlCl_4 (0.25 M). Scanning rate: 0.25 V/sec. Reference electrode: Cs. 0.8 V/cm, 0.25 mA/cm.

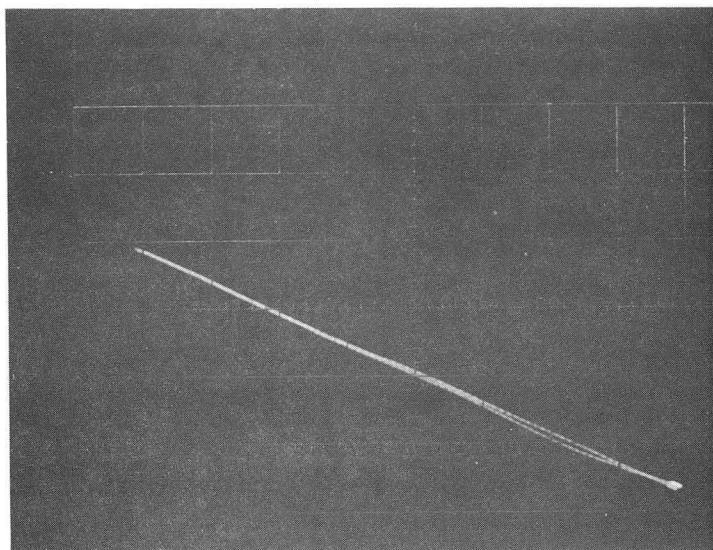
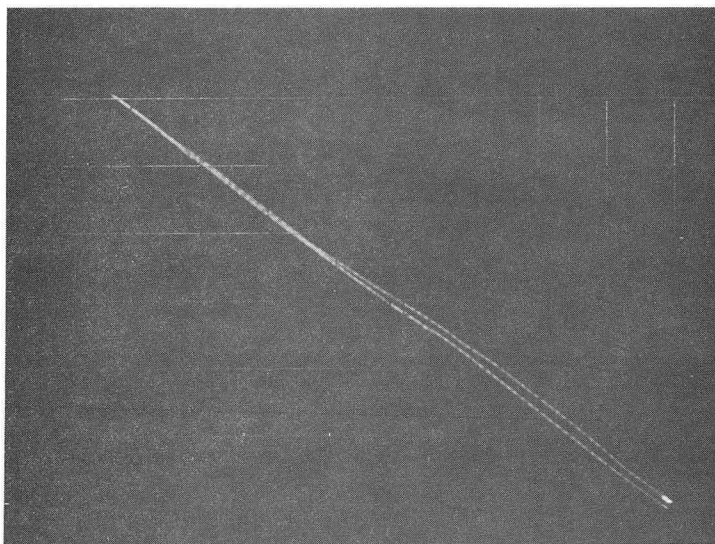


Fig. 3-29. Cyclic voltammogram of pure Cs electrode in CsAlCl_4 (0.25M). Scanning rate: 0.25 V/sec. Reference electrode: ^4Cs . 0.5 V/cm, 0.5 mA/cm.



XBB 728-4111

Fig. 3-30. Cyclic voltammogram of Cs(Hg) electrode 0.302%wt. in CsAlCl_4 (0.25M). Scanning rate: 0.25 V/sec. Reference electrode: Cs. 0.5 V/cm, 0.5 mA/cm.

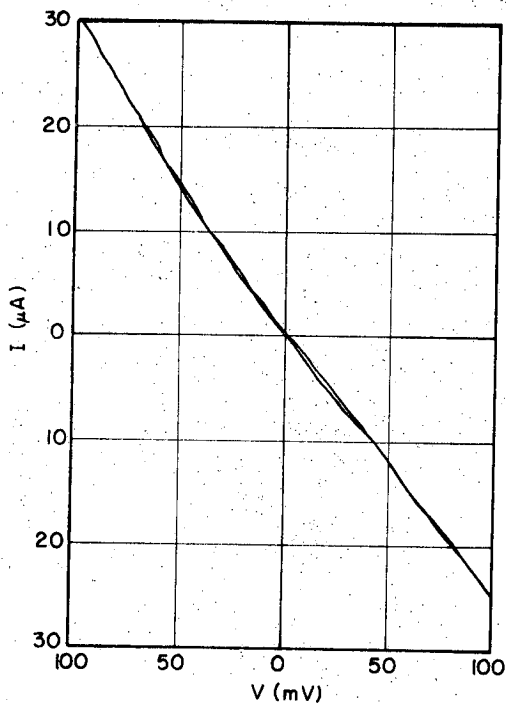


Fig. 3-31.
Cyclic voltammogram for Cs in
 $\text{CsAlCl}_4(0.25\text{M})\text{-PC}$.
Reference electrode: Cs
Sweep rate: 4 mV/sec.

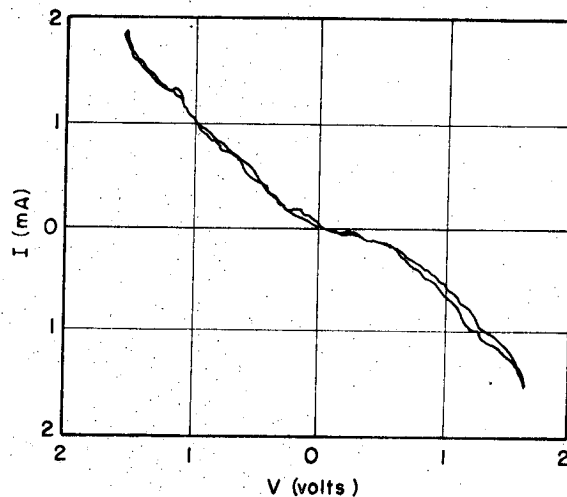


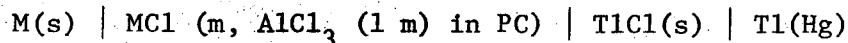
Fig. 3-32.
Cyclic voltammogram for Cs in
 $\text{CsAlCl}_4(0.25\text{M})\text{-PC}$.
Reference electrode: Cs
Sweep rate: 4 mV/sec.

behavior is again quite reversible. The solution was stirred during these experiments with a small magnetic stirrer to minimize concentration overpotential.

Figure 3-31 shows a cyclic voltammogram of Cs in CsAlCl_4 (0.25 M) in the linear region. Very good reversibility was observed. Figure 3-32 shows a cyclic voltammogram in the Tafel region. The behavior is reversible and symmetrical.

3.2. Cell Potentials of the Alkali Metal Chlorides in AlCl_3 (1 M)-PC Solutions

Tables 3-2 to 3-6 contain the results of the experimental measurements of the general cell:



at 25° and 35°C, where M represents Li, Na, K, Rb and Cs. The measurements were repeated for each metal at different alkali metal chloride molalities. The concentration of the thallium amalgam, the same in all experiments, was 4.749%wt.

The first column in each table gives the concentration of the alkali metal chloride in molality units (moles of MCl per 1000 gr of pure PC). The measured cell potential in volts is listed in the second column. This value for each concentration is the average value of the potential of the two alkali metal electrodes vs. the two reference electrodes. The potential difference between two thallium amalgam-thalious chloride reference electrodes was always smaller than 1 mV. The bias potential between the two alkali metal electrodes was different for the various metals. The bias potential was smaller than 1, 1, 10, 5, 5 millivolts for the Li, Na, K, Rb and Cs systems, respectively. The higher bias potential of the potassium

Table 3-2. Results of cell potential measurements, lithium system.

m	25°C			35°C		
	E	E ₁	E ₂	E	E ₁	E ₂
1.0	2.35715	2.26215	2.26215	2.35945	2.26145	2.26145
0.5	2.38480	2.28980	2.25419	2.38910	2.29110	2.25429
0.25	2.40440	2.30940	2.23818	2.40750	2.30950	2.23589
0.25	2.41790	2.32290	2.25168	2.42100	2.32300	2.24939
0.10	2.41600	2.32100	2.20270	2.41935	2.32135	2.19908
0.10	2.40900	2.31400	2.19570	2.41235	2.31535	2.19308
0.10	2.41990	2.32490	2.20660	2.42335	2.32535	2.20308
0.05	2.43710	2.34210	2.18819	2.44040	2.34240	2.18333
0.01	2.46010	2.36510	2.12550	2.46415	2.36615	2.12161
0.005	2.47070	2.37570	2.10349	2.47695	2.37895	2.09761
0.005	2.47400	2.37900	2.10679	2.48005	2.38205	2.10071
0.002	2.45915	2.36415	2.04486	2.46930	2.37130	2.04130

Table 3-3. Results of cell potential measurements, sodium system.

m	25°C			35°C		
	E	E ₁	E ₂	E	E ₁	E ₂
0.5	2.17905	2.08405	2.04844	2.18740	2.08940	2.05260
0.25	2.18750	2.09250	2.02128	2.19860	2.10060	2.02700
0.10	2.18630	2.09130	1.97300	2.20370	2.10570	1.98340
0.01	2.23400	2.13900	1.90240	2.25210	2.15410	1.90960
0.01	2.24460	2.14960	1.91300	2.26070	2.16270	1.91816

Table 3-4. Results of cell potential measurements, potassium system.

m	25°C			35°C		
	E	E ₁	E ₂	E	E ₁	E ₂
1.0	2.40420	2.30920	2.30920	2.42160	2.32360	2.32360
1.0	2.41305	2.31805	2.31805	2.43055	2.33255	2.33255
0.5	2.43620	2.34120	2.30560	2.45200	2.35400	2.31720
0.5	2.43320	2.33820	2.30260	2.44900	2.35100	2.31420
0.25	2.47260	2.37760	2.30640	2.51560	2.41760	2.34400
0.25	2.46850	2.37350	2.30230	2.51150	2.41350	2.33990
0.1	2.50715	2.41215	2.29385	2.52625	2.42825	2.30600
0.01	2.51085	2.41585	2.17925	2.53600	2.43800	2.19350
0.0025	2.50945	2.41445	2.10660	2.53050	2.43280	2.11435
0.0025	2.55075	2.45575	2.14790	2.57180	2.47410	2.15565

Table 3-5. Results of cell potential measurements, rubidium system.

m	25°C			35°C		
	E	E ₁	E ₂	E	E ₁	E ₂
1.0	2.35320	2.25820	2.25820	2.35365	2.25565	2.25565
0.5	2.45210	2.35710	2.32150	---	---	---
0.25	2.48670	2.39170	2.32050	---	---	---
0.10	2.47900	2.38400	2.26570	2.48950	2.39150	2.16920
0.10	2.47600	2.38100	2.26270	2.48720	2.38920	2.26690
0.05	2.47500	2.38000	2.22610	2.49160	2.39360	2.23450
0.01	2.49700	2.40200	2.16540	2.52380	2.42580	2.18130
0.0025	2.54000	2.44500	2.13720	2.59555	2.49755	2.17940

Table 3-6. Results of cell potential measurements, cesium system.

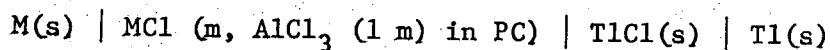
m	25°C			35°C		
	E	E ₁	E ₂	E	E ₁	E ₂
1.0	2.40265	2.30765	2.30765	2.41615	2.31815	2.31815
1.0	2.40350	2.30850	2.30850	2.41420	2.31620	2.31620
1.0	2.39700	2.30200	2.30200	2.41200	2.31400	2.31400
0.5	2.47550	2.38050	2.34490	2.49570	2.39770	2.36090
0.25	2.50815	2.41315	2.34190	2.53920	2.44120	2.36760
0.10	2.49020	2.39520	2.27690	2.52570	2.42770	2.30540
0.10	2.50470	2.40970	2.29140	2.53680	2.43880	2.31650
0.01	2.51510	2.42010	2.18350	2.55580	2.45780	2.21330
0.01	2.50980	2.41480	2.17820	2.55120	2.45320	2.20870
0.0025	2.55530	2.46030	2.15250	2.60580	2.50780	2.18965
0.0010	2.52900	2.43500	2.08000	2.58120	2.48320	2.11640

electrodes is due mainly to the reactivity of this metal towards the solvent. The bias potential of the Rb and Cs electrodes is due mainly to the great difficulties in handling these metals in the liquid state and to their reactivity towards the solvent.

The potential E_1 is tabulated in the third column and represents the corrected value of E for the thallium amalgam concentration. The correction was taken from the work of Daniels and Richards,¹³⁸ who measured the potentials between different thallium amalgam concentrations and pure thallium.

The function E_2 is listed in the fourth column and the method used to obtain this function is given below:

the potential of the cell



is given by

$$E_1 = E_1^{\circ} - RT/F \ln (m_{Cl^-} m_{M^+} \gamma_{Cl^-} \gamma_{M^+}) \quad (3-1)$$

where m is the molality and γ the activity coefficient of a particular ion. Since the molality of $AlCl_3$ is held constant, it is convenient to choose the reference state as $AlCl_3$ (1 m) in PC. By this convention, the solvent is considered to be a unit molality solution of $AlCl_3$ in PC and not pure PC as usual. The cell potential according to this convention is given by

$$E_1 = E_2^{\circ} - 2RT/F \ln (m_{MCl} \gamma_{MCl}) \quad (3-2)$$

where E_2° is the standard potential of the cell in $AlCl_3$ (1 m)-PC solution. The standard state of the solute is taken at infinite dilution of the alkali metal chloride in $AlCl_3$ (1 m)-PC solution where the activity coefficient of the alkali metal chloride approaches unity. The problem of determining E_2° and thus the activity coefficients at different concentrations of MCl involves extrapolation to infinite dilution. The method of extrapolation to infinite dilution using the Guggenheim equation¹⁵⁰ cannot be employed here since the ionic strength is very high. Instead, rearranging Eq. (3-2) gives

$$E_2 = (E_1 + 2RT/F \ln m_{MCl}) = E_2^{\circ} - 2RT/F \ln \gamma_{MCl} \quad (3-3)$$

Following the method presented by Lewis, Randall, Pitzer and Brewer¹⁵¹ pp. 315-316, if we plot the left-hand side of Eq. (3-3) as ordinate against some function of m_{MCl} as abscissa, the limit approached by the ordinate at dilution is equal to E_2° . It is common to extrapolate with $(m_{MCl})^{1/2}$ as abscissa since such a choice should give a curve approximating to linearity at high dilution following Debye-Hückel limiting law.

However, here this dependence is used to expand the low concentration range. Figures 3-33 and 3-34 show the plot of E_2 vs. $(m_{MCl})^{1/2}$ for all the alkali metals at 25° and 35°C, respectively. The intercepts at zero molalities give E_2^0 , the standard potentials at $AlCl_3$ (1 m)-PC solution. The difference between the extrapolated values at 25° and 35°C gives the temperature dependence of the standard potential at constant pressure. The results of the extrapolations are given in Table 3-7.

Table 3-7. Standard cell potentials at 25° and 35°C.

Metal	E_2^0 25°C	E_2^0 35°C	$(\partial E_2^0/\partial T)_p$
Li	2.045±0.010	2.037±0.010	-0.8 10^{-3}
Na	1.885	1.878	-0.7 10^{-3}
K	2.116	2.120	+0.4 10^{-3}
Rb	2.116	2.140	+2.4 10^{-3}
Cs	2.122	2.165	+4.3 10^{-3}

From the standard cell potentials and their variation with temperature, the standard free energy ΔG_2^0 , entropy ΔS_2^0 and enthalpy ΔH_2^0 can be calculated:

$$\Delta G_2^0 = -n F E_2^0 \quad (3-4)$$

$$\Delta S_2^0 = -n F (\partial E_2^0/\partial T)_p \quad (3-5)$$

$$\Delta H_2^0 = -n F (E_2^0 - T(\partial E_2^0/\partial T)_p) \quad (3-6)$$

These functions are related to the following cell reaction:

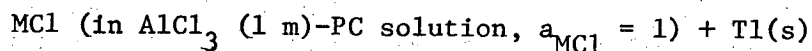
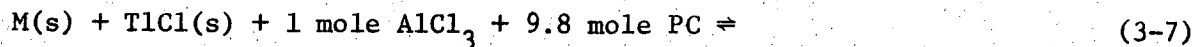


Table 3-8 presents ΔG_2^0 , ΔS_2^0 and ΔH_2^0 on the molal scale for the above cell reaction at 25° and 35°C. The uncertainty in ΔS_2^0 and ΔH_2^0 is quite high

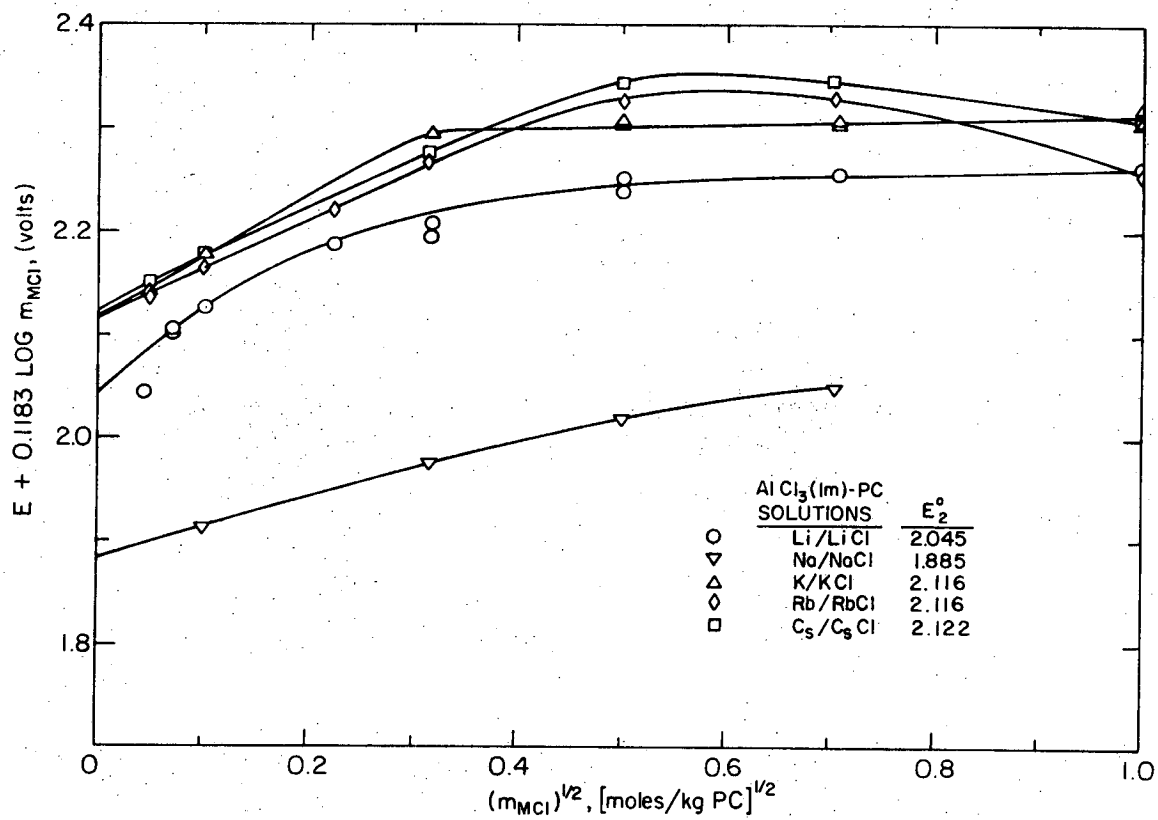
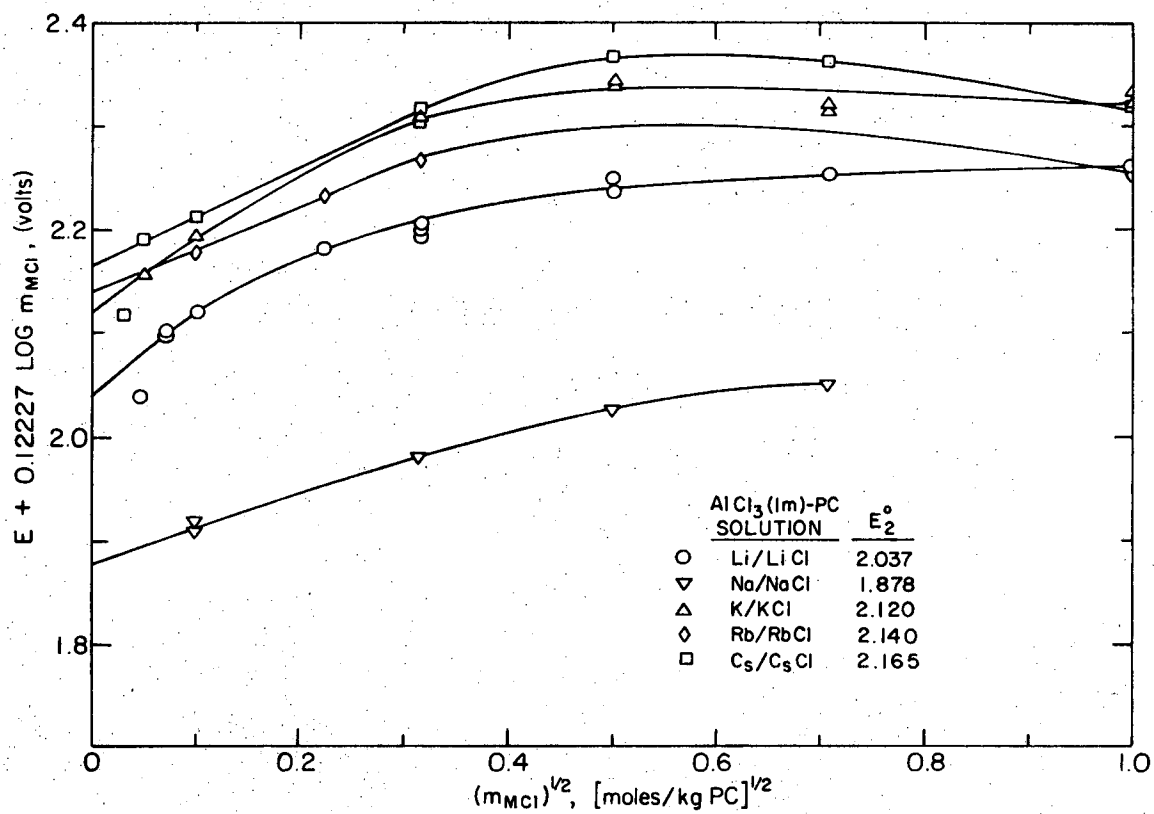


Fig. 3-33.

XBL725-6286

EMF measurements of the cell: M/MCl(m), AlCl₃(lm)-PC/TlCl(s), Tl(s) at 25°C.



XBL725-6287

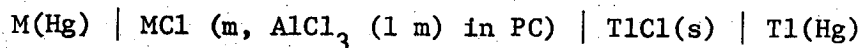
Fig. 3-34. EMF measurements of the cell: M/MCl(m), AlCl₃(lm)-PC/TlCl(s), Tl(s) at 35°C.

because they were calculated from the difference between extrapolated values.

Table 3-8. Standard free energies, entropies and enthalpies for reaction (3-7) for all the alkali metals.

Metal	ΔG_2° kcal/mol		ΔS_2° , e.u.	ΔH_2° kcal/mol	
	25°C	35°C	25°C	25°C	35°C
Li	-47.17	-46.98	-18.4	-52.7	-52.7
Na	-43.47	-43.31	-16.1	-48.3	-48.3
K	-48.80	-48.90	+ 9.2	-46.0	-46.1
Rb	-48.80	-49.36	+55.3	-32.3	-32.3
Cs	-48.94	-49.93	+64.7	-29.6	-29.6

In addition, EMFS of the cell



were measured. In this cell, the alkali metal amalgam was substituted for the pure alkali metal. The results are presented in Tables 3-9 to 3-13. The concentrations of the alkali metal amalgams were adjusted to the exact concentrations of the amalgams used by G. N. Lewis and his co-workers,^{28,62,63,66} and H. E. Bent and his co-workers.⁶⁷ This was done in order to be able to make comparisons with EMF data for the single amalgam concentrations listed in the literature. In the case of lithium amalgam, the activity coefficient data of lithium was obtained from the work of Cogley and Butler.³⁹ The potential differences between the amalgams and the pure alkali metals obtained from these references were added to the cell potentials in order to obtain the potentials between the pure metals and the thallium amalgam-thallos chloride reference electrode. The results were corrected as before for the thallium amalgam composition. The first column in Tables 3-9 to 3-13 gives the concentrations of the

alkali metal chlorides in molality units (moles of NCl per 1000 gr of pure PC). The measured cell potentials are listed in the second column. The third column gives the corrected potentials, i.e. the sums of the measured potentials and the potentials of the amalgams obtained from the literature. The fourth column presents the potential E_1 , which is the corrected value of E for the thallium amalgam composition.¹³⁸ The function E_2 is listed in the fifth column. The method used for obtaining E_2 has been described previously with regard to Tables 3-2 to 3-6. The cesium amalgam concentration did not match the concentration used by Bent, et al.,⁶⁷ and the correction was obtained from the average of 5 measurements of the potential difference between this amalgam and pure cesium in CsCl-AlCl_3 (1 m)-PC solutions. The agreement between the measurements based on the alkali metal amalgams and those based on the pure alkali metals increases the confidence in the data.

Table 3-9. Results of cell potential measurements at 25°C, lithium amalgam.

Lithium amalgam composition: 0.0672%wt

$E_{\text{Li-Li(Hg)}} = 1.004$ volt

$E_{\text{Li-Li(Hg)}} = 1.0037$ volt D. R. Cogley and J. N. Butler.³⁹

Table 3-10. Results of cell potential measurements at 25°C, sodium amalgam.

m	E'	E	E ₁	E ₂
0.5	1.33640	2.18200	2.08700	2.05140
0.25	1.34700	2.19290	2.09790	2.02670
0.25	1.34780	2.19370	2.09870	2.02750
0.10	1.36955	2.21545	2.12045	2.00215
0.10	1.36805	2.21395	2.11895	2.00065
0.01	1.41210	2.25800	2.16300	1.92600
0.01	1.39380	2.23970	2.14470	1.90810

Sodium amalgam composition: 0.2062%wt

$E_{\text{Na-Na(Hg)}} = 0.843$ volts

$E_{\text{Na-Na(Hg)}} = 0.8456$ volts G. N. Lewis and
C. A. Kraus.⁶³

Table 3-11. Results of cell potential measurements at 25°C, potassium amalgam.

m	E'	E	E ₁	E ₂
1.0	1.38950	2.43760	2.34260	2.34260
0.5	1.38235	2.43045	2.33545	2.29985
0.5	1.40145	2.44955	2.35455	2.31895
0.5	1.40660	2.45540	2.36040	2.32480
0.25	1.42900	2.47710	2.38210	2.31090
0.10	1.45800	2.50610	2.41110	2.29280
0.10	1.46000	2.50810	2.41310	2.29480
0.01	1.45985	2.54795	2.41295	2.17635
0.01	1.45965	2.50775	2.41275	2.17615
0.0025	1.50265	2.55075	2.45575	2.14790

Potassium amalgam composition: 0.2216%wt.

$E_{\text{K-K(Hg)}} = 1.0523$ volt.

$E_{\text{K-K(Hg)}} = 1.0481$ volts G. N. Lewis and F. G. Keyes.⁶²

Table 3-12. Results of cell potential measurements at 25°C, rubidium amalgam.

m	E'	E	E ₁	E ₂
1.0	1.28200	2.35650	2.26150	0.26150
0.1	1.40780	2.48230	2.38730	2.26900

Rubidium amalgam composition: 0.2306%wt.

$E_{\text{Rb-Rb(Hg)}} = 1.0766$ volts

$E_{\text{Rb-Rb(Hg)}} = 1.0745$ volts G. N. Lewis and
W. L. Argo⁶⁶

Table 3-13. Results of cell potential measurements at 25°C, cesium amalgam.

m	E'	E	E ₁	E ₂
1.0	1.36350	2.38050	2.28550	2.28550
0.5	1.45650	2.47350	2.37850	2.34290
0.25	1.45400	2.47100	2.37600	2.30480
0.10	1.47400	2.49100	2.39600	2.27770
0.01	1.50750	2.52450	2.42950	2.19290

Cesium amalgam composition: 0.302%wt.

$E_{\text{Cs-Cs(Hg)}} = 1.017$ volts.

H. E. Bent, G. S. Forbes and A. F. Forziati:⁶⁷

Cesium amalgam composition: 0.1875%wt

$E_{\text{Cs-Cs(Hg)}} = 1.119$ volts.

3.3 Activity Coefficients of the Alkali Metal Chlorides in AlCl₃ (1 m)-PC Solution

Mean molal activity coefficients of the alkali metal chlorides in AlCl₃ (1 m) solution in PC were calculated from

$$\ln \gamma_{MCl} = (2RT/F) (E_2^{\circ} - E_2) - \ln m_{MCl} \quad (3-8)$$

where E_2° is the extrapolated value of the standard cell potential given in Table 3-7. The calculated activity coefficients at 25°C are given in Tables 3-14 to 3-18. Figure 3-35 presents the plots of $\ln \gamma_{MCl}$ vs. $(m_{MCl})^{1/2}$ for all the alkali metal chlorides. It should be mentioned again that the reference state is AlCl₃ (1 m) in PC and not the pure solvent.

Table 3-14. Activity Coefficients of LiCl in AlCl₃ (1 m)-PC at 25°C

m_{LiCl}	$-\ln \gamma_{LiCl}$
1.0	4.0513
0.5	3.8922
0.25	3.5936
0.25	3.8444
0.10	2.9004
0.10	2.7411
0.10	2.9470
0.05	2.6037
0.01	1.4271
0.005	0.9623
0.005	0.9888

Table 3-15. Activity coefficients of NaCl in AlCl₃ (1 m)-PC at 25°C

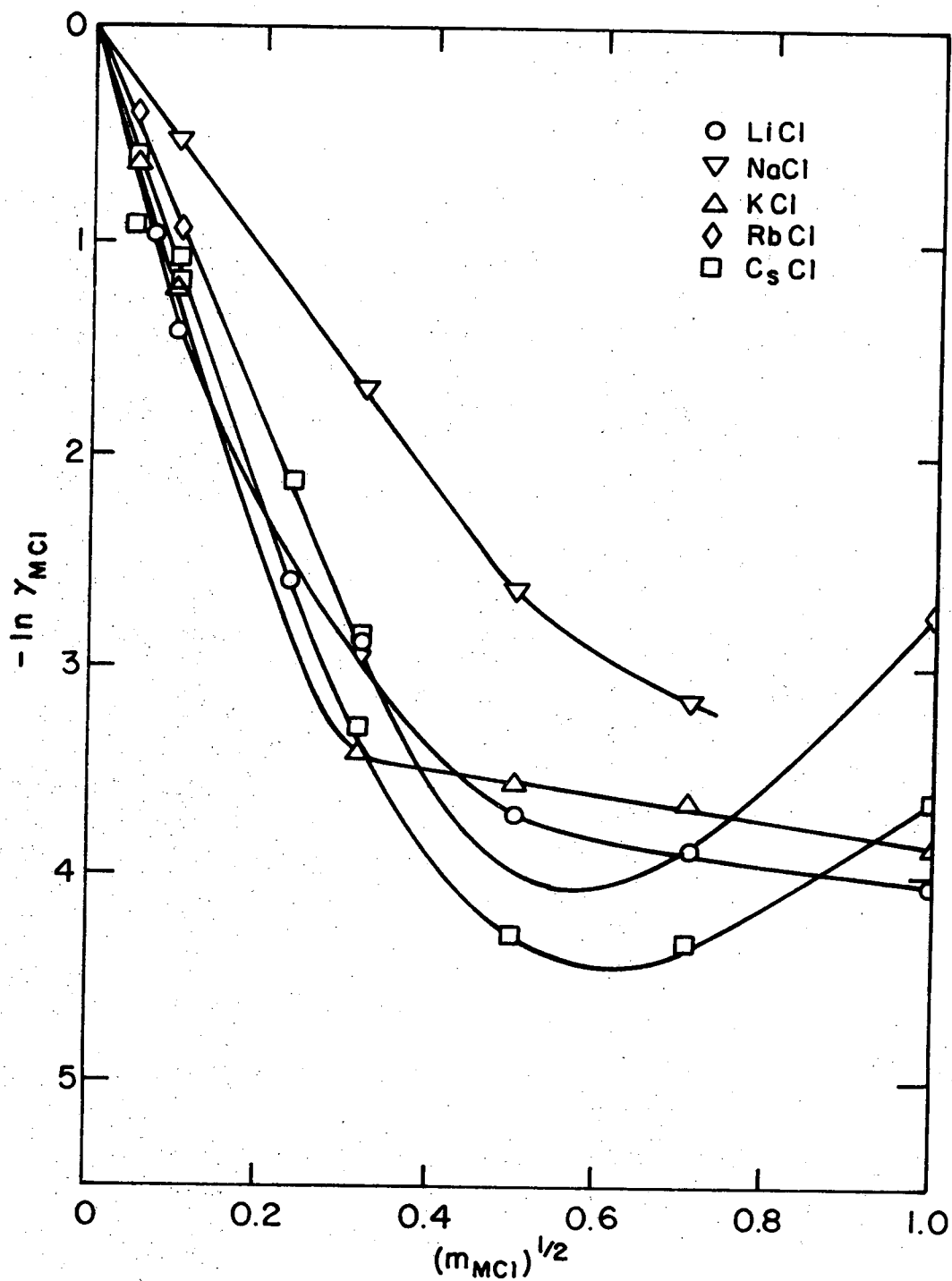
m_{NaCl}	$-\ln \gamma_{NaCl}$
0.5	3.1811
0.25	2.6521
0.10	1.7129
0.01	0.3387
0.01	0.5450

Table 3-16. Activity coefficients of KCl in AlCl_3 (1 m)-PC at 25°C.

m_{KCl}	$-\ln\gamma_{\text{KCl}}$
1.0	3.722
1.0	3.894
0.5	3.652
0.5	3.593
0.25	3.667
0.25	3.586
0.10	3.423
0.01	1.193
0.0025	0.631

Table 3-17. Activity coefficients of RbCl in AlCl_3 (1 m)-PC at 25°C.

m_{RbCl}	$-\ln\gamma_{\text{RbCl}}$
1.0	2.7678
0.5	
0.25	
0.1	2.913
0.1	2.856
0.05	2.143
0.01	0.961
0.0025	0.412



XBL 725-6280

Fig. 3-35. Activity coefficients of the alkali metal chlorides in $AlCl_3(lm)$ -PC solution at $25^\circ C$.

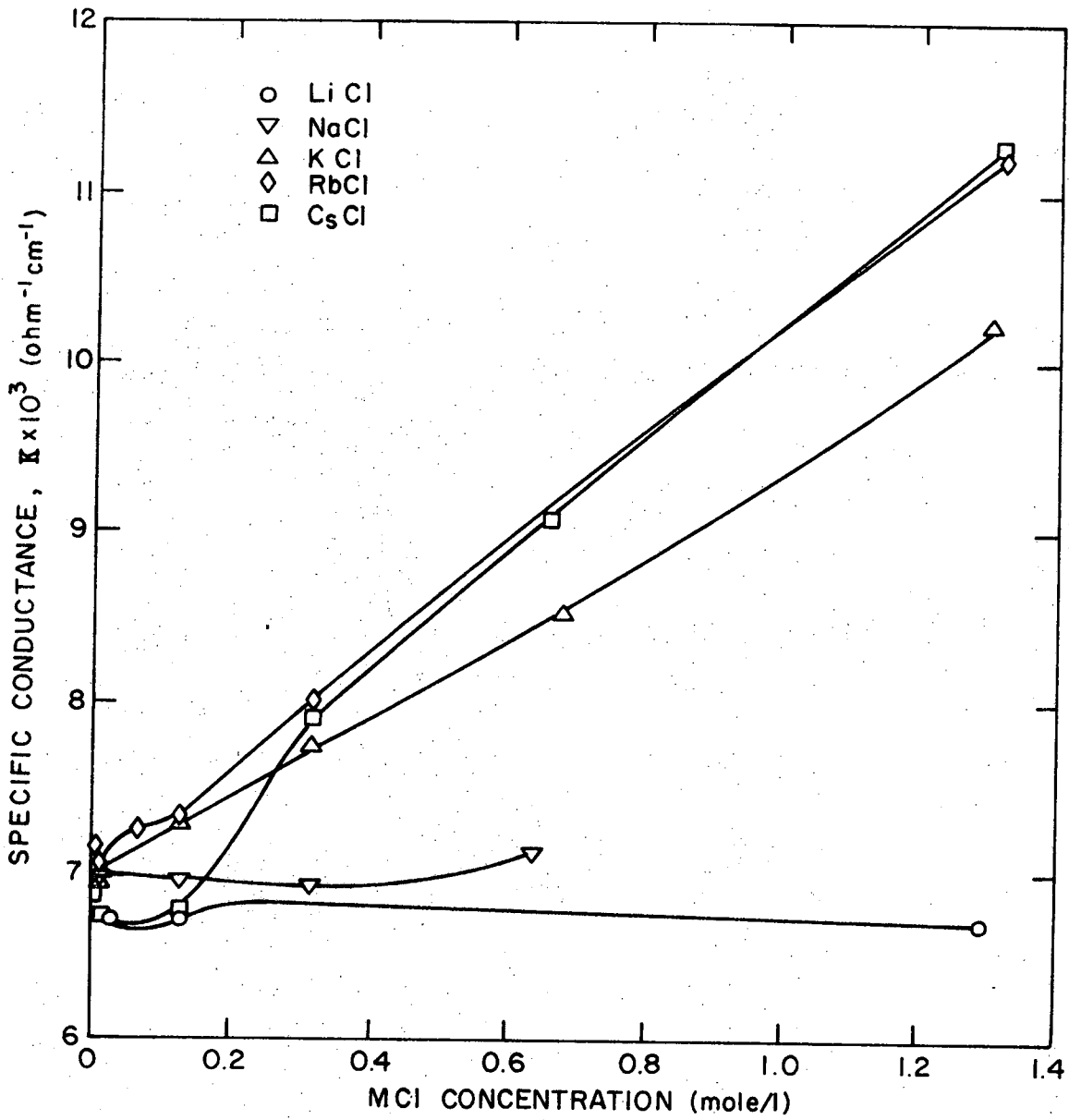
Table 3-18. Activity coefficients of CsCl in AlCl₃ (1 m)-PC at 25°C.

m_{CsCl}	$-\ln \gamma_{\text{CsCl}}$
1.0	3.730
1.0	3.746
0.5	4.455
0.25	4.398
0.10	3.132
0.10	3.414
0.01	1.314
0.01	1.211
0.0025	0.710
0.0025	1.035

3.4. Conductance of the Alkali Metal Chlorides in AlCl₃ (1 m)-PC Solution

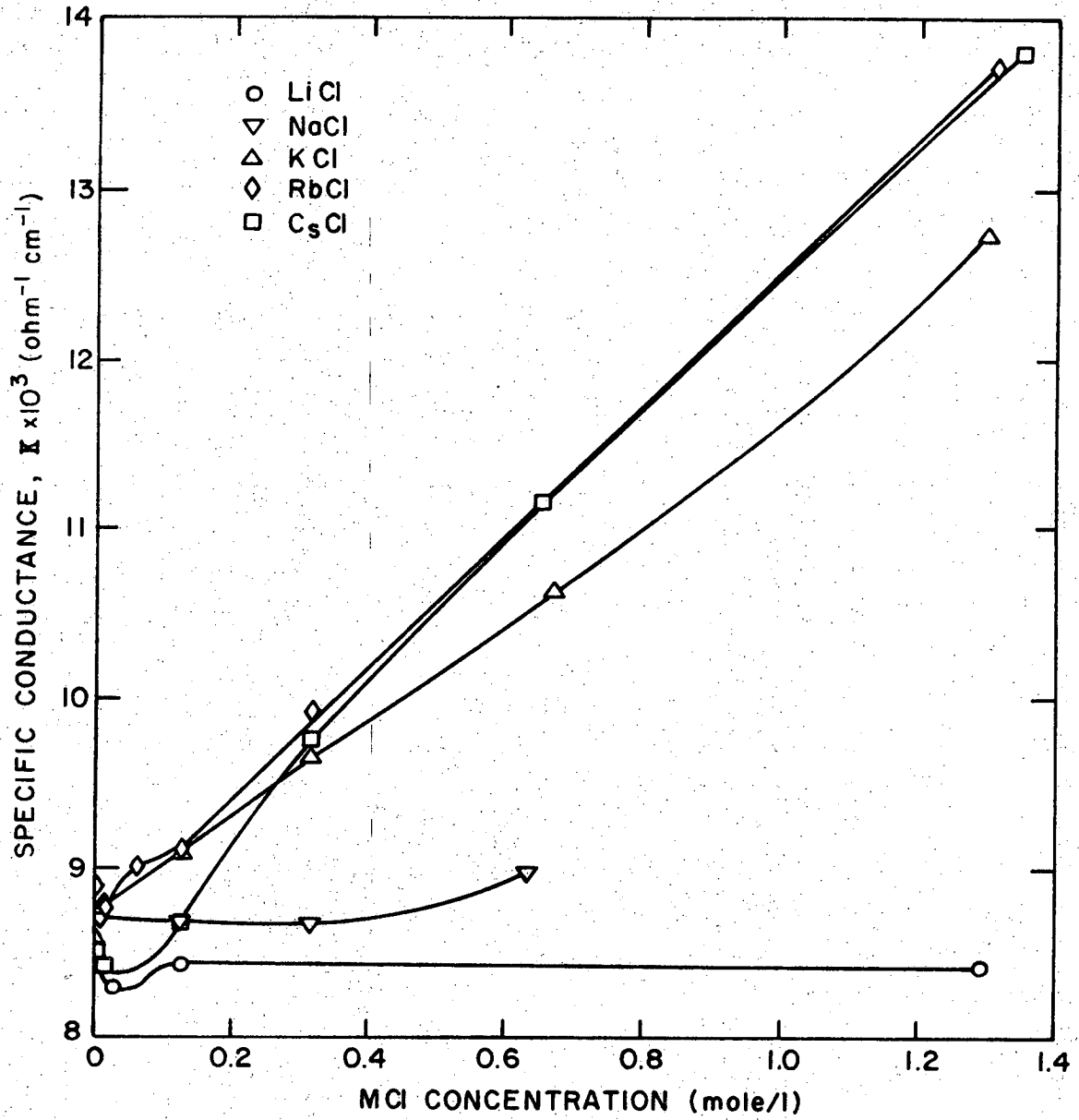
The specific conductance of the alkali metal chlorides in AlCl₃ (1 m)-PC solution at 25° and 35°C is given in Tables 3-19 to 3-23. The concentration is given on molarity basis (mole/lit.) and was transferred from the molality basis by multiplying by the density of the solution. The densities of solutions of different alkali metal chloride molalities are measured and the results are presented in the next section.

The concentration of the alkali metal chlorides were measured from zero up to 1 m, which corresponds to 1:1 ratio between MCl and AlCl₃. Figure 3-36 and Fig. 3-37 present the specific conductance of the alkali metal chlorides vs. their molarities at 25° and 35°C, respectively.



XBL725-6283

Fig. 3-36. Specific conductance of the alkali metal chlorides in AlCl₃(lm)-PC solution at 25°C.



XBL725-6282

Fig. 3-37. Specific conductance of the alkali metal chlorides in AlCl₃(lm)-PC solution at 35°C.

Table 3-19. Specific conductance of LiCl in AlCl₃ (1 m)-PC solution at 25° and 35°C.

m(mole/Kg PC)	C(mole/l)		10 ³ κ(ohm ⁻¹ cm ⁻¹)	
	25°C	35°C	25°C	35°C
0.02	0.0251	0.0250	6.7089	8.3150
0.1	0.1262	0.1253	6.7419	8.4429
1.0	1.2594	1.2512	6.7007	8.4348

Table 3-20. Specific conductance of NaCl in AlCl₃ (1 m)-PC solution at 25° and 35°C.

m(mole/Kg PC)	C(mole/l)		10 ³ κ(ohm ⁻¹ cm ⁻¹)	
	25°C	35°C	25°C	35°C
0.01	0.01262	0.01253	6.9710	8.7023
0.10	0.1264	0.1253	6.9555	8.6937
0.25	0.3163	0.3138	6.9100	8.6628
0.50	0.6330	0.6279	7.1190	8.9416

Table 3-21. Specific conductance of KCl in AlCl₃ (1 m)-PC solution at 25° and 35°C.

m(mole/Kg PC)	C(mole/l)		10 ³ κ(ohm ⁻¹ cm ⁻¹)	
	25°C	35°C	25°C	35°C
0.0025	0.00315	0.00313	6.915	8.5916
0.01	0.01262	0.01253	6.9943	8.7631
0.10	0.1261	0.1254	7.2784	9.1085
0.25	0.3167	0.3143	7.7540	9.6490
0.50	0.6390	0.6330	8.5166	10.630
1.00	1.300	1.292	10.2100	12.7256

Table 3-22. Specific conductance of RbCl in AlCl_3 (1 m)-PC solution at 25° and 35°C.

m(mole/Kg PC)	C(Mole/l)		$10^3 \kappa(\text{ohm}^{-1} \text{cm}^{-1})$	
	25°C	35°C	25°C	35°C
0.0025	0.00315	0.00313	7.1573	8.9144
0.01	0.01263	0.01254	7.0414	8.7439
0.05	0.06325	0.06266	7.2424	9.0206
0.10	0.1272	0.1261	7.2947	9.1010
0.25	0.3194	0.3168	8.0225	9.9509
0.50				
1.00	1.3195	1.3091	11.0033	13.7197

Table 3-23. Specific conductance of CsCl in AlCl_3 (1 m)-PC solution at 25° and 35°C.

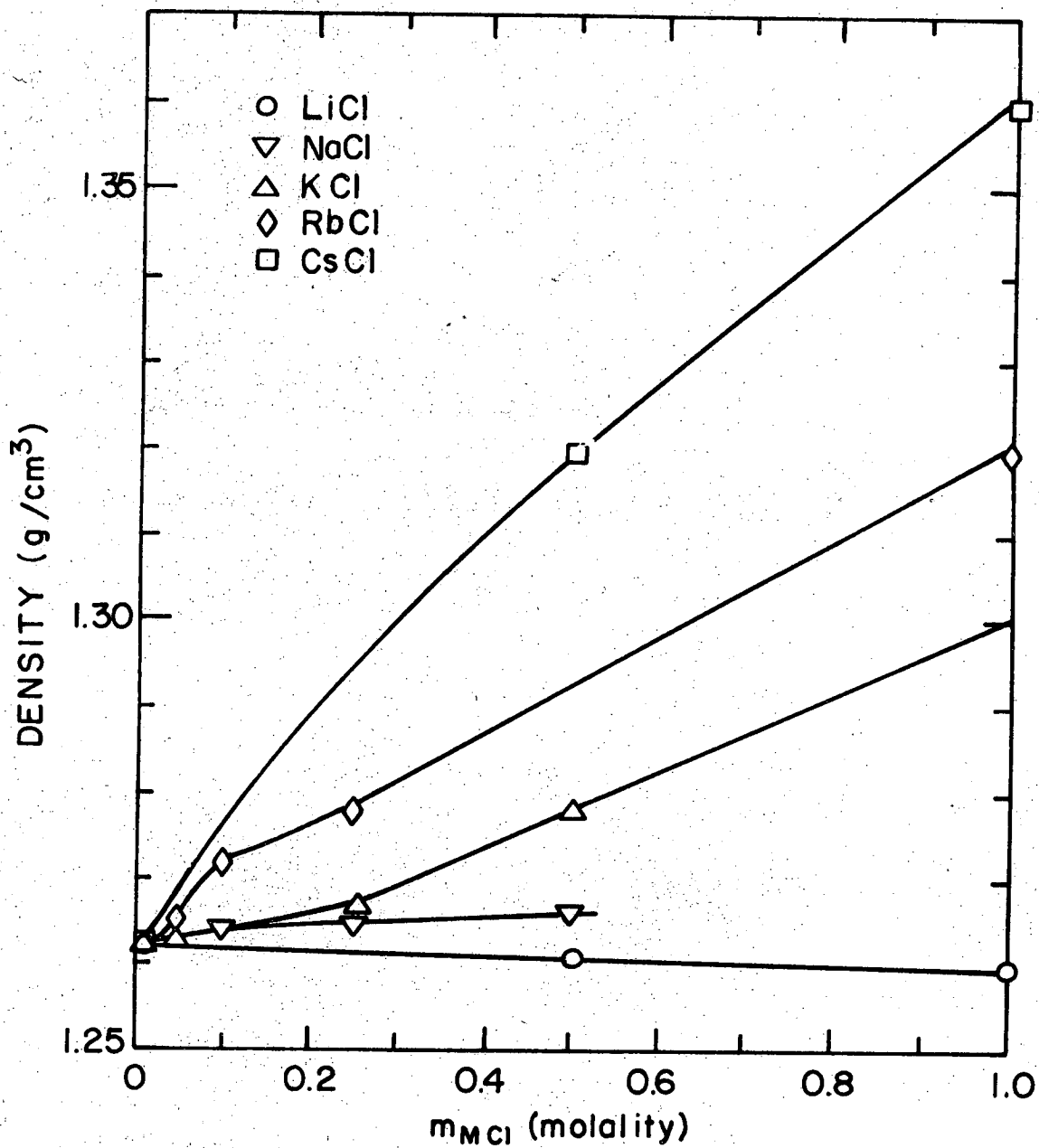
m(mole/Kg PC)	C(Mole/l)		$10^3 \kappa(\text{ohm}^{-1} \text{cm}^{-1})$	
	25°C	35°C	25°C	35°C
0.0025	0.00313	0.3133	6.8481	8.5084
0.01	0.01264		6.7326	8.4106
0.10	0.1264		6.7731	8.6765
0.25			7.9105	9.7563
0.50	0.6597	0.6555	9.0709	11.1713
1.00	1.3597	1.3481	11.2572	13.8060

3.5. Density Measurements

Densities of different molalities of the alkali metal chlorides in AlCl_3 (1 m)-PC solution at 25° and 35°C are presented in Table 3-24. Figure 3-38 and Fig. 3-39 show the density vs. the molality for each alkali metal chloride in AlCl_3 (1 m)-PC at 25° and 35°C, respectively.

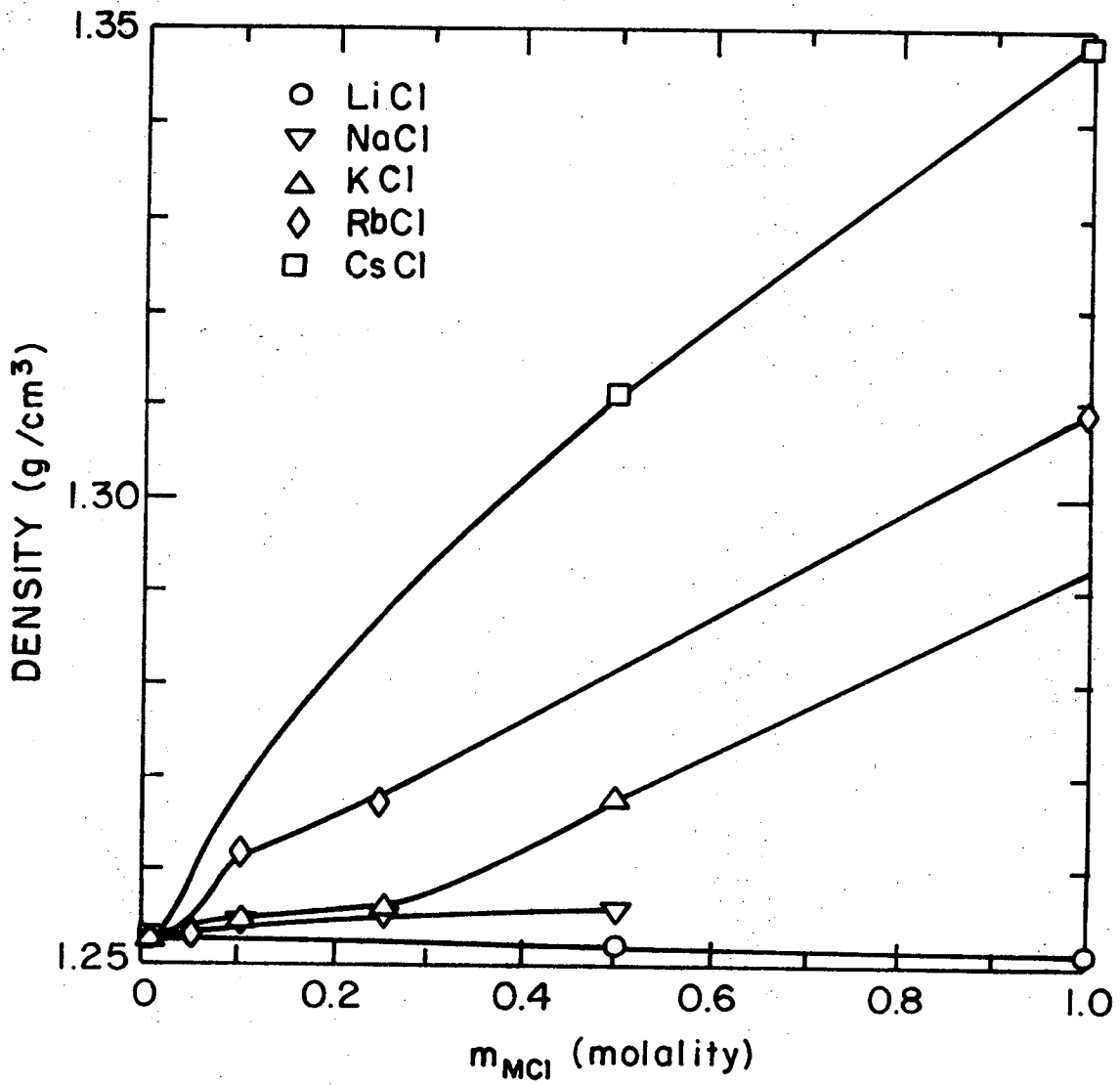
Table 3-24. Densities of the alkali metal chlorides
in AlCl_3 (1 m)-PC at 25° and 35°C.

Salt	m(Mole/Kg PC)	ρ 25°C(gr/cc)	ρ 35°C(gr/cc)
----	----	1.26284	1.25296
LiCl	0.5	1.26135	1.2185
	1.0	1.25945	1.25122
NaCl	0.01	1.26214	1.25262
	0.10	1.26378	1.25349
	0.25	1.26503	1.25516
	0.50	1.26608	1.25579
KCl	0.0025	1.26158	1.25251
	0.01	1.26245	1.25272
	0.10	1.26151	1.25432
	0.25	1.26692	1.25736
	0.50	1.27805	1.26789
	1.00		
RbCl	0.01	1.26319	1.25370
	0.05	1.26507	1.25317
	0.10	1.27236	1.26140
RbCl	0.25	1.27770	1.26723
	0.50		
	1.00	1.31955	1.30909
CsCl	0.0025	1.26367	1.25314
	0.01	1.26367	
	0.50	1.31942	1.31097
	1.00	1.35967	1.34812



XBL 727-6625

Fig. 3-38. Densities of the alkali metal chlorides in $\text{AlCl}_3(\text{lm})\text{-PC}$ solution at 25°C .



XBL 727 - 6626

Fig. 3-39. Densities of the alkali metal chlorides in AlCl₃(1m)-PC solution at 35°C.

3.6. Micropolarization Measurements of the Alkali Metals
in their chloride solutions in AlCl₃ (1 m)-PC

Micropolarizations of the alkali metals in different molalities of alkali metal chlorides in AlCl₃ (1 m)-PC solution are presented in Figs. 3-40 through 3-44. The temperature was held constant at 25°±0.01°C. The overpotentials are IR-free, and the ohmic drop was estimated from the current interrupter technique (see Section 2.4-1). At low overpotentials, linear behavior was observed for all the metals; deviation from linearity was observed at potentials above approximately 50 mV, where the non-linear Tafel behavior became appreciable. Deviations from linearity were also caused by concentration overpotential, which becomes significant at higher currents, especially in the cases of Rb and Cs, where the metals were placed in the cup electrodes, the active surfaces facing upward, and the solutions stirred from underneath the cups.

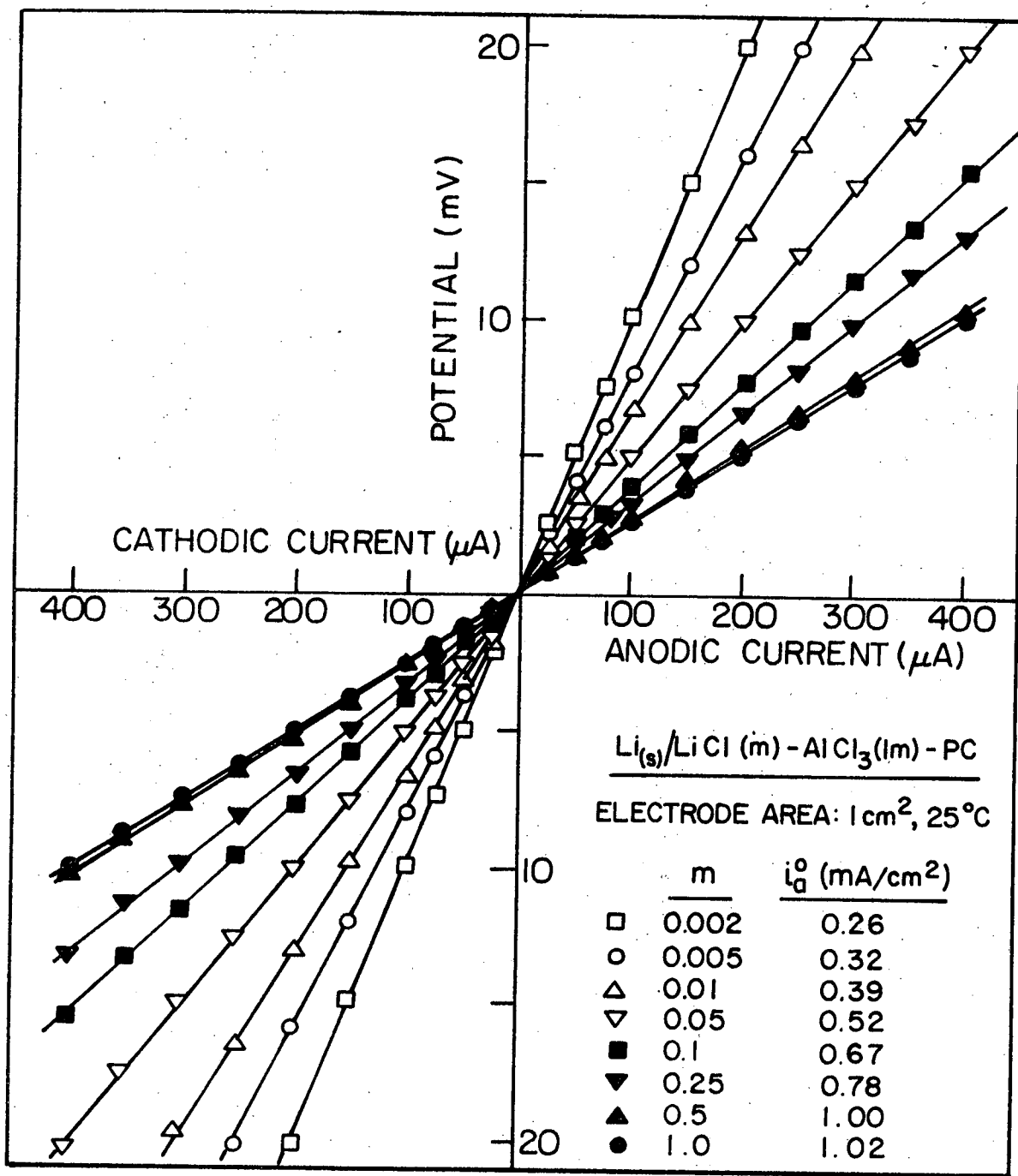
The exchange current densities were calculated from the slopes of the linear polarizations, according to the equation

$$i_a^o = \frac{1}{A} \frac{RT}{F} \frac{\partial i}{\partial \eta} \Big|_{i=0} \quad (3-9)$$

and the results are presented in each figure (Fig. 3-40 through 3-44).

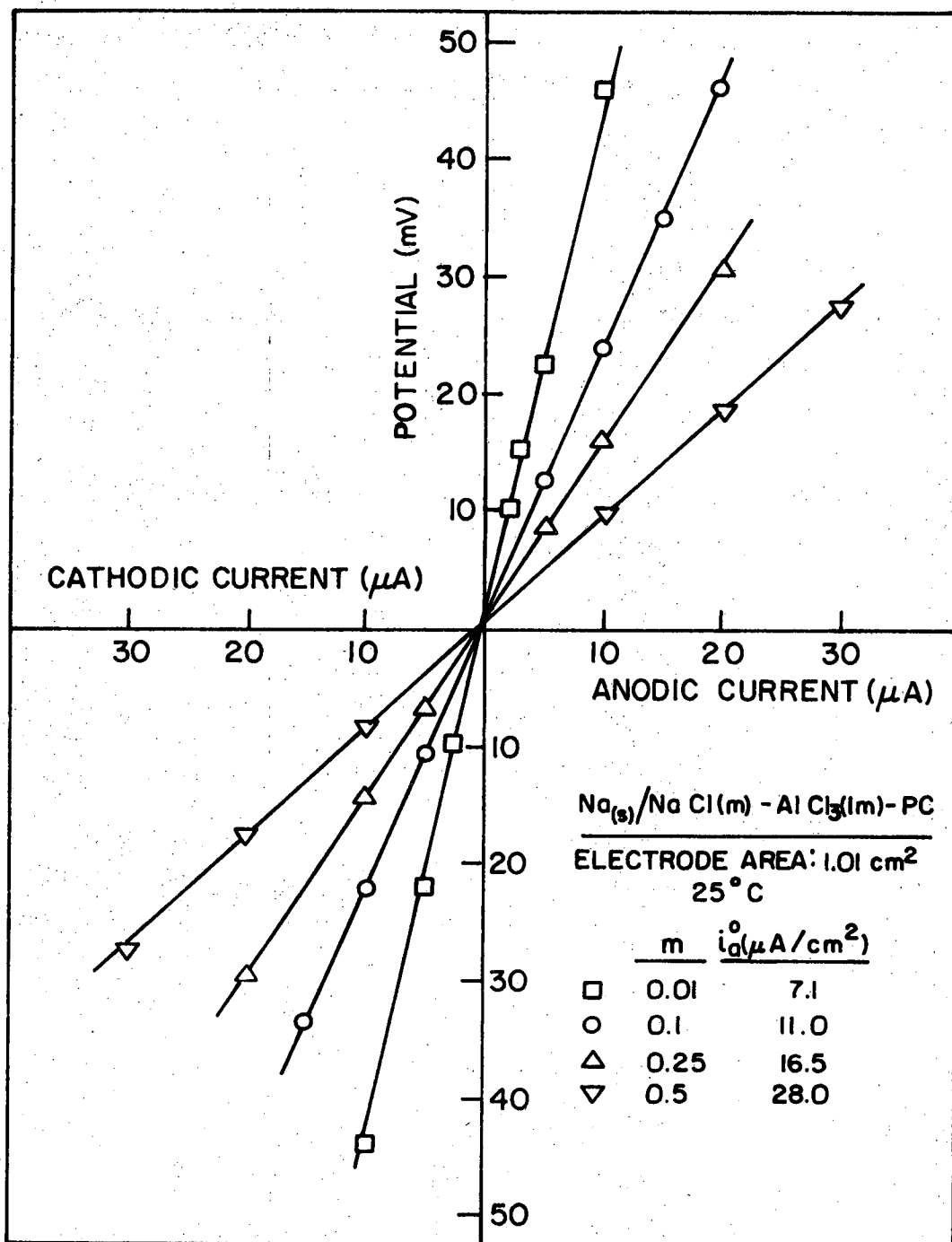
3.7. Enthalpy of Activation at Zero Polarization of
Lithium in LiCl Solution in AlCl₃ (1 m)-PC

Micropolarizations of lithium electrode in different LiCl concentrations in AlCl₃ (1 m)-PC were performed at three different temperatures: 25°, 30° and 35°C. Figure 3-45 presents the plot of the apparent exchange current densities, i_a^o , vs. 1/T for the various LiCl molalities. The slopes of the lines are about equal, and the average enthalpy of activation at zero polarization was calculated as



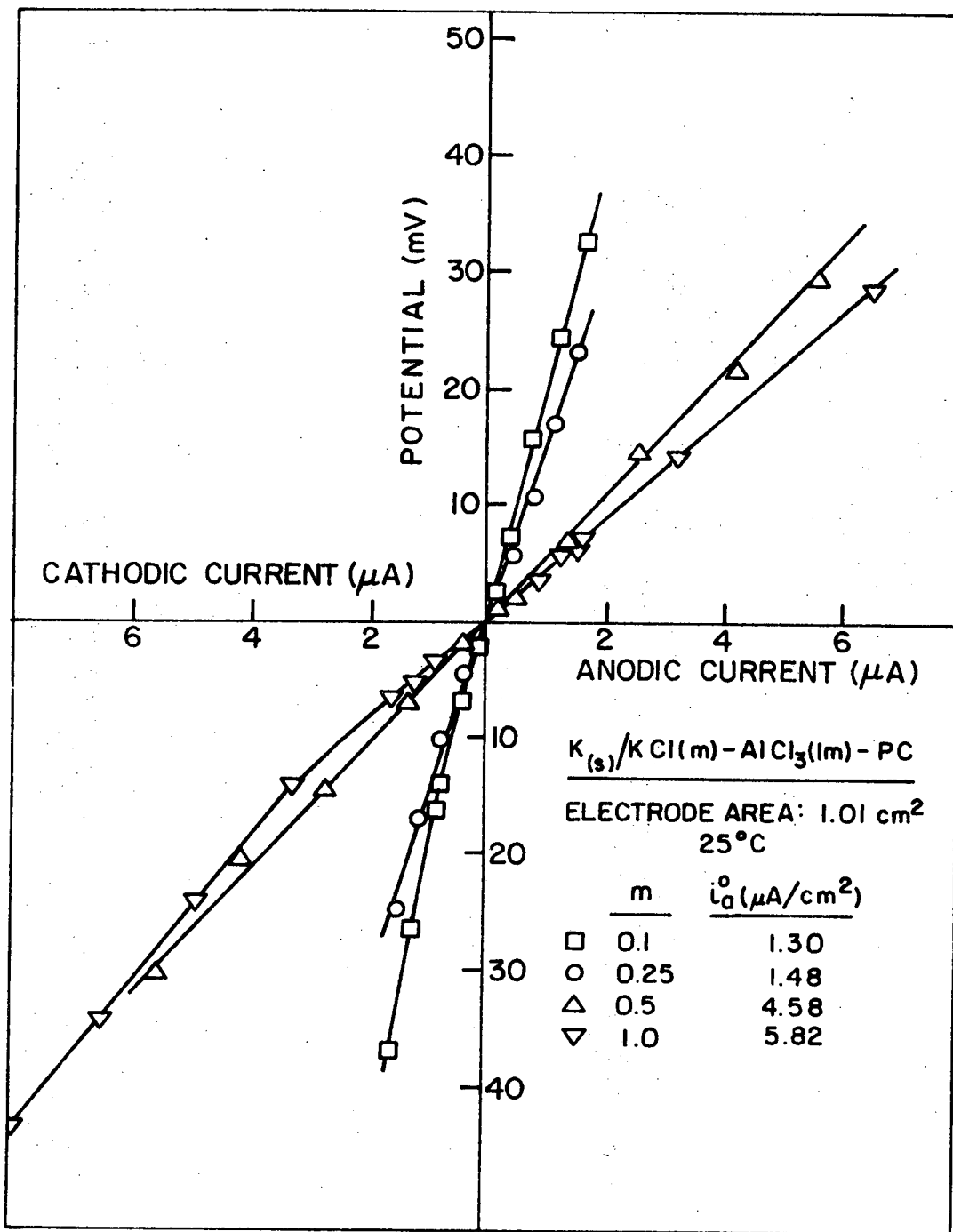
XBL 725-6272

Fig. 3-40. Micropolarization of $\text{Li}(s)/\text{LiCl}(m)$ in $\text{AlCl}_3(lm)\text{-PC}$ solution.



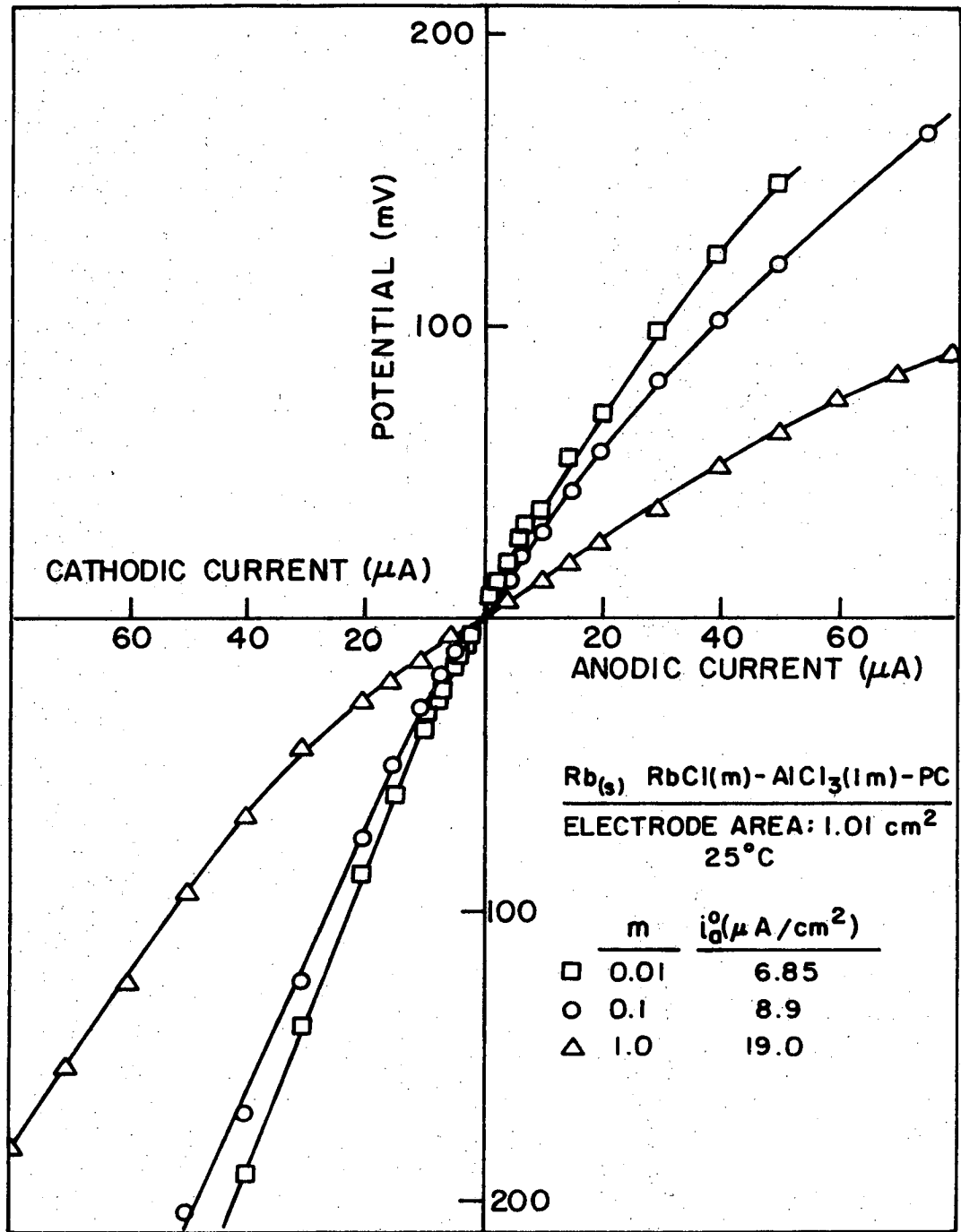
XBL 725-6273

Fig. 3-41. Micropolarization of Na(s)/NaCl(m) in AlCl₃(lm)-PC solution.



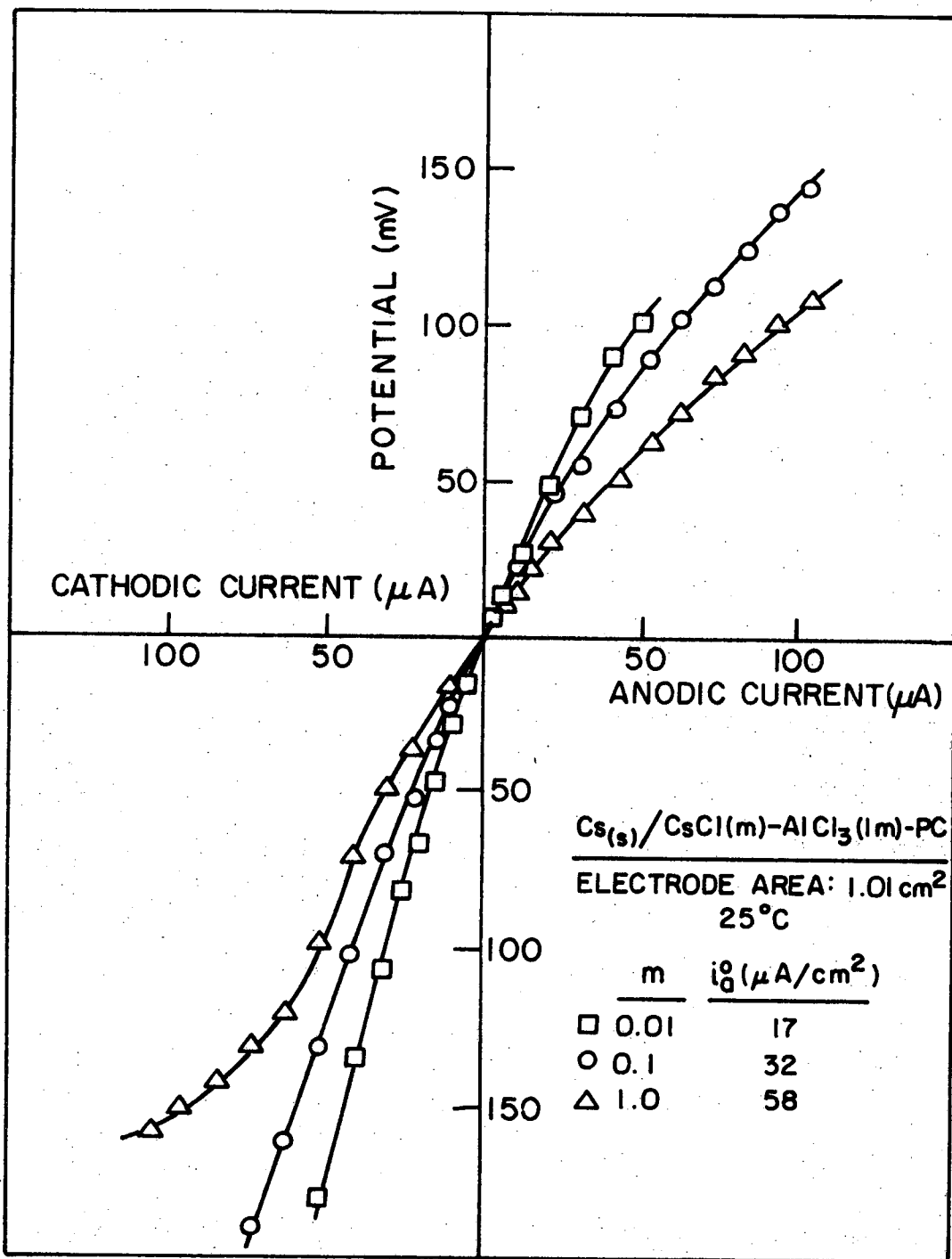
XBL725-6271

Fig. 3-42. Micropolarization of $K(s)/KCl(m)$ in $AlCl_3(lm)-PC$ solution.



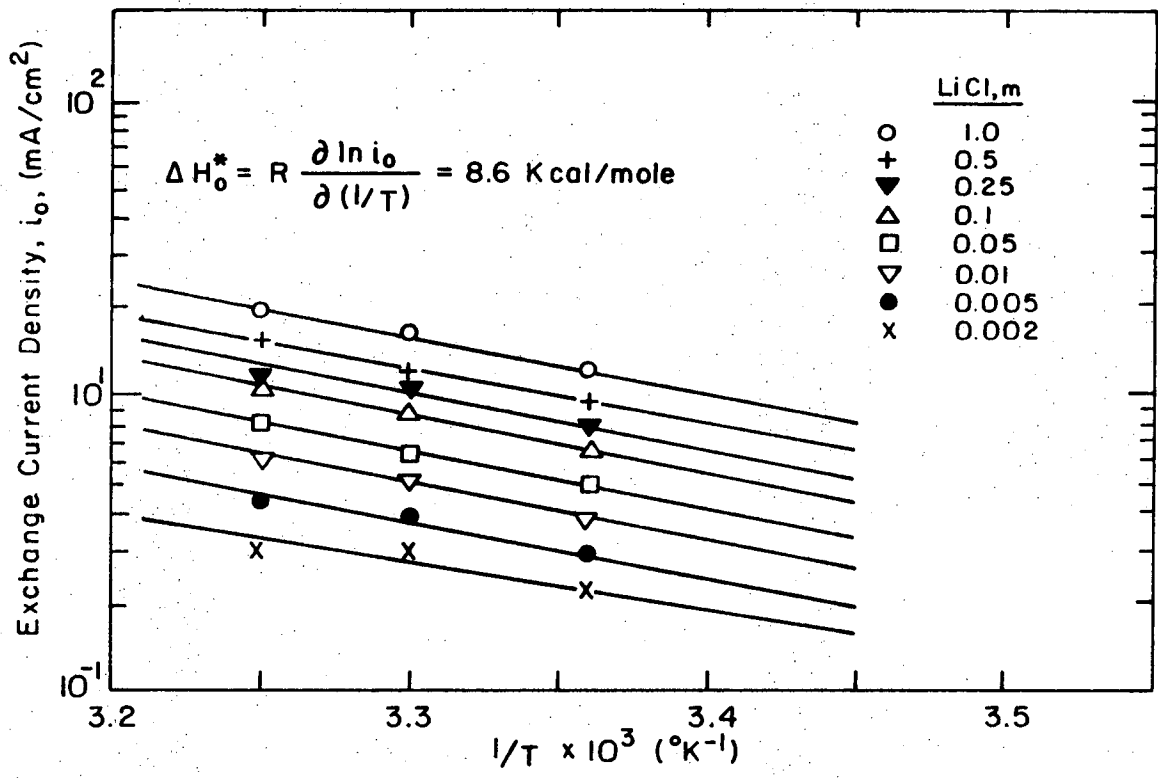
XBL725-6274

Fig. 3-43. Micropolarization of $Rb(s)/RbCl(m)$ in $AlCl_3(lm)-PC$ solution.



XBL 725-6270

Fig. 3-44. Micropolarization of $\text{Cs}(s)/\text{CsCl}(m)$ in $\text{AlCl}_3(lm)-\text{PC}$ solution.



XBL 721-6002

Fig. 3-45. Determination of the enthalpy of activation at zero polarization for Li/LiCl(m) in AlCl₃(lm)-PC solution.

$$\Delta H_o^* = -R \frac{\ln i_a^o}{(1/T)} = 8.6 \text{ kcal/mole} \quad (3-10)$$

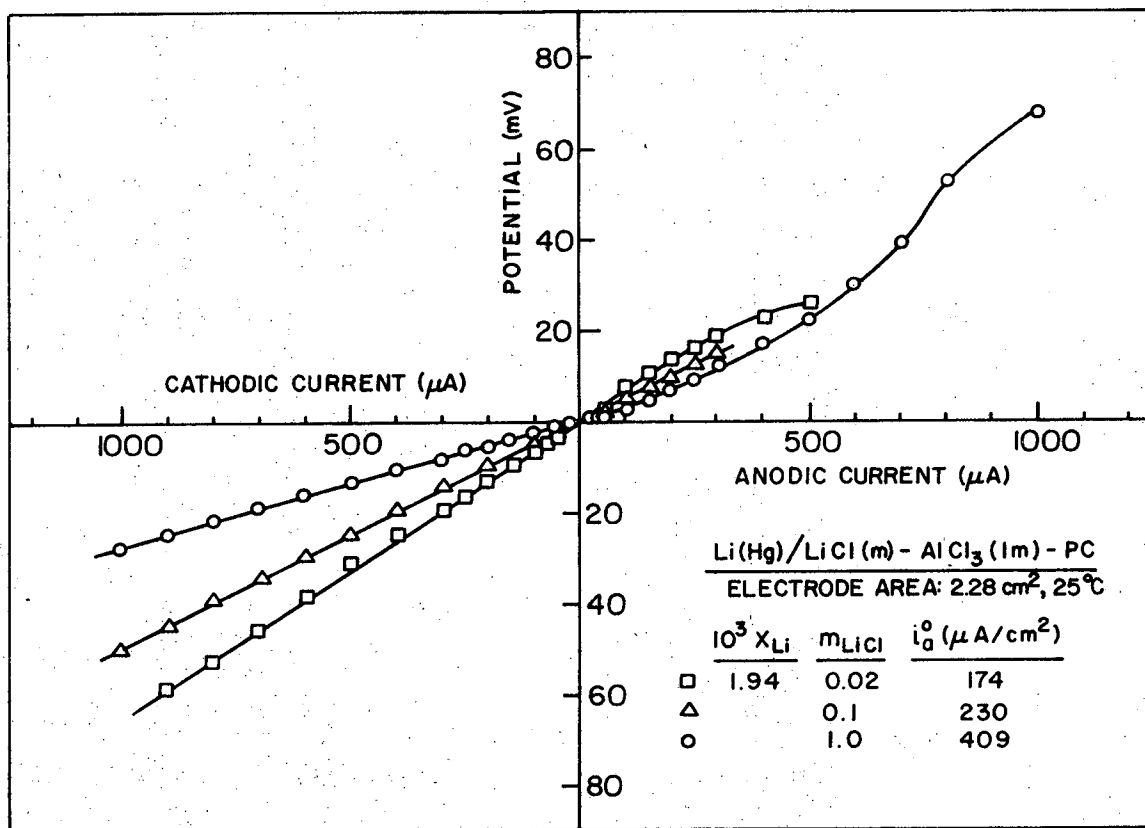
The value of ΔH_o^* is within the order of magnitude expected for soft metals. A similar value of 7.1 kcal/mole was obtained for the sodium electrode in NaClO_4 solution in PC (Fig. 3-7).

The micropolarization behavior of cesium electrode in CsAlCl_4 (0.25 M) solution in PC is presented in Fig. 3-25. The plot of i_a^o vs. $1/T$ is presented in Fig. 3-26, from which the enthalpy of activation at zero polarization is 10.4 kcal/mole. Somewhat lower exchange current density was obtained for Cs electrode at 23.5°C. At this temperature cesium is solid, while the other temperatures employed are above the melting point of cesium, 28.5°C.

3.8. Micropolarization Experiments of the Alkali Metal Amalgams in Their Chloride Solutions in AlCl_3 (1 m)-PC

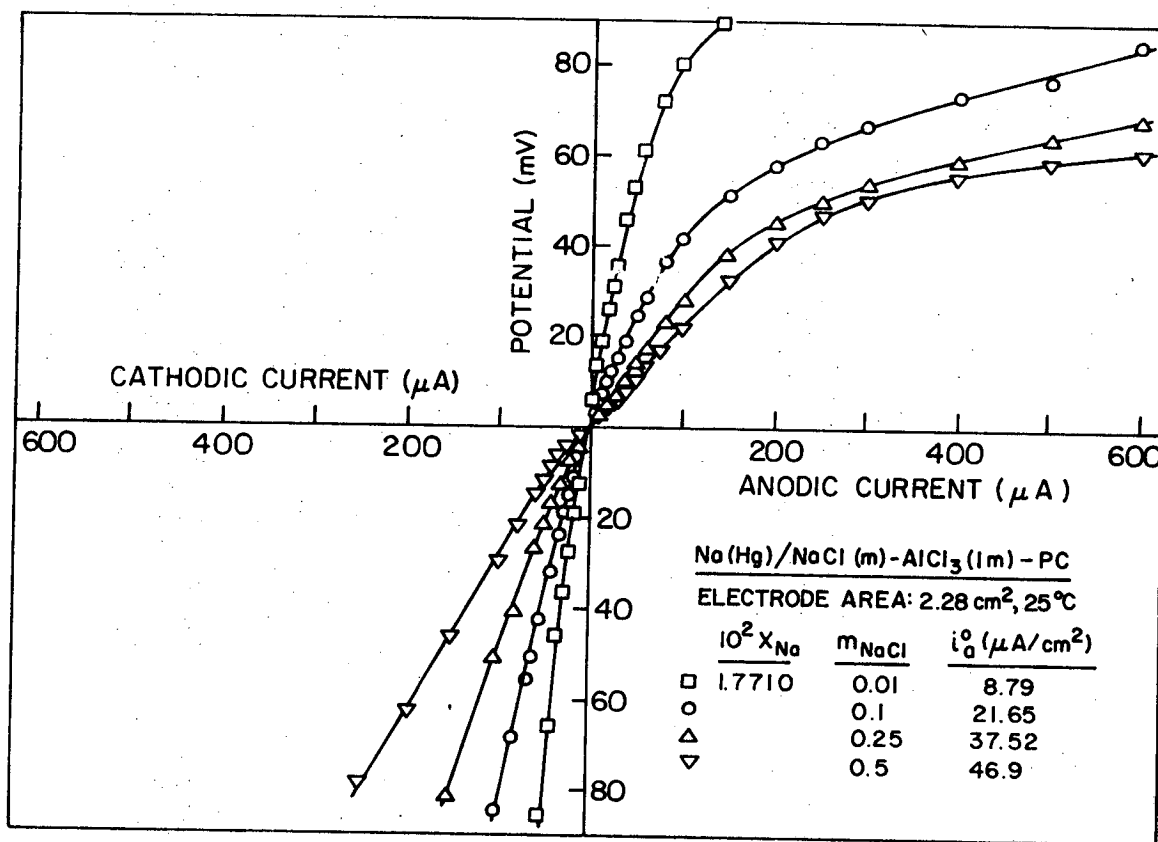
Figures 3-46 to 3-50 present the micropolarization behavior of the alkali metal amalgams at different molalities of the alkali metal chloride in AlCl_3 (1 m)-PC solution. The temperature was held constant at $25 \pm 0.01^\circ\text{C}$. The overpotentials were corrected for ohmic drops (see Section 2.4-1). Linear polarization is observed up to approximately 50 mV, above which non-linear behavior starts to be appreciable, especially in the cathodic direction; Tafel behavior and concentration overpotentials are probably the cause for this behavior.

Exchange current densities were calculated from the linear region, according to Eq. (3-9). More emphasis was given to the anodic branches, where the linearity extended over a wider range. In some cathodic polarization runs, especially at low chloride concentrations, the overpotential increased rapidly, and in some cases the limiting current was



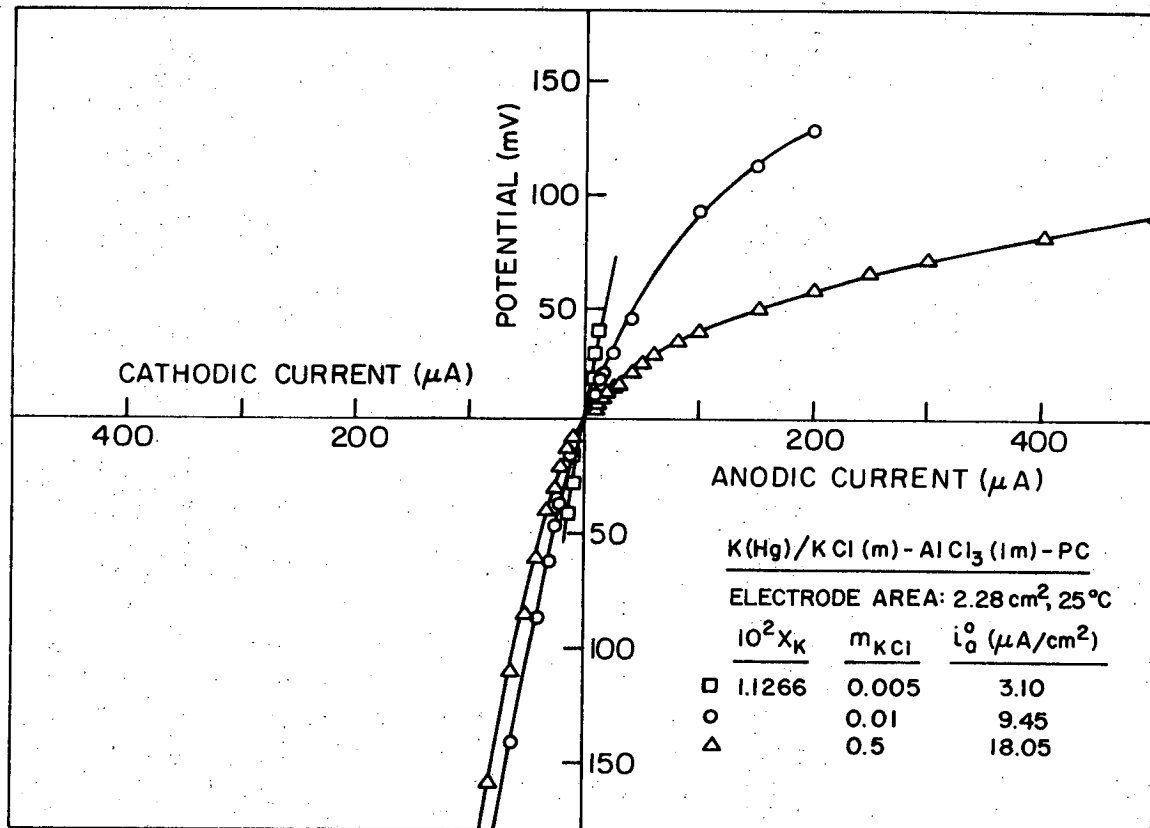
XBL 725-6277

Fig. 3-46. Micropolarization of Li(Hg)/LiCl(m) in AlCl₃(lm)-PC solution.



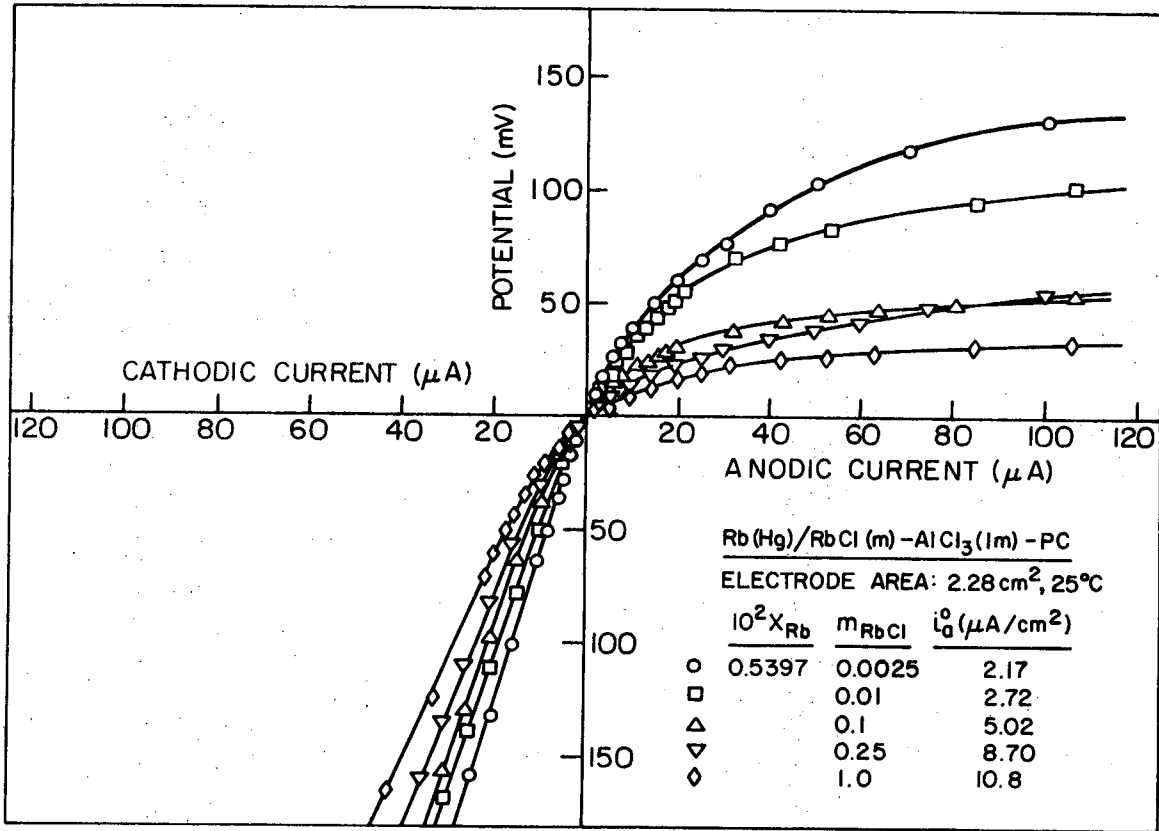
XBL 725- 6278

Fig. 3-47. Micropolarization of Na(Hg)/NaCl(m) in AlCl₃(1m)-PC solution.



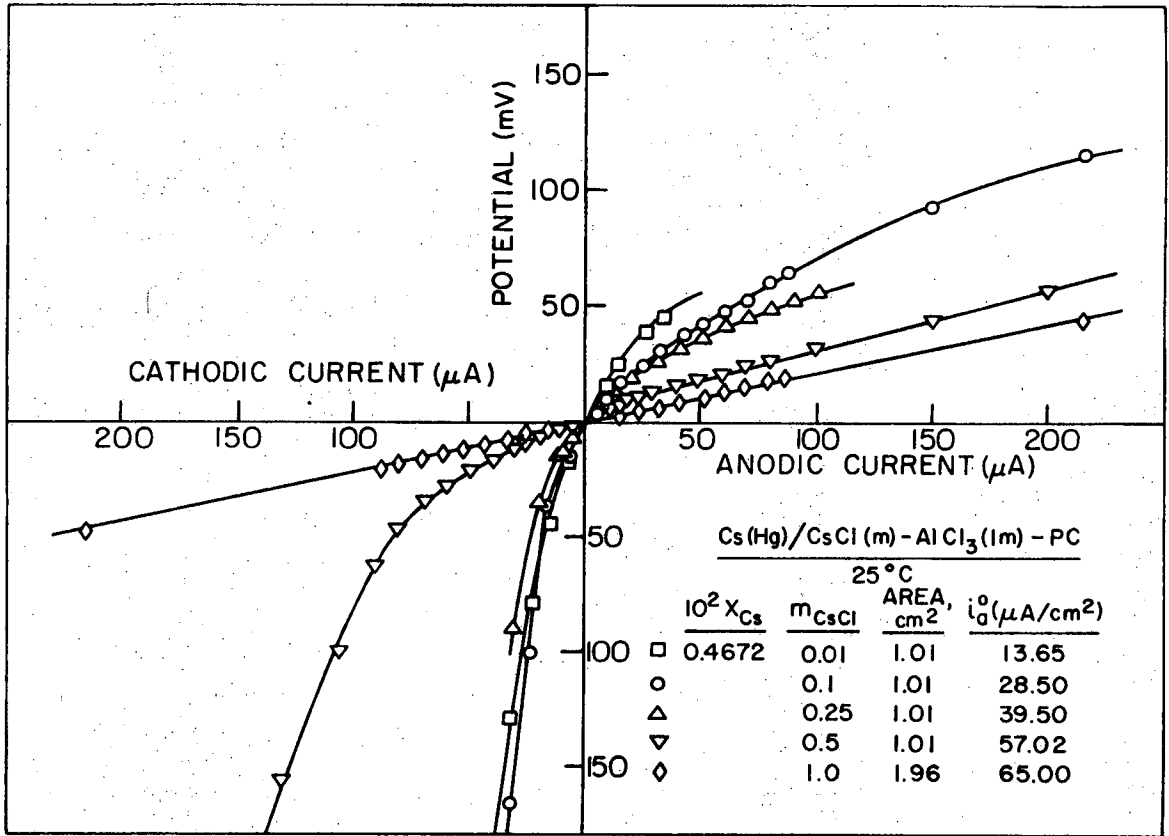
XBL 725- 6276

Fig. 3-48. Micropolarization of K(Hg)/KCl(m) in AlCl₃(lm)-PC solution.



XBL725-6279

Fig. 3-49. Micropolarization of Rb(Hg)/RbCl(m) in $\text{AlCl}_3(\text{lm}) - \text{PC}$ solution.



XBL 725-6275

Fig. 3-50. Micropolarization of Cs(Hg)/CsCl₃(lm)-PC solution.

reached. It is not clear whether at low chloride concentration the limiting current arose from a mass transport or kinetic limitation, or from an insulating layer covering the surface, which possibly formed during cathodic deposition, but was destroyed during anodic dissolution.

The calculated exchange current densities are presented in each figure, along with the mole fraction of the amalgams, and the molalities of the alkali metal chlorides in AlCl_3 (1 m)-PC. The behavior in the Tafel region was tested for the potassium amalgam system, and the results are presented, separately, in Section 3.9. Because of the relatively high current densities applied in this region, the KAlCl_4 (1 m) solution was stirred by bubbling dry argon through it.

3.9. Tafel Polarization of Potassium Amalgam in KAlCl_4 (1 m)-PC Solution

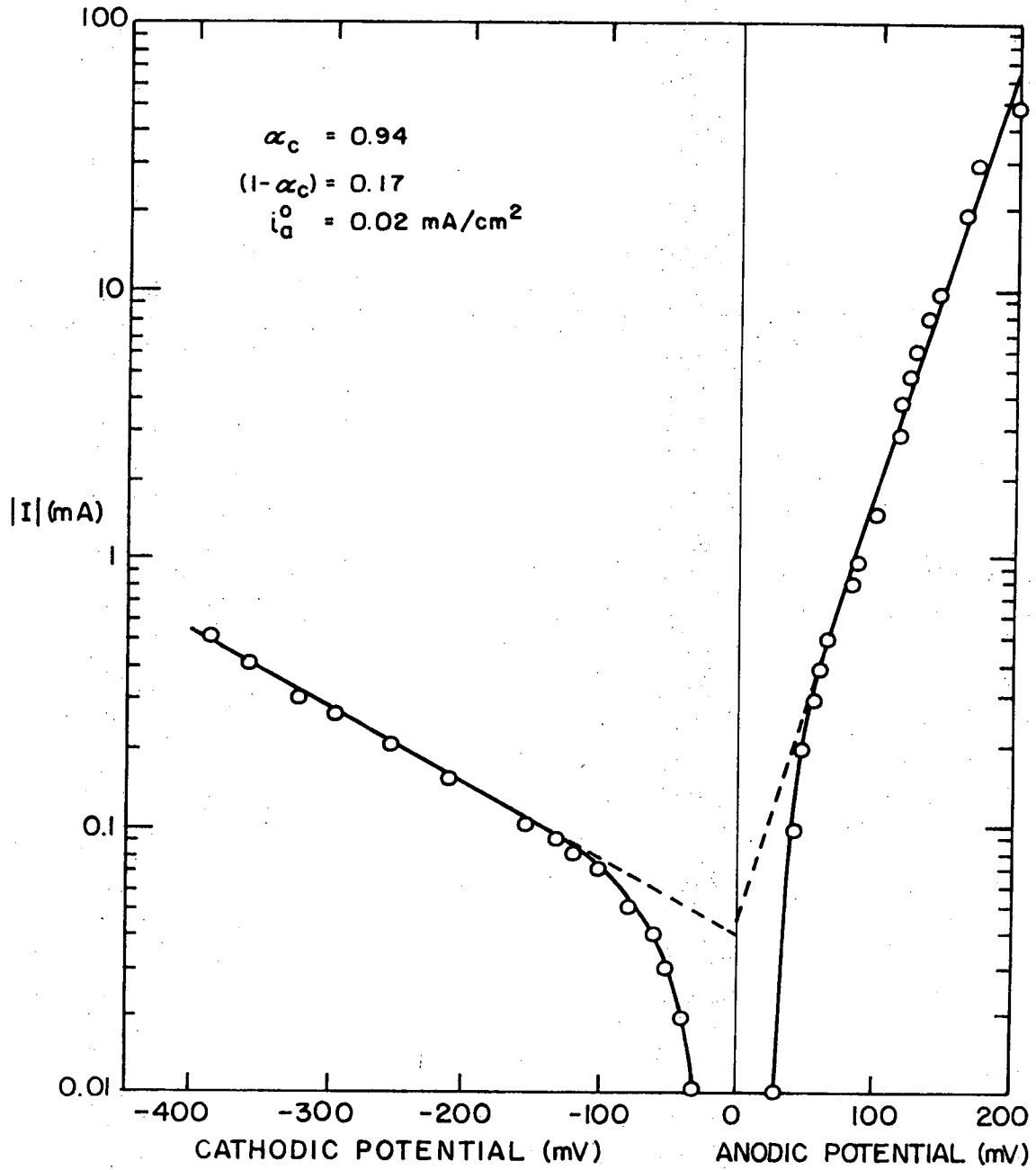
The polarization measurements of the alkali metal amalgams in AlCl_3 (1 m)-PC solutions, presented in Section 3.8, were performed in stagnant solutions, and were restricted to low current densities where concentration overpotentials are negligible. In order to investigate the behavior in the Tafel region, the potassium amalgam system was tested under relatively high currents, and the kinetic parameters obtained from the Tafel plot were compared to those obtained from the linear plot (see Fig. 3-48). Concentration overpotentials were minimized by bubbling dry argon through the solution. A small capillary was introduced from the top of the cell (Fig. 2-15), the tip being located just a few millimeters above the amalgam's surface. Stirring in this way was quite efficient, as the argon stream was directed toward the amalgam's surface. The polarization procedure was identical to the one described in Section 2.4-2. The ohmic drop was estimated by the current interrupter technique.

Polarization of potassium amalgam ($1.1266 \cdot 10^{-2}$ mole fraction) in KAlCl_4 (1 m) in PC at 25°C was performed at moderately high current densities, up to about 40 mA/cm^2 . The results were plotted according to the Tafel equations:

$$\eta = \frac{RT}{\alpha F} \ln i^0 + \frac{RT}{\alpha F} \ln i \quad \eta \gg \frac{RT}{F} \text{ anodic} \quad (3-11)$$

$$\eta = \frac{RT}{(1-\alpha)F} \ln i^0 - \frac{RT}{(1-\alpha)F} \ln |i| \quad \eta \gg \frac{RT}{F} \text{ cathodic} \quad (3-12)$$

and are shown in Fig. 3-51. The exchange current density was calculated from the intercepts of the cathodic and the anodic branches, and is in good agreement with the values obtained from the linear region (Fig. 3-48). The cathodic transfer coefficient, calculated from the anodic branch, is $\alpha_c = 0.94$, and the cathodic transfer coefficient, calculated from the cathodic branch, is given by $(1-\alpha_c) = 0.17$. The average cathodic transfer coefficient is, therefore, $\alpha_c = 0.88$, which is higher than the value $\alpha_c = 0.61$ obtained from the linear region (see Fig. 4-4). The plot presented in Fig. 3-51 is the type of Tafel plot expected for an electrode reaction with a high cathodic transfer coefficient ($\alpha_c > 0.5$). The reader is referred to illustrations of similar behavior in Ref. 173. The high transfer coefficient obtained for the Tafel region indicates that the deposition process requires a higher activation energy than the dissolution process.



XBL 728-6765

Fig. 3-51. Tafel plot for K(Hg) in $\text{KAlCl}_4(1\text{M})\text{-PC}$ solution at 25°C . The solution was stirred by strong argon bubbling. Amalgam composition: $X_K = 1.1266 \times 10^{-2}$ Electrode area: 2.28 cm^2

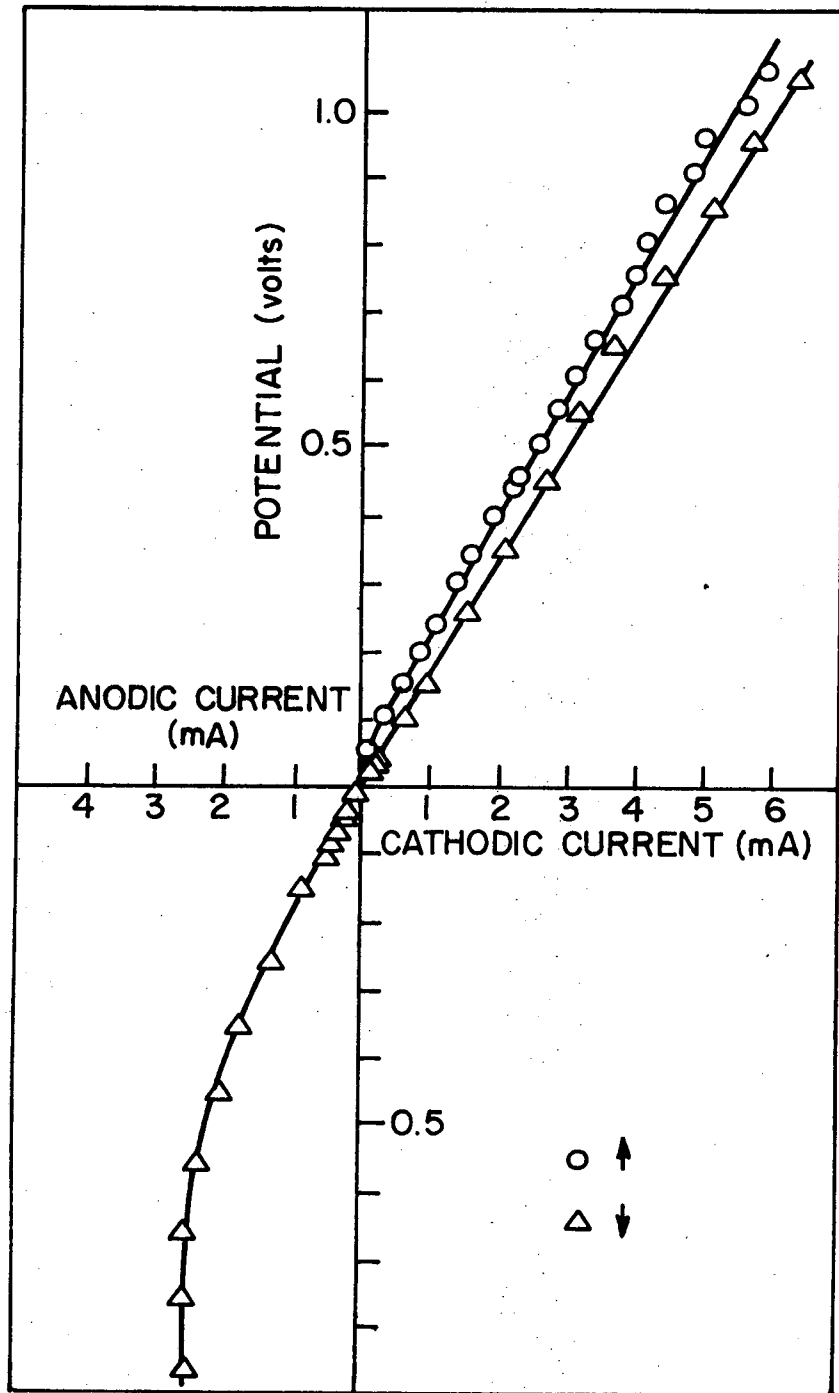
3.10. Electrodeposition of Lithium in the Tafel Region

Lithium was deposited on a rotating disk electrode from LiAlCl_4 (1 m) in PC. The current-potential plots at rotation speeds 360 and 180 rpm are represented in Fig. 3-52 and Fig. 3-53, respectively. The disk was made of teflon, and the central electrode of stainless steel. The electrode area was 0.0855 cm^2 . The counter electrode was a lithium amalgam pool at the bottom of the cell, and the lithium amalgam reference electrode was placed in a separate compartment connected to the main cell by a small capillary. The ohmic drop was estimated by the current interrupter technique (see 2.4-1) and was compared to the calculated value of the ohmic using the equations of Newman.^{152,153} The calculation was based on Eq. (2-4) using the geometry and dimensions of the rotating disk system. For LiAlCl_4 (1 m) in PC at 25°C , the specific conductance is $\kappa = 7.7 \cdot 10^{-3} \text{ ohm}^{-1} \text{ cm}^{-1}$ (see Table 3-19) and the estimated ohmic drop is

$$R = \frac{1.8034}{6.7 \cdot 10^{-3}} = 269 \text{ ohm} \quad (3-11)$$

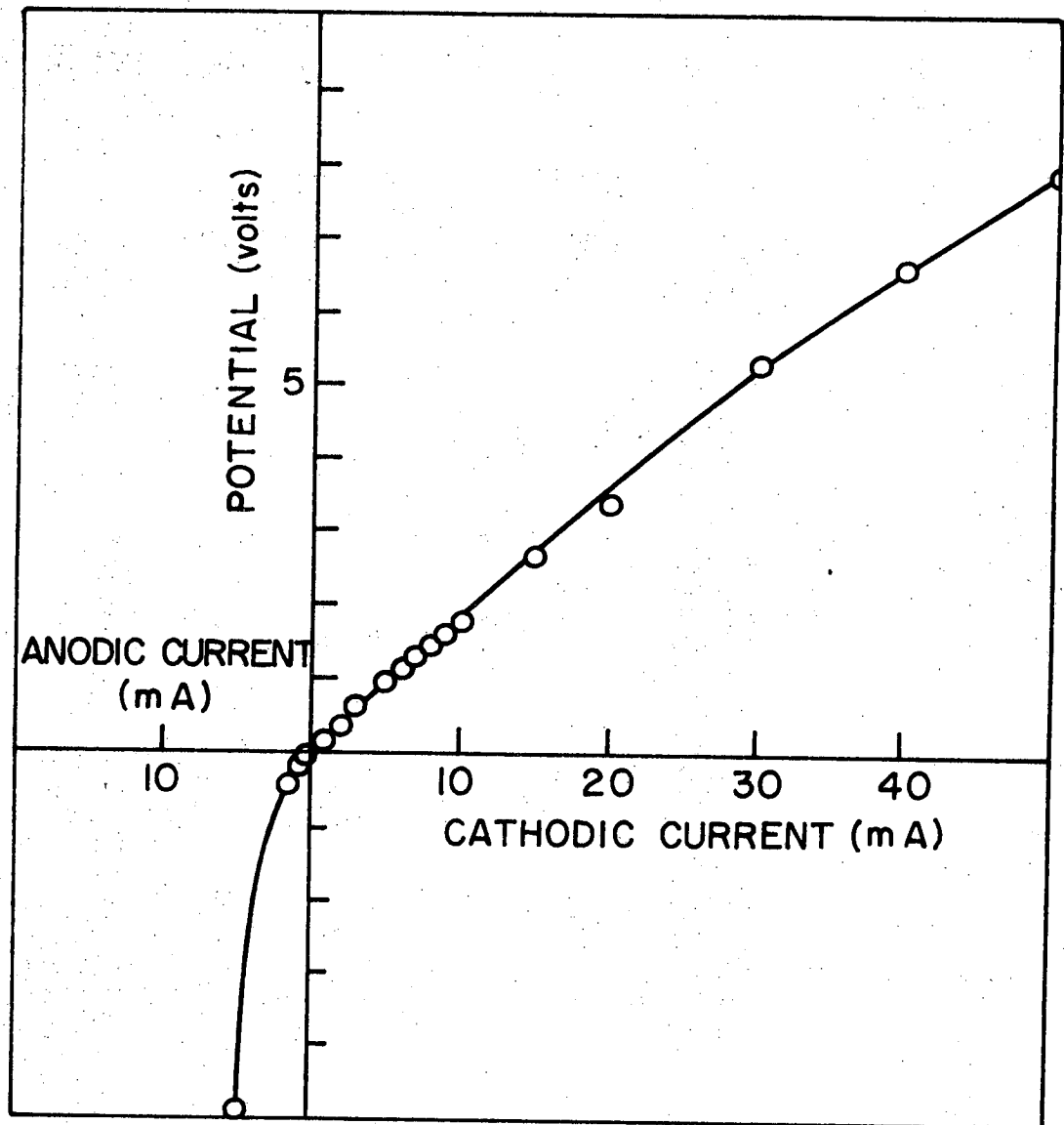
The potential trace of the current interrupter pulse is shown in Fig. 2-10, from which the ohmic resistance was estimated at 280 ohm, in good agreement with the calculated value.

The anodic portions of the curves are included in Figs. 3-52 and 3-53. Since the deposit of lithium was not adherent, the possibility exists that the stainless steel substrate was exposed during the anodic dissolution, thus the high overpotentials seen in Figs. 3-52 and 3-53 may have been caused by the absence of active lithium on the electrode surface (i.e. solvent decomposition).



XBL 727- 6630

Fig. 3-52. Polarization of stainless steel rotating disk in $\text{LiAlCl}_4(\text{lm})\text{-PC}$ at 25°C . $A = 0.0855 \text{ cm}^2$, $\omega = 360 \text{ rpm}$, $i^0 = 1.635 \text{ mA/cm}^2$.



XBL 727-6631

Fig. 3-53. Polarization of stainless steel rotating disk in $\text{LiAlCl}_4(1\text{m})\text{-PC}$ solution at 25°C . $A = 0.0855 \text{ cm}^2$, $\omega = 1800 \text{ rpm}$, $i^0 = 1.72 \text{ mA/cm}^2$.

The apparent exchange current density was calculated from the linear portions of the polarization curves (Eq. (3-9)). At 360 rpm, the exchange current density is $i_a^0 = 1.635 \text{ mA/cm}^2$, and at 180 rpm, $i_a^0 = 1.72 \text{ mA/cm}^2$. The agreement between the two values is good, and they both are close to the value of $i_a^0 = 1.02 \text{ mA/cm}^2$, which was obtained in the micropolarization experiments (see Fig. 3-40).

IV. DISCUSSION

4.1. The Electrodeposition of the Alkali Metals

The alkali metals were electrodeposited in a satisfactory form from their chloride solutions in AlCl_3 (1 m)-PC. In addition, lithium, sodium and potassium were deposited from various of their other salt solutions in PC. Perchlorate solutions were found to be promising for the deposition of lithium and sodium. LiPF_6 and LiBF_4 are suitable for lithium deposition; however, their solubilities in PC are somewhat lower. The kinetics of lithium in various solutions in PC was investigated by Meibuhr,^{46,47} who reported on the effect of various anions on the exchange current densities. LiAlCl_4 , LiPF_6 and LiBF_4 showed moderately high exchange current densities, in the order of $0.3\text{-}0.5 \text{ mA/cm}^2$ at 20°C . Deliberate addition of water decreased the exchange currents by an order of magnitude.⁴⁷ The exchange current density for LiAlCl_4 (1 m) in PC obtained in the present work, 1.0 mA/cm^2 , is in reasonable agreement with a value of approximately 0.5 mA/cm^2 , reported by Meibuhr⁴⁷ for LiAlCl_4 (1 M) in PC at 25°C .

Sodium was electrodeposited from NaClO_4 solution in PC. The deposition-dissolution of sodium in NaClO_4 (1 M) in PC at three different temperatures (Fig. 3-6) involves high reversibility and moderately high exchange current densities. At 25°C $i^0 = 0.43 \text{ mA/cm}^2$, in good agreement* with a value of 0.21 mA/cm^2 at 19°C , reported by Meibuhr.⁶⁰ The enthalpy of activation at zero polarization was calculated from the temperature dependence of the exchange current (Fig. 3-7). A value of $\Delta H_o^* = 6.0 \text{ kcal/mole}$ was

* Exchange current densities are regarded to be in good agreement when they are within the same order of magnitude because of the experimental difficulties and the uncertainty regarding the water content of the solvent used.

obtained, in comparison to 14.6 kcal/mole obtained by Meibuhr. The present result seems more reasonable for a soft metal like sodium, and is in better agreement with $\Delta H_o^* = 8.5$ kcal/mole obtained for Li/LiClO₄ in PC.⁴⁶ The micropolarization of NaClO₄ in PC, reported by Meibuhr, was performed only in the anodic direction, whereas in the present work the cathodic portion is included, and the linearity and the identical slopes in both cathodic and anodic directions indicate high reversibility of the dissolution-deposition process.

The system of NaPF₆ in PC was also investigated; however, the exchange current densities were much lower for both sodium metal and sodium amalgam (Figs 3-8 and 3-9, respectively). Polarization of sodium in NaPF₆ (0.5 M) in the Tafel region (Figs 3-10 and 3-11) shows that an appreciable cathodic overpotential (about 1 volt) is necessary to deposit sodium at the rate of about 3 mA/cm², while the anodic dissolution process can be carried out at a lower overpotential. The reversible behavior of sodium in NaPF₆ (0.5 M) in PC is demonstrated by the cyclic voltammogram (Fig. 3-11). Despite the relatively high sweep rate, 120 mV/sec., only small hysteresis can be observed in the cathodic direction, probably due to different concentration gradients generated when the potential was swept back and forth.

The kinetics and transport behavior of NaAlCl₄ in PC is discussed later. It seems that on the basis of kinetic considerations alone, NaClO₄ is superior to NaPF₆ although other considerations (e.g., conductance or stability) might be of greater importance.

Potassium exhibits the most reactive behavior toward PC. Potassium electrodes were stable in PC only after the solutions were carefully dried with molecular sieves. Even then, most erratic and irreproducible results were obtained during the potential and the micropolarization

experiments. Although the instability was assumed to be mainly caused by water traces, further work should be done to clarify this point. Potassium was deposited from KPF_6 (0.5 M) in PC; polarization experiments (Fig. 3-12) show, in general, a Tafel behavior. The bias potentials of up to 20 mV, between the potassium deposit on a platinum substrate and a potassium reference electrode, is attributed to the loose form of the deposit. It should be noted that even between identical potassium electrodes in some cases, the bias potential was in the range of 10 mV.

Potassium was deposited from $LiAlCl_4$ solution in PC, and again the deposit was loose and showed bias potentials of up to 20 mV. The potential measurements between potassium and potassium amalgam (0.231%wt) (Table 3-2) yielded the correct EMF range and temperature dependence. Potassium amalgam, of the same composition as the amalgam used by G. N. Lewis,⁶² showed a potential of 1.0523 volts with respect to a pure potassium electrode, in comparison to 1.0481 volts obtained by G. N. Lewis (see Table 3-11).

Linear cyclic voltammetry results show good reversibility at 25° and 43°C. (Figs. 3-13 and 3-14, respectively.) Sweeping the potential into the Tafel region (Figs. 3-15 and 3-16) shows hysteresis, especially when the sweep rate was high (40 mV/sec). The hysteresis is probably caused by different concentration profiles when the potential was swept in the anodic and the cathodic directions. Figure 3-17 shows several cyclic voltammograms of Pt electrode in $KAlCl_4$ (0.5 M). Negligible anodic current can be observed when the potential is swept in the cathodic direction. The cathodic behavior is linear; however, cycling back in the anodic direction, anodic current peaks can be observed, caused

by the re-dissolution of the deposited potassium from the platinum surface.

Potassium amalgam behaves reversibly as indicated by the voltammogram of $K(Hg)/KAlCl_3$ (0.5 M) in PC (Fig. 3-18). Figures 3-19 and 3-20 show several consecutive cycles of potassium and potassium amalgam in $KAlCl_4$ (0.5 M), respectively. In both cases, the currents dropped after each cycle. This can be explained by the formation of loose potassium deposit on the surface, resulting in an increase of the ohmic drop, which is included in the scanned potential. Another possibility is the formation of an insulating film on the surface which gradually reduced activity of the electrode. The cyclic voltammogram of $K(Hg)$ (Fig. 3-20) shows stabilization and steady state behavior after the third cycle. The last two cycles are practically identical.

Rubidium was electrodeposited from $RbAlCl_4$ solution in PC. Bias potentials of less than 25 mV were obtained between the deposited rubidium and a metallic rubidium reference electrode. The agreement between the potential difference between Rb and $Rb(Hg)$ obtained in the present work, and the value reported by G. N. Lewis⁶⁶ for an identical amalgam, increases confidence in the stability of rubidium in PC solution (see Table 3-12).

Cesium was electrodeposited from $CsAlCl_4$ solution in PC. The bias potential between the electrodeposited Cs, and metallic cesium was below 20 mV. The cesium amalgam composition did not match exactly the composition of the amalgam used by Bent, et al.,⁶⁷ which is the only source of data for cesium amalgams. However, the value of 1.017 volt for 0.302%wt Cs is in the right direction when compared to 1.119 volt obtained by Bent, et al.⁶⁷ for a 0.1875%wt cesium amalgam. These two values are the only potential measurements for cesium amalgams, at room temperature.

Micropolarization of cesium in CsAlCl_4 (0.25 M) in PC at different temperatures shows reversible behavior in both cathodic and anodic directions, although the exchange currents were quite low (Fig. 3-25). The enthalpy of activation at zero polarization was calculated from Fig. 3-26, $\Delta H_{\text{O}}^* = 10.4$ kcal/mole, reasonable for alkali metal deposition at room temperature. The exchange current density below the melting point of cesium is somewhat lower than expected. Cyclic voltammetry experiments of cesium and cesium amalgam in CsAlCl_4 solution show reversible behavior both in the cathodic and the anodic direction. Fig. 3-29 shows the voltammogram of metallic cesium, which is almost identical to the one for electrodeposited cesium on Pt substrate, Fig. 3-28. Figure 3-27 shows the voltammogram of clean Pt electrode in CsAlCl_4 (0.25 M). Negligible anodic current was observed because of the absence of cesium on the surface. This verifies the high stability of the solvent toward reduction. After the Pt electrode was swept in the cathodic direction, a small anodic current could be observed, a result of the re-dissolution of the electrodeposited cesium from the platinum electrode. Reversible behavior was observed for Cs(Hg) in CsAlCl_4 (0.25 M). Figure 3-31 demonstrates again the high reversibility of Cs electrode, and Fig. 3-32 shows the cyclic voltammetry of Cs in the Tafel region, where the potential was scanned between ± 2 volts, and the current varied between ± 1.5 mA. The slow sweep rate insured the high reversibility of the electrode over this wide potential range; the small fluctuations in Fig. 3-32 are the result of the long duration of the experiment.

4.2. Cell Potentials of the Alkali Metal Chlorides
in AlCl_3 (1 m)-PC Solution

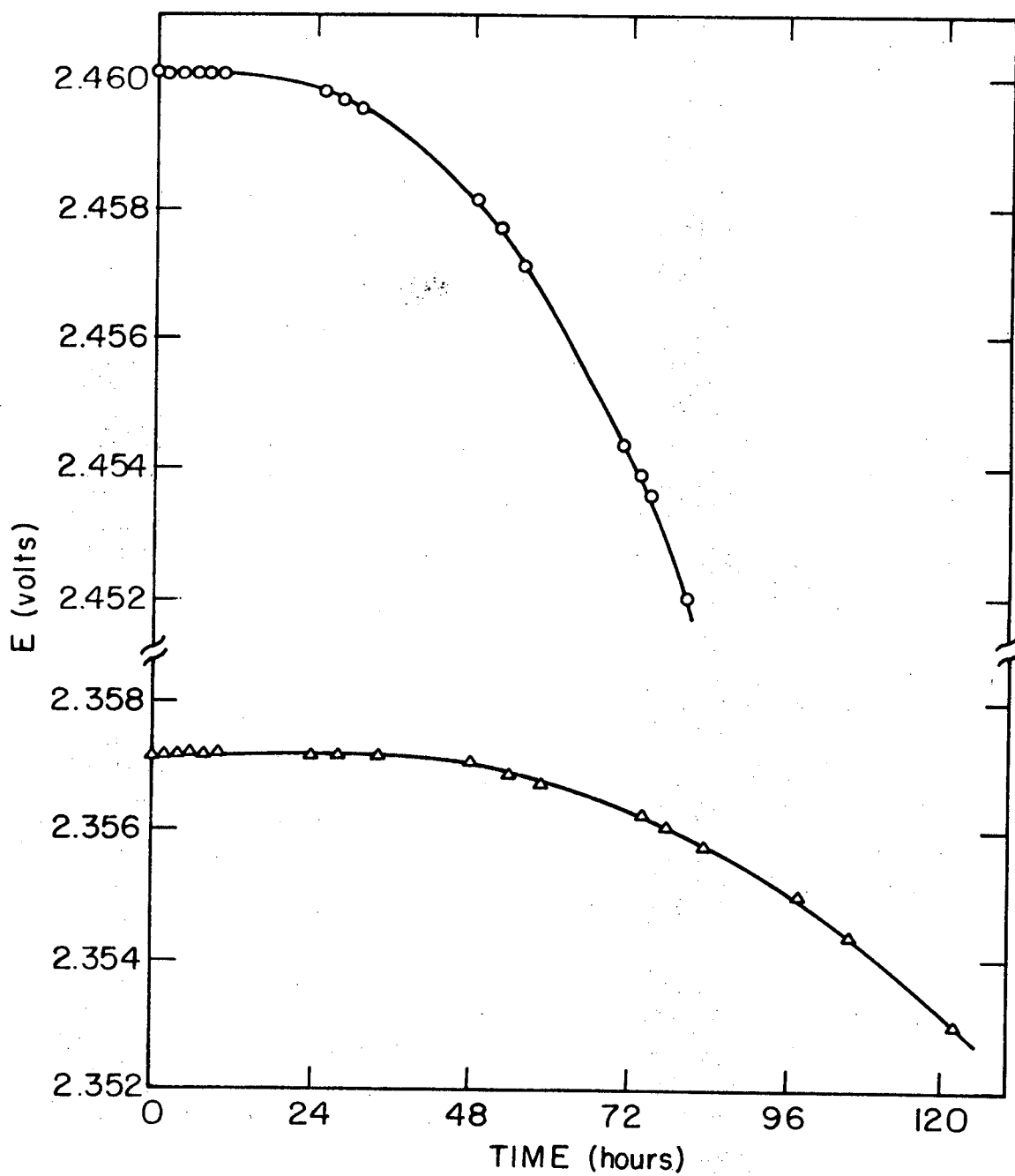
EMF measurements of the cell without transferences: $\text{M(s)}/\text{MCl(m)}$, AlCl_3 (1 m)-PC/ $\text{TlCl(s)}/\text{Tl(Hg)}$ gave reproducible results. Potential measurements involving the lithium and sodium systems were especially reproducible. The greatest scattering of data points was experienced with the potassium system. Potassium electrodes were less stable in PC and in some cases turned purple after a few days of repeated measurements. Lithium and sodium gave reproducible results within ± 5 mV, while rubidium and cesium were somewhat less reproducible, and their bias potentials varied within ± 10 mV, probably because of difficulties experienced in preparing the electrodes in the molten state. The scatter of potentials is believed to be caused by the preparation of AlCl_3 solution in PC. The dissolution of AlCl_3 in PC is a very exothermic process, and the accidental addition of "large granules" of AlCl_3 resulted in local heating and solvent decomposition, as evidenced by the solution turning yellow or even brown. The reproducibility of the preparation of AlCl_3 solution in PC is unknown, and solutions which were more than slightly yellow were discarded.

The change in cell potential with time was followed by measuring the potentials every 10-15 minutes in the first two hours, and checking them every hour for the first day. The potentials were measured then for at least four days before the cell was disassembled. For the first half hour, especially for solutions having a low concentration of alkali metal chloride, changes in potentials were observed. The potential was then steady within ± 5 mV for a few hours, followed by a steady decrease

in the cell potential, during the next day. In every case the potential drifted toward the discharge of the cell. The decrease in potential was faster for low alkali metal chloride concentrations, and was minimal when the molality of MCl approached unity or 1:1 ratio with respect to AlCl_3 molality in PC. Figure 4-1 presents the time dependence of the potential for two lithium cells. The lower curve represents the change in potential of a cell containing LiCl (1.0 m) in AlCl_3 (1 m)-PC. The upper curve shows the behavior of a cell containing LiCl (0.01 m) in AlCl_3 (1 m)-PC.

Similar behavior of cell discharge was observed by Salomon⁹⁵ for the alkali metal halides in PC. A steady decrease in cell potentials was observed for lithium halides in DMSO,^{92,154,115} dimethylformamide,⁹⁸ and N-methylformamide.¹¹⁰ A strong decrease of cell potential with time was observed in the cell Pt, $\text{H}_2/\text{HCl}(m)/\text{AgCl}, \text{Ag}$ in formamide;^{118,119,120} the true cell potentials were obtained by extrapolating the observed potentials to zero time. A decrease of approximately 20 mV was observed during a period of 2 hours.

The reasons for the steady decrease in cell potentials have been attributed to either solubility and diffusion of the thallos halide and subsequent reaction with the alkali metal,^{92,154,115} or the reaction of the alkali metal with the solvent or with solvent impurities such as water.⁹⁵ Salomon attributed the phenomena to the reactivity of the alkali metals with impurities rather than to TlCl diffusion across the cell, because the solubility of TlCl in pure PC is extremely low ($K_{sp} = 10^{-12.4}$). However, TlCl is probably somewhat more soluble in the presence of an excess of chloride ions.

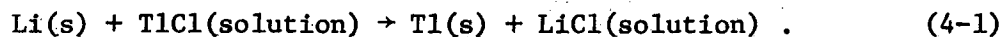


XBL728-6678

Fig. 4-1. Time dependence of lithium cell potential at 25°C.

- Δ $m_{\text{LiCl}} = 1.0$
- \circ $m_{\text{LiCl}} = 0.01$

The behavior of the cell potentials in the present work was similar to the one reported by Smyrl and Tobias for LiCl in DMSO,⁹² where, after a period of several hours of relatively constant potential, the potential started to decrease steadily due to the reaction:



Since identical cells were used in the present work and by Smyrl and Tobias, the time for the diffusion of the thallium species across the cell should be of the same order of magnitude. The fact that the potentials decreased more rapidly in the present work indicates that the solubility of thallium chloride in PC in the presence of AlCl_3 is higher than in DMSO. The stable behavior of the potentials measured by Salomon in PC⁹⁵ can be attributed to the low solubility of thallic halides in PC, and to the fact that fritted glass was used to slow the diffusion of the thallium species across the cell from the reference electrode to the alkali metal electrode.

The standard cell potentials of the alkali metals in AlCl_3 (1 m)-PC solution, relative to Tl, TlCl, are presented in Table 3-7 along with the cell potential temperature coefficients. These results were obtained by extrapolation to infinite dilution with respect to the alkali metal chloride molalities. The order of the standard potentials in the alkali metal series does not follow that in aqueous solution, where lithium has the highest standard potential. The standard potentials of the alkali metals in water and in several other solvents are presented in Table 4-1a, along with the present results. The present results, as well as Salomon's data assign a noticeably higher standard potential to potassium than to lithium. The difference of approximately 70 mV between the standard

potential of K and that of Li cannot explain the high reactivity of potassium in PC. Since the work of Salomon does not include measurements of the rubidium and cesium cells, further comparison cannot be made. Cesium, followed by rubidium shows the highest oxidation potentials in AlCl_3 (1 m)-PC. This is not the case in acetonitrile, N-MF, and water, where lithium has the highest oxidation potential. It may be proper to quote the prediction made by G. N. Lewis and W. L. Argo in 1915, concerning the peculiarity of the order of the standard potentials in the alkali metal series: "The potentials of the alkali metals follow a curious order, namely, lithium, rubidium, potassium, and sodium. It is interesting, however, to observe that this is the order of the heats of formation of the several ions in aqueous solution. In order to illustrate this fact, the heat of formation of the chlorides of the four metals in aqueous solution are: 102, 101, 101, 96 kcal/mole for LiCl, RbCl, KCl and NaCl, respectively. The heat of formation of aqueous cesium chloride is given as 105 kcal/mole, and if this figure is correct, we might predict the potential of cesium to be higher than any of the other alkali metals."⁶⁶ However, this prediction did not materialize when 14 years later Bent, Forbes and Forziani⁶⁷ obtained the normal electrode potential of cesium, $E^{\circ} = 2.923$ volts, "...very close to the corresponding value for rubidium, but still 34 millivolts below that for lithium."

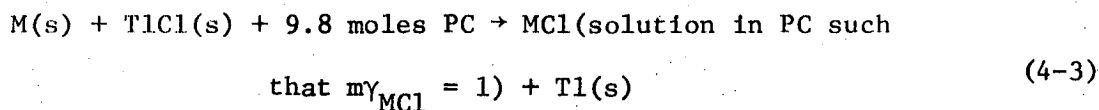
In order to verify the standard oxidation potential sequence obtained in AlCl_3 (1 m)-PC, the following estimates can be made of the standard oxidation potentials of rubidium and cesium in pure PC: The free energies of solvation of RbCl and CsCl in PC were reported by Salomon:¹³⁹

$$\Delta G_{\text{solv}}^{\circ} (\text{RbCl}) = -142.7, \Delta G_{\text{solv}}^{\circ} (\text{CsCl}) = -140.9 \text{ kcal/mole. By using}$$

Eq. (5-10) backward, the free energy of the cell reaction (Eq. 4-3) can be calculated:

$$\Delta G_{\text{emf}}^{\circ} = \Delta G_{\text{solv}}^{\circ} (\text{MCl}) - \Delta G_{\text{f}}^{\circ} (\text{TlCl}_{(\text{s})}) + \Delta G_{\text{f}}^{\circ} (\text{MCl}_{(\text{s})}) - \Delta G_{\text{lat}}^{\circ} (\text{MCl}_{(\text{s})}) \quad (4-2)$$

Following the values of Table 1-8, the free energies of the cell reaction



for rubidium and cesium are

$$\Delta G_{\text{emf}}^{\circ} (\text{M=Rb}) = -142.7 + 44.46 - 98.48 + 149.0 = -47.72 \text{ kcal/mole} \quad (4-4)$$

$$\Delta G_{\text{emf}}^{\circ} (\text{M=Cs}) = -140.9 + 44.6 - 96.60 + 144.9 = -48.14 \text{ kcal/mole} \quad (4-5)$$

The standard oxidation potentials of the cells are then

$$E^{\circ}_{\text{Rb/RbCl,PC/TlCl,Tl}} = 2.07 \text{ volt}$$

$$E^{\circ}_{\text{Cs/CsCl,PC/TlCl,Tl}} = 2.08 \text{ volt}$$

These estimated values are both higher than the standard oxidation potentials of Li, Na and K obtained by Salomon (Table 4-1a).

The estimated standard oxidation potential of Cs is over 200 mV higher than that Li. This agrees qualitatively with the finding of the present work, where Cs has a higher potential than Li in AlCl_3 (1 m)-PC solution.

It should be emphasized here that the estimated standard oxidation potentials of Rb and Cs in pure PC are very crude ones, since they are based on estimated values for the free energies of solvation of RbCl and CsCl in PC. However, at least qualitatively, it shows that the high standard potentials for Rb and Cs are not unexpected even in pure PC.

The fact that K also has a higher potential than Li in AlCl_3 -PC solution agrees with the results, based on the alkali metal iodide measurements (see Table 4-1a), of Salomon.

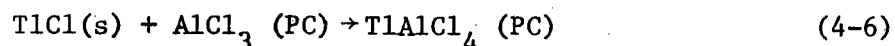
Table 4-la. Standard oxidation potentials in nonaqueous solvents.

	Acetonitrile	N-MF	Formamide	Propylene Carbonate	PC-AlCl ₃ (1 m)	H ₂ O	
Li	3.23	3.124	---	1.85080 1.84223	1.8452 2.045	3.045	
Na	2.87	2.807	---	(1.83480) ---	1.6188 1.885	2.714	
K	3.16	3.021	2.872	---	1.934 2.116	2.925	
Rb	3.17	---	2.855	---	2.116	2.925	
Cs	3.16	2.987	---	---	2.122	2.923	
Ref.	H ₂ /H ⁺	Ag/AgCl	H ₂ /H ⁺	Tl/TlCl	Tl/TlBr	Tl/TlI	H ₂ /H ⁺
Reference	(155,156)	(157)	(158)	(95)	(95)	(97,96)	(182)
						(present work)	

Figures 3-33 and 3-34 present the potential measurements and the extrapolation to infinite dilution. The fact that almost linear behavior is obtained by plotting the potential E_2 vs. $(m_{\text{MCl}})^{1/2}$ is very helpful in obtaining the standard potentials, although it should be remembered that this behavior is not necessarily attributed to the Debye-Huckel limiting law, because the reference solvent was a solution of AlCl_3 in PC, in which the ionic strength is very high. The plotting of the results vs. the square root of the molality was adopted to expand the dilute region and to obtain a better accuracy in the extrapolation.

The potentials for lithium cells in which the molality of LiCl was less than 0.005 m showed a substantial drift to lower values. This can be observed in Fig. 3-33 and Fig. 3-34 by the tailing off at the very low LiCl concentration. The potential at 0.002 m LiCl was not included in the extrapolation. This deviation was observed also in the cesium system. Tailing off at low concentration was observed by others, especially for lithium cells in DMSO,^{92,154} N-methyl formamide,¹¹⁰ and in dimethyl formamide.⁹⁸ Smyrl and Tobias¹⁵⁴ explained the decrease in potential at low LiCl concentration in DMSO by the diffusion of TlCl from the reference electrode to the lithium electrode, where it spontaneously reacts. This concentration gradient is of importance only when the LiCl concentration is of the same order of magnitude as the solubility of the sparingly soluble TlCl. However, the solubility of TlCl in PC is much lower than in DMSO ($K_{\text{sp}} = 10^{-12.66}$ in PC, in comparison to $10^{-6.2}$ in DMSO). On this basis, Salomon concluded that the decrease in potential is due to a reaction between lithium and the solvent.⁹⁵ The observed deviations in the present work can be due to diffusion of

TlCl across the cell, since it is quite possible that the solubility of TlCl increases in the presence of AlCl_3 in PC, perhaps according to



It is not clear why the tailing off at low concentration was observed almost exclusively in lithium cells. Deviations were not observed in sodium and potassium cells in PC^{96,97} or in sodium, potassium and rubidium cells in N-methyl formamide.¹¹⁰ In addition, the deviations seem to be observed only in lithium chloride and lithium bromide cells. Deviations were not observed in LiI solution in PC,⁹⁷ nor in LiI solution in DMSO.⁹⁴ The fact that LiCl was found to be associated in PC⁹⁷ might explain these deviations.

The standard potentials in the present work are given on a molal basis. The molal basis has been chosen because the molecular weight of PC is more than 5 times larger than that of water. Since many authors present their results on a molar basis, it should be remembered that the standard potential, on a molal basis, can be converted into a molar basis, according to the following relation:

$$E_c^{\circ} = E_m^{\circ} + \frac{2RT}{F} \ln \rho_0 \quad (4-7)$$

where E_c° and E_m° are the standard potentials on a molar and molal basis, respectively, and ρ_0 is the density of the solvent. The solvent in the present case is an AlCl_3 (1 m)-PC solution, and its density is reported in Section 3.5 as 1.2628 and 1.2530 gr/cm^3 at 25° and 35°C, respectively. The standard potentials of the alkali metals, on a molar basis are presented in Table 4-1. In addition, the standard potentials on a mole fraction basis are presented as well. The mole fracture basis is probably the most

suitable way to present thermodynamic data, where the solute mole fracture is comparable with the solvent mole fraction. The standard potential on a mole fraction basis can be obtained from the following equation:

$$E_N^{\circ} = E_m^{\circ} + \frac{2RT}{F} \ln \frac{1000}{M.W.} + 1 \quad (4-8)$$

where E_N° is the standard potential on a mole fraction basis, and M.W. is the molecular weight of the solvent. In the present case, the reference state is a 1 m solution of $AlCl_3$ in PC. The standard potentials on a mole fraction basis are presented in Table 4-1.

Table 4-1. Standard oxidation potentials on a molar and a mole fraction basis for $AlCl_3$ (1 m)-PC cells.

	$E_{2,c}^{\circ}$		$E_{2,N}^{\circ}$	
	25°C	35°C	25°C	35°C
Li	2.054	2.046	2.162	2.158
Na	1.894	1.887	2.002	1.998
K	2.125	2.127	2.233	2.241
Rb	2.125	2.149	2.116	2.261
Cs	2.131	2.174	2.239	2.286

The potential measurements of cells containing alkali metal amalgams were undertaken in order to increase the confidence in the standard potential and activity coefficient data. The concentrations of the sodium, potassium and rubidium amalgams were adjusted to the exact concentrations of the amalgams used by G. N. Lewis and his co-workers. The potential difference between the metal and the amalgam, $E_{M-M(Hg)}$, is independent of the solvent and of the alkali metal salt concentration in

it. The potential depends only on the amalgam's composition. The agreement between the present results and G. N. Lewis' results is remarkable; in no case is the difference larger than 4.2 mV (see Tables 3-9 to 3-13). The agreement between the potential $E_{\text{Li-Li(Hg)}}$ and data of lithium amalgam³⁹ is less than 1 mV (Table 3-9). The composition of the cesium amalgam used did not match the only amalgam composition reported in the literature;⁶⁷ however, the potentials are in qualitative agreement (Table 3-13). The good agreement with these highly reliable sources increases confidence in stability and reversibility of the alkali metals and their amalgams in AlCl_3 -PC solution. The agreement between the cells containing alkali metal amalgams and those containing alkali metals is good. It was observed that the self-discharge rate of an alkali metal amalgam cell was slower than that of an alkali metal one. However, after a few days the surfaces of the alkali metal amalgams were covered with a thin transparent layer. Stirring the cell and gently shaking the cup electrode helped in exposing a fresh surface, and in restoring the potential close to its original value.

The behavior of the sodium curves in Figs. 3-33 and 3-34 is different from the rest of the alkali metals. The solubility of NaCl in AlCl_3 (1 m)-PC solution was around 0.5 m, in contrast to the rest of the alkali metal chlorides, which dissolved, corresponding to a 1:1 ratio with respect to AlCl_3 . There is no explanation for this unexpected behavior, although there are indications that the solubilities of RbCl and CsCl in AlCl_3 (1 m)-PC were not exactly 1.0 m, but drop slightly upon standing. The decrease in the potentials at high concentrations for the rubidium and cesium and cesium systems, given in Fig. 3-33, indicates probable solvate formation.

The activity coefficients of the alkali metal chlorides in $\text{AlCl}_3\text{-PC}$ solution are shown in Fig. 3-35. The sharp decrease in the activity coefficients at low concentrations is due to the reaction between the chloride ions and Al^{3+} species yielding the AlCl_4^- . Since AlCl_3 is part of the solvent, this decrease in the activity coefficients is equivalent to systems where the solute reacts with the solvent, e.g., NH_3 in water or hydrate formation in aqueous solution.

4.3. Estimation of the Standard Potentials of the Alkali Metals in Pure PC

The standard potentials obtained in Chapter III were calculated with respect to the cell $\text{M(s)}/\text{MCl}, \text{AlCl}_3 (1 \text{ m})\text{-PC}/\text{TlCl(s)}, \text{Tl(s)}$ where the standard state was chosen as infinite dilution of MCl in $\text{AlCl}_3 (1 \text{ m})\text{-PC}$ solution. The standard potentials of the alkali metals in pure PC can be measured from the cell $\text{M(s)}/\text{MCl}, \text{PC}/\text{TlCl(s)}, \text{Tl(s)}$. However, the solubilities of the alkali metal chlorides in PC are very low, and only LiCl is soluble enough to permit accurate potential measurements. Salomon measured the standard potential of lithium in LiCl solution in PC; however, in order to establish a scale of standard potentials in PC for the rest of the alkali metals, he switched to the alkali metal iodides which are soluble in PC. The standard potentials for Li, Na and K systems were given in Table 1-7. Salomon did not measure the standard potentials of rubidium and cesium.

An estimation of the standard potentials of cells of the alkali metal chlorides in pure PC can be made on the basis of the results of the present work and the standard potential of the LiCl cell as reported by Salomon:⁹⁵ The standard potential of the cell $\text{Li(s)}/\text{LiCl(m)}, \text{AlCl}_3(1 \text{ m}),$

PC/TlCl(s), Tl(s) is given by

$$E_1 = E_1^{\circ} - \frac{RT}{F} \ln \left(m_{Li^+} \gamma_{Li^+} m_{Cl^-} \gamma_{Cl^-} \right) \quad (4-9)$$

where E_1° is the standard potential at infinite dilution. The cell potential on the basis of $AlCl_3$ (1 m)-PC as a reference state is given by

$$E_1 = E_2^{\circ} - \frac{2RT}{F} \ln \left(m_{LiCl} \gamma_{\pm LiCl} \right) \quad (4-10)$$

As $m_{LiCl} \rightarrow 0$

$$E_2^{\circ} - E_1^{\circ} = - \frac{RT}{F} \ln \left(m_{Li^+} \gamma_{Li^+} m_{Cl^-} \gamma_{Cl^-} \right) \quad (4-11)$$

The left-hand side of Eq. (4-11) can be calculated, since E_2° was measured in the present work, and E_1° for lithium is reported by Salomon as, $E_1^{\circ} = 1.85080$ volt (This value is the corrected one, since Salomon made a mistake in the thallium amalgam correction, see Section 1.9).

$$- \frac{RT}{F} \ln \left(m_{Li^+} \gamma_{Li^+} m_{Cl^-} \gamma_{Cl^-} \right)_{m_{LiCl} \rightarrow 0} = 2.045 - 1.851 = 0.194 \text{ volt}$$

If we assume that this value does not change much going through the alkali metal series, we can estimate the standard potentials E_1° for the rest of the alkali metals:

$$E_1^{\circ} = E_2^{\circ} - 0.194 \quad (4-12)$$

Table 4-2 summarizes the approximated standard potentials of the cell $M(s)/MCl, PC/TlCl(s), Tl(s)$.

Table 4-2. Estimated standard oxidation potentials for the alkali metals in pure PC.

Cell	E_1° volt	ΔG_1° kcal/mole
Li/LiCl,PC/TlCl,Tl	1.85080*	-42.9*
Na/NaCl,PC/TlCl,Tl	1.691	-39.0
K/KCl,PC/TlCl,Tl	1.922	-44.3
Rb/RbCl,PC/TlCl,Tl	1.922	-44.3
Cs/CsCl,PC/TlCl,Tl	1.928	-44.5

* Measured by Salomon.⁹⁵

The estimated standard oxidation potentials for Rb and Cs, presented in Table 4-2, are lower by approximately 150 mV than the crude estimations made in Section 4.2. The standard oxidation potentials in Section 4.2 were estimated from the free energy of solvation data for RbCl and CsCl, given by Salomon.¹³⁹ These free energies of solvation are based on solubility measurements and are believed to be only crude approximations. Therefore, the estimated standard oxidation potentials in Table 4-2 are believed to be more reliable.

4.4. Conductance Measurements

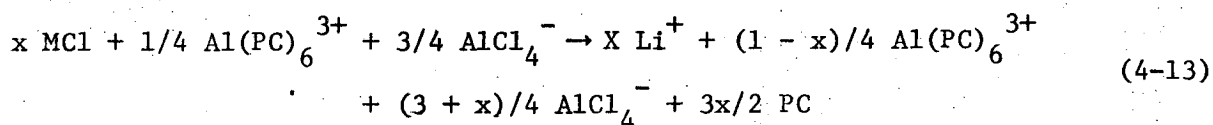
The specific conductance of the alkali metal chlorides in $AlCl_3$ (1 m)-PC solution was presented in Fig. 3-34 and Fig. 3-37 at 25° and 35°C, respectively. The general trend, with the exception of LiCl, is that the specific conductance increases with an increase in the concentration of the alkali metal chloride, MCl. In the case of NaCl, the specific conductance is almost constant over the entire concentration range. A steady increase in the specific conductance can be observed for KCl, RbCl and CsCl solutions in $AlCl_3$ (1 m)-PC. Small minima can be

observed at low concentrations of LiCl and CsCl. A comparison of the specific conductance of the alkali metal chlorides shows that the specific conductance increases as we pass along the alkali metal series, from Li to Cs. Despite the fact that Li is the smallest ion, its chloride solutions have the lowest conductance, while Rb and Cs, which are large ions, have the highest. These observations can be explained on the basis of ionic equilibrium, solvation and viscosity considerations.

A comparison of the present results with other data can be made only for the lithium system, on which several conductance measurements were made. Our value for the specific conductance of AlCl_3 (1 m) at 25°C in PC is $6.9 \cdot 10^{-3} \text{ ohm}^{-1} \text{ cm}^{-1}$. The molarity of this solution is 1.263 M. Boden⁸⁷ gives the specific conductance of AlCl_3 (1 M) as $9 \cdot 10^{-3}$, however, his measurements were performed at low frequency.⁸² Keller, et al.⁸¹ measured the conductance of AlCl_3 (1 M) as $6.96 \cdot 10^{-3}$ at 25°C (see Fig. 1-3), in good agreement with the present results. Extrapolation of the conductance curve of Breivogel and Eisenberg⁸⁸ results in a somewhat smaller value of approximately $6 \cdot 10^{-3} \text{ ohm}^{-1} \text{ cm}^{-1}$. Chilton and Cook¹⁵⁹ report a specific conductance of approximately $7.1 \cdot 10^{-3}$ for AlCl_3 (1 M) at 25°C . The specific conductance of LiAlCl_4 (1 m) at 25°C was measured in the present work as $6.7 \cdot 10^{-3} \text{ ohm}^{-1} \text{ cm}^{-1}$. The molarity of this solution is 1.26 M. Keller, et al.⁸¹ reports a value of $6.58 \cdot 10^{-3}$ for saturated solution of LiCl in AlCl_3 (1 M) in PC at 25°C , in good agreement with the present results. In addition, Keller's data confirm the present observation that the addition of LiCl to AlCl_3 (1 m) solution reduces the conductance of the resultant solution. Eisenberg, et al.'s conductance measurements of LiAlCl_4 in PC⁸⁸ were restricted to concentrations

of up to 0.6 M. However, crude extrapolation of their data to 1 M (Fig. 1-3) gives a value of approximately $7 \cdot 10^{-3} \text{ ohm}^{-1} \text{ cm}^{-1}$ at 25°C . The temperature coefficient of the specific conductance of AlCl_3 (1 m) solution in PC can be calculated from the data at 25° and 35°C . Our value of $0.15 \cdot 10^{-3} \text{ ohm}^{-1} \text{ cm}^{-1} \cdot \text{K}^{-1}$ is in reasonable agreement with $d\kappa/dT = 0.17 \cdot 10^{-3}$, calculated after Keller, et al.⁸¹ The temperature coefficient of the specific conductance of LiAlCl_4 (1 m) in PC is $0.17 \cdot 10^{-3} \text{ ohm}^{-1} \text{ cm}^{-1} \cdot \text{K}^{-1}$, again in good agreement with a value of $0.18 \cdot 10^{-3}$, after Keller, et al.⁸¹ In general, good agreement was found between the present results of AlCl_3 and LiAlCl_4 solutions in PC, and the corresponding results found in the literature. This agreement also should lend credibility to the data obtained for the rest of the alkali metal chloride- AlCl_3 system. Unfortunately, the latter results cannot be compared to earlier results obtained elsewhere; previous work was restricted to the $\text{LiCl}-\text{AlCl}_3$ system.

The addition of x moles of alkali metal chloride, MCl , to AlCl_3 (1 m) solution in PC is accompanied by the following reaction:



The number of charge carriers increases by $0.5x$ moles, and therefore, purely on this basis, the specific conductance should increase. The equivalent conductances of all the species are not known. The equivalent conductance of LiAlCl_4 in PC is reported as $34.5 \text{ ohm}^{-1} \text{ cm}^2 \text{ eq}^{-1}$.⁸⁸ The equivalent ionic conductance of Li^+ in PC is $7.30 \text{ ohm}^{-1} \text{ cm}^2 \text{ eq}^{-1}$.⁸² Hence the estimated equivalent conductance of AlCl_4^- is relatively quite high: $27.2 \text{ ohm}^{-1} \text{ cm}^2 \text{ eq}^{-1}$ (see Table 1-4 for comparison). The equivalent ionic conductances of the alkali metal ions in PC increases from Li^+ up to Cs^+ ,

despite the fact that the ionic crystal radius of Li^+ is the smallest, and that of Cs^+ the largest. This reversed trend was observed in most aprotic solvents as well as in water, and is caused by the tightly held sheath of solvent molecules attracted by the intense electric field of the small ion. The equivalent ionic conductances of Li^+ , Na^+ and K^+ in PC are 7.30, 9.40 and 12.0, respectively (see Table 1-4), and it is expected that the equivalent ionic conductances of Rb^+ and Cs^+ are even higher. The solvated radius of ions in nonaqueous solvents is discussed by Della Monica and Senatore.¹⁶⁰ The radii of the solvated alkali metal ions increase from Li^+ to Cs^+ in most solvents (methanol, formamide, N,N-dimethylformamide, dimethylacetamide, pyridine, acetonitrile and sulfolane). The same trend was observed by Yao and Bennion⁸⁴ in DMSO. Mukherjee, Boden and Lindauer⁷⁹ report equivalent conductances for Li^+ and K^+ in PC of 7.30 and 11.97, respectively.

The addition of MCl to AlCl_3 solution in PC results in two effects: addition of M^+ ions, and a conversion of $\text{Al}(\text{PC})_6^{3+}$ to AlCl_4^- ions. On the basis of the discussion so far, both effects tend to increase the conductance, and the increase is larger as we move along the alkali metal series from Li to Cs . The equivalent conductance of $\text{Al}(\text{PC})_6^{3+}$ is not known since extrapolation to infinite dilution of AlCl_3 in PC is tenuous (because of the minimum at low concentrations (see Fig. 1-3)), and therefore quantitative analysis is not possible. An additional and opposing effect is the change in the viscosity of the solution. Since viscosities were not measured in the present work, the discussion of this effect is based primarily on data in the literature. Keller, et al.⁸¹ report viscosities at 25°C of 5.72 and 7.16 cp for AlCl_3 (1.03 M) solution,

and for saturated LiCl solution in AlCl_3 (103 M), respectively. The viscosity of pure PC is 2.48 and 1.33 cp at 25° and 60°C, respectively.⁸¹ Eisenberg¹⁶¹ measured viscosities of LiAlCl_4 solutions in PC. The viscosities of 0.75 M and 1.25 M LiAlCl_4 solutions in PC at 25°C are 4.42 and 7.57 cp, respectively.

It is well known that viscosities do not change in the same manner as conductivities. Viscosities of electrolytic solutions have been used as an indication of the degree of structuredness within the solvent. In aqueous solutions the effects are generally ascribed to the ability of the various ions to increase or decrease the structure of water over that of the pure solvent. Small ions, such as lithium, are structure makers, while large simple ions, such as cesium, are structure breakers. This is the reason why the viscosities of aqueous alkali metal solutions decrease as the cations change along the series from Li^+ to Cs^+ . According to this consideration, the effect should not be observed for solvents exhibiting only a small amount of structure. However, Criss and Mastroianni¹⁶² discuss this matter, and show that even in structureless solvents, the B_η coefficients in the Jones-Dole equation¹⁶³

$$\eta/\eta_0 = 1 + A_\eta c^{1/2} + B_\eta c \quad (4-14)$$

decrease with the increase in the size of the ion. This can only be explained in terms of structuring the solvent by the smaller cations. In the present system, the original solution is AlCl_3 (1 m)-PC and not pure PC. This solution possesses a large degree of order to begin with. The addition of LiCl to this solution destroys the previous order by converting $\text{Al}(\text{PC})_6^{3+}$ to AlCl_4^- , but the small Li^+ ion is a structure

maker, and therefore the viscosity increases. On the other hand, the addition of CsCl, for example, destroys the initial order, but the large Cs⁺ ion is a poor order maker, and it is predicted, therefore, that the increase in the viscosity with concentration will be small or even reversed in the case of RbCl and CsCl solutions in AlCl₃-PC.

Evidence that the viscosity decreases with the size of the cation can be found in the viscosity measurements of Mukherjee and Boden.⁸² The B_η coefficients in PC follow the order LiClO₄ > n-Bu₄N ClO₄ > Et₄N ClO₄, in agreement with the increasing size order.

The minimum in the conductance curve for LiCl in AlCl₃ (1 m)-PC can be the result of ionic association of LiCl in PC.^{82,95,96,97} The association constant for LiCl was estimated to be 557 from conductance measurements,⁸² and as 59 from emf measurements.⁹⁶ The minimum in the conductance curve of CsCl in AlCl₃ (1 m)-PC can be the result of a combination of the opposing factors which determine the conductance of the solution.

The minimum in the plot of the equivalent conductance of AlCl₃ in PC was observed by several workers^{81,88,159} (see Section 1.5). There is no conclusive explanation for this behavior at low concentration. An attempt to explain the minimum by the water content of the solvent seems questionable because the minimum was observed by three independent laboratories and the water contents were probably different. Moreover, if we assume that the minimum is the result of the water content, we can extrapolate to infinite dilution, neglecting the minimum (see Fig. 103), and obtain the molar conductance at infinite dilution, $\Lambda_0 = 18 \text{ ohm}^{-1} \text{ cm}^2 \text{ mole}^{-1}$. The equivalent conductance of AlCl₄⁻ was estimated

before at 27.2, and according to this, the equivalent ionic conductance of $\text{Al}(\text{PC})_6^{3+}$ would be

$$\Lambda_{\text{Al}(\text{PC})_6^{3+}}^{\circ} = 4/3 \ 18 - 27.2 = -3.2 \ \text{ohm}^{-1} \text{cm}^2 \text{eq}^{-1}$$

On the basis of this discussion it seems that the minimum in the equivalent conductance of AlCl_3 is not the result of impurities, and is probably associated with multiple ionic equilibria.

4.5. Density Measurements and Excess Volumes

Density measurements at various molalities of the alkali metal chlorides in AlCl_3 (1 m)-PC solution at 25° and 35°C (see Section 3.5) show that adding NaCl, KCl, RbCl or CsCl increases the density of the solution, while adding LiCl decreases it slightly. The order of the increase in the density follows the order of the molecular weights of the alkali metals. This was quite expected because, for example, 1 mole of CsCl weighs 168.36 gr, while 1 mole of LiCl only weighs 42.39 gr. The density of 1 molal CsCl solution in AlCl_3 (1 m)-PC is 1.35967 and that of LiCl only 1.25945 gr/cm^3 .

In order to isolate the influence of the addition of alkali metal chloride to AlCl_3 (1 m)-PC solution, the excess volumes were calculated. The excess volume is the difference between the experimental specific volume and the calculated specific volume, under the assumption that the volumes of the solvent and the solute are additive. The specific molar volumes of LiCl, NaCl, KCl, RbCl and CsCl at 25°C are 20.498, 26.993, 37.58, 43.1857 and 42.2166 cm^3/mole , respectively. The calculated specific volume of a solution of molality m_{MCl} in AlCl_3 (1 m)-PC was calculated according to

$$v_{\text{calc}} = \frac{m_{\text{MCl}} v_{\text{MCl}}^m + v_{\text{AlCl}_3\text{-PC}} (1133.34)}{m_{\text{MCl}} (\text{M. W.})_{\text{MCl}} + 1133.34} \quad (4-15)$$

where m_{MCl} is the molality of MCl, v_{MCl}^m is the molar volume of MCl, $v_{\text{AlCl}_3\text{-PC}}$ is the specific volume of AlCl₃ (1 m)-PC solution (0.79187 and 0.79811 cm³/gr at 25° and 35°C, respectively), and (M. W.)_{MCl} is the molecular weight of MCl. The number 1133.34 is the sum of 1000 gr PC and 133.34 gr AlCl₃ (1 mole of AlCl₃).

Table 4-3 presents the experimental specific volumes, the calculated specific volumes, and the excess specific volumes for various molalities of MCl in AlCl₃ (1 m)-PC solution at 25°C. Table 4-4 presents the similar results at 35°C.

The specific excess volume of 1 mole of AlCl₃ in 1000 gr pure PC can be calculated from the specific volumes of pure PC, AlCl₃ salt and AlCl₃ (1 m)-PC solution. The excess volume of AlCl₃ (1 m)-PC is then 0.687 10⁻² and 0.811 10⁻² cm³/gr, at 25° and 35°C, respectively.

In general, the specific excess volumes are positive, except in the case of KCl(0.5 m), RbCl(0.1 m) and CsCl(0.0025 m). The negative excess volume for CsCl(0.0025 m) might be due to experimental error because of the low concentration; however, in the case of KCl(0.5 m) and RbCl(0.1 m) it is not clear whether the negative values are in error or are meaningful. The excess volumes are in the order of 1-2%, which means that the volume of a unit molality solution of alkali metal chloride in AlCl₃ (1 m)-PC increases by 1-2% over the sum of the volumes of the solute and the solvent. It seems that reorientation of the solvent's molecules does not change the volume significantly, and the

Table. 4-3. Excess specific volumes of alkali metal chlorides in AlCl_3 (1 m)-PC at 25°C.

Salt	m_{MCl}	v_{exp} (cm^3/gr)	v_{calc} (cm^3/gr)	$10^2 v_{\text{excess}}$ (cm^3/gr)
LiCl	0.5		0.78625	
	1.0	0.79399	0.78075	+1.325
NaCl	0.01	0.79230	0.79170	+0.060
	0.10	0.79128	0.79017	+0.111
	0.25	0.79049	0.78766	+0.283
	0.50	0.78984	0.78357	+0.627
	0.0025	0.79265	0.79182	+0.083
KCl	0.01	0.79211	0.79168	+0.043
	0.10	0.79270	0.78999	+0.271
	0.25	0.78930	0.78721	+0.209
	0.50	0.78240	0.78270	-0.030
	0.01	0.79160	0.79140	+0.020
RbCl	0.05	0.79047	0.78872	+0.175
	0.10	0.78590	0.78728	-0.138
	0.25	0.78265	0.78057	+0.208
	1.00	0.75783	0.74995	+0.788
	0.0025	0.79134	0.79167	-0.033
CsCl	0.01	0.79134	0.79106	+0.028
	0.50	0.75790	0.75445	+0.345
	1.00	0.73547	0.72188	+1.359

Table 4-4. Excess specific volumes of alkali metal chlorides in AlCl_3 (1 m)-PC at 35°C.

Salt	m_{MCl}	v_{exp} (cm^3/gr)	v_{calc} (cm^3/gr)	$10^2 v_{\text{excess}}$ (cm^3/gr)
LiCl	0.50		0.79238	
	1.00	0.79922	0.78677	+1.245
NaCl	0.01	0.79830	0.79794	+0.036
	0.10	0.79777	0.79639	+0.138
	0.25	0.79670	0.79383	+0.287
	0.50	0.79630	0.78966	+0.664
KCl	0.0025	0.79840	0.79806	+0.034
	0.01	0.79826	0.79792	+0.034
	0.10	0.79724	0.79619	+0.105
	0.25	0.79532	0.79335	+0.197
	0.50	0.78870	0.78874	-0.004
RbCl	0.01	0.79764	0.79764	0.000
	0.05	0.79798	0.79492	+0.306
	0.10	0.79277	0.79345	-0.068
	0.25	0.78912	0.78665	+0.247
	1.00	0.76389	0.75560	+0.829
CsCl	0.0025	0.79800	0.79791	+0.009
	0.50	0.76280	0.76027	+0.253
	1.00	0.74177	0.72731	+1.446

ions fit comfortably between the solvent's molecules without causing changes in volume. The excess volume increases with the size of the alkali metal ion, with the exception of lithium chloride, for which the excess volume is close to that of CsCl. The excess volume of adding AlCl_3 to pure PC is also quite low, despite the fact that $\text{Al}(\text{PC})_6^{3+}$ complex is formed.

4.6. Micropolarization of the Alkali Metals in Their Chloride Solutions in AlCl_3 (1 m)-PC

Micropolarizations of the alkali metals in alkali metal chloride solutions in AlCl_3 (1 m)-PC were presented in Fig. 3-40 to Fig. 3-44. The apparent exchange current densities were calculated from the slopes at the point of zero current. A linear behavior can be observed for all the alkali metals over a wide range of alkali metal chloride concentrations. Using a low current and moderate stirring ensured the elimination of concentration overpotential. The apparent exchange current densities were not corrected for the nonuniform current densities across the surface of the electrodes. The influence of the nonuniformity of the current across the electrode is discussed in Section 4.7, where it is shown that, despite relatively low conductivities, this correction is negligible for the present case, because of low exchange current densities.

The comparison of the magnitude of the exchange currents to corresponding values in the literature is restricted to the lithium system, because no information is available for the rest of the alkali metals. The exchange current density of Li in LiAlCl_4 (1 m), according to the present results, are 1.02, 1.5 and 2.0 mA/cm^2 at 25°, 30° and 35°C,

respectively. These values are in general agreement with the exchange currents of 0.40, 1.05, 1.49 and 2.35 mA/cm² reported by Meibuhr⁴⁷ for LiAlCl₄ (1 M) at 19°, 35°, 46° and 55°C, respectively. A plot of the exchange current densities vs. 1/T is presented in Fig. 3-45, and the calculated enthalpy of activation at zero polarization, $H_o^* = 8.6$ kcal/mole, is in agreement with an enthalpy of 6.4 kcal/mole, reported by Meibuhr.⁴⁷ Kinetic measurements of Li in LiClO₄ solutions in PC were performed by Meibuhr⁴⁶ and Scarr.⁴⁸ The exchange current densities in LiClO₄ (1 M) solution were 0.95, 1.8, 3.4 and 5.25 mA/cm² at 28°, 43°, 58° and 67.5°C, respectively,⁴⁶ and 1.78 mA/cm² at 23°C.⁴⁸ The i^o values for LiClO₄ solution in PC are of the same order of magnitude as those obtained here for LiAlCl₄. Butler, et al.⁴⁹ found that the current density changes significantly during the first few minutes after the preparation of a clean fresh Li surface. However, all earlier experiments, as well as the present ones, were performed on aged surfaces, which is a more practical condition. Pre-anodization of the surface was necessary to obtain reproducible results. It is not clear whether this procedure removes adsorbed impurities or breaks an insulating film on the electrode. Scarr⁴⁸ reports two levels of activities of Li electrode in LiClO₄ solution in PC, depending on the pre-treatment of the surface, and the lower level of activity was associated with film formation.

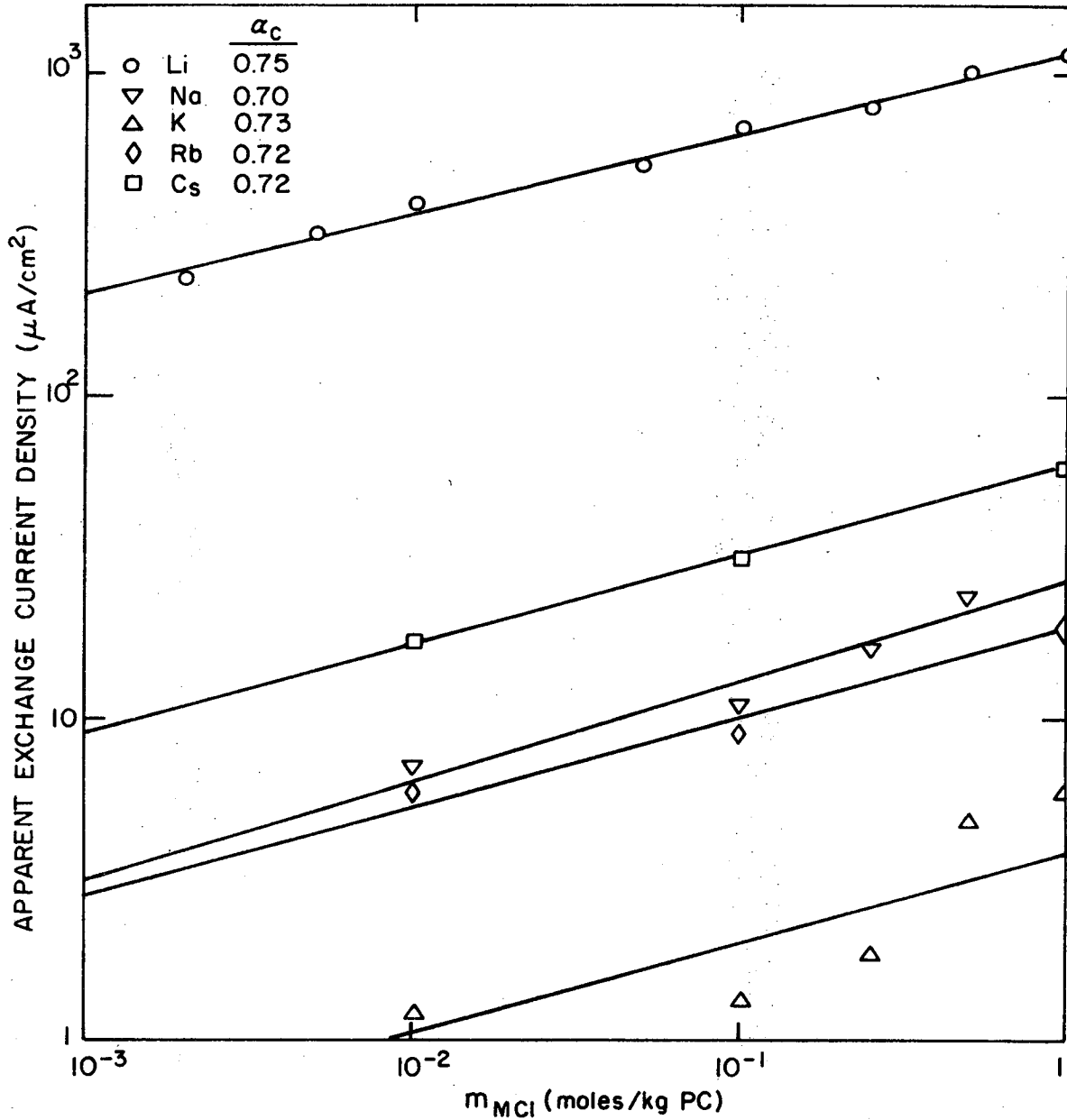
The exchange current densities for the rest of the alkali metals are lower than those for Li. The wide differences in the exchange currents in the alkali metal series are discussed in detail in Chapter VI, where the medium effect and the influence of the individual ionic energetics on the electrode kinetics is discussed with regard to the

alkali metal amalgams. The order of activity of the alkali metals is $\text{Li} > \text{Cs} > \text{Na} > \text{Rb} > \text{K}$. This order might also be the result of the reactivity of some of the alkali metals toward impurities, water and even the solvent itself. This is especially true for potassium, which showed reactivity toward PC solutions which were not treated with molecular sieves. The exchange current density of Na electrode in $\text{NaCl}(0.5 \text{ m})$ solution in $\text{AlCl}_3(1 \text{ m})\text{-PC}$ is $28 \mu\text{A}/\text{cm}^2$ at 25°C , which can be compared qualitatively to a value of $12 \mu\text{A}/\text{cm}^2$ for Na electrode in $\text{NaClO}_4(0.5 \text{ M})$ solution in PC at 19°C .⁶⁰ The low exchange currents for potassium are definitely the result of the relatively unstable behavior of this metal in PC. The relatively high exchange current densities for Cs electrode might be the result of the fact that the metal melts at 28.5°C , and therefore the metal is very soft at room temperature.

The transfer coefficients of the electrochemical reaction at the alkali metal electrode interface can be calculated from the dependence of the exchange current density on the concentration of the reduced ion:^{164,165}

$$1 - \alpha_c = \frac{\partial \log i_a^0}{\partial \log C_M^+} \quad (4-16)$$

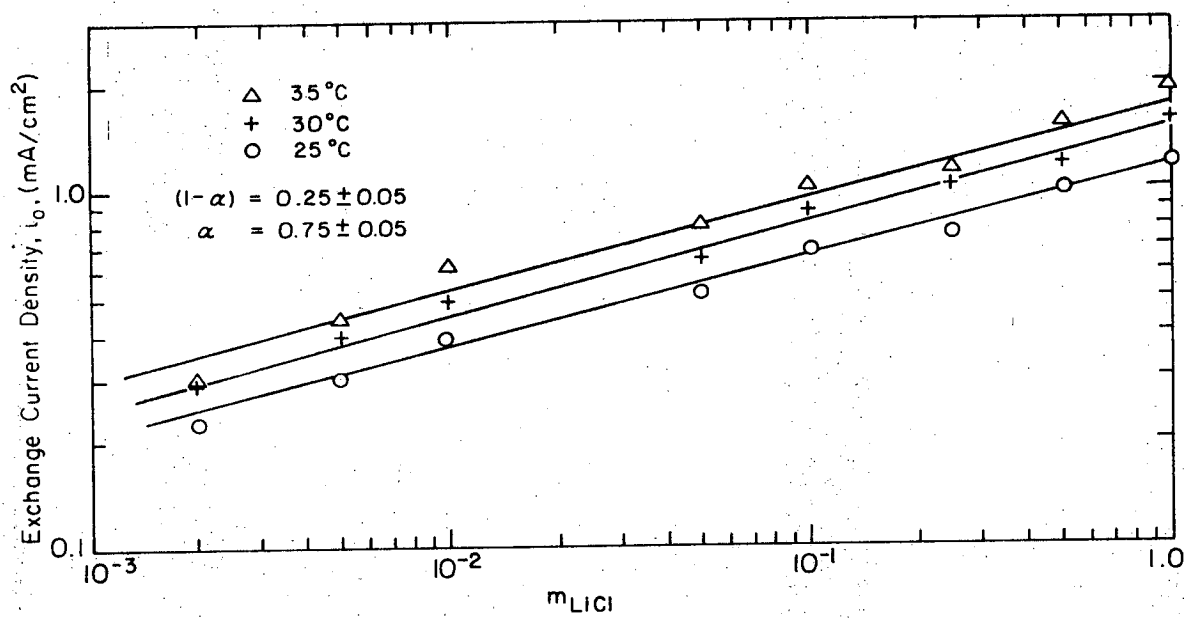
where α_c is the cathodic transfer coefficient. Figure 4-2 presents the plot of $\log i_a^0$ vs. $\log m_{\text{MCl}}$ for all the alkali metals, as well as the calculated α_c . The cathodic transfer coefficient for Li is $\alpha_c = 0.75$, in agreement with $\alpha_c = 0.8$ reported for LiAlCl_4 in PC, and $\alpha_c = 0.62 - 0.72$ for LiClO_4 in PC.^{46,47,48} The lithium system was further investigated at three different temperatures, 25° , 30° and 35°C . The plots of $\log i_a^0$ vs. $\log m_{\text{LiCl}}$ at the three temperatures are presented in Fig. 4-3,



XBL 725-6284

Fig. 4-2. Determination of the cathodic transfer coefficients of the alkali metals in $\text{AlCl}_3(1 \text{ m})\text{-PC}$.

-181-



XBL72I-600I

Fig. 4-3. Determination of the cathodic transfer coefficients of Li in $AlCl_3(1\text{ m})-PC$ at 25°, 30° and 35°C.

and the parallel lines show that the transfer coefficient does not change over this temperature range. An average $\alpha_c = 0.75 \pm 0.05$ was calculated for the three temperatures.

Lithium was also deposited from LiAlCl_4 (1 m) solution in PC on a rotating disk electrode (see Section 3.9) at moderately high current densities, well in the Tafel region. The exchange current density derived from this range was $i_a^0 = 1.7 \text{ mA/cm}^2$, in fairly good agreement with the exchange current obtained from the micropolarization experiments. The cyclic voltammograms, which were obtained for K, Rb and Cs (see Sections 3.1-3 to 3.1-5) are covering the Tafel region and are also in qualitative agreement with the micropolarization results. Although the voltammograms include the ohmic drop between the working and the reference electrodes, Tafel behavior can nevertheless be observed qualitatively in some of these figures. The behavior of the rest of the alkali metals in the Tafel region, where practical currents in the order of at least 10 mA/cm^2 are being applied, should be investigated in the future. It is believed that the exchange currents in this region are higher than the values obtained in the micropolarization experiments, because of continuous renewal of the active surface, and the breakage of possible film formation at high deposition or dissolution rates.

4.7. Nonuniform Current Distribution and Ohmic Drop Effects in Micropolarization Measurements

The micropolarization method is used frequently to determine the exchange current density of an electrode reaction. According to this method, the exchange current density can be calculated from the slope of the linear polarization curve at the point of zero current.

This method is valid only when the current distribution is uniform at the surface of the electrode. The nonuniformity of the current is dictated by the geometry of the system. Nevertheless, many kinetic measurements were performed under nonuniform conditions, and serious errors can result under certain conditions, especially when the exchange current density is relatively high, the conductance of the solution is low, or when the linear dimension of the electrode is large.

When the overpotential is measured between the working electrode and the reference electrode placed somewhere in the solution, this quantity includes the surface activation overpotential, the ohmic drop, and concentration overpotential. In order to isolate the surface overpotential (or the charge transfer overpotential), the last two contributions should be subtracted. The concentration overpotential can be calculated for certain systems.^{166,167} In the case of relatively slow electrode reaction, when $i^0 < 1.0 \text{ mA/cm}^2$, the micropolarization experiments are carried out at low currents, and the concentration overpotentials may be negligible. In addition, forced convection, in the form of agitation or flow, can eliminate the concentration gradients. A pulse technique can also be used for this purpose.¹⁶⁸

The ohmic drop can be calculated analytically for certain geometries¹⁶⁷ by solving the Laplace's equation, or can be estimated experimentally by interrupting the current and following the immediate potential drop within a few microseconds.^{168,169} Since the current interrupter technique was frequently used in kinetic measurements of nonaqueous systems,^{46,48,49} including the present one, the validity of such measurements will be examined. Concentration overpotential will be ignored by assuming uniform

bulk concentration up to the electrode's surface. The analysis is restricted to a disk electrode embedded in an insulating plane. The alkali metal electrodes used in the present polarization experiments can fit into this geometry because the wire electrodes were coated with epoxy and cut, exposing disk-shaped active surfaces. The nonuniform current distribution is associated with a nonuniform ohmic potential drop. The question arises, according to Newman: ". . . What ohmic potential drop is measured by an interrupter technique?"¹⁶⁹ The ohmic drop is some average value which does not prevail everywhere on the electrode. On interrupting the current, the double layer capacity remains charged, and the potential just outside the double layer changes by a uniform amount over the entire surface of the electrode. Therefore, the measured ohmic drop corresponds to the primary current distribution.¹⁶⁹

Under nonuniform current density conditions, the exchange current, i^0 , determined from the linear polarization, depends on the location of the reference electrode, because the measured overpotential is related to the local current density which differs from the average current density. The correction can be obtained by solving the secondary current distribution subjected to a boundary condition of linear polarization. The present analysis follows the treatment of Tiedemann, Newman and Bennion¹⁷⁰ concerning the error in measurements of electrode kinetics caused by nonuniform ohmic potential drop to a disk electrode. The local current density is given by

$$i(r) = i^0 \frac{F}{RT} \eta \quad (4-17)$$

The average current density is related to the apparent overpotential, calculated by the current interrupter technique,

$$i_{(ave)} = i_{\text{apparent}}^{\circ} \frac{F}{RT} \eta_{\text{apparent}} \quad (4-18)$$

The local overpotential, η , is the difference between the electrode potential V , and the potential just near the electrode at a particular position, r . The correction for the apparent exchange current is given by

$$\frac{i^{\circ}}{i_{\text{apparent}}^{\circ}} = \frac{i(r)}{i_{\text{apparent}}} \frac{\eta_{\text{apparent}}}{\eta} \quad (4-19)$$

The correction was solved for the general arbitrary location of the reference electrode:¹⁷⁰

$$\frac{i^{\circ}}{i_{\text{apparent}}^{\circ}} = \frac{\pi J}{4} \frac{4k_{\infty} r_o V}{I} - 1 - \sum_{n=1}^{\infty} \frac{B_n}{B_o} P_{2n}(\eta) M_{2n}(\xi) \quad (4-20)$$

The nomenclature is given in Ref. 170, and follows the usual Newman's nomenclature.¹⁶⁷

The solutions for three special cases are given in Fig. 4-4, where:
 A. The reference electrode is placed at the center of the disk, B. The reference electrode is far away from the electrode and C. The reference electrode is located at the edge of the disk electrode. The correction is plotted against J :

$$J = (\alpha_a + \alpha_c) \frac{Fr_o i^{\circ}}{RTk_{\infty}} \quad (4-21)$$

J represents, in a way, the throwing power of the system. At the center of the disk the apparent exchange current is larger than the true one because the local current is lower than the average.

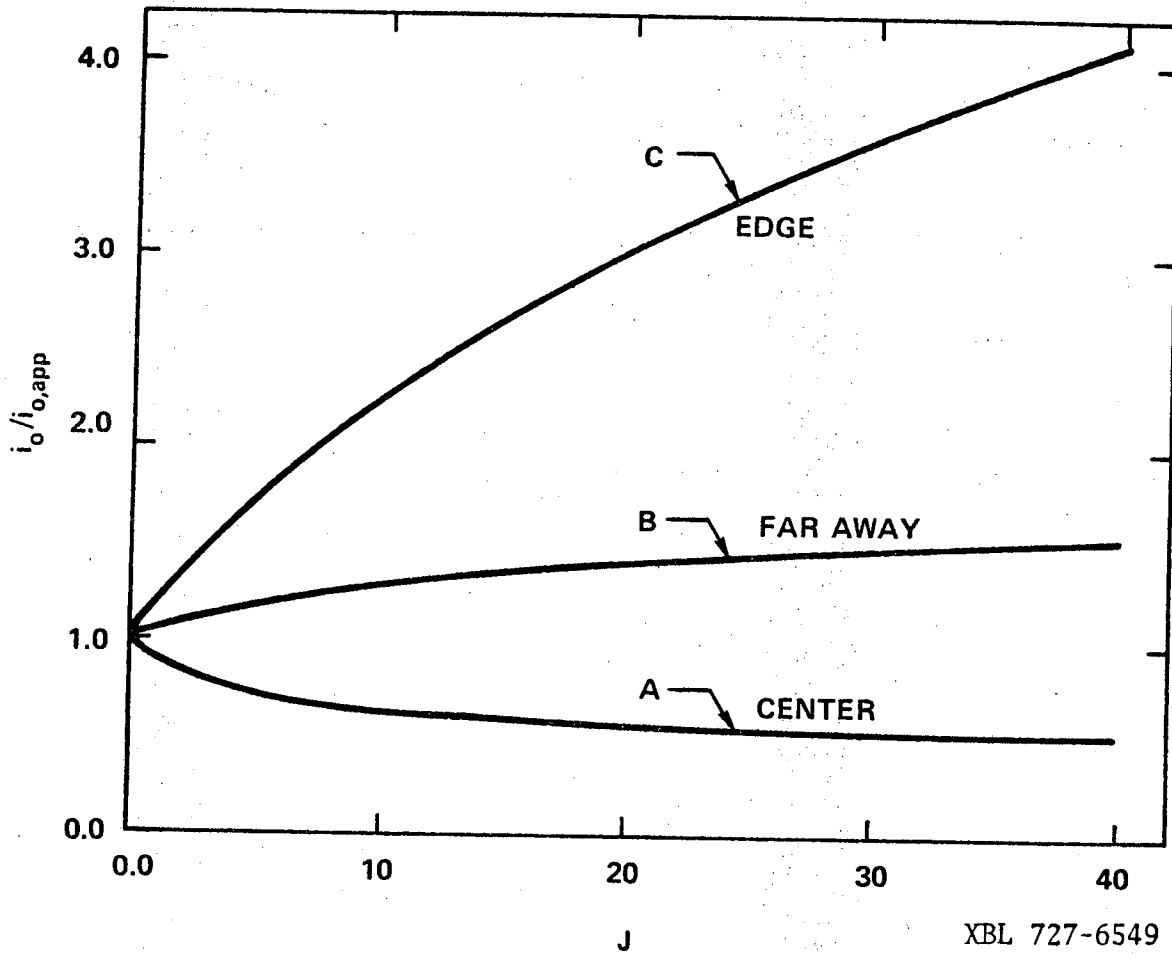


Fig. 4-4 Correction in i_o determination for linear polarization for various positions of the reference electrode relative to the disk electrode.¹⁷⁰
Curve A approaches 0.5 for large J , while Curve C approaches infinity.

The situation is opposite at the edge, where the local current is higher. Large error can result from measurements where the reference electrode is located at the edge. The best location is far away from the electrode; however, under this condition the ohmic drop becomes a significant part of the total overpotential, and the resulting error is probably higher than the error due to the nonuniformity of the current.

The exchange current densities reported in the present work (Section 3.6) are the apparent ones; however, the corrections are negligible. Considering the extreme conditions, $r = 0.5 \text{ cm}$, $\kappa_{\infty} = 5 \cdot 10^{-3} \text{ ohm}^{-1} \text{ cm}^{-1}$, $i^{\circ} = 1.0 \text{ mA/cm}^2$ and assuming $(\alpha_c + \alpha_a) = 1$, we can estimate the largest possible J for the present systems to be

$$J = 4$$

Since the reference electrodes were located far away from the disk electrode, the correction, according to curve B in Fig. 4-4, is about $i^{\circ}/i_{\text{apparent}}^{\circ} = 1.1$, which is negligible, especially since the errors in the exchange current values are probably more than 10%. It should be mentioned here that the extreme conditions given above were realistic only for the lithium system. For the rest of the alkali metals the exchange current densities are ten times lower, and the conductivities are somewhat higher, both resulting in lower J , and the correction is probably in the order of 1%. This analysis is not applied for the polarizations of the alkali metal amalgams because the specially designed cell ensured uniform current distribution (see Fig. 2-15). Tiedemann and Bennion¹⁷¹ have criticized Scarr's results about the kinetics of Li in LiClO_4 solution in PC. Scarr⁴⁸ placed his reference electrode near the edge of the electrode, and the J number of his system is about

10, resulting in a correction in the order of a factor of 2 to the reported i^0 apparent. The criticism of Meibuhr's results,⁴⁶ that it was not corrected for the nonuniform current distribution, seems unjustified because in this work, the reference electrode was placed far away from the working electrode, and therefore, the approximate J number is very small, resulting in a negligible correction of the exchange current density. In trying to find an agreement between their results in dimethyl sulfite and kinetic measurements in PC,^{46,48} Tiedemann and Bennion¹⁷¹ seem to have overlooked the fact that their kinetic measurements were performed in a different solvent, and medium effects must be considered as partly responsible for the higher exchange currents in dimethyl sulfite. The effects of the solvent on the electrode kinetics is discussed in Chapter VI.

4.8. Micropolarization of the Alkali Metal Amalgams in Their Chloride Solutions in AlCl_3 (1 m)-PC

Micropolarizations of the alkali metal amalgams in the corresponding alkali metal chlorides in AlCl_3 (1 m) solution in PC are presented in Fig. 3-46 to Fig. 3-50. The experiments were performed in a cell especially designed to eliminate nonuniform current distribution at the amalgam electrode, and to minimize ohmic drop (see Fig. 2-15).

The potential associated with the passage of an applied current is the sum of: 1. Charge transfer overpotential, 2. IR drop between the working and the reference electrode and 3. Concentration overpotential. The IR drop was small due to the short distance between the tip of the capillary and the surface of the amalgam. The IR drop was estimated by the current interrupter technique and subtracted from the total overpotential. Concentration overpotentials were small because of the low

currents and the short time of the micropolarization. The current was applied only for a few seconds, the minimal time necessary to read the overpotential on the differential voltmeter. However, the increase in the potential at the cathodic direction in some of the micropolarization curves in Fig. 3-46 to Fig. 3-50, and the appearance of an "almost limiting current" like behavior at low concentrations, suggest that concentration overpotential might explain the large cathodic overpotentials. The concentration overpotential and the transition time can be estimated from the solution given by Sand^{172,173} for the case of diffusion from a semi-infinite column of electrolyte, under galvanostatic conditions. The difference between the bulk concentration, C_b , and the surface concentration, $C_{(0,\theta)}$, at time θ is given by

$$C_b - C_{(0,\theta)} = \frac{2i}{nF} \sqrt{\frac{\theta}{\pi D}} \quad (4-21)$$

The transition time, τ , which is the time when the interfacial concentration of the ions being discharged drops to zero, is given by

$$\tau = \frac{\pi D}{4} \left(\frac{nFC_b}{i} \right)^2 \quad (4-22)$$

and the concentration overpotential can be expressed by

$$\eta_c = \frac{RT}{nF} \ln \left(1 - \sqrt{\frac{\theta}{\tau}} \right) \quad (4-23)$$

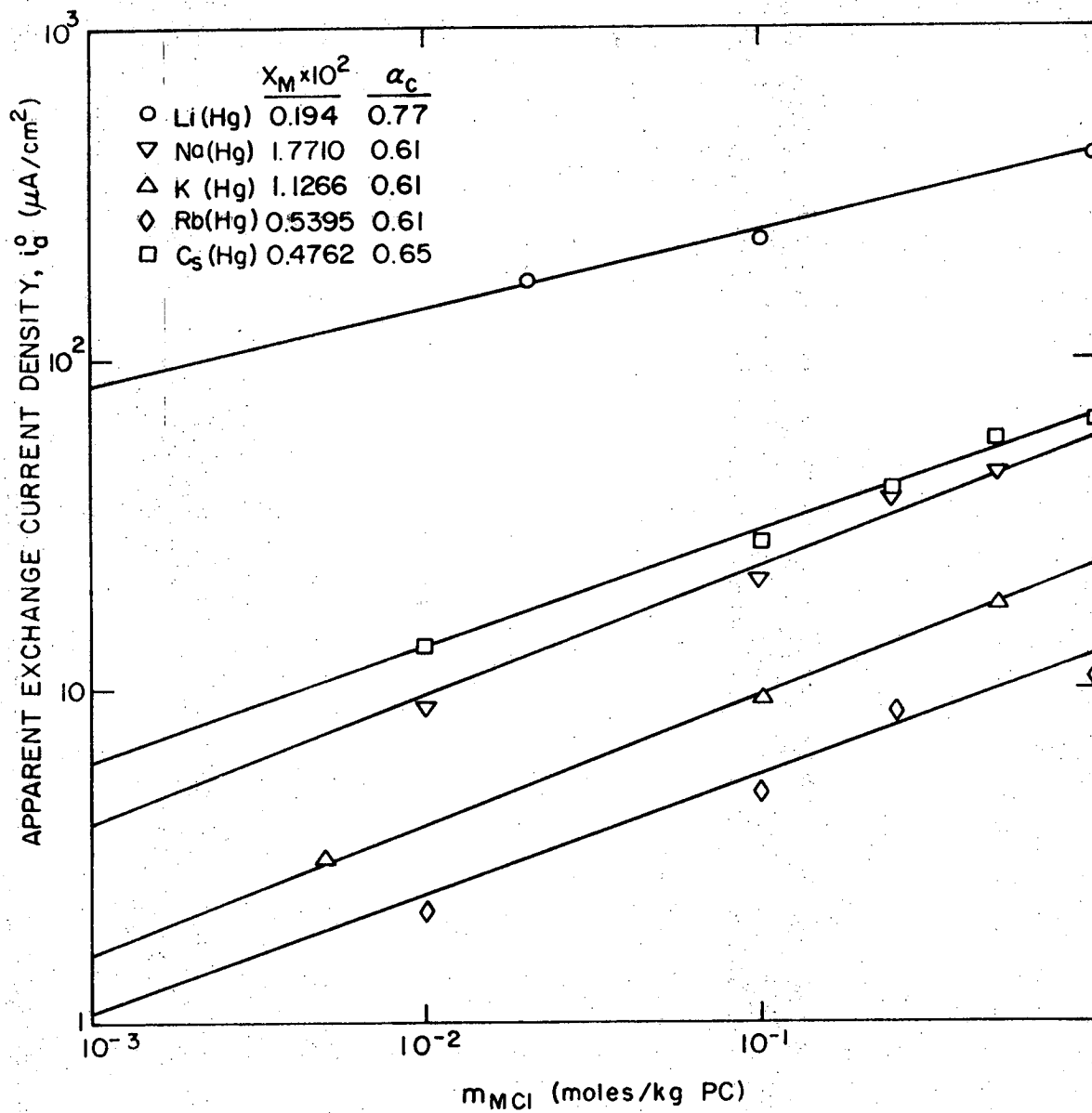
The diffusion coefficient in the present system is in the order of $D = 3 \cdot 10^{-6} \text{ cm}^2/\text{sec}$.¹⁷⁴ The maximum current was in the order of $i = 0.1 \text{ mA/cm}^2$. The lowest concentration was in the range of $C_b = 0.01 \text{ m}$. The transition time for these extreme conditions is about 250 sec, which is about ten fold the time of each measurement. The concentration

overpotential can be estimated as

$$\eta_c = 0.059 \log (1 - 0.1) = 0.010 \text{ volt} .$$

Therefore, under these extreme conditions, the concentration overpotential starts to become significant, and is probably the reason for the sharp increase in the cathodic overpotential. The exchange current densities were calculated from the linear zones, where the currents were less than about 0.02 mA/cm^2 . For this current, and under the same extreme conditions, the transition time is in the order of 100 minutes, and the concentration overpotential is negligible. For concentrations in the order of 0.1-1.0 m the concentration overpotentials were negligible under all conditions. For example, the concentration overpotential for 0.1 m MCl solution in AlCl_3 (1 m)-PC at 0.050 mA/cm^2 , after one minute, is $\eta_c = 1.3 \text{ mV}$, which is negligible compared to the total overpotential of about 50 mV. In conclusion, it is quite possible that the sharp increase in the cathodic overpotentials is the result of concentration overpotentials, especially when the alkali metal concentration was low, and the current was relatively high. The micropolarization experiments were completed as quickly as possible, and the manual increase of the current was preferred over a pulse technique because of the accuracy in measuring the steady state overpotential using a very accurate differential voltmeter.

The transfer coefficients of the alkali metal amalgams were obtained by plotting $\log i_a^0$ vs. $\log m_{\text{MCl}}$, and the cathodic transfer coefficients were calculated from the slopes of the straight lines. The transfer coefficients are presented in Fig. 4-5. The transfer coefficient of Li(Hg) is the highest, $\alpha_c = 0.77$. The transfer coefficients of Na(Hg) , K(Hg) and Rb(Hg) are equal, $\alpha_c = 0.61$. The transfer coefficient of Cs(Hg)



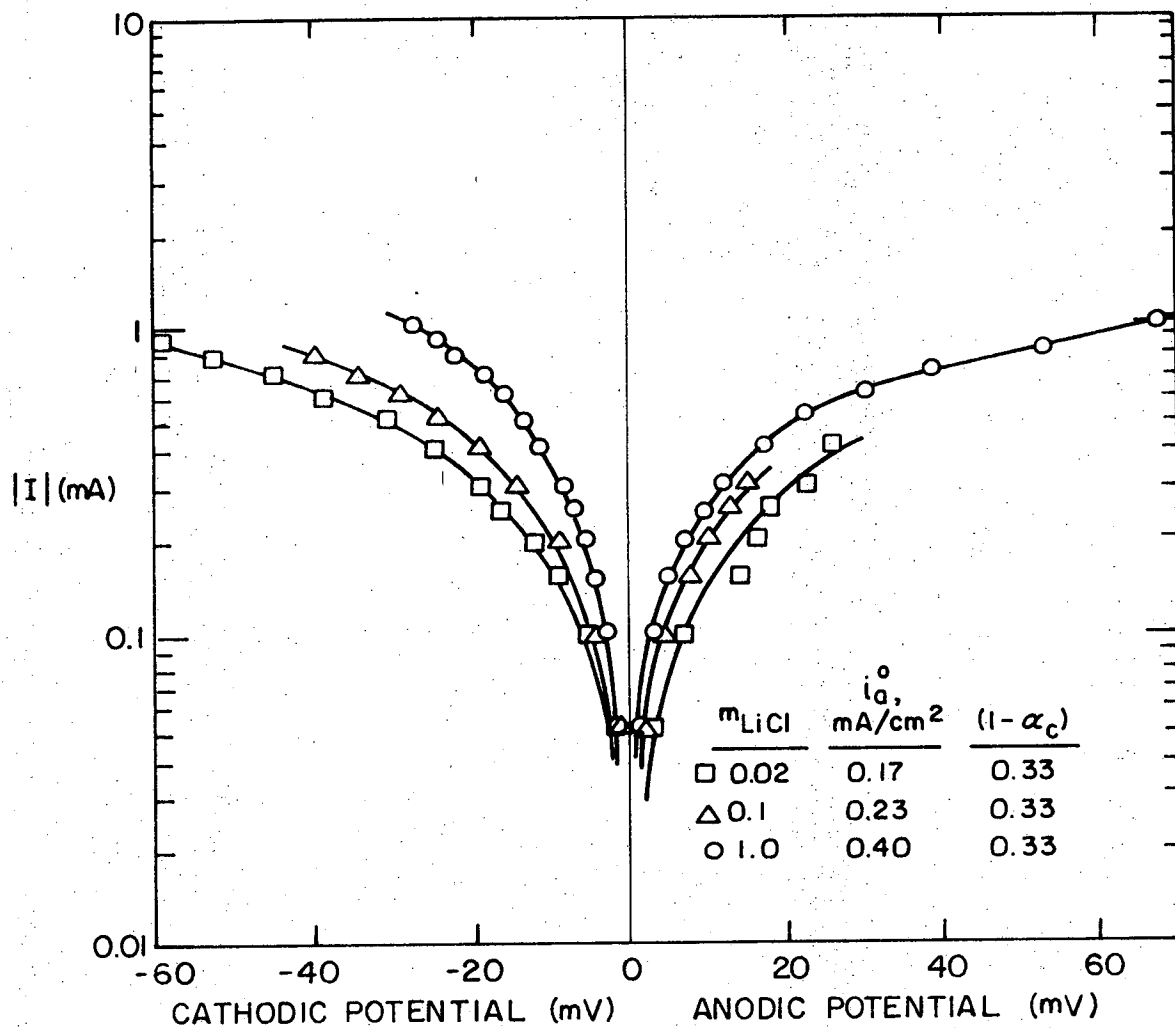
XBL725-6285

Fig. 4-5. Determination of the cathodic transfer coefficients of the alkali metal amalgams in AlCl_3 (1 m)-PC solution.

is somewhat higher, $\eta_c = 0.65$.

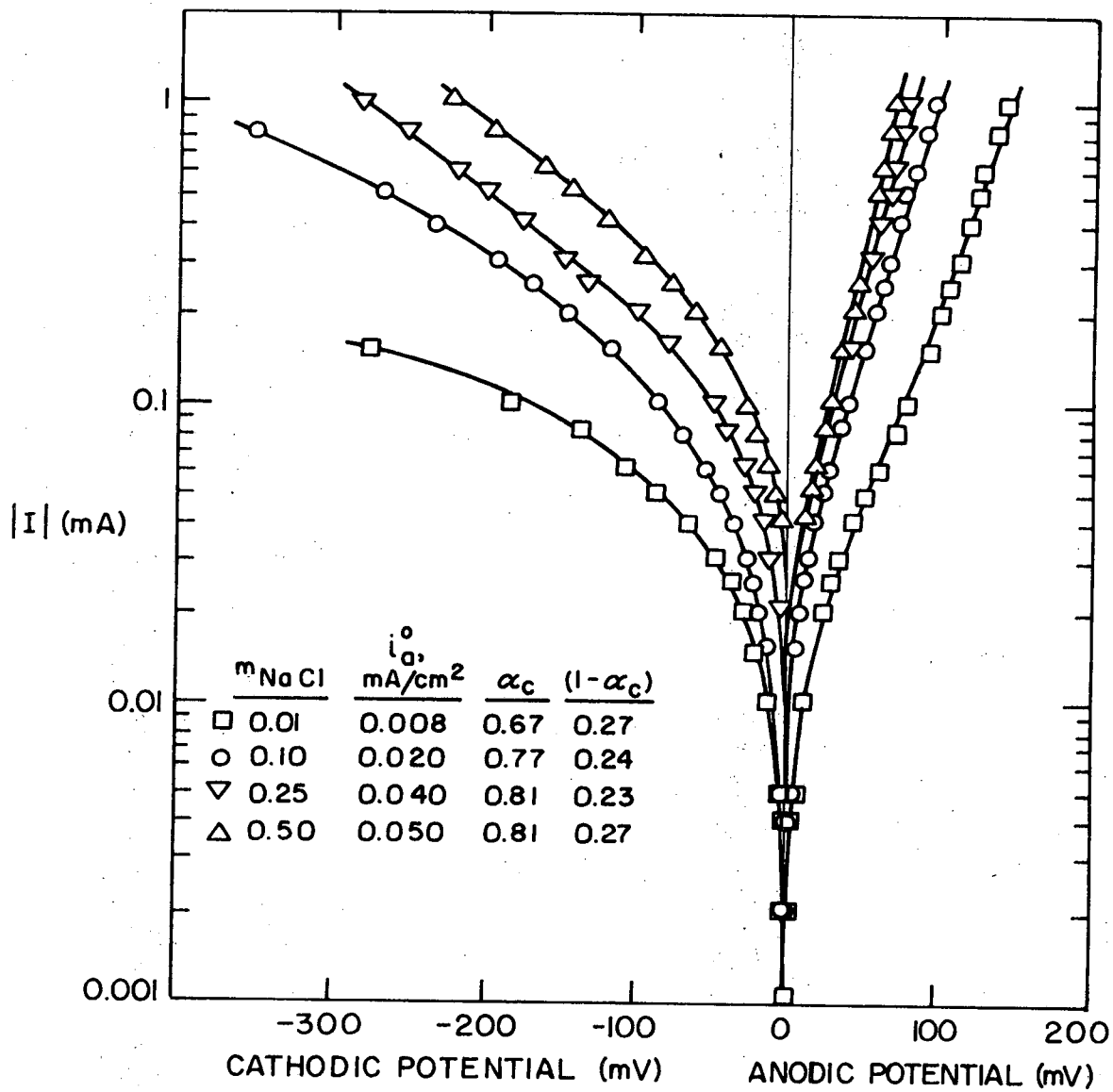
In order to compare the kinetic parameters obtained from the linear polarization and from the concentration dependence of the exchange current densities, the polarization data is replotted according to the Tafel equations (see Eq. (3-11) and (3-12)). Figures 4-6 to 4-10 present the Tafel plots for all the alkali metal amalgams in different alkali metal chloride molalities in AlCl_3 (1 m)-PC solution. The Tafel plots are asymmetrical because the cathodic transfer coefficients are greater than 0.5. Similar plots are illustrated by Vetter.¹⁷³ The exchange current density, in each case, was calculated from the intercepts of the cathodic and the anodic asymptotes. The cathodic transfer coefficient, α_c , was obtained from the slope of the anodic asymptote, and the anodic transfer coefficient was obtained from the slope of the cathodic asymptote. The exchange current densities, the cathodic and the anodic transfer coefficients are presented as well in Fig. 4-6 to 4-10. Comparison of the present results with the exchange current densities obtained in Fig. 3-46 to 3-50 shows good agreement. The exchange current densities in both cases are of the same order of magnitude. The sums of the cathodic and anodic transfer coefficients in each case vary between 0.72 to 1.11, and in most cases the sum is very close to 1.0, as can be predicted from the charge transfer theory. In all cases the cathodic transfer coefficients are greater than 0.5, and generally are in good agreement with the coefficients obtained in Fig. 4-5. The results for Li(Hg) , presented in Fig. 4-6, are somewhat doubtful as the overpotentials were below the Tafel region which starts at around $|\eta| > 70$ mV.

The averages of the cathodic transfer coefficients were calculated



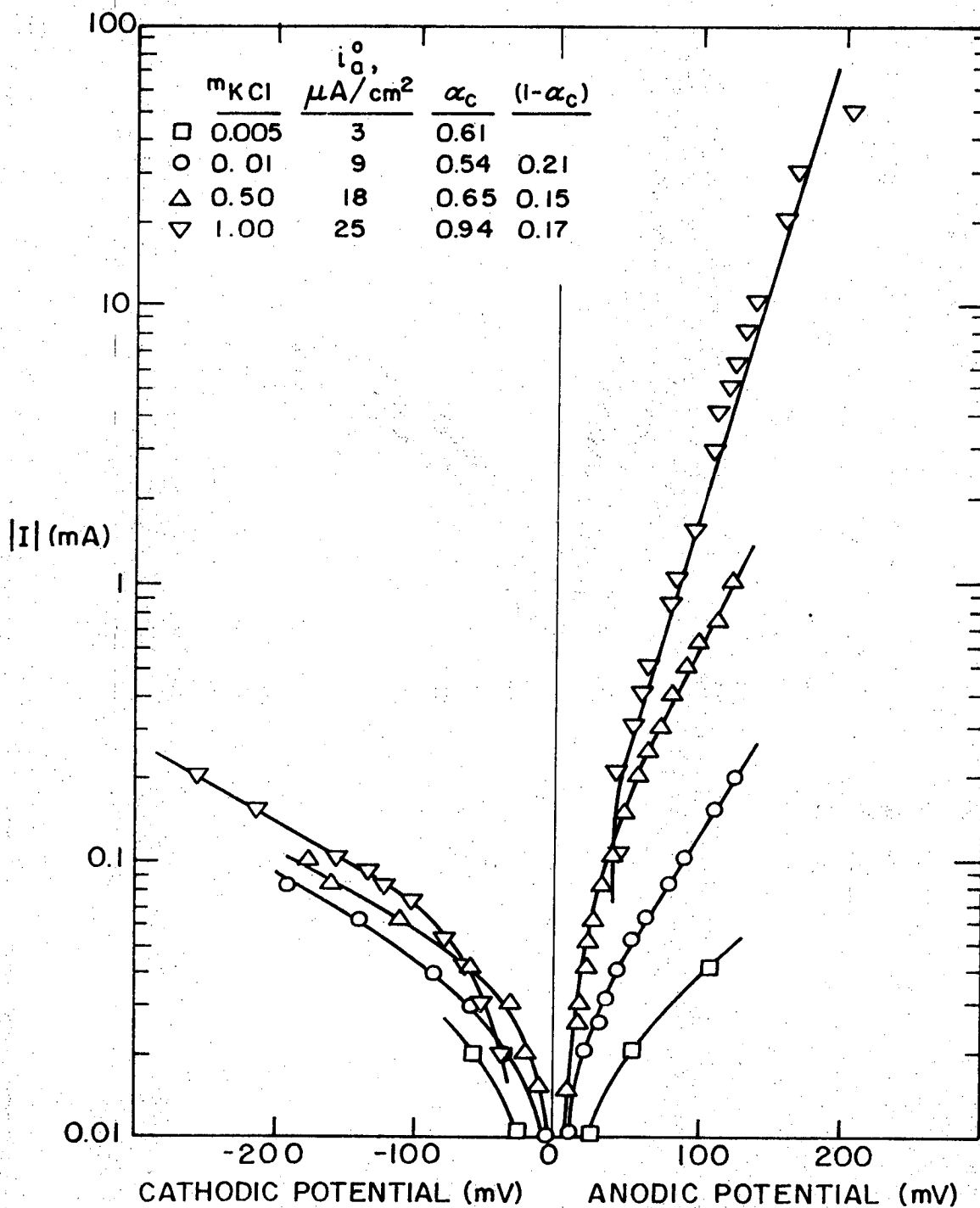
XBL 728-6766

Fig. 4-6. Tafel plot for Li(Hg)/LiCl(m) in AlCl₃(lm)-PC solution. Electrode area: 2.28 cm². Temperature: 25°C. Amalgam mole fraction: 1.94 10⁻³.



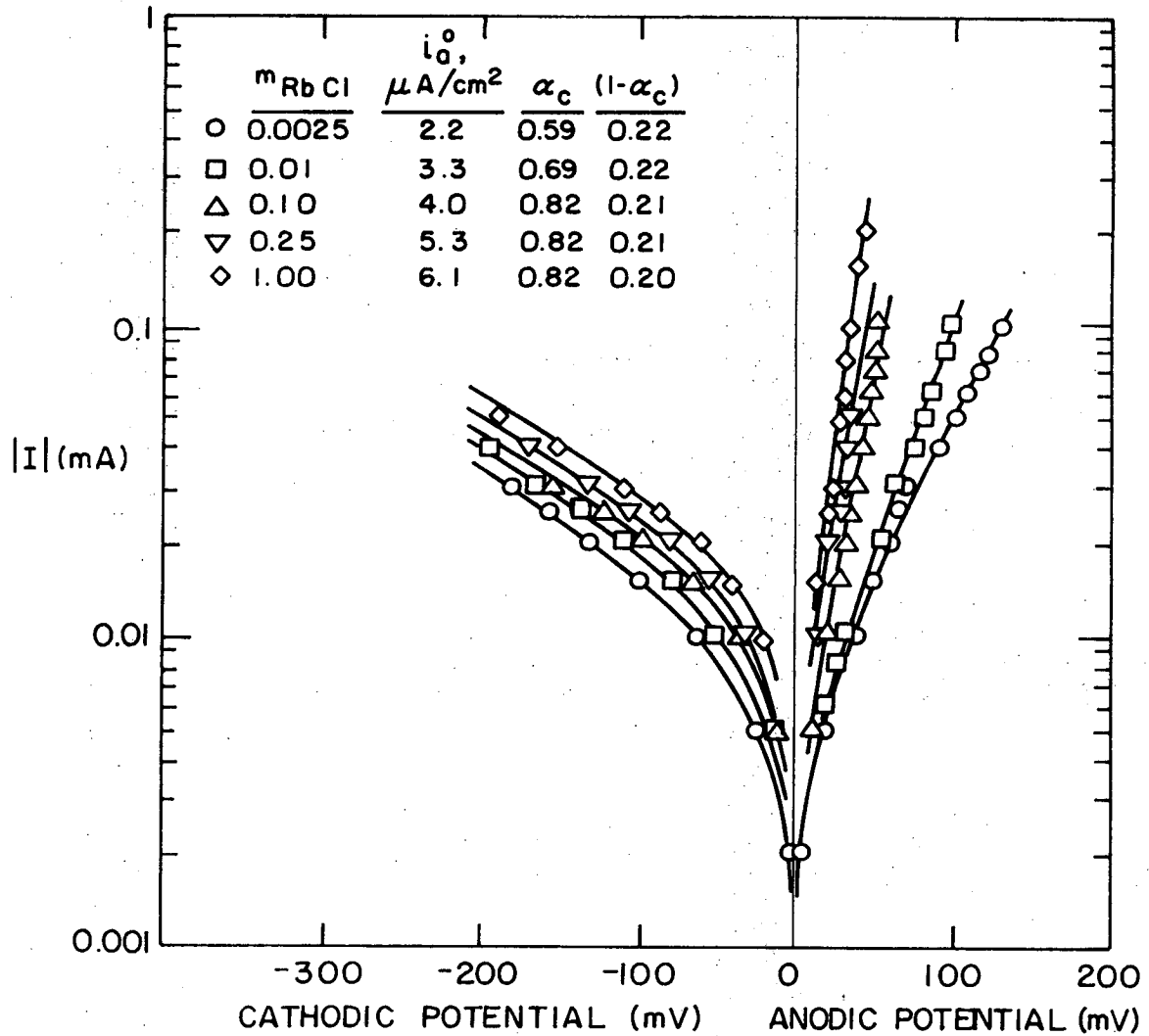
XBL 728 6767

Fig. 4-7. Tafel plot for Na(Hg)/NaCl(m) in AlCl₃(lm)-PC solution. Electrode area: 2.28 cm². Temperature: 25°C. Amalgam mole fraction: 1.771 10⁻².



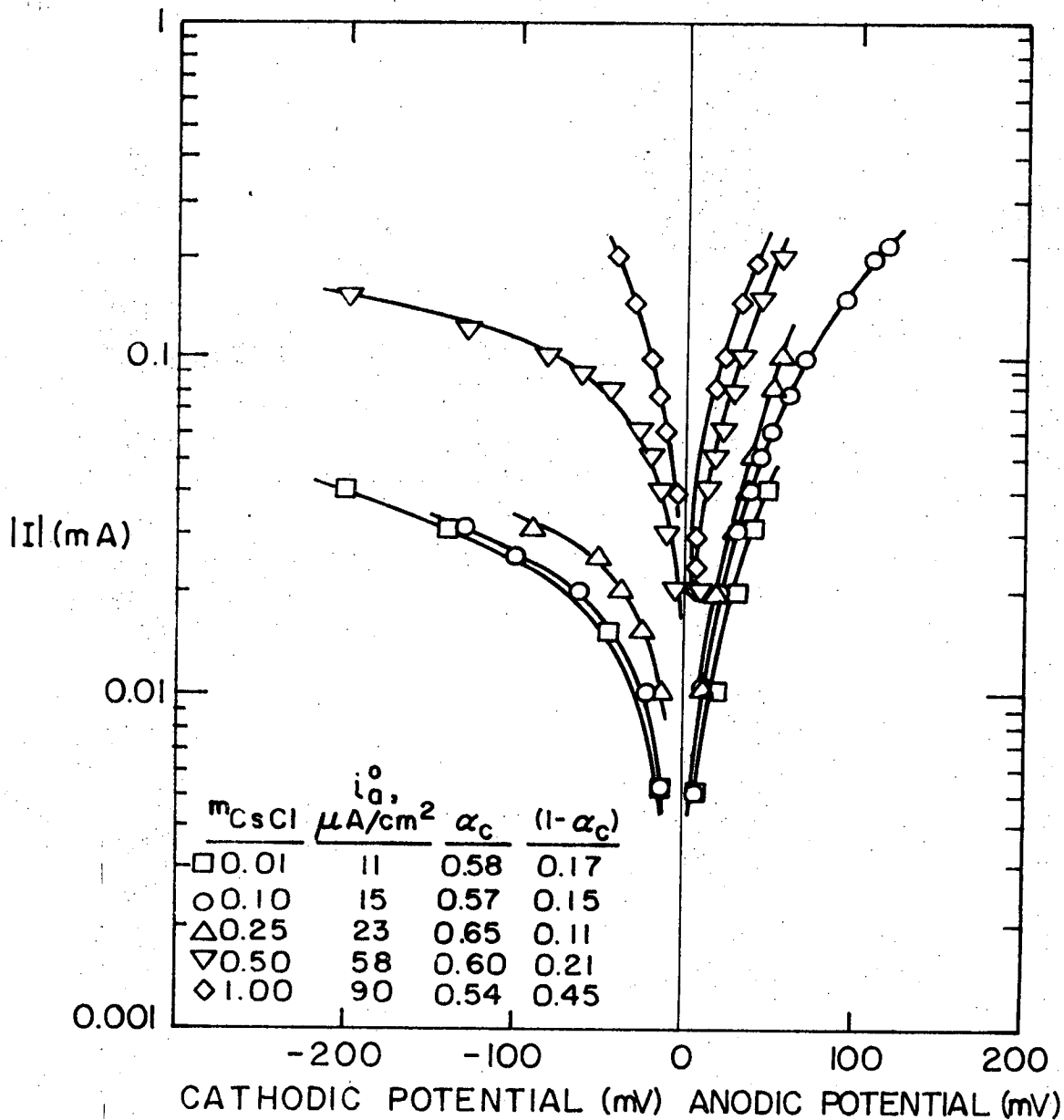
XBL728-6768

Fig. 4-8. Tafel plot for $\text{K(Hg)/KCl}(m)$ in $\text{AlCl}_3(lm)\text{-PC}$ solution. Electrode area: 2.28 cm^2 . Temperature: 25°C . Amalgam mole fraction: $1.1266 \cdot 10^{-2}$.



XBL 728-6769

Fig. 4-9. Tafel plot for Rb(Hg)/RbCl(m) in AlCl₃(lm)-PC solution. Electrode area: 2.28 cm². Temperature: 25°C. Amalgam mole fraction: 0.5397 · 10⁻².



XBL728-6770

Fig. 4-10. Tafel plot for Cs(Hg)/CsCl(m) in AlCl₃(lm)-PC solution. Electrode area: 1.01 cm². Temperature: 25°C. Amalgam mole fraction: 0.4672 10⁻².

for each alkali metal amalgam. The average cathodic transfer coefficients are 0.67, 0.76, 0.69, 0.75, 0.59 for Li(Hg), Na(Hg), K(Hg), Rb(Hg), and Cs(Hg), respectively. These values are within general agreement with the values of 0.77, 0.61, 0.61, 0.61 and 0.65, respectively, which were obtained in Fig. 4-5 from the concentration dependence of the exchange current densities. As a general rule, the transfer coefficients for the alkali metal amalgams are approximately equal to $2/3$.

The kinetic parameters of the alkali metal amalgams in AlCl_3 -PC solutions are discussed further in Chapter VI, where the influence of the solvent on the rate of an electrochemical reaction is investigated. The kinetic parameters of the alkali metal amalgams in PC are compared to the parameters in aqueous solution, and the relative rate constants are related to the energetics of the individual ions in each solvent.

V. THE THERMODYNAMICS OF ION SOLVATION IN PROPYLENE CARBONATE

5.1. Introduction

The evaluation of single-ion solvation energies and the variations from one solvent to another is a fundamental problem in solution chemistry. The solvation free energies, enthalpies and entropies of individual ions are of great importance because they reveal the nature of the ion-solvent interactions. For a long time attempts have been made to establish a universal scale of standard potentials, independent of the solvent. In order to establish universal scales of standard potentials and medium effects, activity coefficients of single ions and liquid junction potentials between different solvents must be fully understood.

Special attention is given here to the estimation of single ion solvation energies. The influence of medium effects on the electrode kinetics of the alkali metals in PC in comparison to water will be discussed in detail in Chapter VI.

5.2. Medium Effect or Solvent Activity Coefficient

The activity of a solute i is commonly referred to infinite dilution standard state in a given solvent:

$$a_i^* = m_i \gamma_i^s \quad (5-1)$$

where m_i is the molality and γ_i^s is the salt-effect activity coefficient, which becomes unity at infinite dilution in the given solvent. The main limitation of this formulation is that the activity scale is specific for each solvent due to the different standard state. In order to compare the activities of a solute in different solvents we have to refer to a common standard state. Usually, an infinitely diluted aqueous

solution is chosen as a standard state:

$$a_i = m_i \gamma_i^w \quad (5-2)$$

where $\gamma_i^w = 1$ at infinite dilution only in water. When the solute molality approaches zero in a nonaqueous solvent, the activity coefficient approaches the medium effect γ_i^m :

$$\gamma_i^w = \gamma_i^m \text{ as } m_i \rightarrow 0$$

Thus the activity coefficient of a solute of molality m in nonaqueous solvent is the product of the medium effect and the salt effect coefficients

$$\gamma_i^w = \gamma_i^s \gamma_i^m \quad (5-4)$$

and

$$a_i = a_i^* \gamma_i^m \quad (5-5)$$

For aqueous solution $\gamma_i^m = 1$ at all concentrations.

The medium effect can be expressed in terms of free energy of transfer from water to the given solvent

$$\Delta G_t^0 = RT \ln \gamma_i^m \quad (5-6)$$

The "medium effect" γ_i^m is referred to by other names, such as "distribution coefficient", "partition coefficient", medium activity coefficient" and "solvent activity coefficient".¹⁴²

The central problem is to split the medium effect of an electrolyte into individual ion medium effects

$$\gamma_i^w = (\gamma_M^{+w}) (\gamma_X^{-w}) \quad (5-7)$$

It is impossible to measure experimentally single ion medium effects. In order to split the measurable total medium effect, some extra-thermodynamic assumptions have to be made.

We prefer here to deal with solvation energies of individual ions rather than medium effect, since solvation energies are more fundamental physicochemical properties.

5.3. Free Energies of Solvation of Individual Ions

The free energy and enthalpy of solvation of single ions are of great importance in understanding solution chemistry. The most common equations for evaluating these quantities are the Born equations:

$$\Delta G_{\text{solv}} = - \frac{(z e)^2}{2 r_i} \left(1 - \frac{1}{\epsilon}\right) \quad (5-7)$$

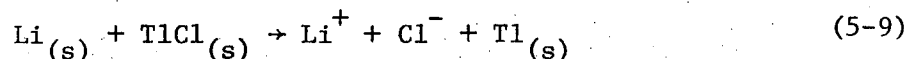
and the Born-Bjerrum equation:

$$\Delta H_{\text{solv}} = - \frac{(z e)^2}{2 r_i} \left(1 - \frac{1}{\epsilon} - \frac{T}{\epsilon} \frac{\partial \ln \epsilon}{\partial T}\right)_p \quad (5-8)$$

The usual approach is to adjust the crystal radii r_i of the cations or the anions in order to get a linear relation between ΔG or ΔH and $1/(r_i + \delta)$, where δ is a free parameter of the solvent.

The wide variation in activities of single ions in different solvents is usually discussed in terms of solvation energies and medium effects,¹⁴² or in terms of the free energy of transfer from one solvent to another.¹⁷⁶

The free energies of solvation can be obtained from emf data. Consider for example the cell reaction



The standard free energy of solvation of LiCl can be obtained in the following way:

$$\Delta G_{\text{solv}}^{\circ} = \Delta G_{\text{soln}}^{\circ} + \Delta G_{\text{lat}}^{\circ} \quad (5-10)$$

where $\Delta G_{\text{lat}}^{\circ}$ is the lattice free energy and is given by

$$\Delta G_{\text{lat}}^{\circ}(\text{LiCl}) = \Delta G_{\text{f}}^{\circ}(\text{Li}_{\text{g}}) + \Delta G_{\text{f}}^{\circ}(\text{Cl}_{\text{g}}) - \Delta G_{\text{f}}^{\circ}(\text{LiCl}_{\text{s}}) + I - A \quad (5-11)$$

where I is the ionization potential of lithium metal, and A is the electron affinity of the chloride. The standard free energy of solution $\Delta G_{\text{soln}}^{\circ}$ is given by

$$\Delta G_{\text{soln}}^{\circ} = \Delta G_{\text{emf}}^{\circ} + \Delta G_{\text{f}}^{\circ}(\text{TlCl}_{\text{s}}) - \Delta G_{\text{f}}^{\circ}(\text{LiCl}_{\text{s}}) \quad (5-12)$$

$\Delta G_{\text{emf}}^{\circ}$ is obtained from the standard cell potential. Thus for LiCl the standard free energy of solvation can be obtained from emf measurements, and from the tabulated values of formation and lattice energies. An alternative to emf data is to estimate the free energy of solution from solubility data

$$\Delta G_{\text{soln}}^{\circ} = -2RT \ln (m_{\text{sat}} \gamma_{\pm}) \quad (5-13)$$

where m_{sat} is the solubility of LiCl and γ_{\pm} is the mean molal activity coefficient. However, solubility measurements are usually less accurate than potential measurements.

The main problem facing us is to split the free energy of solvation of solute MX into the free energy of solvation of the individual ions, $\Delta G_{\text{solv}}^{\circ}(\text{M}^{+})$ and $\Delta G_{\text{solv}}^{\circ}(\text{X}^{-})$. It is impossible to determine these quantities experimentally, since it is impossible to transfer ions without dragging along the counter ions in an equivalent amount. Estimations of individual free energies of solvation can provide important physicochemical information and are very useful in predictions and correlations of experimental data. In order to split the measurable free energy of solvation we have to make some extra-thermodynamic assumptions. If a number of independent extra-thermodynamic assumptions give the same single ion energy of solvation, then the values obtained are believed to be confident. The

most common extra-thermodynamic assumptions are:

a) The tetraphenylarsonium-tetraphenylboride assumption.

It is assumed that $\Delta G_{\text{solv}}^{\circ}(\text{Ph}_4\text{As}^+) = \Delta G_{\text{solv}}^{\circ}(\text{Ph}_4\text{B}^-)$. This assumption became very popular since the cation and the anion are symmetrical species of the same size and shape, but the great disadvantage is that it assumes that the solvent orientation about an anion is the same as that around a cation, which is mostly wrong.

b) The large anion-large molecule assumption.

It is assumed that $\Delta G_{\text{solv}}^{\circ}(\text{X}^-) = \Delta G_{\text{solv}}^{\circ}(\text{A})$, where X^- and A are similar except that X^- is anion where the negative charge is buried beneath ligands, and therefore, the electrostatic interaction with the solvent is negligible. The solvation energy of A can be determined experimentally since it is not an ion.

c) The large cation-large molecule assumption.

It is assumed that $\Delta G_{\text{solv}}^{\circ}(\text{A}) = \Delta G_{\text{solv}}^{\circ}(\text{A}^+)$, where it is again assumed that the electrostatic interactions are negligible.

d) Zero solvation energy for Rb and Cs.

Large alkali metals like Rb and Cs are assumed to have no specific interactions with solvents, $\Delta G_{\text{solv}}^{\circ}(\text{Cs}^+ \text{ or } \text{Rb}^+) = 0$.

e) Negligible liquid junction potential.

It is assumed that the liquid junction between the two solvents has zero potential. This assumption can be justified only when the individual free energy of solvation matches values obtained under other assumptions.

5.4. Empirical Methods of Estimation of the Free Energies of Solvation of Individual Ions

Single ion solvation energies can be estimated by different methods, most of them empirical in nature. The Born equation and the Born-Bjerrum equation (Eqs. 5-7 and 5-8) are often used. The method of Latimer, Pitzer and Slansky¹³² was used by adjusting the crystal radii r_i of cations and anions until the plot of ΔG or ΔH behaves linearly vs. $1/(r_i + \delta)$. This method was subject to several modifications considering the effect of dielectric saturation.¹⁷⁷ Halliwell and Nyberg,¹⁷⁸ followed by Salomon,¹³⁹ proposed that solvation energies of single ions may be estimated from the empirical relation

$$d\Delta G_{\text{conv}}^{\circ} = \frac{\text{Constant}}{r} - 2\Delta G_{\text{solv}}^{\circ}(\text{RI}) \quad (5-14)$$

where $\Delta G_{\text{solv}}^{\circ}(\text{RI})$ is the solvation energy of the reference ion, and $\Delta G_{\text{conv}}^{\circ}$ is the difference in the conventional energies of solvation between a cation and anion of equal ionic (crystal) radii r . For monovalent ions the conventional energies, referred to the solvated proton, are given by

$$\Delta G_{\text{conv}}^{\circ}(\text{M}^+) = \Delta G_{\text{solv}}^{\circ}(\text{M}^+) - \Delta G_{\text{solv}}^{\circ}(\text{H}^+) \quad (5-15)$$

$$\Delta G_{\text{conv}}^{\circ}(\text{X}^-) = \Delta G_{\text{solv}}^{\circ}(\text{X}^-) + \Delta G_{\text{solv}}^{\circ}(\text{H}^+) \quad (5-16)$$

therefore

$$\Delta G_{\text{conv}}^{\circ} = (\Delta G_{\text{solv}}^{\circ}(\text{M}^+) - \Delta G_{\text{solv}}^{\circ}(\text{X}^-)) - 2\Delta G_{\text{solv}}^{\circ}(\text{H}^+) \quad (5-17)$$

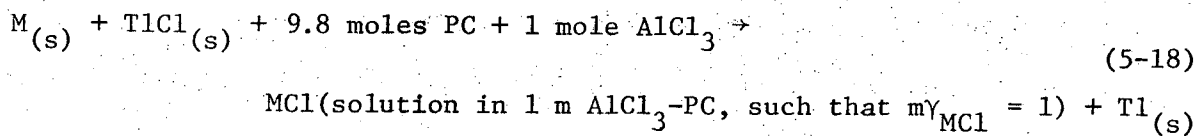
Plotting the left-hand side against $1/r$ gives a straight line, and the intercept at $(1/r) = 0$ gives the free energy of solvation of H^+ .

This method is based on the assumption of cancellation of the ion-dipole

term for $r_+ = r_-$. Clearly this assumption is valid only when the orientations of the solvent at the cation and the anion are mirror images.¹⁷⁹ Based on this method, Salomon¹³⁹ estimated the free energies and enthalpies of single ions in water and propylene carbonate, and by extrapolation found that $\Delta G_{\text{solv}}^{\circ}(\text{H}^+ \text{ in } \text{H}_2\text{O}) = -235.0 \text{ kcal/mole}$, and $\Delta G_{\text{solv}}^{\circ}(\text{Li}^+ \text{ in } \text{PC}) = -95.0 \text{ kcal/mole}$.

5.5. Free Energies of Solvation of Single Ions in AlCl_3 (1 m)-PC solution

Using the standard cell potentials which were obtained for the alkali metals in AlCl_3 (1 m)-PC solution (Table 3-7), it is now possible to calculate the free energy of solvation for the salt MCl (where M is Li, Na, K, Rb, or Cs) in AlCl_3 (1 m)-PC. The free energy of solvation of single alkali metal ions will then be estimated according to Latimer, Pitzer and Slansky's method.¹³² Using $\Delta G_{\text{emf}}^{\circ}$ for the cell reaction:



plus the formation and lattice energies, it is possible to calculate the free energies of solvation of MCl for all the alkali metals.

$$\Delta G_{\text{solv}}^{\circ}(\text{MCl}) = \Delta G_{\text{emf}}^{\circ} + \Delta G_{\text{f}}^{\circ}(\text{TlCl}_{(s)}) - \Delta G_{\text{f}}^{\circ}(\text{MCl}_{(s)}) + \Delta G_{\text{lat}}^{\circ}(\text{MCl}_{(s)}) \quad (5-19)$$

where

$$\Delta G_{\text{lat}}^{\circ}(\text{MCl}_{(s)}) = \Delta G_{\text{f}}^{\circ}(\text{M}_{\text{g}}) + \Delta G_{\text{f}}^{\circ}(\text{Cl}_{\text{g}}) - \Delta G_{\text{f}}^{\circ}(\text{LiCl}_{\text{g}}) + I - A \quad (5-20)$$

Free energies of formation, G_{f}° , were taken from several sources.^{180,181,182}

Ionization potentials, I, were obtained from Jesson and Muettelies,¹⁸³

and the electron affinity, A, of the chloride ion was obtained from

Berry and Reimann.¹⁸⁴ Table 5-1 presents the results. The last column gives the crystal ionic radii of the corresponding alkali metal, according to Pauling.¹⁸⁵

Table 5-1. Free Energies of solvation of the alkali metal chlorides in AlCl₃ (1 m)-PC solution.

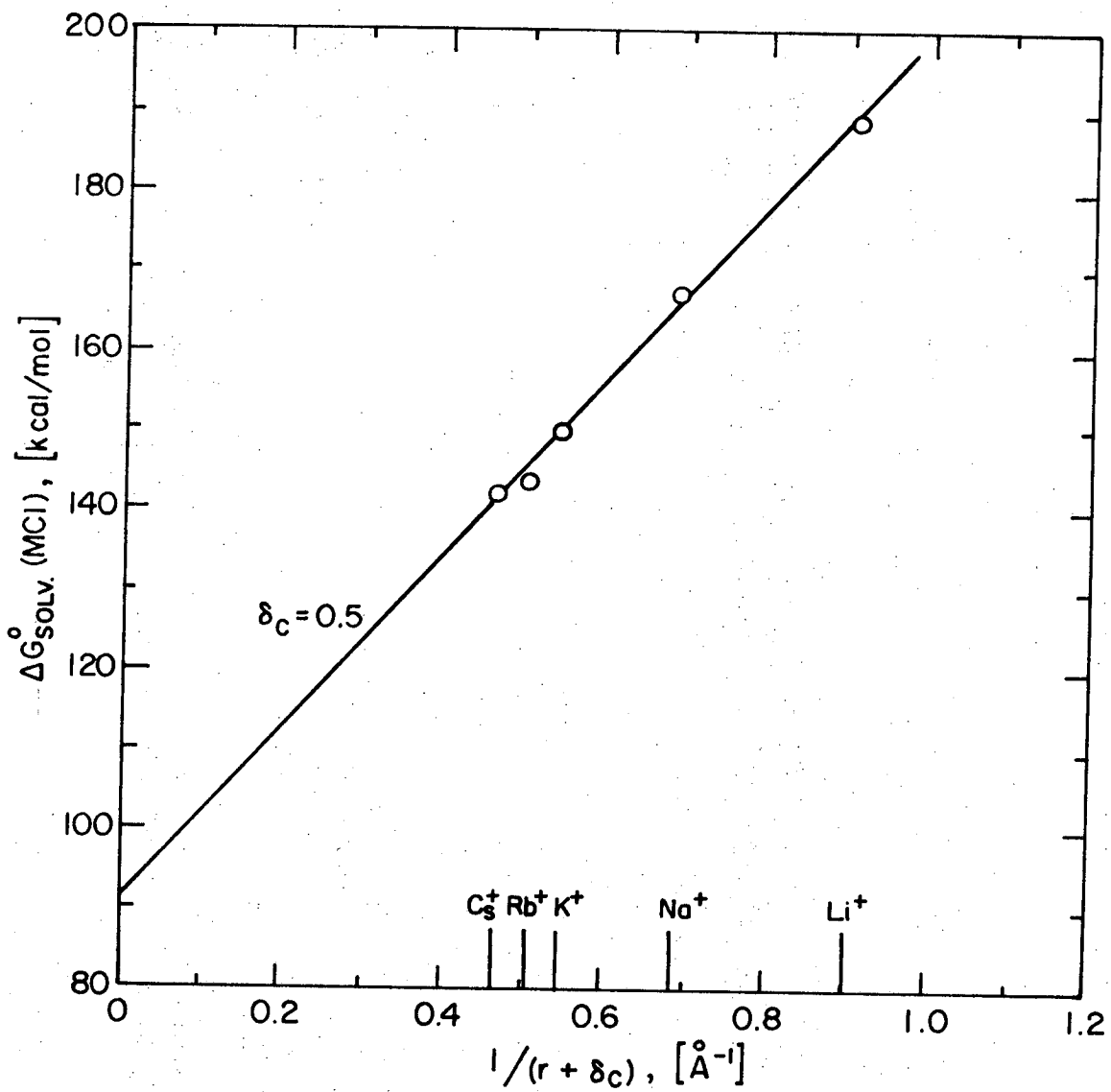
Salt	E ₂ ^o	ΔG _{emf} ^o	ΔG _f ^o (TlCl _s)	ΔG _f ^o (MCl _s)	ΔG _{lat} ^o (MCl)	ΔG _{solv} ^o (MCl)	r _p , Å
LiCl	2.045	-47,170	-44,460	-91,700	-188,500	-188,430	0.607
NaCl	1.885	-43,475	-44,460	-91,894	-170,600	-166,640	0.958
KCl	2.116	-48,800	-44,460	-97,760	-154,100	-149,600	1.331
RbCl	2.116	-48,800	-44,460	-98,480	-149,000	-143,780	1.484
CsCl	2.122	-48,940	-44,460	-96,600	-144,900	-141,700	1.656

The free energies are given in cal/mole, and the potentials in volts.

Since the chloride ions are being complexed by the Al³⁺ ions to form AlCl₄⁻ ions, one can assume that the free energy of solvation of chloride ion in AlCl₃ (1 m)-PC solution is constant and independent of the nature of the alkali metal cation. Therefore, we assume that the free energy of solvation of the alkali metal chloride in AlCl₃ (1 m)-PC solution behaves according to

$$\Delta G_{\text{solv}}^{\circ}(\text{MCl}) = \Delta G_{\text{solv}}^{\circ}(\text{Cl}^{-}) + \frac{A}{r_i + \delta_c} \quad (5-21)$$

where r_i is the crystal radii of the alkali metal and δ_c is the Latimer, Pitzer and Slansky's parameter¹³² for cations in PC. The data of Pauling was used for the crystal radii. Figure 5-1 presents the plot of $\Delta G_{\text{solv}}^{\circ}(\text{MCl})$ vs. $1/(r_i + \delta_c)$. A linear plot was obtained for the alkali metal cations for $\delta_c = 0.50$. The intercept at infinite crystal radii



XBL725-6281

Fig. 5-1. Free energies of solvation of the alkali metal chlorides vs. $1/(r+\delta)$ in $\text{AlCl}_3(\text{lm})\text{-PC}$ solution at 25°C .

gives the free energy of solvation of Cl^-

$$\Delta G_{\text{solv}}^{\circ}(\text{Cl}^-) = -90.0 \text{ kcal/mole}$$

Using this result, the free energies of solvation of the individual alkali metal cations can be estimated. Table 5-2 summarizes the estimated free energies of solvation of single ions at 25°C in AlCl_3 (1 m)-PC solution. Also included, for comparison, are the free energies of solvation in pure PC and in water estimated by Salomon.¹³⁹

Table 5-2. Free energies of solvation of individual ions at 25° in AlCl_3 (1 m)-PC in pure PC and in water.

Ion	$\Delta G_{\text{solv}}^{\circ}(\text{M})_{\text{AlCl}_3\text{-PC}}$ (a)	$\Delta G_{\text{solv}}^{\circ}(\text{M})_{\text{PC}}$ (b)	$\Delta G_{\text{solv}}^{\circ}(\text{M})_{\text{H}_2\text{O}}$ (b)
Li^+	-98.4	-95.0	-97.8
Na^+	-76.6	-71.9	-72.4
K^+	-59.6	-56.6	-54.9
Rb^+	-53.8	-54.5	-50.7
Cs^+	-51.7	-52.7	-46.7
Cl^-	-90.0	-88.2	-100.3

(a) Present work. Solvent: AlCl_3 (1 m)-PC solution.

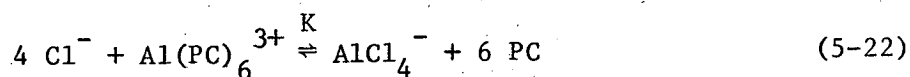
(b) M. Salmon, J. Phys. Chem. 74, 5219 (1970).

Free energies of solvation in kcal/mole, on a molal basis.

It can be seen from Table 5-2 that the free energies of solvation of the individual cations, obtained in the present work in AlCl_3 (1 m) solution in PC, are similar to the values estimated by Salomon¹³⁹ in pure PC. The presence of AlCl_3 in the solvent changes the free energies of solvation by approximately 1-5 kcal/mole. Li^+ , Na^+ and K^+ are more solvated in the presence of AlCl_3 . However, the solvation of Rb^+ and Cs^+ remain almost the same, probably due to their large size, and in

agreement with the popular assumption that the large alkali metal cations have no specific interaction with solvents, and therefore their energies of solvation are independent of the solvent. The free energies of solvation of all the alkali metals are lower in AlCl_3 (1 m)-PC than in water, which means that the cations are more strongly solvated in AlCl_3 -PC than in water.

The free energy of solvation of the chloride ion in AlCl_3 (1 m)-PC solution is lower than in pure PC. The chloride ions are believed to be complexed by the Al^{3+} ions according to the following exchange reaction:



The free energy of transfer of Cl^- from pure PC to AlCl_3 (1 m)-PC solution is estimated at -1.8 kcal/mole, hence the equilibrium constant for the exchange reaction can be estimated from

$$4(\Delta G_{\text{solv}}^{\circ}(\text{Cl}^-)_{\text{AlCl}_3\text{-PC}} - \Delta G_{\text{solv}}^{\circ}(\text{Cl}^-)_{\text{PC}}) = -RT \ln K \quad (5-23)$$

$$K = \exp \frac{4 \times 1,800}{1.98 \times 298} = \exp(12.203) = 1.99 \times 10^5$$

This is the molal association constant of Cl^- with $\text{Al}(\text{PC})_6^{3+}$ in PC solution. It should be mentioned here that a large association constant of Cl^- with $\text{Al}(\text{PC})_6^{3+}$ was predicted by NMR studies.⁸¹ Indeed, this should be the reason for the high solubility of the alkali metal chlorides in AlCl_3 -PC solution, while they are nearly insoluble in pure PC. The association constant can be used to estimate Cl^- concentrations in AlCl_3 -PC systems. The accuracy of the estimated value of K is unknown, since it was established from the difference between two values which were obtained by extrapolation. K is a measure of the expected strong tendency of the free chloride ions

to substitute the PC molecules around the Al^{3+} ions, which is responsible for "forcing" metal cations into the solution.

5.6. Free Energy of Transfer

Frequently, the medium effect or the free energy of solvation is expressed in the form of the free energy of transfer of a solute from a reference solvent (usually water) to the particular solvent. This interpretation of the free energy of transfer as the difference between the solvation energies in the two solvents is precise only for neutral molecules. For individual ions, the free energy of transfer includes an additional term $ze\chi$, where χ is the potential difference across the interface between the two phases. A distinction should be made between a "real" and a "chemical" solvation energy of single ions. "Chemical" solvation energies express only the solute-solvent interactions, while "real" solvation energies include the potential step across the vacuum-solvent interface. Free energies of transfer, in the present work, are referred to as the "chemical" free energy. Table 5-3 summarizes the estimated free energies of transfer of individual ions from water to AlCl_3 (1 m)-PC solution and to pure PC. The negative values for the alkali metal cations indicate that these ions are more tied in PC than in water. The positive free energy of transfer of chloride ion means that Cl^- is loose in PC and poorly solvated, in agreement with the general observation that anions are poorly solvated in aprotic solvents. ¹⁴¹

Table 5-3. Free energies of transfer of individual ions from water to AlCl_3 (1 m)-PC and Pure PC.

Ion	$\Delta G_t^\circ (\text{M})_{\text{H}_2\text{O} \rightarrow \text{AlCl}_3\text{-PC}}$ (a)	$\Delta G_t^\circ (\text{M})_{\text{H}_2\text{O} \rightarrow \text{PC}}$ (b)
Li^+	-0.6	+2.8
Na^+	-4.2	+0.5
K^+	-4.7	-1.7
Rb^+	-3.1	-3.8
Cs^+	-5.0	-6.0
Cl^-	+10.3	+12.1

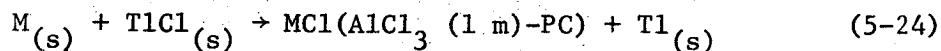
(a) Present work. Aqueous values were taken from Salomon.¹³⁹

(b) M. Salomon, J. Phys. Chem. 74, 2519 (1970).

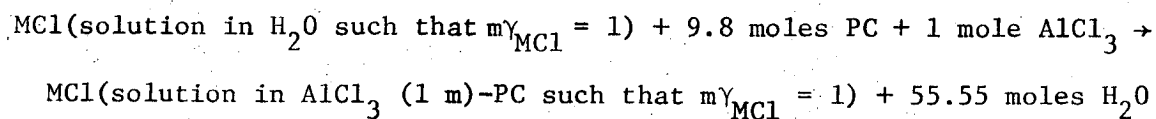
Free energies of transfer in kcal/mole, on a molal basis.

5.7. Standard Entropies of Transfer of the Alkali Metal Chlorides in AlCl_3 (1 m)-PC Solution

The standard free entropies for the general cell reaction



were calculated from the temperature dependence of the standard cell potentials, and are presented in Table 3-8. These values are tabulated again in Table 5-4, along with the values for the corresponding cell reactions in water. The aqueous standard entropies were calculated from Latimer's tables.¹⁸² The difference between the standard entropies corresponds to the following transfer process:



However, a small correction is necessary for the difference in the specific volumes of the two solvents:¹⁸⁶

$$R \ln (v_{\text{AlCl}_3 (1 \text{ m})\text{-PC}}) - R \ln (v_{\text{H}_2\text{O}}) \quad (5-25)$$

The specific volume of water at 25°C is 1.0019 cm³/gr, and the specific volume of AlCl₃ (1 m)-PC solution was measured to be 0.7919 cm³/gr (see Table 3-5). The correction is therefore -0.46 eu, which was added to the difference between the standard entropies. The calculated standard entropies of transfer are presented in the last column of Table 5-4.

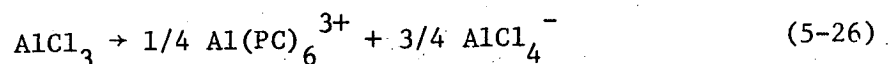
Table 5-4. Standard entropies of transfer of the alkali metal chlorides from water to AlCl₃ (1 m)-PC

	$\Delta S_{2 \text{ AlCl}_3\text{-PC}}^{\circ}$	$\Delta S_{2 \text{ H}_2\text{O}}^{\circ}$	ΔS_t°
LiCl	-18.4	-0.6	-18.3
NaCl	-16.1	+4.9	-21.5
KCl	+ 9.2	+12.0	- 3.3
RbCl	+55.3	+15.8	+39.0
CsCl	+64.7	+14.7	+49.5

Entropies in eu (cal/mole °K) and on a molal basis.

The uncertainty in the calculated entropies is quite high, because these values were calculated from differences between extrapolated values. Therefore, we will refer here only to the sign and the order of magnitude of the standard entropies of transfer. The standard entropies of transfer are negative for lithium, sodium and potassium chlorides, while the values for rubidium and cesium chlorides are

positive. This can be explained in terms of the internal structures of the solvents. Water exhibits a large amount of hydrogen bonding, which causes a high degree of order in the pure state. Pure PC shows a low degree of order; it is considered to be an ideal orderless solvent. However, we are dealing here with AlCl_3 solution in PC as the solvent, and this reference state exhibits a high degree of order because of the orientation of the PC molecules around the Al^{3+} ions. AlCl_3 dissociates in PC solution according to



The addition of alkali metal chloride MCl to this solution reduces the amount of solvated $\text{Al}(\text{PC})_6^{3+}$ species and converts them into AlCl_4^- ions, which are poorly solvated. Consequently, the addition of MCl reduces the initial order in AlCl_3 -PC solution and increases the entropy. On the other hand, the introduction of alkali metal ions causes reorientation of the solvent molecules around the ions, causing an entropy decrease. In the case of lithium, sodium and potassium, the order gained by the introduction of these ions, due to strong reorientation of the PC molecules around them, is larger than the disorder gained by the conversion of $\text{Al}(\text{PC})_6^{3+}$ ions to AlCl_4^- . In the case of Rb and Cs, these large cations are poorly solvated, and the reorientation due to their presence is smaller than the loss of order due to the disappearance of $\text{Al}(\text{PC})_6^{3+}$ species.

VI. ELECTRODE KINETICS AND MEDIUM EFFECTS

6.1. Introduction

The fact that the exchange current densities of the alkali metal amalgams in PC are several orders of magnitude lower than those in water raises the very fundamental question: What is the influence of the solvent on the rate of an electrochemical reaction? The data obtained for the electrode kinetics of the alkali metal amalgams in PC enables us to try to answer this question by comparing the true constants for the electrochemical reaction in water and PC, and to correlate it with medium effects or the energetics of transfer between the two solvents.

Very little attention has been given to electrode kinetics in nonaqueous solvents, and to the influence of the solvent on the exchange current density. Early attention was given to the hydrogen evolution reaction in alcoholic solution.¹⁸⁷⁻¹⁹² Bockris and Parsons found that the exchange current density decreases as the mole fraction of methanol increases in methanol-water mixture, but the exchange current density starts to increase at a high percent of methanol. The exchange current density of hydrogen in pure methanol is higher than in water. Salomon¹⁹³ discussed the medium effects on the rate of hydrogen evolution. Using a simple electrostatic model for the activated complex, and using estimated values of free energy of transfer of hydrogen ion from water to water-methanol mixtures, Salomon was able to predict the ratio of the exchange current densities in water to that in water-methanol mixtures.

The kinetics of alkali metal amalgams in nonaqueous solvents is almost an untouched field. The kinetics of discharge of alkali metals on their amalgams in aqueous solutions were studied by faradaic impedance

by Randles and Somerton.¹⁹⁴ They calculated the approximate apparent standard rate constants ($k_a^0 = 0.4, 0.1$ and 0.2 cm sec^{-1} for Na, K and Cs, respectively) in aqueous solutions of 1 M tetramethylammonium hydroxide. Imai and Delahay¹⁹⁵ used the faradaic rectification method to determine exchange current densities i^0 , and transfer coefficients of various alkali metal amalgam electrodes $M(\text{Hg})/0.498\text{M MCl} + 0.002\text{M MOH}$. The values measured for the alkali metals Li, Na, K, Rb and Cs were $\alpha = 0.35$ to 0.43 for the transfer coefficients, and $i^0 = 72$ to 219 mA/cm^2 for the exchange current densities. The standard rate constants, corrected for double layer effects using Gouy-Chapman theory, from Li to Cs are: $0.02, 0.04, 0.01 (0.02) \text{ cm sec}^{-1}$, and the transfer coefficients: $0.35, 0.39, 0.41, 0.42, 0.43$. The results for cesium are doubtful because of the evidence of specific adsorption of Cs at mercury-water interface.

Recent interest in high energy batteries has given a considerable incentive for research on the deposition and dissolution of those active metals having low equivalent weights which can be used as anodes in high energy batteries.²⁹ The kinetics of solid lithium in PC was treated by Burrows and Jasinski,³³ Scarr⁴⁸ and Meibuhr.^{46,41} The kinetics of solid sodium was investigated by Meibuhr.⁶⁰ Butler, et al.⁴⁹ discussed the dependence of the apparent exchange current of solid lithium in PC on the age of the surface, and found that even at very low concentration of water (below 0.001 m) the exchange current drops by a factor of 10 during the first hour. The kinetics of lithium amalgam in LiCl-DMSO solutions was investigated by Cogley and Butler.^{50,109} The apparent exchange current densities were in the range of $0.08-0.16 \text{ mA/cm}^2$. The Tafel equation with cathodic transfer coefficient $\alpha = 0.75 \pm 0.02$ was

obeyed over the current density range of 10^{-2} to 3 mA/cm^2 . The standard rate constant, corrected for double layer effects, is $(2.9 \pm 0.2) 10^{-5} \text{ cm sec}^{-1}$.

Parker¹⁴¹ gives a very interesting review of the solvent effects on the rates of bimolecular organic reactions. For anion nucleophilic substitution reaction, the rates in dipolar aprotic solvents are approximately 10^6 times faster than they are in water. Parker explains this observation by the positive values of free energy of transfer for anions. This means that anions are poorly solvated by dipolar aprotic solvents and therefore are looser in these solvents compared to water and other protic solvents. Solvent activity coefficients of anions and cations in several aprotic solvents are presented; in general, the activity coefficients are negative for most cations, which indicates negative free energies of transfer from water to aprotic solvents. The activity coefficients are positive for small anions, which indicates weaker solvation compared to aqueous solution.

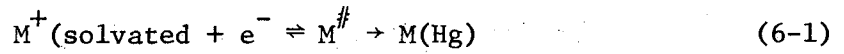
Cogley, Butler and Grunwald¹⁴⁰ measured the equilibrium constants for association of water with individual ions in PC. The molal association constants are 6.5, 1.4, 0.4 and 6.2 for Li^+ , Na^+ , K^+ and Cl^- , respectively. The affinity of water at low concentrations in PC for alkali metal cations correlates well with the free energies of transfer of these ions from PC to bulk water. The fact that 1) the anionic substitution reactions are 10^6 times faster in aprotic solvents than in water, 2) equilibrium constants for association of water with individual ions in aprotic solvents correlate well with the free energies of transfer, and 3) the exchange currents for alkali metal deposition at their amalgams are much lower (10^{-3} times lower for Li(Hg) in DMSO compared to water), all suggest that the rate of electrochemical or ionic reaction depends strongly on the free energies

of solvation of individual ions in different solvents.

In the next sections the relation between electrode kinetics and medium effects (free energy of transfer) is presented. The wide reactivity of ions in different solvents is explained by the relative energetic states of single ions in these solvents. The ratio between the rate constants is expressed in terms of the free energy of transfer from the reference solvent to the solvent under study. The proposed theory is then discussed in light of the rate constants and the free energies of transfer obtained in the present work for the alkali metals in the $AlCl_3$ -PC system.

6.2. Kinetics of Simple Electrode Process

Our discussion will be restricted to simple electrode processes in which the rate-determining step is the over-all charge transfer reaction in the absence of coupled chemical reaction and specific adsorption. It is well accepted that charge transfer represents the slow step in the discharge of an alkali metal ion at a mercury electrode.¹⁹⁵ Considering the general electrode reaction:



in which $M^\#$ is the activated complex and $M(Hg)$ is the metal in the amalgam state. This electrode reaction can be described by the Volmer's current-overpotential relation

$$i = i_a^0 \exp(-\alpha n F \eta / RT) - \exp((1 - \alpha) n F \eta / RT) \tag{6-2}$$

in which i_a^0 is the apparent exchange current density which depends on the concentrations of the solution and the amalgam, and on the potential of the outer Helmholtz double layer ϕ_2 .¹⁶⁴ α is the transfer coefficient,

i is the current density and η is the charge transfer overpotential. The true exchange current density is defined as the value corrected for double layer effect:

$$i_t^0 = i_a^0 \exp(1 - \alpha)nF\phi_2/RT \quad (6-3)$$

Exchange currents in the literature are almost never corrected for the double layer effect.

The true exchange current density is given according to the transition state theory¹⁶⁴

$$i_t^0 = nF \frac{kT}{h} \exp \left[\frac{(-\Delta G_{\#}^{\rightarrow 0} - \alpha F\phi_M^e)/RT}{1} \right] a_M^+ \quad (6-4)$$

$$= nF \frac{kT}{h} \exp \left[\frac{(-\Delta G_{\#}^{\leftarrow 0} + (1 - \alpha)F\phi_M^e)/RT}{1} \right] a_M \quad (6-5)$$

where $\Delta G_{\#}^{\rightarrow 0}$ is the difference in the chemical standard free energy of the transition state and the solvated ion, and $\Delta G_{\#}^{\leftarrow 0}$ is the difference between the transition state and the metal or the amalgam state. ϕ_M^e is the equilibrium potential and can be expressed by the Nernst equation

$$\phi_M^e = \phi_M^0 + RT/nF \ln(a_M^+/a_M) \quad (6-6)$$

where ϕ_M^0 is the standard potential of the reaction. Equation (6-5) now becomes

$$i_t^0 = nFk_t^0 a_M^+^{1-\alpha} a_M^{\alpha} \quad (6-7)$$

where the true standard rate constant k_t^0 is

$$k_t^0 = \frac{kT}{h} \exp \left(\frac{-\Delta G_{\#}^{\rightarrow 0} - \alpha nF\phi_M^0}{RT} \right) \quad (6-8)$$

$$= \frac{kT}{h} \exp \left(\frac{-\Delta G_{\#}^{\leftarrow 0} + (1 - \alpha)nF\phi_M^0}{RT} \right) \quad (6-9)$$

An apparent standard rate constant can be defined as the rate constant uncorrected for double layer effect

$$k_a^0 = k_t^0 \exp[(\alpha - 1)F\phi_2/RT] \quad (6-10)$$

In order to summarize this brief review on the concept of exchange current for simple charge transfer electrode reaction, let us approach it from two directions: experimental and energetic:

a) Experimental treatment of the apparent exchange current.

The apparent exchange current can be obtained from micropolarization in the linear zone, when $|\eta| \ll nF/RT$, or $|\eta| \ll RT/(1 - \alpha)nF$ where $i = i_a^0 nF\eta/RT$, or from the Allen-Hickling equation:^{175,164,165}

$$\ln \frac{i}{1 - \exp(nF\eta/RT)} = \ln i_a^0 - nF\eta/RT \quad (6-11)$$

The slope of the plot of Eq. (6-11) yields α , and the intercept yields i_a^0 . The apparent exchange current can be converted into the true standard rate constant by correcting for double layer effect and by correcting to unit activities both for the solution and the amalgam side. Correction is not needed for metallic electrode for which the activity is unity. The true standard rate constant is given by

$$k_t^0 = \frac{i_a^0}{nF} \exp \left[-(1 - \alpha)nF\phi_2/RT \right] \left(\frac{1}{a_{M^+}} \right)^{1-\alpha} \left(\frac{1}{a_M} \right)^\alpha \quad (6-12)$$

The transfer coefficient α can be calculated from the dependence of the apparent exchange current on the activities of either M^+ in the solution or M in the amalgam.

$$\left(\frac{\partial \ln i_a^0}{\partial \ln a_{M^+}} \right)_{a_M} = 1 - \alpha \quad (6-13)$$

$$\left(\frac{\partial \ln i_a^0}{\partial \ln a_M} \right)_{a_{M^+}} = \alpha \quad (6-14)$$

It is important to note that in order to correct for double layer effect we have to know ϕ_2 , the potential of the outer Helmholtz double layer relative to the bulk solution. ϕ_2 can be estimated from integration of the differential capacitance-potential curves, which yields the charge density q

$$q = \int_{E_z}^E C dE \quad (6-15)$$

where E_z is the potential of the point of zero charge, and q is related to the potential of the outer Helmholtz layer ϕ_2 through the Gouy-Chapman theory

$$q = \pm \left[\frac{RT}{2} \sum c_i^s \exp(-z_i F \phi_2 / RT - 1) \right]^{1/2} \quad (6-16)$$

which can be simplified for the case of symmetrical electrolyte to

$$q = 2 \left(\frac{kT c}{2\pi} \right)^{1/2} \sinh \left(\frac{zF\phi_2}{2RT} \right) \quad (6-17)$$

In many cases, because of lack of data, the exchange currents or the standard rate constants are given in their apparent forms.

b) Energetic form of the exchange current.

The true standard rate constant k_t^0 can be evaluated theoretically from free energy and potential data.

$$k_t^0 = \frac{kT}{h} \exp [(-\Delta G_{\#}^{\ddagger} - \alpha n F \phi_M^0) / RT] \quad (6-18)$$

To evaluate k_t^0 we have to know the change in the chemical free energy between the transition state M^{\ddagger} and the ionic state M^+ , and the standard potential of the overall reaction. ϕ_M^0 presents great difficulty when we have to compare the rate constants or the exchange currents in different

solvents, since there is no general scale for standard potentials in different solvents. $\Delta G_{\ddagger}^{\circ}$ also presents difficulty, since very little is known about the energetic level of the transition state.

6.3. Exchange Currents in Different Solvents

A comparison between the rate constants in different solvents is very desirable since it might enable us to predict the exchange currents in different solvents from their thermodynamic properties with respect to a reference state (usually water) in which reliable data is readily available. This will help us also in selecting a specific solvent for a desired electrochemical reaction, on the basis of physical and thermodynamic properties.

Let us restrict ourselves again to the simple electrode process:



where (s) refers to the solvated ionic state and M is the metal or the amalgam state. Water is our reference state, since it is the only solvent for which kinetic and thermodynamic data are available. The relative true rate constant is defined as the ratio between the true rate constants in solvent (s) and water

$$k_r^{\circ} = \frac{(k_t^{\circ})_s}{(k_t^{\circ})_w} = \exp[\Delta G_t^{\circ}(M^+) - \Delta G_t^{\circ}(M^{\ddagger}) + F(\alpha_w \phi_w^{\circ} - \alpha_s \phi_s^{\circ})]/RT \quad (6-20)$$

where $\Delta G_t^{\circ}(M^+)$ and $\Delta G_t^{\circ}(M^{\ddagger})$ are the standard chemical free energies of transfer of ion M^+ and the activated complex M^{\ddagger} from water to solvent (s), respectively. α_s and α_w are the corresponding transfer coefficients in the two solvents.

In the same way the relative standard exchange currents can be defined

$$(i_t^0)_r = \frac{(i_t^0)_s}{(i_t^0)_w} = \frac{(k_t^0)_s}{(k_t^0)_w} \exp \frac{F}{RT} (1 - \alpha_w)(\phi_2)_w - (1 - \alpha_s)(\phi_2)_s \quad (6-21)$$

Converting the standard values into apparent exchange currents involves the concentrations of the solutions and the amalgams.

It can be seen from Eqs. (6-20) and (6-21) that the main factors influencing the change in the rate constant are the free energies of transfer of the solvated ion and the activated complex, the difference between the standard potentials in the two solvents, and the difference between the outer Helmholtz layer potentials in the two solvents. The difference between the transfer coefficients in both solvents is probably minor, and it is expected that setting $\alpha_s = \alpha_w$ is a good approximation.

6.4. Rate Constants of the Alkali Metal Amalgams in AlCl₃ (1 m)-PC

The apparent exchange currents i_a^0 obtained for the alkali metal amalgams in AlCl₃ (1 m)-PC (see Section 3.8) can be converted into the apparent rate constants, k_a^0 , which still include the influence of the potential of the double layer. The apparent rate constant, defined on a molarity basis, is given by

$$i_a^0 = nFk_a^0 (C_M^+)^{1-\alpha} (C_{M(Hg)})^\alpha \quad (6-22)$$

where C_M^+ and $C_{M(Hg)}$ are the concentrations in mol/cm³ of the alkali metal ion in solution and the alkali metal in the amalgam, respectively, and α is the cathodic transfer coefficient. The amalgam's mole fractions were converted into molar concentrations using the density of pure mercury, since the amalgams used were very dilute. The molarities of the alkali metal ions in AlCl₃ (1 m)-PC solutions were obtained from the molal concentrations, using the density measurements in Section 3-5. The

transfer coefficients were calculated in Section 3.8. Table 6-1 summarizes the calculated apparent standard rate constants, on a molar basis. These results were calculated from the apparent exchange currents at (1 m) MCl solution in AlCl₃ (1 m)-PC. At this concentration, the ratio of MCl to AlCl₃ is 1:1, and the solute can be considered as MA1Cl₄.

Table 6-1. Apparent standard rate constants of the alkali metal amalgams in AlCl₃ (1 m)-PC solutions.

	$10^2 X$	α_c	$i_a^0, \text{ mA/cm}^2$	$10^5 k_a^0, \text{ cm/sec}$
Li(Hg)	0.194	0.77	0.420	1.97
Na(Hg)	1.7710	0.61	0.058	0.0492
K(Hg)	1.1266	0.61	0.025	0.0277
Rb(Hg)	0.5395	0.61	0.013	0.0224
Cs(Hg)	0.4672	0.65	0.070	0.136

X is the mole fraction in the amalgam, and i_a^0 is the apparent exchange current for unit molality of the alkali metal chloride in AlCl₃ (1 m)-PC solution.

In order to compare the true rate constants in AlCl₃ (1 m)-PC to the data of Imai and Dalahay¹⁹⁵ on the kinetics of the alkali metal amalgams in aqueous solution, it is necessary to correct k_a^0 for double layer effects. The true rate constant represents the heterogeneous reaction, free of the effect of the potential of the double layer with respect to the solution. Since data for the capacitance vs. potential in PC is available only for sodium perchlorate,¹⁰⁴ the true rate constant was estimated only for sodium, assuming that the nature of the anions does not influence the double layer capacitance because of strong

repulsion at the far cathodic potentials. For the rest of the alkali metals, the rate constants were approximated, using the capacitance-potential curve of sodium (i.e. assuming that their behavior is similar to that of sodium). These estimations are quite crude, especially in the case of cesium, which is believed to be specifically adsorbed in aqueous as well as in nonaqueous solutions. The estimated true standard rate constant of sodium in AlCl_3 (1 m)-PC, along with the approximated values for the rest of the alkali metals, are presented in Table 6-2. The true standard rate constants in aqueous solution, as measured by Imai and Delahay,¹⁹⁵ are presented as well for comparison. The details of the correction for the potential of the double layer, including the integration of the capacitance-potential curve, are presented in the next section.

Table 6-2. True standard rate constants for the alkali metal amalgams in AlCl_3 (1 m)-PC solution and in aqueous solution.

	AlCl_3 (1 m)-PC	H_2O
	$10^5 k_t^0$, cm/sec	k_t^0 , cm/sec
Li(Hg)	0.95*	0.022
Na(Hg)	0.0139	0.040
K(Hg)	0.00793*	0.011
Rb(Hg)	0.0064*	0.011
Cs(Hg)	0.042*†	0.016†

* Approximation, because the double layer correction was based on the integration of the capacitance-potential plot of sodium perchlorate in PC.

† Approximation, because specific adsorption of Cs^+ was not considered.

6.5. Double Layer Correction of the Rate Constant

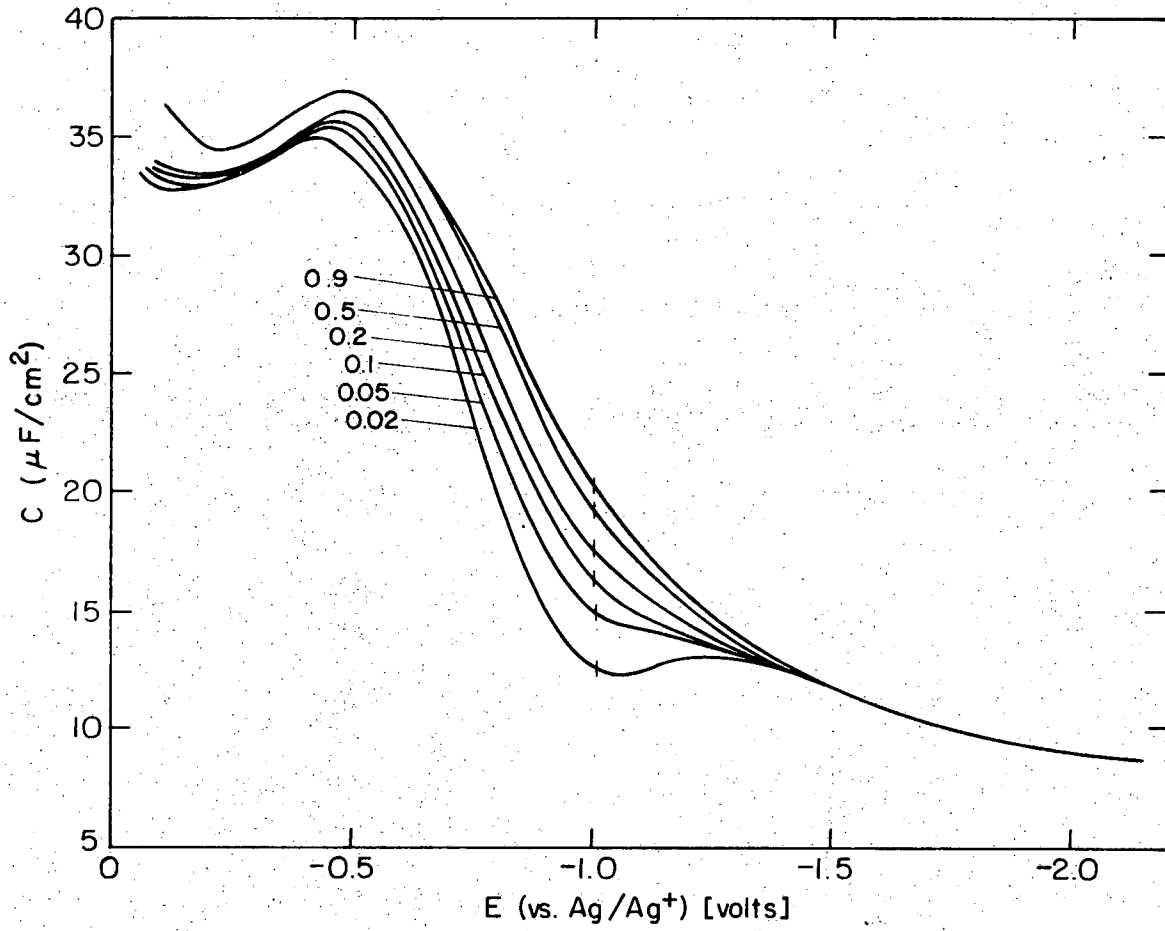
The potential of the outer Helmholtz layer ϕ_2 was calculated in Eq. (6-16) or (6-17) from the Gouy-Chapman theory, according to the simplified equation for symmetrical electrolyte:

$$q = 2(RT \epsilon \epsilon_0 C / 2\pi)^{1/2} \sinh(zF\phi_2/RT) \quad (6-23)$$

The excess charge q at the amalgam solution interface was obtained by graphical integration of the double layer capacitance vs. potential curve (Fig. 6-1) for 1 M NaClO₄ solution in PC, after Biegler and Parsons.¹⁰⁴ The potential of zero charge vs. normal calomel electrode in PC was obtained from the work of Payne^{143,144} as $-E_z(\text{PC}) = 0.33$ volts. On the negative side of the point of zero charge the capacity becomes almost independent of concentration, and at highly negative potentials the capacity is almost independent of the species present. The integration was performed, according to Eq. (6-15), from the potential of zero charge to the potentials corresponding to the concentrations of the amalgams used in the polarization experiments. Table 6-3 gives the calculated charge density values and the resulting potentials of the outer Helmholtz plane for the alkali metals in AlCl₃ (1 m)-PC.

6.6. Individual Ion Solvation and Its Effect on Electrode Kinetics in AlCl₃ (1 m)-PC Solution

The relative true rate constant of a simple electrode reaction in nonaqueous solvent compared to water is given by Eq. (6-20). The true rate constants of the alkali metals were estimated in Table 6-2. However, only the data for sodium amalgam is reliable since double layer correction in PC is available only for the sodium system. The relative true rate constant of sodium in NaCl solution in AlCl₃ (1 m)-PC is then given by



XBL 727-6629

Fig. 6-1. Capacity-potential curves for mercury electrode in NaClO₄ (M) in PC at 25°C.¹⁰⁴

Table 6-3. The evaluation of the potentials of the outer Helmholtz plane in AlCl_3 (1 m)-PC solution.

	%wt	$E_{M(\text{Hg})}$ vs. aq SCE**	$q, \mu\text{C}/\text{cm}^2$	ϕ_2, volts
Li(Hg)	0.0672	2.2823	36.83	-0.081*
Na(Hg)	0.2062	2.4201	38.76	-0.083
K(Hg)	0.2216	2.3739	38.05	-0.082*
Rb(Hg)	0.2311	2.3984	38.05	-0.082*
Cs(Hg)	0.302	2.0716	34.00	-0.079*

*Approximation--Using the capacity-potential plot of NaClO_4 (1 M) in PC.¹⁰⁴

**Based on $E_{\text{SCE}} = 0.2676$ volts.

$$(k_r^o)_{\text{Na}} = \frac{(k_t^o)_{\text{AlCl}_3\text{-PC}}}{(k_t^o)_{\text{H}_2\text{O}}} = \frac{0.0139 \cdot 10^{-5}}{0.040} = 0.347 \cdot 10^{-5} \quad (6-24)$$

The rate of the reaction $\text{Na}^+ + e^- \rightarrow \text{Na}(\text{Hg})$ is five orders of magnitude slower in AlCl_3 -PC solution than in water. As has been mentioned before, the sharp changes in the reactivity are due primarily to the large negative free energy of transfer of the alkali metal cations from water to aprotic solvents. The free energy of transfer of Na^+ from water to AlCl_3 (1 m)-PC solution was estimated (Table 5-3) as $\Delta G_t^o(\text{Na}^+)_{\text{AlCl}_3\text{-PC}} = -4.2$ kcal/mol. In order to predict the relative true rate constant (see Eq. (6-20)) we have to know the free energy of transfer of the activated complex. The structure and the degree of solvation of the activated complex are not known. We assume here that the free energy of transfer of the activated complex is negligible compared to that of the fully solvated cation. The rationale behind this assumption is that the activated complex is either not fully solvated and therefore its

energetic state is not influenced by the solvent, or the activated complex M^\ddagger is not charged and is weakly solvated by the solvent. In addition, the difference in the absolute electrode potentials in the two solvents is not known (see Eq. (6-20)) and therefore it was chosen as a free parameter, which might include possible inaccuracy in the assumption that $\Delta G_t^\circ(M^\ddagger) \approx 0$. This assumption was found reasonable for bimolecular anionic substitution in aprotic solvents.¹⁴¹

Substituting $\Delta G_t^\circ(\text{Na}^+) = -4.2 \text{ kcal/mol}$, $k_r^\circ(\text{Na}^+) = 0.347 \cdot 10^{-5}$, $\Delta G_t^\circ(\text{Na}^\ddagger) = 0$ and $\alpha_{\text{AlCl}_3\text{-PC}} = \alpha_{\text{H}_2\text{O}} = 0.61$ (the values of the transfer coefficients in the two solvents happen to be exactly equal), the difference in the absolute potential is

$$\phi_{\text{AlCl}_3\text{-PC}}^\circ - \phi_{\text{H}_2\text{O}}^\circ = +0.228 \text{ volts}$$

This difference corresponds to the real free energy of transfer

$$\Delta\alpha_t^\circ(\text{Na}^+) = F(\phi_{\text{AlCl}_3\text{-PC}}^\circ - \phi_{\text{H}_2\text{O}}^\circ) \quad (6-25)$$

The real free energy of transfer $\Delta\alpha_t^\circ$, is the sum of the chemical free energy of transfer $\Delta G_t^\circ(\text{Na}^+)$ and the difference in the surface potential of the two solvents

$$\Delta\alpha_t^\circ(\text{Na}^+) = \Delta G_t^\circ(\text{Na}^+) + F(\chi_{\text{AlCl}_3\text{-PC}} - \chi_{\text{H}_2\text{O}}) \quad (6-26)$$

For neutral molecules, the real and the chemical free energies of transfer are the same. The surface potential difference can be calculated from Eq. (6-26):

$$+0.228 = \frac{-4200 \cdot 4.184}{96500} + (\chi_{\text{AlCl}_3\text{-PC}} - \chi_{\text{H}_2\text{O}}) \quad (6-27)$$

$$\chi_{\text{AlCl}_3\text{-PC}} - \chi_{\text{H}_2\text{O}} = +0.410 \text{ volts}$$

The surface potential of AlCl_3 (1 m)-PC solution is +0.410 volts more positive than water. The surface potential of water is about +0.1 volt,¹⁹⁶ therefore, the surface potential of AlCl_3 -PC is $\chi_{\text{AlCl}_3\text{-PC}} = +0.510$ V. This is, in qualitative agreement with the capacitance measurements of Payne¹⁴³ in PC, who concluded that the PC dipoles are preferentially oriented with the positive end toward the mercury interface.

Similar calculations can be made for the kinetics of lithium amalgam in LiCl solution in DMSO. Cogley and Butler⁵⁰ measured the exchange currents and the transfer coefficient for lithium in DMSO. The standard real rate constant, after double layer correction, is $k_t^0(\text{Li}^+) = 2.9 \cdot 10^{-5}$ cm/sec, and the cathodic transfer coefficient $\alpha_c = 0.70$. Comparing these values to the data of Imai and Delahay¹⁹⁵ for Li^+ in aqueous solution, $k_t^0(\text{Li}^+)_{\text{H}_2\text{O}} = 0.02$ cm/sec, the relative true rate constant is $k_r(\text{Li}^+) = 1.45 \cdot 10^{-3}$. The chemical free energy of transfer of Li^+ from water to DMSO can be estimated in the following way: The chemical free energy of transfer of LiCl, LiBr and LiI were measured by emf method:^{92,93,94} +4.865, 2.515, -0.625 kcal/mole, respectively. The chemical free energy of transfer of the anions Cl^- , Br^- and I^- are reported by Parker:¹⁴¹ +12.1, +8.6, +4.2 kcal/mole, respectively. (Parker's data is given in terms of solvent activity coefficients of anions, rather than free energies of transfer. However, the free energies of transfer were calculated according to Eq. (5-6).) Assuming $\Delta G_t^0(\text{LiX}) = \Delta G_t^0(\text{Li}^+) + \Delta G_t^0(\text{X}^-)$, three values were obtained for $\Delta G_t^0(\text{Li}^+)$: -7.2, -6.1 and -4.85 kcal/mole. The average was taken as the estimated value, $\Delta G_t^0(\text{Li}^+)_{\text{DMSO}} = -6.1$ kcal/mole. The average cathodic transfer coefficient is $\alpha_c = (0.70 + 0.65)/2 = 0.675$. Substituting these values in Eq. (6-20) results in the absolute potential

difference for Li in the two solvents:

$$\phi_{\text{DMSO}}^{\circ} - \phi_{\text{H}_2\text{O}}^{\circ} = - 0.144 \text{ volts .}$$

The surface potential difference between DMSO and water can be estimated from Eq. (6-26):

$$\chi_{\text{DMSO}} - \chi_{\text{H}_2\text{O}} = +0.1205 \text{ volt .}$$

The surface potential of water is about +0.1 volt; therefore, the surface potential of DMSO is $\chi_{\text{DMSO}} = +0.22$ volt. Again, the positive value indicates that the positive parts of the DMSO dipoles are oriented toward the metallic interface.

6.7. Conclusions

The true rate constant for the deposition of Na at the Na(Hg) electrode in AlCl_3 (1 m)-PC solution was calculated from the micropolarization results, after being corrected for double layer effect. The true rate constant was then compared to the rate constant in aqueous solution. The difference in the absolute potential between AlCl_3 (1 m)-PC solution and water was estimated as +0.228 volts, and the difference in the surface potential as +0.410 volts, indicating that the positive part of the PC dipole is oriented toward the interface. These results can be used to predict the relative rate constants, and hence the exchange currents, in AlCl_3 -PC solution. Further kinetic measurements with different metals should be undertaken to verify these results.

VII. ELECTROREFINING AND SEPARATION OF THE ALKALI METALS AT AMBIENT TEMPERATURE

7.1. Conclusions of the Present Work

The results of the present work established the feasibility of the electrodeposition of the alkali metals from their solutions in propylene carbonate at ambient temperature. The following conclusions were obtained:

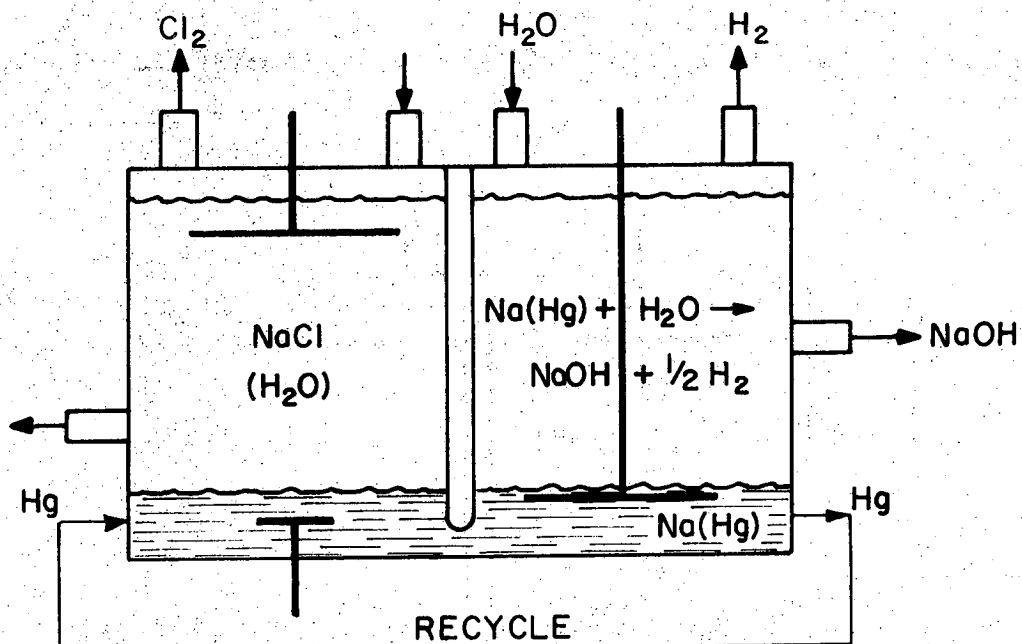
- a) Li, Na, K, Rb and Cs can be reduced from various salt solutions in PC, with high efficiency. Among the salts employed, best results were obtained from ClO_4^- , PF_6^- , BF_4^- and particularly from double salts involving the chloride of the metal and AlCl_3 in PC. From the latter, a typical composition of the electrolyte would involve 1 molal alkali metal chloride in 1 molal AlCl_3 -PC solution.
- b) The alkali metals behave chemically reversibly in PC and demonstrate moderately high exchange currents, which insure low charge transfer overpotentials during the deposition process.
- c) A scale of the standard potentials of the alkali metals in AlCl_3 (1 m)-PC solution was established, revealing a different order than in water. The order of increasing standard potential in AlCl_3 (1 m)-PC is: $\text{Cs} > \text{Rb} > \text{K} > \text{Li} > \text{Na}$.
- d) Dilute amalgams of the alkali metals behave also reversibly in alkali metal chloride solutions in AlCl_3 (1 m)-PC, and the alkali metal can be anodically dissolved from, and cathodically deposited in, the amalgam.
- e) The specific conductance of the alkali metal chlorides in AlCl_3 (1 m)-PC solution at 25°C is in the order of $10^{-2} \text{ ohm}^{-1} \text{ cm}^{-1}$. This relatively high conductance insures that the ohmic drop across a cell of 0.5 cm gap, operating at 50 mA/cm^2 , will not exceed 2.5 volts. Furthermore, raising the temperature to 60°C can reduce the ohmic drop by 50%.

These favorable results led us to propose a new process for the electrorefining and separation of the alkali metals at ambient temperature, using PC as the medium for the electrochemical process. The process is described schematically in the next section.

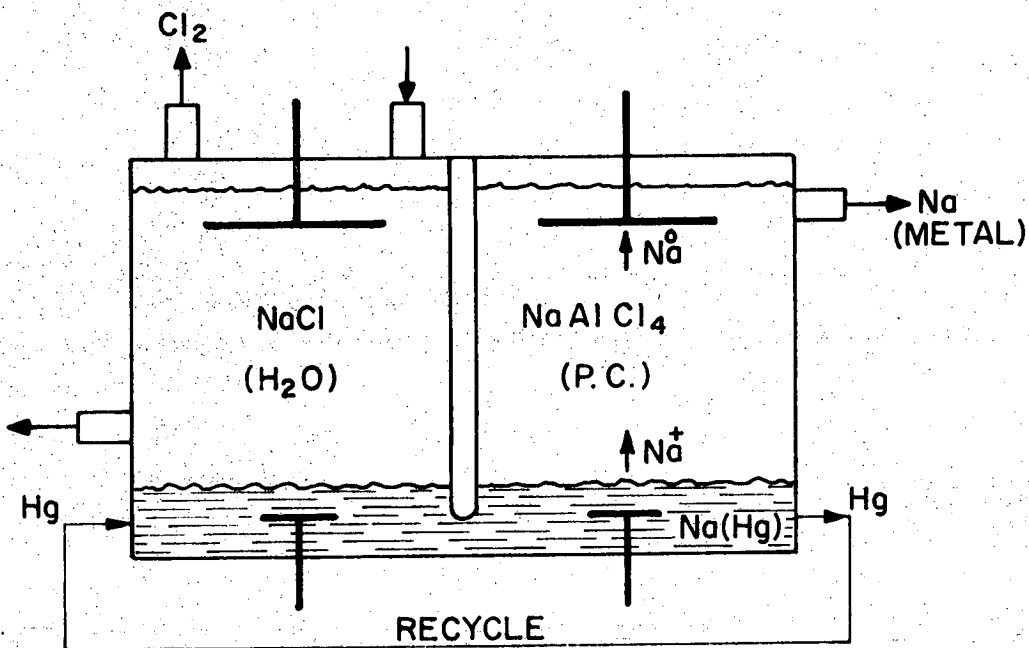
7.2. Electrorefining and Separation of the Alkali Metals at Ambient Temperature

The feasibility of the reversible deposition-dissolution of all the alkali metals and their amalgams in PC is suggested as new electrorefining and separation processes at ambient temperature.²⁰⁹ The proposed process complements the commercial mercury-chlorine cell, in which amalgam is produced by aqueous electrolysis. It is proposed that the amalgam, which is produced by aqueous electrolysis, be transferred into a nonaqueous cell containing a solution of the alkali metal chloride in $\text{AlCl}_3\text{-PC}$; the alkali metal would then be transferred from its solution in Hg to the pure metallic state, by a process akin to electrorefining: anodic dissolution of the metal from its amalgam, and cathodic deposition in the pure form. The lean amalgam would then be recycled to the aqueous cell, where it would pick up, by cathodic deposition, the alkali metal. The new process could be applied to any of the alkali metals; electrolysis of their aqueous chloride solutions would be the first stage, followed by the PC electrorefining cell.

A schematic diagram of the proposed process is shown in Fig. 7.1. Figure A is a schematic representation of the mercury-chlorine cell, where chlorine and sodium hydroxide are the two main products. Figure B represents the modified process: the first stage is identical to the one in Fig. A; however, the second stage is a nonaqueous PC cell which substitutes the decomposition stage. The main products of the modified



A.



B.

XBL 725-6265

Fig. 7-1. Schematic diagrams of the proposed electrorefining process.
 A. Mercury-chlorine cell.
 B. Chlorine cell in combination with PC electrorefining cell.

process are therefore: chlorine (as before) and metallic sodium (instead of NaOH solution). The new process is particularly promising for the production of lithium, potassium and cesium. It is quite possible that the use of the effluent amalgam from the present sodium amalgam-chlorine cell, for the recovery of sodium metal, rather than NaOH, may also offer economic advantages.

7.3. Notes on the Preliminary Design of a PC Electrorefining Cell

Consider an electrorefining cell in which the alkali metal is dissolved anodically from a dilute amalgam, and electrodeposited cathodically in a pure form. The electrolyte is an alkali metal chloride (1 m) in $AlCl_3$ (1 m) solution in PC. The gap between the amalgam and the cathode is approximately 1 cm, and the temperature of operation is $60^\circ C$. The elevated temperature was selected to decrease the ohmic drop and the charge transfer overpotential. Assuming the cell is operating at current density of approximately 50 mA/cm^2 , the total applied potential is given by

$$V_{\text{total}} = V_{\text{ohmic}} + (V_R)_{\text{Hg}} + (V_R)_M + V_{\text{eq}} + V_{\text{M.T.}}$$

where V_{ohmic} is the ohmic drop potential, $(V_R)_{\text{Hg}}$ and $(V_R)_M$ is the charge transfer reaction overpotentials of the amalgam anode and the metal cathode, respectively, V_{eq} is the open circuit equilibrium potential, and $V_{\text{M.T.}}$ is the mass transfer overpotential. The last term will be neglected, assuming that we are operating at one fourth of the limiting current. The necessary mass transfer boundary layer thickness, δ , based on a limiting current of 160 mA/cm^2 is given by

$$\delta = \frac{FDC_b}{i_{\text{lim}}} = \frac{10^5 \times 4 \times 10^{-3}}{0.2} = 0.2 \times 10^{-2} \text{ cm}$$

This boundary layer thickness can be achieved by moderate stirring or flow.

The ohmic drop can be estimated from the specific conductance of 1 molal solution in PC at 60°C, approximately $2 \times 10^{-2} \text{ ohm}^{-1} \text{ cm}^{-1}$.

$$V_{\text{ohmic}} = (0.04 \text{ A/cm}^2) \times (0.5 \times 10^2 \text{ ohm cm}) \times (1.0 \text{ cm}) = 2.0 \text{ volts}$$

The charge transfer overpotential for the amalgam and the metallic cathode can be estimated from the Tafel equation using the exchange current densities measured in the present work. Being pessimistic, and assuming exchange current densities in the order 0.1 mA/cm^2 , the total charge transfer overpotential is:

$$(V_R)_{\text{Hg}} + (V_R)_M = 2 \frac{RT}{F} \ln \frac{i}{i^0} = \frac{2 \times 2 \times 333 \times 4.184}{10^5} \ln \frac{50}{0.1} = 0.35 \text{ volts}$$

The open circuit equilibrium potential between the alkali metal and its dilute amalgam is in the order of 1 volt (see Tables 3-9 to 3-13).

The total applied potential is therefore:

$$V_{\text{total}} = 2.0 + 0.35 + 1.0 = 3.35 \text{ volt}$$

Assuming ohmic losses in the electrical contacts in the order of 0.5 volt, the total applied potential is in the order of 4 volts. The electric energy needed for the deposition of 1 g mole of pure alkali metal is

$$\text{Energy} = n F V_{\text{total}} = 1 \times 26.8 \text{ AH} \times 4.0 \text{ V} = 0.107 \text{ KWH/g mole}$$

Assuming a rate of 1¢/KWH, the total cost of electricity is 0.10 ¢/g mole. This corresponds to the following power costs per pound of metal: Li-6.52 ¢/lb., Na-1.97 ¢/lb., K-1.15 ¢/lb., Rb-0.53 ¢/lb., Cs-0.34 ¢/lb.

With the exception of sodium, these energy costs, relative to differences between current raw material and sales prices, are negligibly small. The

methods may even be economically attractive for sodium: value of sodium per pound in effluent amalgam is quite low, ~6.1 ¢/lb Na, while sodium metal, in the form of regular fused material in drums, is currently quoted at \$0.275 per pound.²¹⁰

APPENDIX I. PROPERTIES OF PROPYLENE CARBONATE

Propylene carbonate is a member of a family of cyclic esters. It is a clear colorless liquid capable of dissolving and ionizing a variety of organic and inorganic salts. It has a wide liquid range (m.p. -49°C , b.p. 241°C), it is colorless, odorless, nontoxic and a very convenient solvent to work with. The high dielectric constant, the ability to dissolve many salts, and the high stability toward oxidation and reduction, make it a very promising solvent for electrochemical purposes.

I.1 Preparation of PC

PC is manufactured in the U. S. by Jefferson Chemical Company by a proprietary reaction of CO_2 and propylene^{86,98} at $100\text{--}270^{\circ}\text{C}$ and 50-150 atm over a catalyst of an alkali or tetraalkylammonium halide, plus an oxide or carbonate of a Group II or Group III metal.

The main application of PC is as a solvent for nylon and polyacrylonitrile and as a plasticizer. The favorable properties of PC as a solvent for ionic solids have led to numerous developmental efforts in the high energy density battery area.

I.2. Purification of PC

Propylene carbonate, as received, contains the following impurities: water, propylene oxide, propylene glycol, propionaldehyde and others.⁷ The solvent is yellow and purification is necessary for practically all electrochemical purposes. The most common procedure is distillation at low pressure. Details of the distillation procedure are given by several workers.^{7,197,8} The distillation is conducted under argon atmosphere at high reflux ratio and at low temperatures, since PC shows signs of thermal decomposition above 150°C . The distilled PC is colorless and

contains about 20 ppm water, which can further be removed with molecular sieves. In addition, several dessicants were found to be effective in removing water from PC. CaO·MgO, molecular sieves, LiCl and Li powder can reduce the water content of "as received" PC significantly. Analysis of PC for impurities usually involves classical methods, such as, Karl-Fischer titration and colorimetric measurements.⁸ However, the most versatile technique for this purpose is gas chromatography.¹⁴⁵ Conductance measurements can also give information about the degree of purity of the solvent. The conductance of pure PC is approximately $2 \cdot 10^{-8} \text{ ohm}^{-1} \text{ cm}^{-1}$, when the water content is less than 10 ppm.⁷² Voltammetric measurements, in which the background current results entirely from the decomposition of the solvent, reveal important information about the purity of the solvent, and the range of potential for which the solvent is stable. The potential range in which negligible background current is observed ranges from -2.5 to +0.4 volts vs. SCE at a mercury electrode, and from -2.0 to +1.7 volts vs. SCE at platinum electrode using Et_4NClO_4 supporting electrolyte.¹⁹⁸ As can be expected, the presence of water reduces the decomposition potential of PC. On a platinum cathode, large current was observed in LiClO_4 solution in "as received" PC containing water at +2.0 V vs. Li/Li^+ reference electrode, but when carefully dried, the current peak disappeared.¹⁹⁹ The presence of propylene oxide also reduces the cathodic decomposition potential to about -2.0 V vs. Ag/AgCl reference electrode.²⁰⁰ The cathodic decomposition potential limit of PC is close to the deposition potential of lithium; therefore, the stability of metallic lithium in PC can be an indication of the purity of the solvent. Lithium electrodes began to show gas evolution in wet LiClO_4 solution,

while remaining stable in carefully dry solution.²⁰¹

I.3. Physical Properties of Propylene Carbonate

Summary of the physical properties of PC are tabulated below:

Table I-1. Physical Properties of PC

		Reference
Molecular weight	102	7
Melting point	-149°C	7
Boiling point	241°C	7
Decomposition temperature	150°C	7
Density		
ρ gr/cc	1.198 at 25°C	6
$(d \ln \rho/dT)$ deg ⁻¹	-1 10^{-3}	6
220.15 < T < 293.15	$\rho = 1.541 - 1.148 \cdot 10^{-3} T$	202
Viscosity		
	2.53 at 25°C	6
	2.43 at 25°C	81
η cp	1.33 at 60°C	81
$(d \ln \eta/dT)$ deg ⁻¹	-0.018	6
Dielectric constant		
ϵ	65.0 at 25°C	202, 203
	64.4 at 25°C	6
$(d \ln \epsilon/dT)$ deg ⁻¹	-0.0037	204, 205
Refractive Index η_D		
20°C	1.4215	206
25°C	1.4202	
30°C	1.4185	
35°C	1.4162	
220.15 < T < 293.15°K	$\eta_D = 1.5314 - 3.752 \cdot 10^{-4} T$	202

Nmr chemical shifts for liquid PC at various temperatures.* Ref.

Temp °K	a Hz	b Hz	c Hz
373	215	191	158
348	214	190	158
328	215	190	158
303	214	192	160

202

*Relative to the high-field peak of the methyl proton doublet.

Static dielectric permittivity ϵ_o (measured at 10 kHz)

T °K	ϵ_o	T °K	ϵ_o
313.15	61.7	253.15	76.9
293.15	66.1	243.15	80.0
283.15	68.4	233.15	83.0
273.15	71.0	223.15	86.1
263.15	73.9	213.15	89.3

202

Decomposition potentials (vs. SCE)

Et ₄ NC10 ₄ at a mercury electrode	-2.5 to +0.4 V
Et ₄ NC10 ₄ at a platinum electrode	-2.0 to +1.7 V

198

Low conductance value of pure PC

Water content below 10 ppm	$\kappa = 2.0 \cdot 10^{-8} \text{ ohm}^{-1} \text{ cm}^{-1}$
Water content of 100 ppm	$\kappa = 2.5 \cdot 10^{-8} \text{ ohm}^{-1} \text{ cm}^{-1}$

The complete liquid-liquid phase diagram at atmospheric pressure was measured for PC-H₂O. The upper critical solution temperature is 61.1°C, at mole fraction of PC $x = 0.575$. 208

APPENDIX II. SELECTED PROPERTIES OF THE ALKALI METALS

	Li	Na	K	Rb	Cs
Atomic number	3	11	19	37	55
Molecular weight	6.939	22.9898	39.102	85.47	132.905
Melting point	180.5°C	97.81°C	63.2°C	39.48°C	28.39°C
Boiling point	1342°C	783°C	759°C	688°C	671°C
Density, g/cc	0.53	0.97	0.86	1.53	1.8785
Crystal lattice	Cubic, b.c.	Cubic, b.c.	Cubic, b.c.	Cubic, b.c.	Cubic, b.c.
Standard potential in H ₂ O	3.045	2.714	2.925	2.925	2.923
Ionization Potential, e.v.:					
1st	5.392	5.139	4.341	4.177	3.894
2nd	75.64	47.29	31.625	27.28	25.1

APPENDIX III. CHEMICALS

Thallium:	The metal in the form of wire was supplied by United Mineral and Chemical corporation, New York, and specified to be 99.999% pure.
Mercury:	Tripled distilled and dried in vacuum. Quicksilver Products Inc., San Francisco.
Lithium:	One-eighth inch diameter wire was supplied by the Lithium Corporation of America and specified to be 99.9% pure.
Sodium:	Baker analyzed reagent.
Potassium:	Mallinckrodt, sticks.
Rubidium:	Alfa Inorganic. m2N+.
Cesium:	United Mineral & Chemical Corporation, New York, 99.8% pure.
TlCl:	Fisher Scientific Company, reagent grade.
LiCl:	Mallinckrodt analytical reagent.
NaCl:	Mallinckrodt analytical reagent.
KCl:	Mallinckrodt analytical reagent.
RbCl:	Alfa Inorganic, analytical reagent, 29.4% Cl ⁻ .
CsCl:	Alfa Inorganic, analytical reagent, 99%.
AlCl ₃ :	Baker analyzed reagent. AlCl ₃ -99.2%.
LiClO ₄ :	Alfa Inorganic
LiBr:	" "
LiPF ₆ :	" "
LiBF ₄ :	" "
NaClO ₄ :	" "
NaPF ₆ :	" "
NaBF ₄ :	" "

- KClO₄: Alfa Inorganic.
- KPF₆: Alfa Inorganic, F-60.8%.
- KBF₄: Alfa Inorganic, 99%.
- RbClO₄: Alfa Inorganic.
- CsClO₄: Alfa Inorganic.
- CsPF₆ Research Inorganic Chemical, Sun Valley, California.

APPENDIX IV. THE DEPOSITION OF MAGNESIUM FROM PC AND RELATED SOLVENTS

Magnesium has not been deposited in a satisfactory condition from organic solvents,⁵ and cannot be deposited from aqueous solution because of its high oxidation potential. Magnesium has some excellent properties in light weight and high strength alloys, and also as a consumable anode for cathodic protection. Since lithium had been deposited from its solution in PC it seemed that magnesium, which has a lower standard potential, could be deposited also. In addition, because of its high energy density, reversible deposition-dissolution behavior of magnesium in PC could lead to important application in the field of high energy batteries.

A review of previous attempts to deposit magnesium from nonaqueous solvents showed that in a very few cases magnesium was obtained in an impure form.⁵ Magnesium was obtained in an impure form by electrolysis of Grignard reagents;⁵ however, this process has no economical application. Magnesium was not obtained from its solutions in ethylenediamine,²¹¹ acetone or monoethanolamine.²¹² Overcash and Mathers²¹³ could not obtain Mg from several organic solvents. Mg was not obtained from $MgBr_2$ in pyridine,²¹⁴ but Mg amalgam was obtained by using a mercury cathode. Müller and his co-workers²¹⁵ claimed to have obtained Mg and Ca from pyridine solutions; however, their results are very doubtful. Connor, Reid and Wood²¹⁵ studied the deposition of Mg from ethereal solutions containing magnesium halides, hydride, borohydride or Grignard reagent. Mg-B alloy containing 90% Mg and 10% B was obtained from $Mg(BH_4)_2$ solution in ether. An alloy containing 7% Mg and 93% Al was obtained from diethylether solution of $MgBr_2$, $AlCl_3$ and $LiAlH_4$. Recently, Brenner²¹⁷

reported a successful deposition of smooth, white, somewhat ductile coating of magnesium. It was obtained by reactions involving decaborane $B_{10}H_{14}$. The solvent was tetrahydrofuran (THF), and the solute is probably $Mg B_{10}H_{12} \cdot 2Et_2O$. Harris and Tobias were not able to deposit magnesium from $MgBr_2$ solution in propylene carbonate.⁶ Jorné and Tobias²¹⁸ deposited 80% pure magnesium from solutions of magnesium halides in PC in the presence of Li or Na borohydride.

IV.1. Experimental

The electrodeposition experiments of magnesium in propylene carbonate (PC) were qualitative in nature. The magnesium salts, or their combination with other solutes, were dissolved in 100 ml distilled PC (water content was less than 40 ppm) inside an argon atmosphere glove box. The salts were dried inside a vacuum oven at low pressure (<50 μ Hg) and high temperature (>200°C). The dissolution of the salts was carried out inside the glove box by stirring the solutions for at least 24 hours. Most of the electrodeposition experiments were performed in an H-type cell, where the cathodic and the anodic compartments were separated by a fritted glass. Magnesium rods or platinum foils served as anodes, and platinum foils served as cathodes, which were examined for possible Mg deposition. A typical deposition experiment lasted for a few hours, and was carried out in a galvanostatic mode. A constant current supply (Electronic measurements C-613) was used, the current was measured by a Keithley electrometer (K-601), and the total applied voltage was recorded, and served as a rough indication for the concentration and the conductance of the solutions. The deposits were removed from the cell, washed carefully with pure PC and were sealed inside small glass test

tubes for observation, and chemical and X-ray analyses. Only deposits which showed metallic or powdery appearance were analyzed chemically. The deposit was dissolved in a dilute nitric acid solution (total volume 10 ml) in water, and 0.1 ml was taken for initial spectroscopic analysis for Mg, Li, Na, K and B. Accurate analysis for Mg was done using EDTA titration (EDTA molarity was 0.00879, and the standard Mg solution was 25 ml of 0.01072 M). The analysis for Li or Na was performed with flame spectroscopy. In addition, some deposits were analyzed by an X-ray diffraction analysis ($K\alpha_1$ radiation of 1.54050\AA , Picker X-ray, Model 3488K). The diffraction pattern was recorded and analyzed by comparing it to related magnesium and alkali metal compounds. Since, in most cases, the deposit was very thin, the peaks corresponding to Pt were subtracted from the diffraction pattern. The deposits were observed under a microscope as well (Zeiss metallurgical microscope). Pictures of the deposits were taken with a polaroid camera.

IV.2. Results and Discussion

IV.2-1. Deposition from PC Solutions

Table IV-1 summarizes the attempts to deposit magnesium from PC solutions. The magnesium salts as well as the complexing agents are listed in the first two columns. The mole ratio, which is the number of moles of the complexing agent per one mole of the Mg salt, is tabulated in the third column. The magnesium salt molarity is given in the fourth column, and the applied current density is given in the fifth. Visual observations of the cathodes and the anodes, as well as the chemical analysis and the X-ray diffraction patterns of the deposits, are listed in the last two columns. The X-ray results are presented in terms of

Table IV-1. Electrodeposition of magnesium from various PC solutions.

Salt	Complexing Agent	Mole Ratio	Conc. (M)	i , mA/cm ²	Cathode	Anode
MgCl ₂	---	---	insol.	10.0	No deposit	---
MgBr ₂	---	---	0.5	10.0	No deposit	---
MgI ₂	---	---	0.5	10.0	Gas evolution	---
Mg(ClO ₄) ₂	---	---	0.5	3.0	Gas evolution and yellow organic deposit. X-ray analysis: 2.53, 2.18, 1.31, 1.11	Gas Evolution
Mg(ClO ₄) ₂	Molecular Seives	---	0.5	5.0	Black deposit disappeared in Ar atmosphere.	Mg anode: Pitts.
MgCl ₂ KCl	---	---	0.5	1.0	Black deposit X-ray analysis: 1.534, 1.307	---
MgCl ₂ 2AlCl ₃	---	---	0.5	1.0	Yellow deposit	---
MgBr ₂ 2AlCl ₃	---	---	0.5	1.0	Yellow deposit	---
MgCl ₂	AlCl ₃	2	1.0	1.0	Yellow deposit	---
MgBr ₂	AlCl ₃	2	1.0	1.0	Metallic deposit	---
MgI ₂	AlCl ₃	2	1.0	10.0	Yellow deposit	Mg anode dissolved
MgF ₂	AlCl ₃	2	1.0	1.0	Yellow deposit	Bright Mg anode.

Salt	Complexing Agent	Mole Ratio	Conc. (M)	i ² mA/cm	Cathode	Anode
Mg(ClO ₄) ₂	AlCl ₃	2	0.6	10.0	Black deposit, disappeared in Ar atmosphere.	Mg anode dissolved
MgF ₂	BF ₃	2.0	1.0	1.0	No deposit	---
MgBr ₂	NaBF ₄	2.0	1.0	1.0	Heavy grey deposit--Na.	---
MgCl ₂ ⁺						
Mg(ClO ₄) ₂	NaBF ₄	2.0	0.5	10.0	Grey deposit and gas evolution. Analysis: Mg-88.3%, Na-11.7% X-ray analysis: 4.04, 2.53, 2.18, 1.31, 1.11.	---
MgF ₂ ⁺						
Mg(ClO ₄) ₂	NaBF ₄	2.0	0.5	10.0	Grey treed deposit analysis; Mg-56.7%, Na-43.3%	---
Mg(ClO ₄) ₂	KBF ₄	2.0	0.5	1.0	Grey deposit-K	---
Mg(BF ₄) ₂	---	---	0.5	1.0	Grey deposit-Mg(?) X-ray analysis: MgO (after exposure).	Anodic dissolution, bright Mg anode.
MgCl ₂	NaBH ₄	2.0	0.25	3.0	Dark deposit	---
MgI ₂	NaBH ₄	2.0	0.25	1.0	Dark deposit	---
MgF ₂	NaBH ₄	2.0	0.5	1.0	Dark deposit	---
Mg(ClO ₄) ₂	NaBH ₄	2.0	0.5	1.0	Dark deposit analysis: Mg-51%, Na-49%	---

Salt	Complexing Agent	Mole Ratio	Conc. (M)	i ² mA/cm ²	Cathode	Anode
MgCl ₂	LiBH ₄	2.0	0.5	10.0	Grey deposit analysis: Mg-22.7%, Li-77.3%	---
MgBr ₂	LiBH ₄	2.0	0.5	20.0	Grey deposit analysis: Mg-23.2%, Li-76.8%	---
Mg(ClO ₄) ₂	LiBH ₄	2.0	0.5	10.0	Grey deposit analysis: Mg-80%, Li-20%	---
Mg(BH ₄) ₂	---	---	0.25	1.0	Grey deposit analysis: Mg-18.8%, Li-81.2%	---
MgH ₂	---	---	insol.	0.1	No deposit	---
MgCl ₂ + mgH ₂	---	---	Sat.	1.0	No deposit	---
MgH ₂	AlCl ₄	2	0.05	1.0	No deposit	Mg anode dissolved
MgCl ₂	KPF ₆	2	0.25	1.0	Grey deposit-K	---
MgCl ₂	PCl ₅	2	0.25	1.0	Violent reaction with Mg anode	---
Mg(NH ₄)Cl ₃	---	---	insol.	1.0	No deposit	---
MgCl ₂	Ethyl Pyridinium Bromide	2	0.5	1.0	Blue solution	Mg anode dissolution

Salt	Complexing Agent	Mole Ratio	Conc. (M)	i^2 mA/cm ²	Cathode	Anode
MgCl ₂ +Mg	Ethyl Pyridinium Bromide	2	0.5	1.0	Blue solution upon Mg addition.	---
MgCl ₂	Mg	2	0.5	1.0	White deposit X-ray analysis: 1.53, 1.32, 1.30	---
Mg(ClO ₄) ₂	Mg	2	0.5	5.0	Heavy grey deposit turned yellow in Ar atmosphere	---
MgMoO ₄	---	---	insol.	1.0	White grey deposit X-ray analysis: 3.38, 2.69, 2.49	---
MgWO ₄	---	---	insol.	1.0	Light white deposit	---
MgTiO ₄	---	---	insol.	1.0	Light white deposit X-ray analysis: 3.16, 2.71, 2.49	---



XBB 701-551

Fig. IV-1. Mg deposit on a Pt rotating-disk electrode. Electrolyte: 0.5M MgCl_2 and 1.0 M NaBH_4 in PC. $i = 1.0 \text{ mA/cm}^2$. Rotation speed $\omega = 3600 \text{ rpm}$.

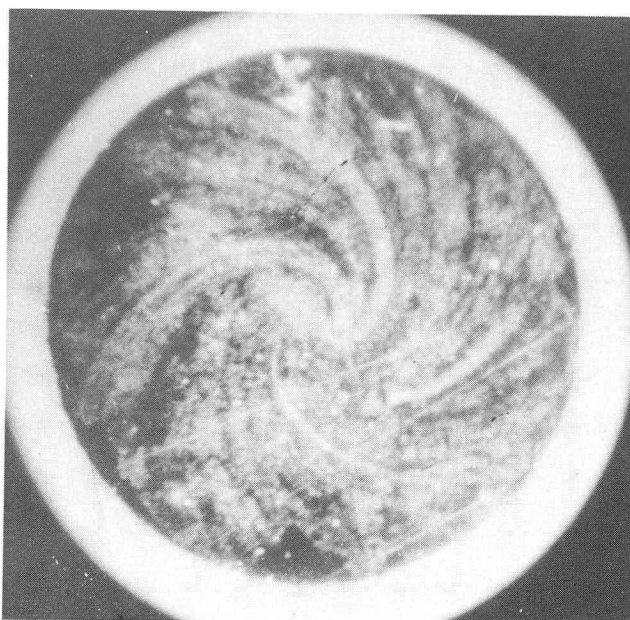
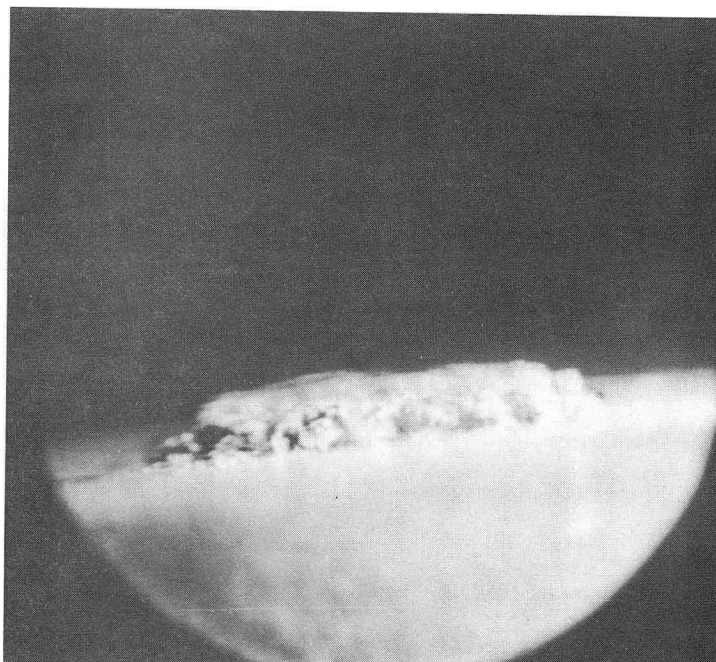


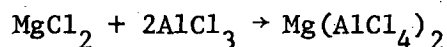
Fig. IV-2. Mg deposit on a Pt rotating-disk electrode. Electrolyte: $\text{MgCl}_2 + \text{NaBH}_4$ in PC. $i = 2 \text{ mA/cm}^2$. Deposition time: 8 hours. Rotation speed: 3600 rpm.



XBB 278-4119

Fig. IV-1. Side view of magnesium deposit from $\text{Mg}(\text{BH}_4)_2$ (0.25M) solution in PC. Current density: 1.0 mA/cm^2 . Temperature: 25°C .

the interplanar spacing d , which corresponds to the angle 2θ . It was found that the presence of some complexing agents increased considerably the solubilities of otherwise insoluble magnesium salts. The presence of AlCl_3 increases the solubility of the magnesium halides according to the following reaction:



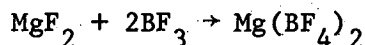
This compound was prepared also by fusing stoichiometric quantities of MgCl_2 and AlCl_3 under argon atmosphere at elevated temperature of 350°C . The same procedure was applied for MgBr_2 and AlCl_3 .

Magnesium perchlorate was dried carefully under high vacuum and elevated temperature 200°C , and was readily dissolved in PC giving a clear though somewhat viscous solution. Treating the solution with Linde molecular sieves 4A changed the nature of the deposit significantly. Without molecular sieve treatment, gas evolution was observed, accompanied by yellow gelatinous deposit. Following molecular sieve treatment, the deposit was dark and disappeared upon exposing the cathode to argon atmosphere leaving a white precipitate on the cathode. Mg anodes dissolved very well in this solution, leaving a bright, almost polished surface.

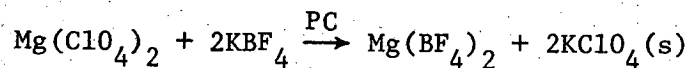
IV.2-2. $\text{Mg}(\text{BF}_4)_2$, $\text{Mg}(\text{PF}_6)_2$ and $\text{Mg}(\text{PCl}_6)_2$

On the basis of the observation that salts having large anions are more soluble in PC, attempts were made to prepare the following salts: $\text{Mg}(\text{BF}_4)_2$, $\text{Mg}(\text{PF}_6)_2$ and $\text{Mg}(\text{PCl}_6)_2$. These salts are unavailable commercially.

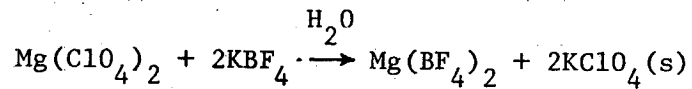
$\text{Mg}(\text{BF}_4)_2$ was prepared in PC according to



MgF₂ was added to PC, and BF₃ gas was bubbled and dissolved in the mixture. The reaction was very exothermic and was cooled with liquid nitrogen. Stirring with a magnetic stirrer was necessary to prevent local heating and decomposition of the solvent. BF₃ is a strong Lewis acid and coordinates strongly with the PC dipoles. The behavior of BF₃ in PC is very similar to that of AlCl₃. MgF₂ dissolved upon adding an excess of BF₃; however, the solution was somewhat brown, and no deposition was obtained at the cathode after the electrodeposition stage. Because of the high toxicity of BF₃ gas, another method was tried. NaBF₄ was added to MgCl₂ or MgF₂ in the presence of an excess of Mg(ClO₄)₂. In both cases, dark deposits were obtained after the electrolysis, containing mostly magnesium and sodium. In the case of MgCl₂, the deposit contained 88.3%wt magnesium. The same procedure was tested with KBF₄ substituting NaBF₄. Since KClO₄ is insoluble in PC, the following precipitation reaction was performed:



However, the reaction did not proceed to completion, and potassium metal was observed at the cathode. The same ionic reaction was also tried in aqueous solution, since KClO₄ is practically insoluble in cold water.

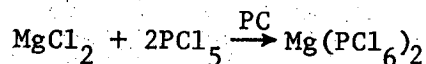


The heavy precipitate was filtered and the resulting clear aqueous solution of Mg(BF₄)₂ was evaporated to dryness under high vacuum and temperature (300°C). The white salt was dissolved in PC and the clear solution was electrolyzed at 1 mA/cm². Gas evolution was initially observed. Heavy treed deposit was obtained at the cathode. The deposit was stable in

air, and was very similar to the one obtained from $\text{Ca}(\text{BF}_4)_2$ solution in PC. X-ray diffraction analysis of the powdered deposit, after a long exposure to air, showed clearly that the oxidized deposit was MgO. The original deposit was probably metallic Mg, which was then oxidized in the air to MgO. The peaks of the X-ray analysis were: 2.43, 2.106, 1.486, 1.216, 1.053, 0.942 and 0.86Å, in good agreement with the MgO diffraction data.

KPF_6 was added to MgCl_2 in PC, but metallic potassium was obtained upon electrolysis at the cathode.

MgCl_2 dissolved in the presence of PCl_5 in PC, probably according to the reaction

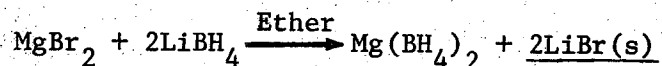


However, immersing magnesium rod in this solution resulted in a violent reaction and strong gas evolution. PCl_5 is a fuming and corrosive salt.

IV.2-3. The Borohydride Solutions

The difficulty of obtaining magnesium deposits from PC is believed to be caused by kinetic rather than thermodynamic factors, since lithium and the rest of the alkali metals, which have higher standard potentials, were deposited successfully. It is believed that the formation of unipositive Mg^{1+} , which attacks the solvent via radical reaction, is the main cause for the failure of obtaining magnesium deposits. Therefore, it was assumed that the addition of strong reducing agents, like the borohydrides, might stabilize the unipositive ion and further reduce it to the metallic state. The results obtained in the National Bureau of Standards,²¹⁶ in which almost pure magnesium deposit was obtained from ethereal solution of $\text{Mg}(\text{BH}_4)_2$, encouraged this approach.

LiBH_4 was found to be reactive in PC, although slow addition of it to MgCl_2 in PC resulted in deposits of Li-Mg alloys. The Mg content in the deposit obtained from $\text{Mg}(\text{ClO}_4)_2$ and LiBH_4 was up to 80% Mg. Magnesium borohydride was prepared in ethereal solution according to the reaction



The solution was filtered and evaporated to dryness under vacuum. The dry $\text{Mg}(\text{BH}_4)_2$ was dissolved slowly in PC. The solution was electrolyzed, but the grey deposit obtained at the cathode contained only 18.8% magnesium, and the rest was lithium. The same procedure was tried using NaBH_4 instead of LiBH_4 because NaBH_4 is not reactive in PC. The addition of NaBH_4 to $\text{Mg}(\text{ClO}_4)_2$ in PC resulted in a deposit containing 51% Mg.

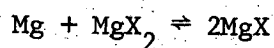
In conclusion, the presence of borohydride ions helped in the deposition of magnesium from PC; however, the reduction of lithium or sodium interfered and gave the corresponding alloys with magnesium. It is believed that solution of $\text{Mg}(\text{BH}_4)_2$ in PC, free of alkali metal ions, might give a pure magnesium deposit, though this process would not have any commercial application since BH_4^- ions are taking part in the reduction mechanism.

IV.2-4. Ethyl Pyridinium Bromide Solution

MgCl_2 was soluble in the presence of ethyl pyridinium bromide in PC. However, ethyl pyridinium bromide was preferentially reduced to give a deep blue solution near the cathode. The reaction product is believed to be diethyldihydro-dipyridyl.^{219,220} Ethyl pyridinium bromide dissolved easily in PC.

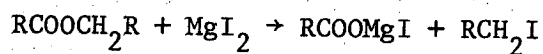
IV.2-5. MgX₂+Mg Mixtures in PC

Since it appeared that stabilizing unipositive magnesium Mg¹⁺ in PC for further reduction to metallic Mg was the key problem in obtaining magnesium deposits, attempts were made to prepare unipositive magnesium solution in PC. The main question was whether PC was stable toward the radical action of Mg¹⁺, which is a strong reducing agent. The use of unipositive magnesium as a reduction agent in organic chemistry was reviewed by Rausch, McEwen and Kleinberg.²²¹ Unipositive magnesium can be produced: 1) anodically in the presence of a number of organic oxidants and 2) by preparation of magnesium-magnesium halide mixtures in inert organic solvent. The same reduction power, as in the case of anodically prepared Mg¹⁺, can be achieved when magnesium and MgBr₂, or more importantly MgI₂, are brought together in the appropriate organic solvent in a ratio of 1:1. The unipositive magnesium is formed probably according to the equilibria



This reaction is ordinarily carried out in ether, benzene or their mixture. The mixture can reduce ketones, aldehydes, carboxylic acids, esters, acid halides, etc. Since PC is a cyclic ester, there is a possibility that the cyclic structure might increase its stability toward reduction.

Esters are reduced by unipositive magnesium according to the following mechanism:²²¹ The first stage is a cleavage by MgX₂



followed by bimolecular reduction of the salt to RC(OMgI) = C(OMgI)R.

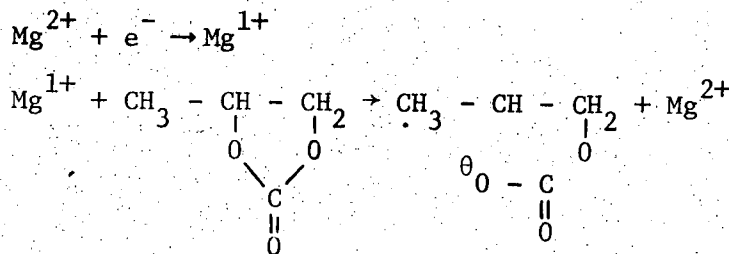
On the basis of this discussion, it seemed doubtful whether PC would be

be stable toward Mg-MgX mixture. Nevertheless, attempts to prepare unipositive magnesium halide solutions in PC were carried out. Mg chips were added, in excess, to MgCl_2 and $\text{Mg}(\text{ClO}_4)_2$ in PC, with the hope that the single stage reduction of the unipositive magnesium would be easy. However, magnesium was not deposited at the cathode, and it seemed doubtful whether the MgX salt was formed at all. Further experiments of this type were performed in ether and benzene and are presented in Section IV.7, which deals with the deposition of magnesium from related solvents.

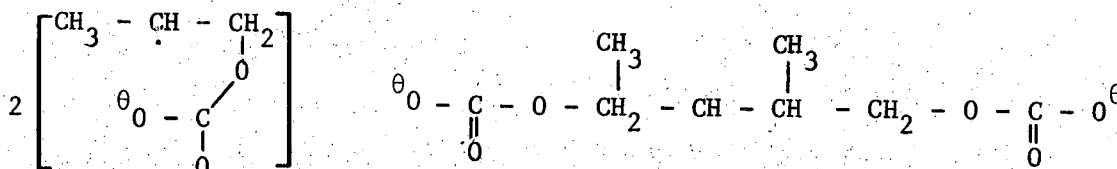
IV.3. The Mechanism of Mg^{2+} Reduction in PC

The inability to reduce Mg^{2+} in PC to its metallic form is due to kinetic reason rather than thermodynamic reasons. The fact that all the alkali metals were deposited from their PC solutions proves that PC has the potential range to achieve the standard potential of magnesium without self decomposition. However, the fact that magnesium ions are bivalent raises the question whether unipositive magnesium, which is believed to be formed as an intermediate step, is stable in PC. Unipositive magnesium is a strong reducing agent, and was reported as being able to reduce esters.²²¹ Despite the stability of PC due to its cyclic structure, it is believed that Mg^{1+} ions attack PC via radical reaction to give an organic product, while they are oxidized back to their bivalent state. This mechanism is supported by the organic yellow deposits which were observed in most of the experiments, and by the evolution of gas (probably propylene or CO_2) at the cathode.

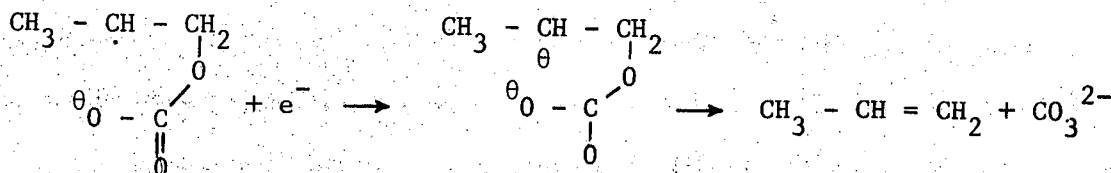
The following mechanisms are suggested during the reduction of simple magnesium salt in PC (e.g. $\text{Mg}(\text{ClO}_4)_2$ or MgBr_2).



Secondary radical,
more stable

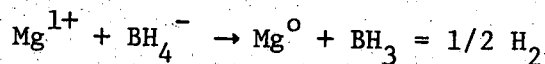


The final product is a Mg salt of the bicarbonate ester of the diol HO-CH₂-CH₂-CH(CH₃)-CH(CH₃)-CH₂-OH. However, the following alternative electrochemical reaction might occur at the cathode:



The final products according to this mechanism are propylene and carbonate ion, which might be identified as a deposit of magnesium carbonate at the cathode. The propylene gas is soluble in PC and probably starts to evolve only after saturation has been reached. Propylene was identified elsewhere as the product of the reduction of pure PC on graphite.²²²

The presence of borohydride ion, which is a strong reducing agent, stabilizes the presence of Mg¹⁺, and furthermore, reduces the unipositive magnesium to its metallic form



Traces of boron might be presented also in the cathodic deposit via further reduction.

IV.4. Electrodeposition of Magnesium From Related Solvents

Along with the attempts to deposit magnesium from its solution in PC, several other nonaqueous solvents were also tried. The results are summarized in Table IV-2. Dimethyl sulfoxide was tried on the basis of its similarity to PC, and the possibility that DMSO would be more stable toward unipositive magnesium ion. However, no magnesium was obtained from DMSO solutions.

The existence of Mg^{1+} ions in solvents like pyridine, ether and benzene was reported.²²¹ These solutions are used as reducing agents in organic chemistry. Since Mg^{1+} is formed as an intermediate step, these solvents were tested as possible media for the reduction $Mg^+ + e \rightarrow Mg$. Also, conflicting reports²¹⁵ regarding the deposition of Mg from pyridine solution encouraged retesting of this solvent. Magnesium was not obtained from $Mg(ClO_4)_2$, $MgCl_2$ or $MgBr_2$ solutions in pyridine. The pyridine was dried by Linde molecular sieves 4A without any further treatment. Attempts to prepare solutions of Mg^{1+} in pyridine, ether and ether-benzene mixture did not produce metallic magnesium. In addition, the conductivities of these solutions were very low. The ether and the benzene were dried by Linde molecular sieves 4A without any further treatment.

Table IV-2. Electrodeposition of magnesium from related solvents.

Solvent	Salt	Conc. (M)	i mA/cm ²	Cathode	Anode
DMSO	Mg(ClO ₄) ₂	0.5	1.0	Dark deposit X-ray peaks: 1.534; 1.307Å	
DMSO	MgBr ₂	Low conductance			
DMSO	Mg(NO ₃) ₂	1.0	10.0	Gelatine deposit and gas evolution	Mg anode dissolution
Pyridine	Mg(ClO ₄) ₂	0.1	1.0	Yellow brown deposit	
Pyridine	MgCl ₂	Satd.	1.0	White deposit X-ray peaks: 1.529; 1.529Å	
Pyridine	MgBr ₂	Low conductance			
Pyridine	MgI ₂ +Mg+2MgI	0.1	1.0	Yellow-transparent deposit. Low conductance	
Ether	MgBr ₂ ⁺ Mg+2MgBr	Low conductance- High voltage			
Ether	MgI ₂ +Mg+2MgI	Low conductance- High voltage			
Ether + Benzene (1:1)	MgI ₂ +Mg+2MgI	Low conductance- High voltage			
Pyridine	Mg(NO ₃) ₂	Insoluble			
TEGDME	Mg(ClO ₄) ₂	Low conductance		No deposit	

VI.5. Electrodeposition of Calcium

Few attempts were made to deposit calcium from its solutions in PC. The experimental procedure was identical to the one used during the deposition of magnesium from PC. Yellow deposit was obtained at the cathode during the electrolysis of CaBr_2 (0.5 M) in PC. Grey treed deposit was obtained from a solution of $\text{Ca}(\text{BF}_4)_2$ (0.5 M) in PC. The deposit was similar to the one obtained from $\text{Mg}(\text{BF}_4)_2$ in PC. X-ray diffraction analysis of the powdered deposit, which was exposed to atmosphere, indicated clearly that the deposit is CaF_2 . (Interplanar space: 3.15, 1.93, 1.647, 1.366, 1.253, 1.115, 1.051, 0.966, 0.9233, 0.864Å.) The solubility of $\text{Ca}(\text{BF}_4)_2$ in PC is 1.44 gr/100 cc.⁶ Yellow deposit was obtained from the electrolysis of $\text{Ca}(\text{ClO}_4)_2$ in PC. Pre-treatment with molecular sieves (Linde 4A) resulted in a dark deposit which disappeared upon exposure to argon atmosphere.

No deposits were obtained from $\text{Ca}(\text{ClO}_4)_2$ or $\text{Ca}(\text{BF}_4)_2$ solutions in tri-ethylene glycol dimethyl ether (TEGDME). In addition, the conductance of these solutions were very low. The solvent was distilled in a single stage distillation column, and since the water content of the solvent was not known, the negative results should not be considered as conclusive.

APPENDIX V. THE ELECTRODEPOSITION OF TITANIUM
FROM PC AND RELATED SOLVENTS

Pure titanium has never been deposited from organic solvents. The excellent properties of titanium as a corrosion resistant metal, and as a very important construction material in the aerospace industry, attracted many attempts to deposit Ti from various organic solvents, though only titanium alloys have been obtained. Reid, Bish and Benner²²³ deposited alloys of titanium and zirconium from etheral solution containing halides, hydrides, borohydrides and organo-metallic compounds of Ti and Zr. Alloys of Ti and Al were obtained, containing up to 6% Ti. Of all the elements of Group IV of the periodic table, only germanium was electrodeposited in a pure form from solution of germanium tetrachloride in propylene glycol.²²⁴ Harris and Tobias⁶ did not obtain titanium from solution of $TiBr_4$ in propylene carbonate at current up to 32 mA/cm^2 , nor from solution resulting when $NaBH_4$ reacted with a solution of $TiBH_4$ in PC. The purpose of the present work was to investigate further possible solutions of titanium salts in PC and related solvents.

V.1. Experimental

The attempts to deposit titanium from PC solutions were exploratory in nature. Titanium salts, or their combination with other solutes, were dissolved in 100 ml distilled PC (the water content was less than 40 ppm) inside an argon atmosphere glove box. The salts were dried prior to use inside a vacuum oven at low pressure and high temperature (200°C). The dissolution of the salts was performed under stirring for at least 24 hours. The electrodeposition experiments were carried

out in an H-type glass cell, in which the cathode and the anode were separated by a fritted glass. Platinum foils served as electrodes. A typical electrodeposition experiment lasted for a few hours at constant current up to 10 mA/cm^2 . The solutions were stirred during the experiments with small magnetic stirrers. A constant current supplier (Electronic Measurements Model C-613) was used; the current was measured by a Keithley electrometer Model K-601 and the applied potential was measured and served as an indicator of the conductance of the solution. The deposits were removed from the cell, washed carefully with pure PC, and sealed in small glass test tubes for optical observations and X-ray analysis. X-ray diffraction analysis was taken with $K\alpha_1$ copper radiation of 1.54050\AA . The diffraction patterns were analyzed, and the peaks corresponding to the platinum substrate were subtracted from the obtained patterns. The deposits were observed under Zeiss metallurgical microscope, and the particular deposit which was obtained from $\text{LiBr} + \text{TiCl}_3$ solution in PC was examined in electron microprobe.

V.2. Results and Discussion

Table V-1 summarizes the attempts to deposit titanium from PC and pyridine solutions. The solutes are presented in the first column, as well as the molarity and the color of the solution. The current densities are given in the fourth column, and the description of the cathodic deposits, along with the results of the X-ray analysis are given in the last column. The X-ray analysis is presented in terms of the interplanar spacings, which correspond to the angle 2θ .

Table V-1. Electrodeposition of titanium from various PC and pyridine solutions.

Solvent	Solute	Color	Conc. (M)	i mA/cm ²	Cathode
PC	TiCl ₃		Insol.		
	TiCl ₃ + AlCl ₃		Insol.		
	TiCl ₃ + Et.Pr.Br	Purple	0.1	1.0	Dark, nonmetallic deposit
	TiBr ₄	Orange	0.1	1.0	Gas evolution and non-metallic green deposit
	TiI ₄	Orange-red	0.1	1.0	Black deposit. X-ray analysis: No peaks.
	TiI ₄ + NaBH ₄	Gas Evolution.			
	TiCl ₃ + NaBH ₄	Dark	0.1	1.0	Heavy dark Na deposit
	TiCl ₃ + LiBr	Dark	0.5	1.0	Black deposit. Li-Pt alloy formation. X-ray analysis: 2.493, 2.928(s), 2.215, 1.93, 1.767, 1.36(s), 1.625(s).

Solvent	Solute	Color	Conc. (M)	i mA/cm ²	Cathode
	TiCl ₃ ⁺ 2LiBF ₄	Dark	0.5	1.0	Li-Pt alloy. X-ray analysis: 4.973, 3.72, 2.88, 2.786, 2.597, 2.396, 2.209, 1.912(s), 1.35(s), 1.180(s).
	TiCl ₃ ⁺ 2LiBF ₄	Dark	0.5	10.0	Li-Pt alloy. X-ray analysis after washing with water: 2.794, 2.252(Pt), 1.95(Pt), 1.38(Pt), 1.18, 1.129 (all peaks were double).
	(C ₂ H ₅) ₂ TiCl ₂	Red	0.25	1.0	No deposit, low conductance
	TiCl ₂ (l)		Insol.		
	TiCl ₂ (?)+ AlCl ₃		Insol.		
Pyridine	TiCl ₃	Dark-green	0.1	1.0	Grey metallic deposit. X-ray analysis: 2.2414(Pt?), 1.9513(Pt), 1.529, 1.377 (Pt), 1.178.
	TiCl ₂ (?)		Insol.		

Of the simple titanium salts, only TiBr_4 and TiI_4 were soluble. From the colorful solutions metallic titanium was not electrodeposited. TiCl_3 was insoluble in PC, but in the presence of LiBr, TiCl_3 dissolved giving a dark solution. The deposit obtained from this solution was heavy and was identified as lithium deposit which formed an alloy with the platinum substrate. A picture of the deposit is given in Fig. 3-5. This pattern was typical for all Li-Pt alloys which were obtained during the electrodeposition of lithium. TiCl_2 was insoluble in PC. Since the salt obtained from the storeroom did not carry the manufacturer's label, it is doubtful whether the salt was indeed TiCl_2 . Grey metallic deposit was obtained from TiCl_3 solution in pyridine, which was pre-treated with Linde molecular sieves 4A. X-ray analysis results were not conclusive as to whether the deposit contained metallic titanium.

APPENDIX VI. THE ELECTRODEPOSITION OF MOLYBDENUM
FROM PC AND PYRIDINE SOLUTIONS

Molybdenum has not been deposited in pure metallic form from organic solvents. Molybdenum could not be obtained by electrolysis of MoCl_5 , MoCl_3 and MoBr_3 in several organic solvents, including formamide and acetamide,²²⁵ acetonitrile, amides, ketones, polyhydroxy alcohols and ethers.²²⁶ The favorable properties of metallic molybdenum attracted attempts to deposit molybdenum from various solutions in PC and pyridine. For a general discussion on the deposition of molybdenum and other rare earth metals, the reader is referred to Brenner's review.⁵

VI.1. Experimental

The electrodeposition attempts to deposit molybdenum from PC and pyridine solutions were qualitative and exploratory in nature. The experimental procedure was identical to the one used in the attempts to deposit titanium from the same solvents (see Appendix V).

VI.2. Results and Discussion

Table VI-1 summarizes the attempts to deposit molybdenum from various PC and pyridine solutions. MoCl_3 was insoluble in PC, while MoCl_4 was quite soluble, (0.5 M) but no deposit was obtained during electrolysis of the dark solution. MoCl_4 was slightly soluble in pyridine, and a very thin deposit was obtained, but the applied potential was very high (>100 volts). Very thin dark deposits were obtained from solutions of molybdenum oxychlorides, and the applied potential was very high due to low conductance solutions and deposits. MoOCl_3 reacted with pyridine to give $\text{MoOCl}_3 \cdot 2\text{C}_5\text{H}_5\text{N}$, but no deposit was obtained.

Table VI-1. Electrodeposition of molybdenum from various PC and pyridine solutions.

Solvent	Solute	Color	Conc. (M)	i / 2 mA/cm	Cathode
PC	MoCl ₃		Insol.		
	MoCl ₄	Dark	0.5	1.0	No deposit.
	MoCl ₃ +AlCl ₃		Insol.		
	MoOCl ₃	Green	0.1	1.0	No deposit.
	MoOCl ₄	Orange	0.25	1.0	Black deposit.
Pyridine	Mo(III)-acetyl acetate		0.1	1.0	Black deposit.
	MoCl ₃		Insol.		
	MoOCl ₃	Purple	0.1	1.0	Yellow deposit.
DMSO	MoCl ₄		0.1	1.0	Very thin deposit.
	MoCl ₃		Insol.		

ACKNOWLEDGEMENTS

I would like to express my appreciation and gratitude to Professor Charles Tobias for his valuable guidance throughout this work, and for five years of personal and scientific growth.

I am grateful to Professors Leo Brewer and Scott Lynn for reviewing the manuscript, and to Dr. Leonard Silvester for valuable suggestions.

And finally, I am grateful to Paula McCarthy for everything.

This work was supported by the U. S. Atomic Energy Commission.

REFERENCES

1. Ludwig F. Audrieth and Jacob Kleinberg, Non-Aqueous Solvents (John Wiley & Sons, New York, 1953).
2. F. Walden, Ber. dtsh. Chem. Ges. 32, 2862 (1899).
3. Paul Walden, Elektrochemie Nichtwassrigen, J. A. Barth (Leipzig, 1924).
4. L. F. Audrieth and H. W. Nelson, Chem. Rev. 8, 335 (1931).
5. Abner Brenner, Electrolysis of Nonaqueous Systems, Advances in Electrochemistry and Electrochemical Engineering, P. Delahay and C. W. Tobias, eds. (Interscience, New York, 1967) Vol. 5.
6. William S. Harris, Thesis, UCRL 8381, University of California, 1958.
7. Raymond Jasinski, Electrochemistry and Application of Propylene Carbonate, Advances in Electrochemistry and Electrochemical Engineering, P. Delahay and C. W. Tobias, eds. (Interscience, New York, 1971) Vol. 8.
8. James N. Butler, Reference Electrodes in Aprotic Organic Solvents, Advances in Electrochemistry and Electrochemical Engineering, P. Delahay and C. W. Tobias, eds. (Interscience, New York, 1970) Vol. 7.
9. C. K. Mann and K. K. Barnes, Electrochemical Reactions in Nonaqueous Systems (Marcel Dekker, New York, 1970).
10. C. K. Mann, Advances in Electroanalytical Chemistry, A. J. Bard, ed. (Marcel Dekker, New York, 1969) Vol. 3.
11. P. H. Geiger, The Chemistry of Non-Aqueous Solvents, J. J. Lagowski, ed. (Academic Press, New York, 1968) Vol. 3.
12. R. N. Adams, Solid Electrode Voltammetry (Marcel Dekker, New York, 1968).

13. H. Strehlow, in The Chemistry of Non-Aqueous Solvents, J. J. Lagowski, ed. (Academic Press, New York, 1966) Vol. 1.
14. I. M. Kolthoff, J. Polarographic Soc. 10, 22 (1964).
15. P. J. Elvin and M. S. Spritzer, *Talanta* 12, 1243 (1965).
16. R. Takahashi, *Talanta* 12, 1211 (1965).
17. Richard Payne, The Electrical Double Layer in Nonaqueous Solutions, Advances in Electrochemistry and Electrochemical Engineering, P. Delahay and C. W. Tobias, eds. (Interscience, New York, 1970) Vol. 7.
18. T. C. Waddington, ed., Non-Aqueous Solvent Systems (Academic Press, New York, 1965).
19. J. J. Lagowski, ed., The Chemistry of Non-Aqueous Solvents (Academic Press, New York, Vol. I, 1966 and Vol. II, 1967).
20. S. v. Laszczynski, *Z. Elektrochem.* 2, 55 (1895).
21. S. v. Laszczynski and S. V. Gorski, *Z. Elektrochem.* 4, 290 (1897).
22. L. Kahlenberg, *J. Phys. Chem.* 3, 602 (1899).
23. M. G. Levi and M. Voghera, *Gazz. Chim. Ital.* 35, 277 (1905).
24. H. E. Patten and W. R. Mott, *J. Phys. Chem.* 8, 153 (1904).
25. H. E. Patten and W. R. Mott, *J. Phys. Chem.* 12, 49 (1908).
26. R. Müller, E. Pinter and K. Pretz, *Monatsh. Chem.* 45, 525 (1924).
27. S. I. Yakubson and M. A. Abramova, *Ukrain. Khim. Zh.* 17, 902 (1951).
28. G. N. Lewis and F. G. Keyes, *J. Am. Chem. Soc.* 35, 340 (1913).
29. Raymond Jasinski, High Energy Batteries (Plenum Press, New York, 1967).
30. R. G. Selim, K. R. Hill and M. L. B. Rao, Research and Development of a High Capacity Nonaqueous Secondary Battery, Final Report, Contract No. NAS 3-6017, 1965, NASA CR-54969; N66-35218; Chem. Abstr. 66, 121447x.

31. J. Chilton, E. Duffek and A. Reed, Final Report, Contract NAS will, April 1961.
- 31a. W. Eliot, S. Hsu and W. Towle, Proc. Annual, Power Sources Conf. 18, 82 (1964); Final Report, Contract NAS 3-2790 (1964).
32. W. Meyers, Final Report, Contract NAS 3-2775 (1964).
33. B. Burrows and R. Jasinski, J. Electrochem. Soc. 115, 365 (1968).
34. B. Burrows and R. Jasinski, J. Electrochem. Soc. 115, 348 (1968).
35. B. Burrows and S. Kirkland, J. Electrochem. Soc. 115, 1164 (1968).
36. S. Abens, W. Merz and C. Walk, Final Report, NASA CR-72331, 1967.
37. N. P. Yao, E. D'Orsay and D. N. Bennion, J. Electrochem. Soc. 115, 999 (1968).
38. W. H. Smyrl and C. W. Tobias, J. Electrochem. Soc. 113, 754 (1966).
39. D. R. Cogley and J. N. Butler, J. Phys. Chem. 72, 1017 (1968).
40. Gianfranco Pistoia, J. Electrochem. Soc. 118, 153 (1971).
41. G. Pistoia, M. DeRoss and B. Scrosati, J. Electrochem. Soc. 117, 500 (1970).
42. I. Fried and H. Barak, J. Electronanal. Chem. 30, 279 (1971).
43. A. N. Dey, J. Electrochem. Soc. 118, 1547 (1971).
44. J. C. Hall, R. C. Murray, Jr. and P. A. Rock, J. Chem. Phys. 51, 1145 (1969).
45. G. Singh, J. C. Hall and P. A. Rock, J. Chem. Phys. 56, 1855 (1972).
46. Stuart G. Meibuhr, J. Electrochem. Soc. 117, 56 (1970).
47. Stuart G. Meibuhr, J. Electrochem. Soc. 118, 1320 (1971).
48. Robert F. Scarr, J. Electrochem. Soc. 117, 295 (1970).
49. J. N. Butler, D. R. Cogley and J. C. Synnott, J. Phys. Chem. 73, 4026 (1969).

50. D. R. Cogley and J. N. Butler, *J. Phys. Chem.* 72, 4568 (1968).
51. H. E. Patten and W. R. Mott, *Electrochem. Ind.* 1, 417 (1903).
52. H. C. Mandell, Jr., W. M. McNabb and J. F. Hazel, *J. Electrochem. Soc.* 102, 263 (1955).
53. N. P. Fedot'ev and R. N. Kinkul'skaya, *Proce. First All-Union Conf. Non-Aqueous Solutions, Kiev (USSR) 1935*, p. 114.
54. G. L. Putnam and K. A. Kobe, *Trans. Electrochem. Soc.* 74, 609 (1938).
55. Ya P. Mezhenii, *Zapiski Inst. Khim. Akad. Nauk Ukr. SSR*, 3, 361 (1936).
56. M. A. Klochko, *Light Metals* 6, 254, 269 (1943).
57. D. A. Pospekhov, *J. App. Chem. USSR, English Translation* 27, 552 (1954).
58. D. E. Couch, *Unpublished Work, Natl. Bur. Std.*, 1957.
59. K. Ziegler, H. Lehmkuhl and W. Grimme, *Ger. Pat.* 1, 114, 330 (May 6, 1961); 1, 146, 258 (March 28, 1963); 1, 114, 490 (Feb. 28, 1963).
60. Stuart G. Meibuhr, *J. Electrochem. Soc.* 118, 709 (1971).
61. M. C. Giordano, J. C. Bazan and A. J. Arvia, *Electrochimica Acta* 11, 741 (1966).
62. G. N. Lewis and F. G. Keyes, *J. Am. Chem. Soc.* 34, 119 (1912).
63. G. N. Lewis and C. A. Kraus, *J. Am. Chem. Soc.* 32, 1459 (1910).
64. E. S. Gilfillan and H. E. Bent, *J. Am. Chem. Soc.* 56, 1505 (1934).
65. H. E. Bent and E. Swift, Jr., *J. Am. Chem. Soc.* 58, 2220 (1936).
66. G. N. Lewis and W. L. Argo, *J. Am. Chem. Soc.* 37, 1983 (1915).
67. H. E. Bent, G. S. Forbes and A. F. Forziati, *J. Am. Chem. Soc.* 61, 709 (1939).
68. R. Fuoss and E. Hirsch, *J. Am. Chem. Soc.* 82, 1013 (1968).
69. A. Lyall, H. Seiger and J. Orshich, *Tech. Report AFAPL-TR-68-71*, July 1968.

70. H. Bauman, Tech. Report APL-TD-R64-59, May 1964.
71. R. Keller, et al., Fourth Quarterly Report, Contract NAS 3-851, July 1967.
72. Y. Wu and H. Friedman, J. Am. Chem. Soc. 70, 501, 2020 (1966).
73. R. Keller, J. Foster and J. Sullivan, NASA Report CR-72106, Sept. 1966.
74. D. Geske and A. Maki, J. Am. Chem. Soc. 82, 2671 (1960).
75. G. McDonald, K. Murphy and J. Gower, Report TID 4500-SG-67-2855, Dec. 1967.
76. S. Abens, R. Corbett and W. Merz, Forth Quarterly NASA Report, CR-72071, June 1966.
77. J. Chilton, New Cathode-Anode Couples, Report ASD-TDR-62-1, April 1962.
78. M. Shaw, et al., NASA Report CR-72377, Jan. 1968.
79. L. Mukherjee, D. Boden and R. Lindauer, J. Phys. Chem. 74, 1942 (1970)
80. A. Dey and M. Rao, Final Report, Contract DA-44-009-AMC-1534(T), Nov. 1967.
81. R. Keller, et al., Final Report, Contract NAS 3-8521, Dec. 1969.
82. L. Mukherjee and D. Bogen, J. Phys. Chem. 73, 3965 (1969).
83. R. Fuoss and F. Accascina, Electrolytic Conductance (Interscience Publishers, New York, 1959).
84. Neng-Ping Yao and D. N. Bennion, J. Electrochem. Soc. 118, 1097 (1971).
85. Neng-Ping Yao and Douglas N. Bennion, J. Phys. Chem. 75, 1727 (1971).
86. Neng-Ping Yao and Douglas N. Bennion, J. Phys. Chem. 75, 3586 (1971).
- 86a. C. Melendres (M. S. Thesis) University of California, 1965.
87. D. Boden, Proc. Annual Power Sources Conf. 20, 63 (1966).
88. F. Breivogel and M. Eisenberg, Electrochemica Acta 14, 459 (1969).
89. J. N. Butler, Anal. Chem. 39, 1799 (1967).

90. J. N. Butler, D. R. Cogley and W. Zorosky, J. Electrochem. Soc. 115, 445 (1968).
91. Friedrich G. K. Baucke and Charles W. Tobias, J. Electrochem. Soc. 116, 34 (1969).
92. William H. Smyrl and Charles W. Tobias, J. Electrochem. Soc. 115, 33 (1968).
93. Mark Salomon, J. Electrochem. Soc. 116, 1392 (1969).
94. Mark Salomon, J. Electrochem. Soc. 117, 325 (1970).
95. Mark Salomon, J. Phys. Chem. 73, 3299 (1969).
96. Mark Salomon, J. Electroanal. Chem. 25, 1 (1970).
97. Mark Salomon, J. Electroanal. Chem. 26, 319 (1970).
98. J. N. Butler and J. C. Synnott, J. Am. Chem. Soc. 92, 2602 (1970).
99. L. F. Silvester, J. J. Kim and P. A. Rock, J. Chem. Phys. 56, 1863 (1972).
100. J. C. Synnott and J. N. Butler, Anal. Chem. 25, 481 (1969).
101. Ilana Fried and Haim Bark, J. Electroanal. Chem. 27, 167 (1970).
102. Ivan Piljac and Reynold T. Iwamoto, J. Electroanal. Chem. 23, 484 (1969).
103. E. Kirowa-Eisner and E. Gileadi, J. Electroanal. Chem. 25, 481 (1970).
104. T. Biegler and Roger Parsons, J. Electroanal. Chem. 21, App 4-6, (1969).
105. A. Caiola, H. Guy and J. C. Sohm, Electrochimica Acta, 15, 1733 (1970).
106. J. N. Butler, D. R. Cogley, J. C. Synnott and G. Holleck, Final Report, Contract AF 19(628)6131, Sept. 1969.
107. A. N. Dey, J. Electrochem. Soc. 114, 823 (1967).
108. G. W. Jackson and G. E. Blomgren, J. Electrochem. Soc. 116, 1483 (1969).
109. D. R. Cogley and J. N. Butler, J. Electrochem. Soc. 113, 1074 (1966).

110. Eugene Luksha and Cecil M. Criss, J. Phys. Chem. 70, 1496 (1966).

111. Robert P. Held and Cecil M. Criss, J. Phys. Chem. 69, 2611 (1965).

112. Robert P. Held and Cecil M. Criss, J. Phys. Chem. 71, 2487 (1967).

113. Cecil M. Criss and Eugene Luksha, J. Phys. Chem. 72, 2966 (1968).

114. Cecil M. Criss, Robert P. Held and Eugene Luksha, J. Phys. Chem. 72, 2970 (1968).

115. G. Holleck, D. R. Cogley and J. N. Butler, J. Electrochem. Soc. 116, 952 (1969).

116. J. S. Dunnett and R. P. H. Gasser, Trans. Faraday Soc. 61, 922 (1965).

117. T. Slerlak, B. Nikov and V. Sislov, Glasnick Drustva Himicara Tehnol SR Bosne Herrcegovine No. 11, 39 (1962). Chem. Abstr. 61, 2461c.

118. R. K. Agarwall and B. Nayak, J. Phys. Chem. 70, 2568 (1966).

119. R. K. Agarwall and B. Nayak, J. Phys. Chem. 71, 2062 (1967).

120. M. Mandel and P. Decroly, Nature, 182, 794 (1958).

121. R. W. C. Broadband, et al., Trans. Faraday Soc. 64, 3311 (1968).

122. G. Spiegel and H. Ulich, Z. Physik. Chem. A178, 187 (1937).

123. J. F. Coetzee and J. J. Campion, J. Am. Chem. Soc. 89, 2513 (1967).

124. J. F. Coetzee and J. J. Campion, J. Am. Chem. Soc. 89, 2517 (1967).

125. H. L. Friedman, J. Phys. Chem. 71, 1723 (1967).

126. G. Somsen, Rec. Trav. Chim. 85, 517 (1966); 85, 526 (1966).

127. Yu. M. Kessler, Elektrokimiya 2, 1467 (1966).

128. L. Weeda and G. Somson, Rec. Trav. Chim. 85, 159 (1966); 86, 263 (1967).

129. R. C. Paul, et al., Indian J. Chem. 3, 300 (1965); 3, 305 (1965).

130. E. M. Arnett and D. R. McKelvey, J. Am. Chem. Soc. 88, 2598 (1966).

131. Y. C. Wu and H. L. Friedman, J. Phys. Chem. 70, 2020 (1966).

132. W. M. Latimer, K. S. Pitzer and C. M. Slansky, *J. Chem. Phys.* 7, 108 (1939).
133. H. L. Friedman, *J. Phys. Chem.* 71, 1723 (1967).
134. C. V. Krishnan and H. L. Friedman, *J. Phys. Chem.* 73, 3934 (1969).
135. C. V. Krishnan and H. L. Friedman, *J. Phys. Chem.* 73, 1572 (1969).
136. C. V. Krishnan and H. L. Friedman, *J. Phys. Chem.* 75, 3606 (1971).
137. C. V. Krishnan and H. L. Friedman, *J. Phys. Chem.* 75, 3598 (1971).
138. T. W. Richards and F. Daniels, *J. Am. Chem. Soc.* 41, 1732 (1919).
139. Mark Salomon, *J. Phys. Chem.* 74, 2519 (1970).
140. D. R. Cogley, J. N. Butler and E. Grunwald, *J. Phys. Chem.* 75, 1477 (1971).
141. A. J. Parker, *Chem. Rev.* 69, 1 (1969).
142. Orest Popovych, *Critical Rev. in Anal. Chem.* 1, 73 (1970).
143. Richard Payne, *J. Phys. Chem.* 71, 1548 (1967).
144. Richard Payne, *The Electrical Double Layer in Nonaqueous Solutions, Advances in Electrochemistry and Electrochemical Engineering*, P. Delahay and C. W. Tobias, eds. (Interscience, New York, 1970) Vol. 7.
145. R. Jasinski and S. Kirkland, *Anal. Chem.* 39, 1663 (1967).
146. F. G. K. Baucke, D. Landolt and C. W. Tobias, *Rev. Sci. Inst.* 39, 1753 (1968).
147. L. Hsueh, (M. S. Thesis) UCRL 16607, University of California, Berkeley, 1966.
148. John Newman, *J. Electrochem. Soc.* 113, 501 (1966).
149. R. A. Robinson and R. H. Stokes, *Electrolytic Solution*, 2nd Edition, (Butterworth Scientific Publication, London, 1959).

150. E. A. Guggenheim, Thermodynamics, 4th Edition, (North-Holland, 1959).
151. G. N. Lewis, M. Randall, K. S. Pitzer and L. Brewer, Thermodynamics, 2nd Edition (McGraw Hill, New York, 1961).
152. John Newman, J. Electrochem. Soc. 113, 501 (1966).
153. L. Hsueh, (M. S. Thesis) UCRL 16607, University of California, 1966.
154. William H. Smyrl and Charles W. Tobias, Electrochem. Acta 13, 1581 (1968).
155. V. A. Pleskov Usp. Khim. 16, 254 (1947).
156. V. A. Pleskov, Zh. Fiz. Khim. 22, 351 (1948); Chem. Abstr. 42, 6249.
157. H. Lund, Acta Chem. Scand. 11, 491 (1957).
158. T. Pavlopoulos and H. Strehlow, Z. Physik. Chem. (Frankfurt) 2, 89 (1954).
159. J. E. Chilton and G. M. Cook, Report ASD-TDR-62-837, Sept. 1962.
160. M. Della Monica and L. Senatore, J. Phys. Chem. 74, 205 (1970).
161. M. Eisenberg, Forth Quarterly Report, Contract N00017-68-C-1401, Sept. 1968.
162. Cecil M. Criss and Martin J. Mastroianni, J. Phys. Chem. 75, 2532 (1971).
163. G. Jones and M. Dole, J. Am. Chem. Soc. 51, 2950 (1929).
164. Paul Delahay, Double Layer and Electrode Kinetics (Interscience Publishers, New York, 1965).
165. Terrell N. Andersen and Henry Eyring, Principles of Electrode Kinetics, Physical Chemistry an Advanced Treatise, Henry Eyring, ed. (Academic Press, New York, 1970) Vol. IXA/Electrochemistry.
166. John Newman, J. Heat and Mass Transfer 10, 983 (1967).
167. John Newman, J. Electrochem. Soc. 113, 1235 (1966).

168. J. D. E. McIntyre and W. F. Peck, Jr., *J. Electrochem. Soc.* 117, 747 (1970).
169. John Newman, *J. Electrochem. Soc.* 117, 507 (1970).
170. William H. Tiedemann, John Newman and Douglas N. Bennion, *J. Electrochem. Soc.* (submitted for publication), University of California, LBL-890, June 1972.
171. William H. Tiedemann and Douglass N. Bennion, Final Report, University of California, Los Angeles, UCLA-ENG-7228, April 1972.
172. H. J. S. Sand. *Phil. Mag.* 1, 45 (1901).
173. Klaus J. Vitter, Electrochemical Kinetics (Academic Press, New York, 1967).
174. J. Sullivan, D. Hansen and R. Keller, *J. Electrochem. Soc.* 117, 779 (1970).
175. P. L. Allen and A. Hickling, *Trans. Faraday Soc.* 53, 1625 (1957).
176. E. Grunwald, G. Baughman and G. Kohnstam, *J. Am. Chem. Soc.* 82, 5801 (1960).
177. K. J. Laidler and C. Pegis, *Proc. Roy. Soc., Ser. A*, 241, 80 (1957).
178. H. F. Halliwell and N. C. Nyberg, *Trans. Faraday Soc.* 59, 1126 (1963).
179. B. E. Conway and M. Salomon, Chemical Physics of Ionic Solutions, B. E. Conway and R. G. Barradas, eds. (John Wiley, New York, 1966).
180. D. D. Wagman, et al., Selected Values of Thermodynamic Properties, N. B. S. Technical Note No. 270, 1968.
181. JANAF Thermochemical Tables, The Dow Chemical Co., Maidland, Mich., August 1965 and addenda.
182. Wendell M. Latimer, Oxidation Potentials (Prentics-Hall, Englewood Cliffs, N. J., 1952).

183. J. P. Jesson and E. L. Muetterties, Basic Chemical and Physical Data, (Marcel Dekker, Inc., New York, 1969).
184. R. S. Berry and C. W. Riemann, J. Chem. Phys. 38, 1540 (1963).
185. Linus Pauling, The Nature of the Chemical Bond, 3rd Edition (Cornell University Press, Ithaca, N. Y., 1960).
186. W. M. Latimer and C. M. Slansky, J. Am. Chem. Soc. 62, 2019 (1940).
187. S. Levinia and S. Sarinsky, Acta Physicochim. 6, 491 (1937).
188. V. M. Novoselski, Russ. J. Phys. Chem. 11, 369 (1938).
189. J. O'M Bockris and R. Parsons, Trans. Faraday Soc. 45, 916 (1949).
190. J. O'M Bockris, R. Parsons and H. Rosenberg, Trans. Faraday Soc. 47, 766 (1951).
191. S. Minc and J. Sobkowski, Bull. Acad. Polon. Sci. 8, 29 (1959).
192. B. E. Conway and M. Salomon, J. Chem. Phys. 41, 3169 (1964).
193. M. Salomon, J. Phys. Chem. 70, 3853 (1966).
194. J. E. B. Randles and K. W. Somerton, Trans. Faraday Soc. 48, 951 (1952).
195. Hideo Imai and Paul Delahay, J. Phys. Chem. 66, 1683 (1962).
196. D. J. Schriffrin, Trans. Faraday Soc. 66, 2464 (1970).
197. Raymond Jasinski and Susan Kirkland, Anal. Chem. 39, 1663 (1967).
198. R. F. Nelson and R. N. Adams, J. Electroanal. Chem. 13, 184 (1967).
199. R. J. Jasinski, B. W. Burrows and P. Malachesky, High Energy Batteries, 3rd Quarterly Report, N0w-66-0621-c, March 1967.
200. D. P. Boden, H. R. Buhner and V. J. Spera, Final Report, DA-28-043-AMC-01394(E), Sept. 1966.
201. R. J. Jasinski, P. Malachesky and B. W. Burrow, 1st Quarterly Report, N000 19-67-C-0680, Sept. 1967.

202. L. Simeral and R. L. Amey, J. Phys. Chem. 74, 1443 (1970).
203. A. Parker, Quart. Rev. (London) 16, 163 (1962).
204. R. Kempa and W. Lee, J. Chem. Soc., 1936 (1958).
205. M. Watanabe and R. Fuoss, J. Am. Chem. Soc. 78, 527 (1956).
206. R. T. Foley and F. D. Bogar, Fifth Progress Report, Research Grant NGR 09-003-005, The American University, April 30, 1967.
207. N. F. Catherall and A. G. Williamson, J. Chem. and Eng. Data 16, 335 (1971).
208. M. Eisenberg, R. E. Kuppinger and K. M. Wong, J. Electrochem. Soc. 117, 577 (1970).
209. Charles W. Tobias and Jacob Jorné, Patent Application, Nov. 9, 1971.
210. L. C. Fuhremeister and A. T. Emergy, Report of the Electrolytic Industries for the year 1971, Sponsored by the Electrochemical Society, May 8, 1972.
211. G. L. Putnam and K. A. Kobe, Trans. Electrochem. Soc. 74, 609 (1938).
212. T. P. Dirkse and H. T. Briscoe, Metal Ind. (New York) 36, 284 (1938).
213. D. M. Overcash and F. C. Mathers, Trans. Electrochem. Soc. 64, 305 (1933).
214. J. Bittrich, R. Landberg and W. Gaube, Wiss. Z. Tech. Hochschule Chem. Leuna-Merseburg 2, 449 (1959-60).
215. R. Müller, et al., Monatsh. Chem. 44, 219 (1923).
216. J. H. Connor, W. E. Reid, Jr. and G. B. Wood, J. Electrochem. Soc. 104, 38 (1957).
217. Abner Brenner, J. Electrochem. Soc. 118, 99 (1971).

218. Jacob Journé and Charles W. Tobias, IMRD Annual Report, Lawrence Berkeley Laboratory, UCRL-19155, p. 48, 1969.
219. F. H. Hurley and T. P. Wier, Jr., J. Electrochem. Soc. 98, 203 (1951).
220. F. H. Hurley and T. P. Wier, Jr., J. Electrochem. Soc. 98, 207 (1951).
221. M. D. Rausch, W. E. McEwen and J. Kleinberg, Chem. Rev. 417 (1956).
222. A. N. Dey and B. P. Sullivan, J. Electrochem. Soc. 117, 222 (1970).
223. W. E. Reid, Jr., J. M. Bish and A. Brenner, J. Electrochem. Soc. 104, 21 (1957).
224. G. Szekely, J. Electrochem. Soc. 98, 318 (1951).
225. T. T. Campbell, J. Electrochem. Soc. 106, 119 (1960).
226. R. E. Meredith and T. T. Cambell, Electrochem. Soc. Meeting, New York, Sept. 30-Oct. 3, 1963.

LEGAL NOTICE

This report was prepared as an account of work sponsored by the United States Government. Neither the United States nor the United States Atomic Energy Commission, nor any of their employees, nor any of their contractors, subcontractors, or their employees, makes any warranty, express or implied, or assumes any legal liability or responsibility for the accuracy, completeness or usefulness of any information, apparatus, product or process disclosed, or represents that its use would not infringe privately owned rights.

TECHNICAL INFORMATION DIVISION
LAWRENCE BERKELEY LABORATORY
UNIVERSITY OF CALIFORNIA
BERKELEY, CALIFORNIA 94720